“Engineering the multigene pathways for CO_2 concentration mechanism and bypassing the photorespiration in C_3 plants”

Von der Fakultät für Mathematik, Informatik und Naturwissenschaften der RWTH Aachen University zur Erlangung des akademischen Grades eines Doktors der Naturwissenscheften genehmigte Dissertation

vorgelegt von

Master of Science

Pratibha Kamble

Amalner, Indien

Berichter

Privatdozent Dr. F. M. Kreuzaler
Universitätsprofessor Dr. Ursula B. Priefer

Tag der mündlichen Prüfung: 17.01.2014

Dedicated to my dear mother

Institute for Biology I (Botany and Molecular Genetics)
RHEINISCH **W**ESTFÄLISCHE **T**ECHNISCHE **H**OCHSCHULE **A**ACHEN

PhD Thesis

"Engineering the multigene pathways for CO_2 concentration mechanism and bypassing the photorespiration in C_3 plants"

Presented by

Master of Science

Pratibha Kamble

From Amalner, India

Examiners
Privatdozent Dr. F. M. Kreuzaler
University professor Dr. Ursula B. Priefer

Developing a world-class skill means that you have the capability to ignore everything else. You have to be able to focus on doing an incredible job or on ignoring it completely. Greatness doesn't come from simply "putting the time in" ... you have to put the time in with effort, energy, and resolve. - Prince Alwaleed

ZUSAMMENFASSUNG

Der Enzymkomplex Ribulose 1,5-bisphosphat-Carboxylase (Rubisco) ist von überragender Bedeutung für das Leben und für die Umwandlung von Lichtenergie in Bioproduckte wie Kohlenhydrate, Lipide, Proteine, Nukleinsäuren, usw. Leider hat dieser wichtige Enzymkomplex einen großen Nachteil, der sich besonders negativ in der Landwirtschaft bemerkbar macht. Neben der Carboxylierungs-Reaktion katalysiert die Rubisco auch die Oxygenierungs-Reaktion. Letztere führt zu einer Verminderung der maximal möglichen Biomasse Produktion, allerdings nur bei C_3-Pflanzen wegen der Photorespiration. Zu diesem CO_2-Fixierungstyp gehören allerdings die wichtigsten Kulturpflanzen wie Weizen, Reis, Kartoffel und die Zuckerübe. Ziel der vorliegenden Arbeit war es, zwei Möglichkeiten zu untersuchen, die Oxygenase-Reaktion der Rubisco zu inhibieren. Die Grundstrategie zur Inhibition der Oxygenase und damit zu Erhöhung der Carboxylase-Reaktion besteht darin, die CO_2 Konzentration in den Chloroplasten, also in der unmittelbaren Nähe der Rubisco zu erhöhen.

Die erste potentielle Möglichkeit zur Erreichung des Zieles besteht darin, einen Biosyntheseweg in C_3-Kulturpflanzen (*N. tabacum*) einzubauen, wie er bei der submers lebenden Pflanze *Hydrilla verticillata* vorgefunden wird. Diese Pflanze kann bei niedrigen CO_2-Konzentrationen in Wasser einen CO_2-fixierungs Mechanismus induzieren, der aber in Gegensatz zu normalen C_4-Pflanzen z.B. Mais, in einer Zelle abläuft und das Leben der Pflanze unter solchen Physiologischen Bedingungen sichert. Die in dieser Arbeit eingesetzten Gene zum aufbauen des modifizierenden Biosyntheseweges sind: Phospho*enol*pyruvat Carboxylase (PEPC) aus *Hydrilla verticillata*; NAD-Malat-Dehydrogenase (MDH) aus Mais; NAD-Malic Enzym (ME) aus *E. coli*; Lactat-Dehydrogenase (*LdhA*) aus Mausleber; Lactat-Dehydrogenase (*LdhB*) aus Ratenherz; Phospho*enol*pyruvat Synthase (PPS) aus *E. coli*; Malat-Lactat Antiporter (Mle) aus *B. subtilis*. Alle Gene wurden erfolgreich mit der Gateway Methode in ein Plasmid integriert und in Pflanzen übertragen. Die Aktivität aller Enzyme wurde gemessen. Leider zeigte sich, dass die gezielte Strategie nicht zu dem gewünschten Erfolg führt. Das hat wohl verschiedene Gründe:

i) Obwohl alle Gene einen Lichtinduzierten Promoter tragen, konnte keine koordinierte Genexpression erhalten werden. Alle Gene wurden zwar exprimiert, die Expressionsraten und damit die Enzymaktivität sind aber sehr unterschiedlich und variieren von Pflanze zu

Pflanze. ii) Die in *H. verticillata* zweifellos vorhandene Regulation der Enzymaktivitäten konnte nicht imitiert werden.
iii) Wir wissen noch zu wenig über die Regulation von Genexpression und Enzymaktivität in C_4-Hydrilla Pflanzen. Die CO_2-Konzentration in C_3-Landpflanzen ist höher als in der submers lebenden *H. verticillata*. Der *H. verticillata* C_4 CO_2 Fixierungsmechanismus ist daher möglicherweise auf C_3-Landpflanzen nicht übertragbar.

Die zweite potentielle Möglichkeit zur Erreichung des Ziels bestand darin, den sogenannten MMPEM-Biosyntheseweg in C_3-Pflanzen zu übertragen. Diese Strategie wurde nach intensiven Diskussionen kreiert. Die beteiligten Enzyme sind: Malat-Synthase (MS) aus *E. coli*; NAD-Malic Enzym (ME) aus *E. coli*; Phospho*enol*pyruvat-Synthase (PPS) aus *E. coli*; Enolase (E) aus *E. coli*; Phosphoglycerat-Mutase (PGM) aus *E. coli*. Alle Gene wurden mit Hilfe der Gateway-Technologie erfolgreich in *N. tabacum* Pflanzen übertragen, die den sogenannten GT-DEF Biosyntheseweg enthielten. Der GT-DEF-Patway führt zu einer Erhöhung der CO_2-Fixierung in C_3-Pflanzen. In dieser Arbeit konnte gezeigt werden, dass der zusätzliche Einbau des MMPEP-Stoffwechselweges zu einer weiteren Erhöhung der CO_2 Fixierung führt. Der gewählte Ansatz war also erfolgreich.

In späteren Arbeiten sollte versucht werden, den Effekt beider Photosynthesewege (GT-DEF/ MMPEM) sowie des MMPEM-Einzelweges zu erhöhen. Das kann mit Hilfe der klassischen Gentechnik erreicht werden. Sowohl durch eine stabile Koordination der Genexpression als auch durch eine besser abgestimmte Aktivität der Enzyme. In Freilandversuchen muss dann gezeigt werden, ob transgene Pflanzen verglichen mit Wildtyp-Pflanzen mehrt Biomasse auf der gleichen Fläche produzieren können.

SUMMERY

The present study shows an improvement in photosynthesis in C_3 plants by two different approaches. The first approach is aimed to increasing the CO_2 concentration in the proximity of Rubisco. The second approach is aimed at bypassing the 'wasteful' reaction of photorespiration in C_3 plants. In both approaches, multiple transgene metabolic pathways are created and successfully introduced in C_3 plants. With the help of multiple transgene metabolic pathways the final products such as CO_2 is observed to successfully reach Rubisco. The multiple transgenes are introduced into the tobacco (*Nicotiana tabacum*) plant through *Agrobacterium* transformation. The MultiRound Gateway technology is used to successfully deliver the combination of two multiple transgene pathways in to the *Agrobacterium*.

The first approach is intended to create a single cell C_4 pathway in a C_3 plant, similar like in *Hydrilla verticillata* C_4 plants, Novel pathway (HC_4l) mimic *Hydrilla* in which carbon channels from cytoplasm to chloroplast ultimately resulting in an increase of CO_2 under the vicinity of Rubisco. In this approach, to create the first multigene transgenic pathway, seven different heterologaus enzymes are used. They are: phospho*enol*pyruvate carboxylase (PEPC) derived from *Hydrilla verticilliata,* NAD malate dehydrogenase (MDH) derived from Maize, NAD malic enzyme (ME) derived from *E. coli*, lactate dehydrogenase (LDHA) derived from mouse liver, lactate dehydrgenase (LDHB) derived from rat heart, phospho*enol*pyruvate synthase (PEPS) from *E. coli*, and malate lactate antiporter (Mle) derived from *Bacillus subtilitis.* The MultiRound Gateway technology is successfully used to transfer these seven transgenes in to plant with the help of two entry vector and one destination vector approach. The RT-PCR is used to quantify the expression level and the efficiency of the expression of transgenes in the study plant. The findings from the RT-PCR indicate successful expression of transgenes in the test plants. The enzymes of respective transgenic are analyzed with enzymatic assays and it also reveals the presence of active protein in the plant studied.

In the second approach, another combination of transgenic pathway is introduced into C_3 plants to bypass the wasteful reaction and flux of photorespiration. The transgenic pathway used in this approach included genes such as malate synthase (MS) from *E. coli*, NAD malic enzyme (ME) from *E. coli*, phospho*enol*pyruvate synthase (PPS), enolase

from *E. coli* and phosphoglycerate mutase (PGM) from *E. coli*. The aim of this transgenic pathway is to reduce the photorespiration to a greater degree than previously observed in plants with GTDEF pathway. The plants used for this approach already possessed the GTDEF pathway. Similar to the first approach, the MultiRound Gateway technology is used to transfer all transgenes by using two entry and one destination vector. The analysis by enzyme assays shows the active presence of the test proteins the plant studied. The influence of introduction of five genes pathway in a plant is measured through physiological, biochemical and by photosynthetic parameters.

Metabolism of glycolate pathway derived from *E. coli* and was established in the chloroplast of *Arabidopsis thaliana* plants (Kebeish *et al*., 2007). This pathway (GTDEF) showed lower compensation point, higher glucose, fructose and end product of the photosynthesis as compared to the wild type plants. The present study reveals that the introduction of the novel pathway consisting five genes (MMPEM pathway) into the plants existing GTDEF pathway results in further decrease in the compensation point (Γ_*), a noticeable increase in glucose, fructose and other end product of photosynthesis. The study also reveals that the plants with combination of GTDEF pathway and five gene pathway has higher fresh as well as dry weight as compared to plants with only GTDEF pathway. The research shows that with the successful introduction of multigene complex metabolic pathways in C_3 plants, the higher rate of photosynthesis is possible.

The present study uses MultiRound gateway recombination technology to create multiple gene pathways in C_3 plants. In this study multiple genes are successfully transferred into the the *Nicotiana tabacum* plant. Transfer of multiple genes located on one vector, created by gateway recombination for both the pathways (MMPEM and HC_4l). Gateway technology was the most advantageous technique among most of the multiple gene transformation techniques. The transformation of multiple transgene pathways by agrobacterium is relatively advantageous because it uses a single T-DNA from single *Agrobacterium tumefaciens* strain rather complex *Agrobacteium* transformation of multiple T-DNA molecules by several *Agrobacterium*, which is more complex for integration pattern (De Neve et al., 1997). The Gateway technique is used in this study is based on vectors (entry vector and destination vector) which have attachments sites sequences that are compatible to each other. It simply means that the destination vector with attL is compatible to entry vector attR. In gateway cloning alternate use of two

gateway entry vectors used to the fusion of multiple transgens into the destination vector by LR recombination (site specific recombination). This technique is used to create single vector from multigene pathway to approach the overexpression of C_4 cycle genes and bypassing the photorespiration in C_3 plant for the improvement in photosynthesis.

Table of Content

Table of Content i

1 Introduction 7

1.1 Photosynthesis 7
1.2 C_3 photosynthesis 8
1.3 Photorespiration 10
1.3.1 The photo respiratory pathway in C_3 plants 12
1.4 The C_4 Photosynthesis 13
1.5 Single cell C_4 photosynthesis 16
1.6 The Crassulacean Acid Metabolism (CAM) photosynthesis 17
1.7 Approaches for improvement of photosynthetic carbon assimilation in C_3 plants 18
1.7.1 Successful approaches for increasing photosynthesis 19
1.7.2 Unsuccessful approaches to expressing C_4 enzymes in C_3 plants 20
1.8 Increasing regenerative capacity of the Calvin cycle 21
1.9 Expression of bacterial glycolate pathway in C_3 plants 23
1.10 The aim of the present study 25

2 Materials and Methods 27

2.1 Materials 27
2.1.1 Chemicals and consumables 27
2.1.2 Instruments 27
2.1.3 Solutions, buffers and media 28
2.1.4 Different Size markers for Gel electrophoresis 29
2.1.5 Used Kits 29
2.1.6 Enzymes 30
2.1.7 Synthetic Oligonucleotide 30
2.1.8 DNA plasmids and vectors 35
2.1.8.1 Entry plasmids for gateway recombination 35

2.1.8.2 Destination vector for gateway recombination 36
2.1.8.3 Plant Vectors and Gateway Entry Vectors 37
2.1.8.4 Plant vectors and entry vector for pYLTAC7 Hydrilla pathway 38
2.1.8.5 Destination vector with Hydrilla pathway genes 41
2.1.8.6 Plant vectors and Gateway Entry Vectors for pYLTAC7 MMPEM pathway 42
2.1.8.7 Destination vector with MMPEM pathway genes 44
2.1.9 Plant materials 46
2.1.10 Bacteria 46
2.1.10.1 *Escherichia coli* cultures 46
2.1.10.2 *Agrobacterium tumefaciens* Culture 47
2.1.11 Used Internet softwares and Computer programs 48
2.2 Methods 48
2.2.1 Molecular biological methods 48
2.2.1.1 Isolation of plasmid DNA from *E. coli* 48
2.2.1.2 Combined isolation of DNA and RNA 50
2.2.1.3 Agarose gel electrophoresis 50
2.2.1.4 Purification of DNA fragments from agarose gels 51
2.2.1.5 Sequencing of DNA 51
2.2.1.6 Polymerase chain reaction (PCR) 52
2.2.1.7 Purification of PCR products 53
2.2.1.8 Multiplex PCR 53
2.2.1.9 First strand cDNA synthesis from RNA 54
2.2.1.10 RNA analysis with RT-PCR 54
2.2.1.11 Restriction Digestion of DNA 55
2.2.1.12 Dephosphorylation of DNA 5´-ends 55
2.2.1.13 "Blunting" of DNA 5 '- or 3'-overhanging ends 56
2.2.1.14 Ligations reaction 56
2.2.1.15 TOPO TA cloning 57
2.2.1.16 Gateway cloning 57
2.2.1 Analysis of plant growth 58
i) Plant growth analysis 58

ii) Determination of the leaf area 59
2.2.2 Microbiological Method 59
2.2.2.1 Transformation of competent *E. coli* (DH5α) by heat-shock 59
2.2.2.2 Preparation of electro competent *E. coli* cells 59
2.2.2.3 Transformation of electro competent *E. coli* cells 60
2.2.2.4 Preparation of electro competent *Agrobacterium* cells 60
2.2.2.5 Transformation of electrocompetent *Agrobacterium* cells 60
2.2.2.6 Transient transformation of *Nicotiana tabacum* 61
2.2.2.7 Stable transformation of *Nicotiana tabacum* 61
2.2.3 Biochemical Methods 63
2.2.3.1 Determination of protein concentration 63
2.2.3.2 Determination of enzyme activities 63
2.2.3.2.1 Hydrilla PEP carboxylase (PEPC) activity measurements 64
2.2.3.2.2 NAD-malic enzyme (ME) activity measurements 65
2.2.3.2.3 NAD-dependent malate dehydrogenase (MDH) activity measurement 65
2.2.3.2.4 PEP synthase (PEPS) activity measurement 66
2.2.3.4 Extraction of soluble and insoluble metabolites from *N. tobacum* leaves 67
I) Determination of glucose and fructose content 68
II) Determination of starch content 68
III) Determination of sucrose content 68
IV Determination of malate content 69
2.2.3.5 Ammonia release assay 70
2.2.3.6 Analysis of metabolites by gas chromatography and mass spectroscopy(GC-MS) 71
I. Gas chromatography 71
II. Mass Spectrometry (MS) 73
III. Preparation, derivatisation and injection of samples 74
IV. Data interpretation 74
2.2.3.7 Measurement of photosynthetic parameters 76
I Measurement of the CO_2 compensation point 76
II The post illumination burst (PIB) 76

3 Results 77

3.1 Project A 77

3.1.1 Establishment a novel pathway in C_3 plants for assimilation of CO_2 under in vicinity of rubisco 77

3.1.2 Construction of Multigene pathway in a single vector 78

3.1.3 Construction of the Gateway Entry Vectors 79

3.1.4 Construction of the destination vector 80

3.1.5 MultiRound Gateway recombination 80

3.1.6 Novel biochemical pathway like single cell *Hydrilla verticilliata* plants, aiming to increase CO_2 concentration in the chloroplast of C_3 plant 82

3.1.7 Construction of gateway plasmids containing genes used for the modified Hydrilla C_4 pathway (HC_4l) 84

3.1.8 Big size destination vector transformation in *A. tumefaciens* 88

3.1.9 Transient expression of Hydrilla pathway (HC_4l) in tobacco 89

3.1.10 Stable expression of C_4 genes in tobacco (T_0 generation) 90

3.1.11 Stable expression of PEPC, MDH, Mle, EcME, LDHA, LDHB, and PPS genes in tobacco (T_1 generation) 92

3.1.12 Enzyme activities and transcription level of a C_4 hydrilla like pathway in transgenic tobacco plants 93

3.1.13 Phenotypic effects of the C_4 Hydrilla pathway on transgenic tobacco plant 96

3.1.14 Measurement of ammonia release during photorespiration 98

3.1.15 Concentration of Malate in C_4 Hydrilla Transgenic plants (T_1 generation) 99

3.1.16 Determintaion of glucose, fructose, sucrose and starch by enzymatically 100

3.1.17 Determination of metabolites by GC-MS 101

3.1.18 Photosynthetic performance of transgenic plants 101

i) Postillumination burst (PIB) as a marker for the rate of photorespiration. 101

ii) Determination of the apparent CO_2 compensation point (Γ) 103

3.1.19 What is the influence of the novel pathway on plant growth? 104

3.2 Project B 105

3.2.1 A novel biochemical pathway aiming to increase CO_2 concentration in the chloroplasts of transgenic GTDEF plants 105

3.2.2 Construction of pathway into single destination vector by MultiRound Gateway technology 106
3.2.3 Analysis of agrobacterium and transgenic plants on DNA level....107
3.2.4 Transient expression of GTDEF+MMPEM pathway....109
3.2.5 Stable expression of the genes of the MMPEM pathway in the chloroplast of transgenic GTDEF tobacco plants (T_0 generation)....110
3.2.6 Stable expression of Enolase, Malate synthase, Mutase, NAD-ME, PPS, DEF, TSR, GCL in T_1 generation 111
3.2.7 Determination of the MMPEM pathway activities and evaluation of the transcription levels in transgenic GTDEF tobacco plants 112
3.2.8 Determination of metabolites by GC-MS....113
3.2.9 Phenotype effect of MMPEM and GTDEF pathway on transgenic tobacco plant....114
3.2.10 Effect of the novel pathway on the plant leaf area and the height of the plant 116
3.2.11 Measurement of the total fresh and dry weight of the transgenic plants....117
3.2.12 Photosynthetic performance of transgenic plants....119
3.2.12.1 The postillumination burst (PIB) as a marker for the rate of photorespiration 119
3.2.12.2 Determination of the apparent CO_2 compensation point (Γ*) of the trans. plants ..121

4 Discussion 123

4.1 Bi-functionality of Rubisco 123
4.2 C_4 syndrome in C_3 plants 124
4.3 The optimized Hydrilla (HC_4l) pathways....126
4 gene experiment (PEPC, Mle, NAD^+-ME, PEPS) 131
4.4 Summarizing discussion for the optimized *Hydrilla* pathway (HC_4lo)....135
4.5 The MMPEM pathway in WT and GTDEF tobacco plants 136
Detail about enyzme used in MMPEM pathway....137
4.6 MMPEM+GTDEF pathway shows positive effect in *N. tabacum*? 140
4.7 MultiRound Gateway technology....141
4.8 Summarizing Discussion 142
4.9 Future work....143

5 Appendixes 145

5.1 List of abbreviations 145

5.2 List of figures 149

5.3 List of Tables 152

6 References 155

Acknowledgements 184

Declaration / Erklärung 185

1 Introduction

1.1 Photosynthesis

Photosynthesis is the primal physiochemical process by which green plants and other photosynthetic organism uses sunlight or other light for converting CO_2 and H_2O into organic compounds. The result of photosynthesis is the release of molecular oxygen and the removal of CO_2 from the ambient air and used to synthesize carbohydrates and it known as oxygenic photosynthesis (Whitmarsh and Govindjee, 1995). Some organisms use sunlight as an energy source to create organic compounds but do not produce oxygen called anoxygenic photosynthesis. Photosynthesis is the great source of molecular oxygen which is necessary for the survival of all oxygen consuming organisms as well as reduced carbon for the survival of nearly all life on earth. It also supplies inexhaustible energy like fossil fuel, burned in day to day activities for us in the form of different oil sources and these fossils were produced by ancient photosynthetic organisms.

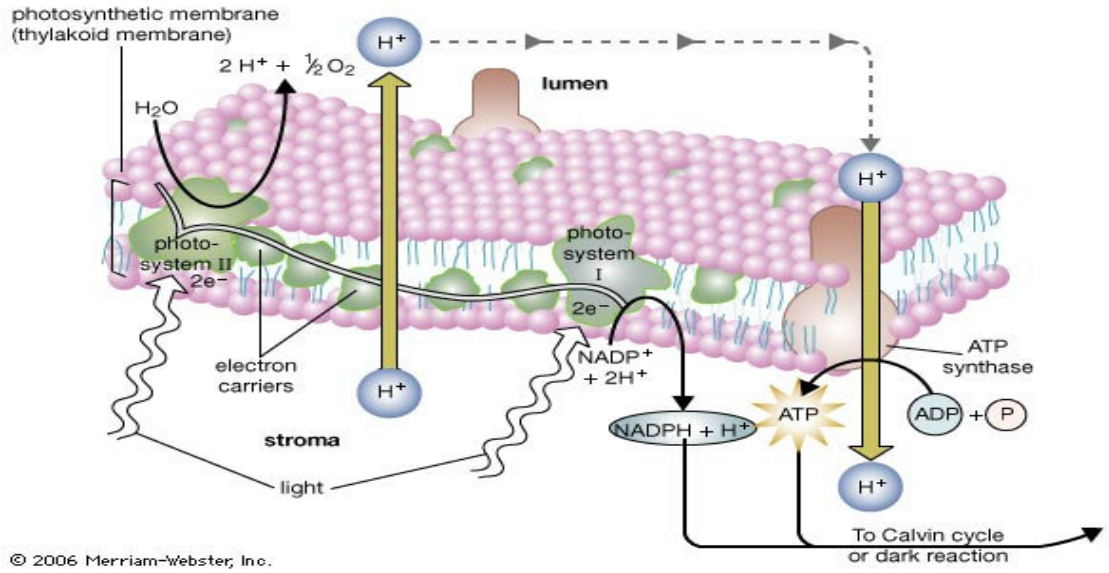

Figure 1.1: The light reaction of photosynthesis
During the electron transport process a proton gradient is form across the thylakoid membrane Photosystem II is excited by absorption of a photon of light energy, and expels an electron to the photosynthetic electron transport chain, the oxidized form of the reaction center chlorophyll molecule is able to accept electrons from water. Water is oxidized on the inner side of the thylakoid membrane, donating electrons to the oxidized PS II reaction center. Oxygen is released as a by product of water oxidation, and the protons released contribute to the H^+ gradient used as the energy source for ATP synthesis. This proton motive force is then used to drive the synthesis of ATP. This process requires PSI, PSII, cytochrome *bf*, ferredoxin $NADP^+$ reductase and chloroplast ATPsynthase (Miles, 2003).

Photosynthesis has a profound effect on atmosphere and climate. By photosynthesis, green plants, photosynthetic bacteria and algae harvest light quanta and convert sunlight into chemical energy, which is used for reduction of CO_2, formation of organic compounds like carbohydrates and store this energy as ATP and NADPH. Photosynthesis is a principally complex set of physical and chemical reactions taking place in a coordinated manner for the synthesis of sugar. The formation of simple sucrose molecule a plant requires ~ 30 distinct proteins that work within a complicated membrane structure (Whitmarsh and Govindjee, 1995). The light reaction occurs in two photosystems. Photosystem I ideally absorbs photons of a wavelength of 700 nm. Photosystem II ideally absorbs photons of a wavelength of 680 nm. Electrons flow from PSII through cytochrome *bf* (a membrane bound protein) to PSI. Photosystem II uses light energy to oxidize two molecules of water into one molecule of oxygen. The 4 electrons removed from the water molecules are transferred by an electron transport chain to eventually reduce $2NADP^+$ to 2NADPH (Miles, 2003). Electrons and H^+ for the reduction of CO_2 come from water and O_2 is produced. Higher plants are divided into three biochemical pathways: the C_3 pathway (Calvin cycle), the C_4 pathway (Hatch-Slack pathway) and the Crassulacean acid metabolism (CAM) (Edwards and Walker, 1983) and these pathways are involved in CO_2 assimilation.

1.2 C_3 photosynthesis

C_3 photosynthesis is an ancestral pathway for CO_2 assimilation and occurs in the vast majority of terrestrial plants and most important crops (wheat, rice, soybean, barley). The term C_3 photosynthesis comes from the observation that the first product of photosynthesis is a 3 carbon molecule. Figure 1.2 represents the CO_2 assimilation pathway in C_3 plants which is known as Calvin cycle. C_3 photosynthesis is a multi step process and it occurs in virtually all leaf mesophyll cells. First, CO_2 reacts with a five carbon compound called ribulose-1,5-bisphosphate (RuBp) (5C) producing an unstable six carbon intermediate that immediately breaks down into two molecules of a three carbon compound phosphoglycerate (PGA)(3C) and therefore the overall raction is called C_3 photosynthesis. In the second step, conversion of PGA to glyceraldehyde 3-phosphate (G3P) takes place with the help of ATP and NADPH produced during the light reaction. The triose phosphate is used either to form carbohydrates and sugars or to regenerate ribulose 1,5-

bisphosphate for the continuity of the Calvin cycle. In the synthesis of carbohydrate, glyceraldehydes 3-phosphate forms dihydroxyacetone phosphate (DHAP) in the presence of triose phosphate isomerase.

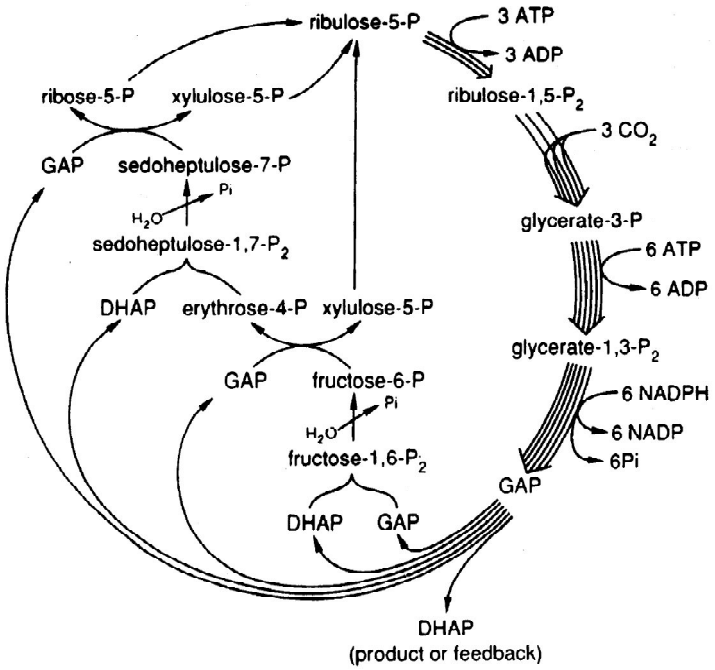

Figure 1.2: Schematic representation of the Calvin cycle
In this diagram ribulose-1,5-bisphosphate (RuBp)(5C) produce unstable phosho glycerate (PGA)(3C). Later stage PGA converted to glyceraldehyde-3-phosphate (G3P). The glyceraldehyde-3-phosphate forms dihydroxy-acetone phosphate (DHAP). DHAP and phospho-glycealdehyde-3-phosphate (GAP) combined by aldolase to form fructose-1,6 bisphosphate which is converted to fructose-6-phosphate and is then with glyceraldehyde-3-phosphate forms ribulose-1,5-bisphosphate (Berg J. et al., 5th edition).

The carboxylation reaction of Rubisco yields two molecules of 3-phosphoglycerate (glycerate 3-P) which is converted into three forms of isomers: glucose 1-phosphate, glucose 6-phosphate, and fructose 6-phosphate and these isomers are interconvertible. Glyceraldehyde 3-phosphate dehydrogenase in chloroplast with NADPH forms DHAP and phospho glycealdehyde 3-phosphate are combined by aldolase to form fructose 1,6-bisphosphate which is then converted into fructose 6-phosphate. Different carbohydrates can be synthesized from fructose 6-phosphate. In a series of reaction, fructosen 6-phosphate and glyceraldehydes 3-phosphate are used for the regeneration of ribulose 1,5-bisphosphate and hexose isomerase converts fructose 6-phosphate into glucose 6-phosphate for the formation of glucose after dephosphorylation. Glyceraldehyde 3-phosphate (GAP) is transported to the cytosol for the carbohydrate synthesis. In the next stage for the regeneration of ribulose 1,5-bisphosphate, the whole process to construct five

carbon sugars from six carbon sugar and three carbon sugar, transketolase and transaldolase play major role in the rearrangement of carbon atoms. Transketolase requires the coenzyme thiamine pyrophosphate (TPP) to transfer two carbon units to form ketoses and aldose. Aldolase catalyzes an aldol condensation between DHAP and an aldehyde. Fructose 6-phosphate with glyceraldehydes 3-phosphate catalyzed by transketolase forms erythrose 4-phosphate and xylose 5-phosphate, and erythrose 4-phosphate with DHAP catalyzed by aldolase forms sedoheptulose 1,7-bisphosphate and sedoheptulose-7-phosphate. Sedoheptulose 7-phosphate with glyceraldehydes 3-phosphate catalyzed by transketolase forms ribose 5-phosphate and xylose 5-phosphate and both catalyzed by phosphopentose isomerase forms ribulose 5-phosphate. Ribulose 5-phosphate is phosphorylated by phosphoribulose kinase and forms ribulose 1,5-bisphosphate (Berg J et al., 5th edition). The whole reaction for the formation of ribulose 1,5-bisphosphate and glucose needs three molecule of ATP and two molecules of NADPH and reducing CO_2 to the oxidative level of carbohydrate.

1.3 Photorespiration

Rubisco (Ribulose-1,5-bisphosphatase), the only enzyme that fixes CO_2 in all photosynthetic organism and capable to fix also O_2 at the active site but Ribulose-1,5-bisphosphate carboxylase/oxygenase favors CO_2 over O_2 by a factor of 100, but the concentration of CO_2 is much lower than O_2 in the atmosphere. As a result, every three molecules of CO_2 is fixed by Rubisco for one molecule of O_2 (Sharkey, 2001), when oxygen is the substrate for Rubisco. The result of the oxygenase reaction is lesser net carbon fixation and later formation of CO_2 in a process known as 'photorespiration' (This problem of photorespiration is overcome by C_4 plants and CAM plants, by concentrating CO_2 at the proximity of Rubisco. Because of the CO_2 concentration mechanism, C_4 plants reduce the oxygenase reaction of Rubisco. Rubisco evolved 3 billion years ago when the concentration of CO_2 in atmosphere was higher than now and concentration of O_2 was almost zero and oxygenation activity was very low. Now the atmospheric oxygen concentration is much higher enough than 3 billion years ago and it supports the Rubisco oxygenase activity and this increases when the temperature rises and this causes a high rate of photorespiration (Ku and Edwords, 1977; Ehleringer, 2001). At current CO_2 level, photorespiration can reduce photosynthesis by 40% at warmer temperature in C_3 plants

(Ehleringer et al., 1991). In photorespiration oxygenation is a wasteful side reaction of Rubisco in many ways like it uses active site of carboxylation, consumes RuBP, recovery of carbon in phosphoglycolate, consumes ATP and reducing equivalents while releasing CO_2 (Sage, 2001).

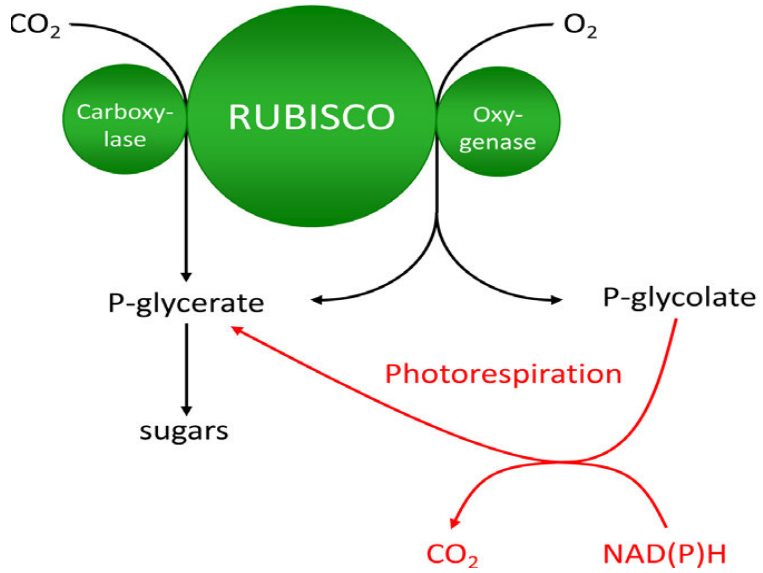

Figure 1.3: Schematic representations of photorespiration and photosynthesis
In above fig shows the bifunctionality of enzyme RUBISCO. At the site of Rubisco shows the competition of CO_2 and O_2 which forms the carboxylase and oxygenase activity respectively. Carboxylase reaction forms the two molecules of phosphoglycerate and which leads to Calvin cycle. The oxygenase reaction forms the one molecule of phophoglycerate and one molecule of phosphoglycolate. Metabolism of phosphoglycolate takes several steps for the formation of phosphoglycerate and the metabolism process called a photorespiration. (The image was kindly provided by Prof. Dr. Christoph Peterhänsel).

Phosphoglycolate is a potent inhibitor for plants. Metabolisms of phosphoglycolate into phosphoglycerate a very energy consuming reaction and performs in three different compartments (chloroplast, peroxisome and mitochondria) with 16 enzymes and more than 6 translocaters (Douce and Neuburger, 1999) so the whole process of photorespiration decreases the efficiency of C_3 plants.

Photorespiration begins when the concentration of oxygen is higher and oxygenation of RuBP forms one phosphoglycolate and phosphoglycerate catalyzed by Rubisco. Photosynthesis happens when RuBP is carboxylated with CO_2 by Rubisco, and forms two phosphoglyceric molecules for the production of carbohydrate and regeneration of RuBP.

1.3.1 The photo respiratory pathway in C_3 plants

The photorespiration pathway in C_3 plants proceeds in the chloroplast, the peroxisome and mitochondria figure 1.4 represents the oxygenation reaction of Rubisco in C_3 plants.

The reaction begins in the chloroplast where the oxygenation reaction of Rubisco results in one molecules of phosphoglycerate and one molecule of phosphoglycolate proceeds to form glycolate after dephosphorylation by phosphoglycolate phosphatase (PGP) in chloroplasts. Glycolate is transported to the peroxisome from the chloroplast. In the peroxisome, glycolate is oxidized to form glyoxalate by the enzyme peroxisomal glycolate oxidase (GOX). This enzyme uses inorganic oxygen as electron acceptor and forms H_2O_2 that is directly cleaved to H_2O and ½ O_2 by catalase (CAT) present in the peroxisome (Tolbert, 1997).

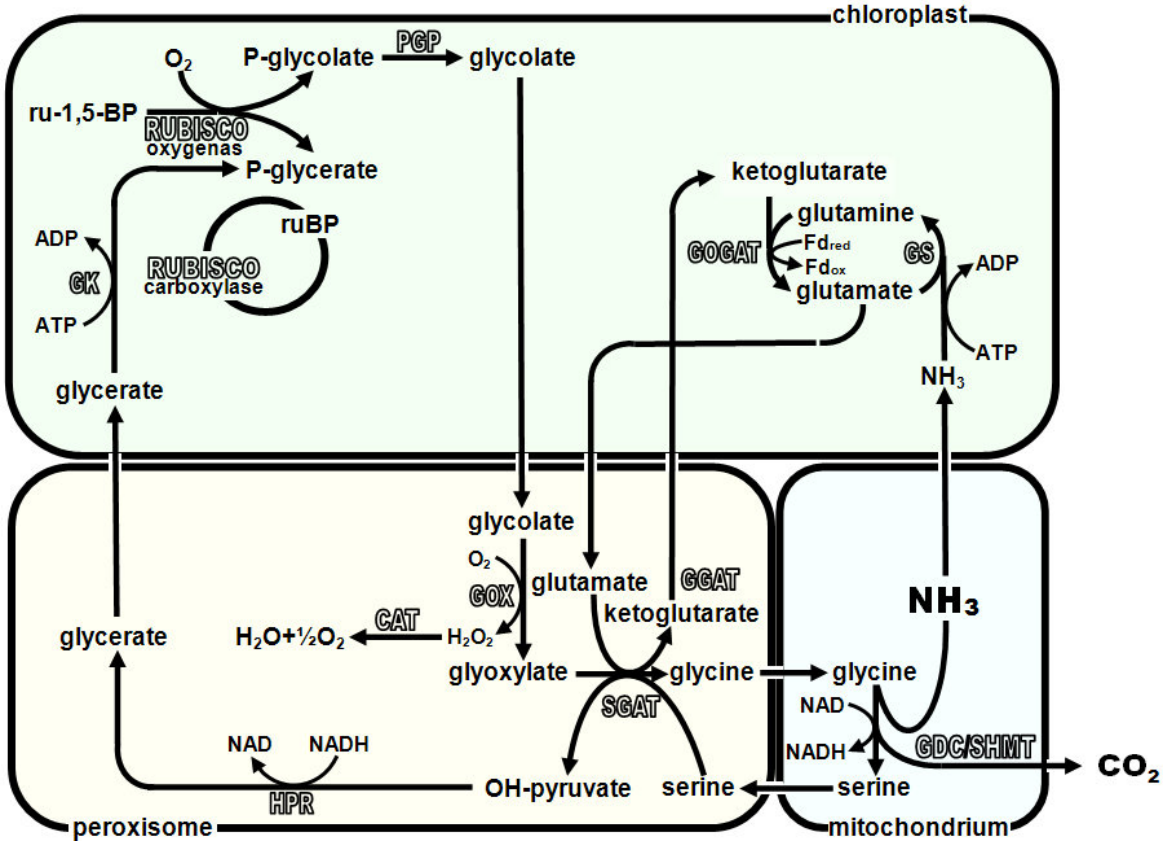

Figure 1.4: Representation of the photorespiratory pathway in C_3 plants
In this pathway oxygenation of RuBP by Rubisco oxygenase results in the formation of one molecule of PGA and one molecule of PG. PGA enters in the Calvin Benson cycle to form carbohydrates and also to regenerate RuBP. PG is processed to form PGA in a reaction sequence occurring in the chloroplast, peroxisomes and mitochondria. PG is converted to glycolate by PGP. Glycolate is transported from the chloroplast into the peroxisome where it is oxidized by GO enzyme to form glyoxylate. Glyoxylate is then converted to glycine by GGAT. Glycine is internally transported to the mitochondria where it is decarboxylated to form serine by GDC/SHMT. The formed serine is transported back to the peroxisome

where it is converted to hydroxypyruvate by SGAT. Hydroxypyruvate is then converted to glycerate by HPR. Glycerate is then transported to the chloroplast where it is converted to PGA by GK, Rubisco = Ribulose-1, 5-bisphosphate carboxylase/oxygenase, PGP = phosphogycolate phosphatase, GOX = glycolate oxidase, CAT = Catalase, GGAT = glyoxylate/glutamate amino transferase, GDC/SHMT = glycine decarboxylase/serinehydroxymethyl transferase, SGAT = serine/glutamate amino transferase, HPR = Hydroxy-pyruvatereductase, GK = glycerate kinase, GS = glutamine synthetase, GOGAT = glutamate synthase.

The glyoxalate is then transaminated to glycine in a reaction including glutamate by the enzyme glyoxalate/glutamate amino transferase (GGAT) by catalyzing the transfer of an amino group. Glycine is transported into mitochondria where it forms serine after decarboxylation and this is mediated by the enzyme glycine decarboxylase/serine hydroxymethyl transferase (GDC/SHMAT). GDC/SHMAT liberates CO_2 and ammonia. Ammonia from mitochondria is transported to the chloroplast where it is used by glutamine synthase (GS) for the catalysis of conversion of glutamate to glutamine. The glutamate oxoglutarate amino-transferase (GOGAT) catalyzed for the conversion of 2-oxoglutarate into glutamate. Glutamate is the amino donor for the glutamate amino transferase in the peroxisome (Sharkey, 2001). The serine formed in mitochondria is transported back to the peroxisome, where it is converted to hydroxyl-pyruvate by serine/glutamate aminotransferase enzyme (SGAT). Glycerate is formed after reduction of hydroxy-pyruvate by enzyme hydroxpyruvate reductase (HPR). Glycerate is phosphorylated in the chloroplast by enzyme glycerate kinase (GK) to 3-phosphoglycerate that reenters into Calvin cycle. The energy cost of the whole pathway is ATP and the reducing power.

1.4 The C_4 photosynthesis

The C_4 pathway is a striking example of convergent evolution, having evolved independently at least 62 times in the angiosperms, and is found in both monocotyledonous and dicotyledonous species (Sage, et al., 2011). In figure 1.5 represents three types of photosynthesis which are dependent on the type of decarboxylating enzyme. C_4 photosynthesis created by nature ~ 20 to 30 million years ago and C_4 plants dominates grassland floras and biomass production in the warmer climates of the tropical and subtropical regions (Edwards, et al., 2010). C_4 plants have many advantages over C_3 species that promote ecological success in warm and latitude habitat. C_4 plants are more productive than C_3 plants as they exhibit more water and

nitrogen efficiencies than C_3 plants and as a result they show increase production of dry biomass (Brown 1999).

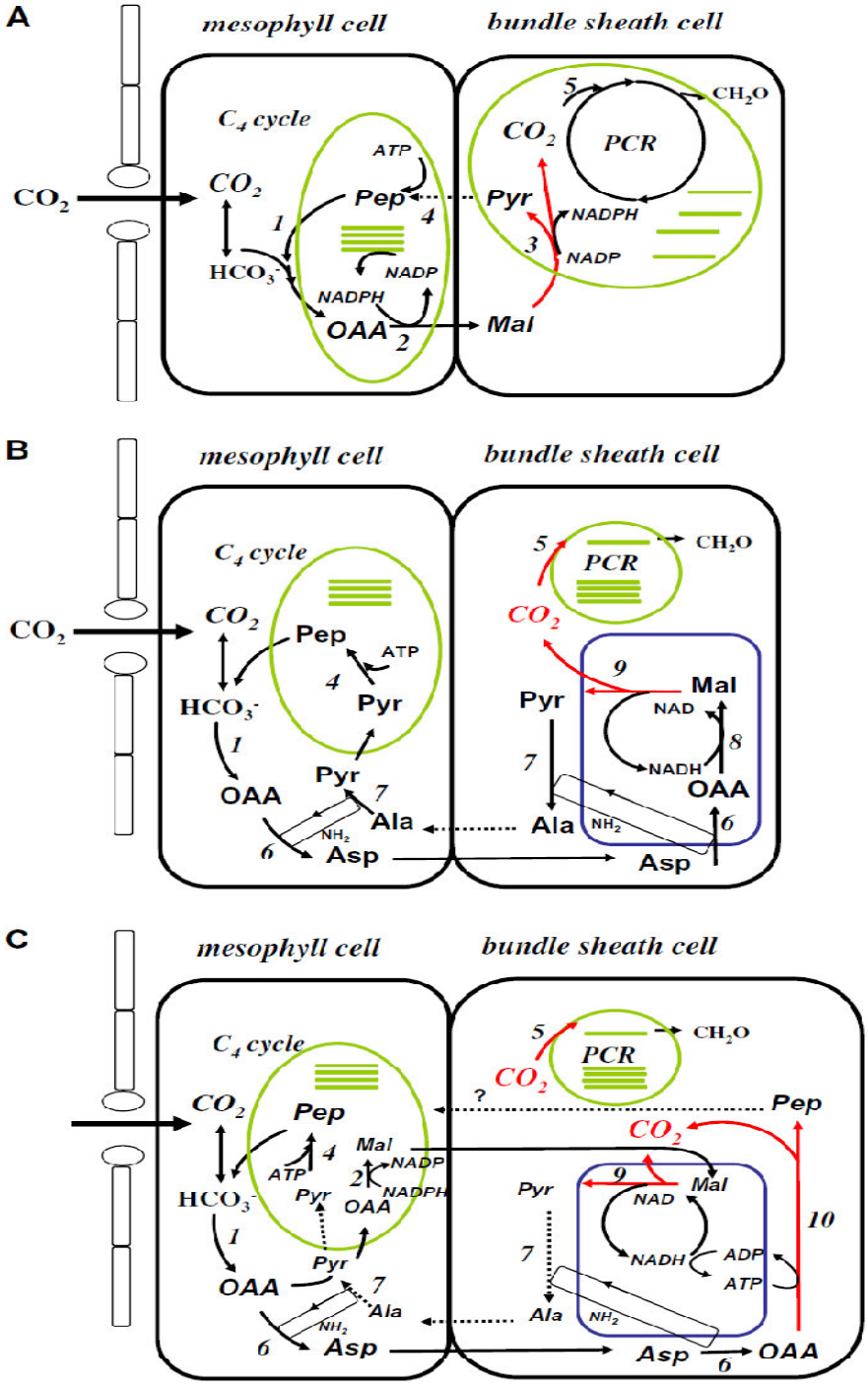

Figure 1.5: Schematic representations of different types of C_4 photosynthesis
Different type of C_4 photosynthesis is dependent on the types of decarboxylating enzymes: (A) NADP-ME; (B) NAD-ME; (C) PEPCK-type. Abbreviations of the metabolites: PEP = phospho*enol*pyruvate; OAA = oxaloacetate; Asp = Aspartate; Ala = Alanine; Pyr = Pyruvate; Mal = Malate; Chloroplast/thylakoid = Green; Mitochondria = Blue: Decarboxylation reaction = Red. The enzymes in metabolic pathways are numbered as follows: (1) phospho*enol*pyruvate (PEP) carboxylase; (2) NADPH-malate dehydrogenase; (3)

NADP-malic enzyme; (4) pyruvate Pi-dikinase; (5) Rubisco; (6) aspartate amino-transferase; (7) alanine aminotransferase; (8) NAD-malate dehydrogenase; (9) NAD-malic enzyme; (10) phospho*enol* pyruvate (PEP) carboxykinase (Furbank, 2011).

In C_4 photosynthesis, CO_2 is fixed by the enzyme phospho*enol*pyruvate carboxylase (PEPC; EC 4.1.1.31) and forms a four carbon compound oxaloacetate and because of the formation of a four carbon compound it is called C_4 photosynthesis. C_4 plants possess a characteristic leaf anatomy with two different rings of photosynthetic cells; one inner ring is formed by bundle sheath cells (BSC) and another outer ring of mesophyll cells (MS). The MS and BSC are connected by plasmodesmata. This peculiar anatomy of cells is called Kranz anatomy (Hatch, 1992). This is the most advantageous function of C_4 pathway which makes the concentration of CO_2 higher for Rubisco and therefore it limits the photorespiration. C_4 plants have been divided into three subgroups based on differences in the enzymes of the decarboxylation step. Common to all is the initial fixation of HCO_3^- by PEP carboxylase (EC 4.1.1.31) to form oxaloacetate in the mesophyll cell cytoplasm. In NADP-ME type, oxaloacetate (OAA) can either enter into the chloroplast of mesophyll cells and is reduced to malate by NADP-malate dehydrogenase otherwise in NAD-ME and PEPCK type cells OAA is converted in the cystol to aspartate catalyzed by aspartate aminotransferase and later transported to the bundle sheath cell (Kanai and Edwards, 1999). Using aspartate aminotransferase, aspartate is converted into OAA in bundle sheath cells.

In PEPCK type, most of the OAA is converted to PEP catalyzed by enzyme the PEP-carboxykinase. NADH used by NAD malic enzyme for oxidative phosphorylation and generate ATP for PEP carboxykinase. NAD-ME might play role to balancing the amino group between the compartments via the return of alanine to the mesophyll compartments (Furbank, 2011). Released CO_2 in the bundle sheath cell is then fixed by Rubisco and continue the pathway for the formation of carbohydrates. After decarboxylation reaction phospho*enol*pyruvate is formed which is inorganic CO_2 acceptor. In NADP-ME type the pyruvate transported again to the chloroplast of mesophyll cell, where phosphorylation is done by the pyruvate orthophosphate dikinase (PPDK) to form phospho*enol*pyruvate. PEP transported to the cystosol by PEP/phosphate translocator. Carbon fixation by PEPC and reduction of OAA to malate as well as regeneration of PEP from pyruvate; this cycle is also known as Hatch-Slack cycle. The segregation in MS and BS cell increased the CO_2 concentration up to 10 times higher compared to surrounding air and decarboxylation at site of RUBISCO resulted in least photorespiration (Carmo-Silva et al., 2008).

1.5 Single cell C_4 photosynthesis

Most terrestrial C_4 plants exhibit "Kranz anatomy" for the concentration of CO_2 around the Rubisco (Hatch, 1987; Sage, 2004). However, in recent years, several terrestrial and aquatic plants have revealed C_4 photosynthesis without any segregation in between two cell types BSC; MC (Kranz anatomy) but both cycle operate within a single cell (Voznesenkay et al., 2001, Edward et al., 2004; Park et al., 2010) e. g. Chenopodiaceae (*Bienertia cyclopeter, suaeda aralocaspia, Bienertia sinuspersici*), *Hydrilla verticilliata* L. f Royle etc.

Hydrilla verticilliata is a single cell C_4 type photosynthetic plant. It is an aquatic monocot facultative C_4 plant (Reiskind, 1997; Rao et al., 2002; Bowes, 2002). It typically exhibits C_3 photosynthesis characteristics but if atmospheric temperature increases and the external CO_2 concentration decline it shifts from the C_3 towards to the C_4 pathway. It shows C_4 system and Calvin cycle in a single cell (Magnin et al., 1997). In the C_4 state, CO_2 from ambient air and initial fixation of HCO_3 by PEP carboxylase forms the four carbon compound oxaloacetate which is transported to the chloroplast and reduced by malate dehydrogenase to malate and it is then decarboxylated by NADP-dependent malic enzyme (Salvucci and Bowes, 1983; Magnin et al., 1997) which makes a steep increase the concentration of CO_2 at the vicinity of Rubisco (Reiskind et al., 1997). In the *Hydrilla verticillata* the CO_2 compensation point is ~ 15 ml CO_2/l in the C_4 stage and 45-50 ml/l in the C_3 stage (Magnin et al., 1997).

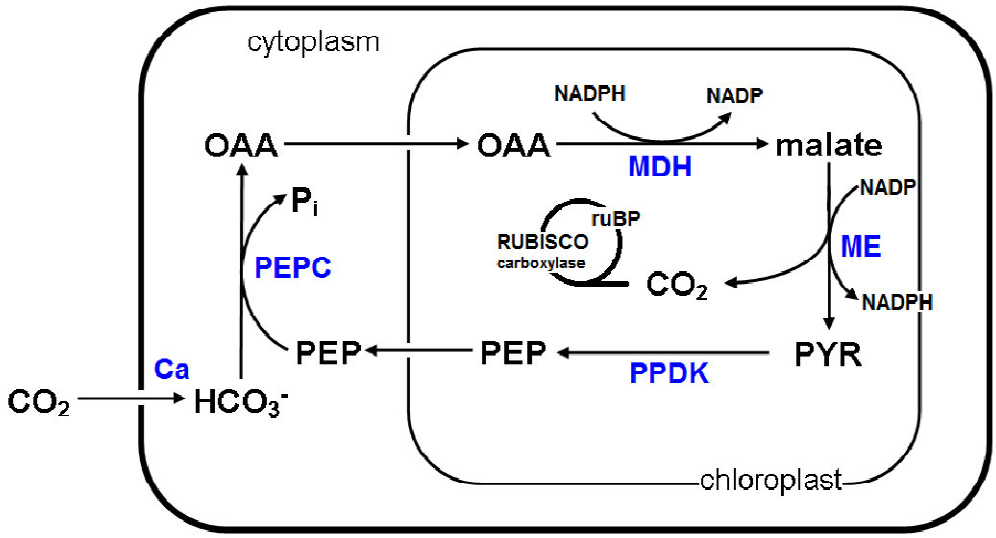

Figure 1.6: "Single cell C_4 photosynthesis" in *Hydrilla verticilliata*

Figure 1.6: The suspected C_4 system in *Hydrilla verticillata* and the localization of key enzymes is shown in fig.1.6. Inorganic carbon is fixed by a carbonic anhydrase (CA) in the form of HCO_3^-. Phosphoenolpyruvate (PEP) forms an oxaloacetate (OAA) by phospho*enol*pyruvate carboxylase (PEPC). This reaction needs inorganic phosphate and ATP. OAA is then transported in to the chloroplast and by malate dehydrogenase (MDH) forms a malate, which is then decarboxylated by a NADP-dependent malic enzyme (ME) form a pyruvate (PYR). A pyruvate orthophosphate dikinase (PPDK) catalyzes the conversion of pyruvate to phospho*enol*pyruvate (PEP), which is again used for the new cycle after transported into the cytoplasm.

1.6 The Crassulacean Acid Metabolism (CAM) photosynthesis

CAM plants use a different strategy to fix CO_2 because these kinds of plants specially grow in dry climate. In these plants, chloroplast containing cells fix CO_2 at night using phospho*enol*pyruvate carboxylase (PEPC) in the cystosol (Cushman, 2001; Cushman and Bohnert, 1997) and the resulting malate accumulates during the night in the vacuole. Subsequently, next day when stomata are closed for preventing the excess loss of water, these organic acids (malate) are decarboxylated by cystolic NADP-ME and create an internal CO_2 source for the Rubisco in the chloroplast. The photosynthetic carbon reduction cycle forms carbohydrates after fixing the internal CO_2. Thus, CAM plants have temporal separation different than spatial separation of C_4 plants. At night, when CO_2 enters into the cytoplasm and meets PEP at this time, CAM plants synthesize the protein PEP carboxylase kinase which is inhibited by malate and high temperature. PEPC kinase phosphorylates PEPC and this phosphorylation makes the enzyme more efficient to catalyze the formation of oxaloacetate which is reduced to malate by malate dehydrogenase. Malate is then stored in the vacuole (Hatch and Slack, 1968; Burnell and Hatch, 1985; Matsuoka et al., 1993; Chastain et al., 2002). During the day time malate forms pyruvate after decarboxylation by malic enzyme or PEP carboxykinase, then the released CO_2 is used by the Rubisco in Calvin cycle. Pyruvate is then transported back to the chloroplast from the cystosol where it is converted to PEP by pyrvate orthophosphate dikinase (PPDK). Finally PEP is converted to 3PGA for the carbohydrate biosynthesis. Generalized carbon fluxes and key regulatory enzymes contribute to CAM plasticity during light and dark phases of the duel cycle of a NADP-ME, in starch accumulating CAM plants such as *M. crystallinum*. Broken lines indicate several intermediates and enzymes between metabolites.

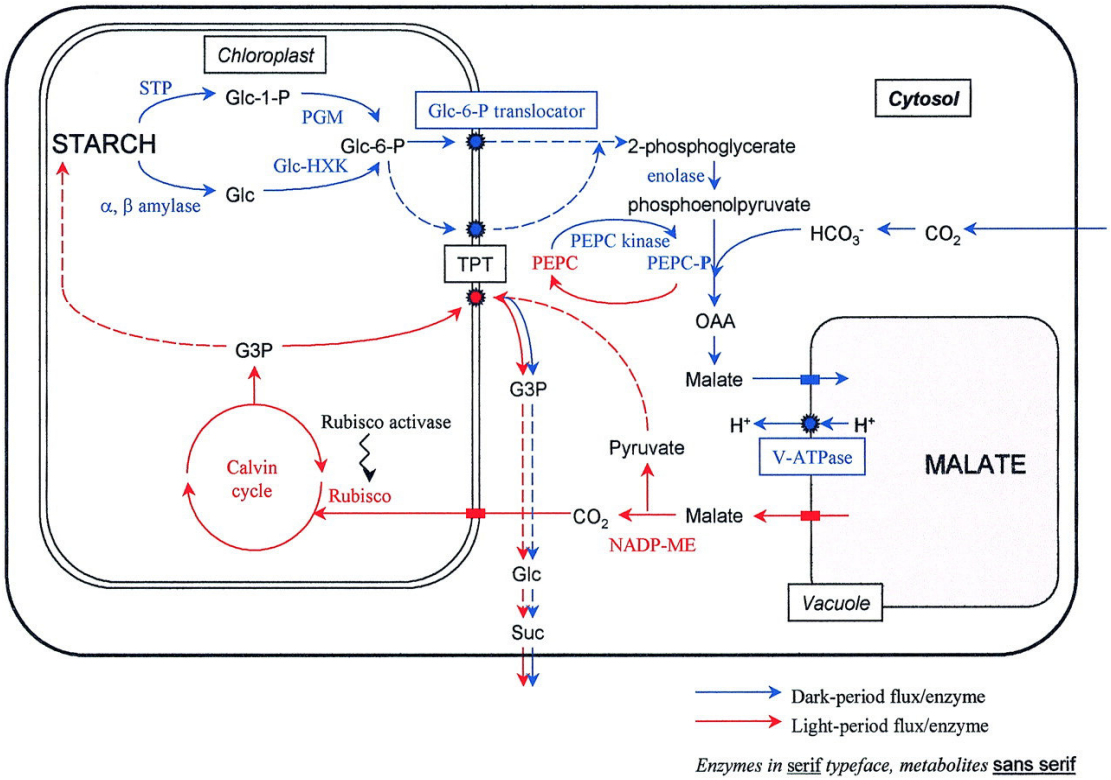

Figure 1.7: Schematic representation of CAM photosynthesis
At night, CAM plants open their stomata and fix the CO_2 in the form of HCO_3^- by PEPC. The resulting oxaloacetate is reduced by the MDH to malate and stored in the vacuoles. During the day, CAM plants close their stomata to water loss then conver the malate by NADP-ME to pyruvate. Then goes the CO_2 free used for the synthesis of carbohydrate in the Calvin cycle. Abbreviations: G3P = glycerate-3-phosphate; Glc = glucose; Glc-1-P = glucose-1-phosphate; Glc-HXK = glucose hexokinase; NADP-ME = NADP dependent malic enzyme; OAA = oxaloacetic acid; PEP = phospho*enol*pyruvate; PEPC kinase = phospho*enol*pyruvate carboxylase kinase; PEPC-P = PEPC in phosphorylated state; PGM = phosphoglucose mutase; STP = starch phosphorylase; TPT = triose phosphate translocator; V-ATPase = vacuolar H^+-ATPase (Dodd et al., 2001).

1.7 Approaches for improvement of photosynthetic carbon assimilation in C_3 plants

Increasing the photosynthetic efficiency in C_3 plants is one of the most demanding challenges for plant biochemists around the world due to the notorious inefficient carboxylating enzyme Rubisco which has a slow catalytic rate and makes the 'wasteful' reaction of photorespiration (Jordan and Ogren, 1984; Ogren, 1984; Brooks and Farquhar, 1985; Sharkey, 1988). There are many attempts have been made for improving photosynthesis by transfer of C_4 traits into C_3 plants by conventional hybridization between C_3 and C_4 plants e. g. *Panicum, Moricandia, Brassica* but most C_3-C_4 hybrids showed infertility because of abnormal chromosome pairing and/or genetic barriers (Matsuko et al., 2001). Nowadays plant genetic engineering has made developments to

introduce desired genes into C_3 plant for improving photosynthesis. There were many attempts to make "C_4 transgenic" C_3 plants.

1.7.1 Successful approaches for increasing photosynthesis

Reengineering rubisco of some of the varieties are more effective than others e.g. red algae species. Expressing the thermostable version of rubisco activase lead to increase in the biomass because the Calvin cycle is sensitive to higher temperature, So making some Rubisco intermediate capable to heat could increase the capacity of Rubisco (Whitney et al., 2011; Kurek et al., 2007). Bypassing the photorespiration by introducing bacterial glycolate oxidizing pathway into the chloroplast (Kebeish et al., 2007; Carvalho et al., 2011) introducing glyoxylate carboligase from *E. coli* and hydroxypyruvate isomerase from *E. coli* was earlier employed. Over expression of seduheptulase bisphosphtase (SBPase) in tobacco and rice showed improved photosynthesis and accumulation of biomass (Tamoi et al., 2006). Expression of cyanobacterial carbonic anhydrase in tobacco increases photosynthesis rate (Lieman-Hurwitz et al., 2003). Engineering the PSII antenna size in *Chlamydomonas* shows increased growth at high light illumination beecause they can transmit more light and are less sensitive to photoinhibition (Beckmann et al 2009). Expressing PEPC from *Corynebacterium glutamicum* and NADP-ME from *Flaveria pringlei* in potato showed enhancement of electron requirement (e/A) for CO_2 Häusler assimilation at higher temperature and also increased respiration in dark (Lipka et al., 1999; et al., 1999, 2001). Expression of C_4 specific PEPC and PPDK from maize, NADP-MDH from Sorghum and C_3 specific NADP-ME from rice show slightly higher CO_2 assimilation rate than wild type plants (Taniguchi et al., 2008). Over expression of either *Chlamydomonas* Sedoheptulose-1,7-bisphosphtase (SBPase)/*cyanobacteria* Fructose-1,6-bisphosphtase-(FBPase) or plant SBPase in tobacco resulted in increased photosynthetic CO_2 fixation and growth (Miyagawa et al., 2001; Lefebvre et al., 2005).

All these approaches showed limited success to get higher biomass in C_3 plants but showed improvement by manipulating Calvin cycle using heterologus genes because each of these approaches give us new information for the behaviour of the foreign gene. Interestingly the expression of the same enzyme in different ways shows different

consequences. Apparently all these approaches of installing C_4 cycle genes in C_3 plants have not succeeded completely for the production of higher biomass.

1.7.2 Unsuccessful approaches to expressing C_4 enzymes in C_3 plants

Using single or multiple C_4 genes in the C_3 plants give us an idea about the role of an individual enzyme in transgenic plants. Expressing maize C_4 specific PEPC in tobacco increased PEPC activity compare to the wild type tobacco but transcripts and protein level were very less. The Table below shows C_4 enzymes in C_3 plants with increased activity in leaves of transgenic C_3 plants. These observations give us a direction for future transformation of C_4 traits into C_3 plants.

Table 1: Approaches to expressing C_4 enzymes in C_3 plants

C_4 enzyme (Location)	**Host C_3 plant**	**Promoter**	**Highest[a] activity (In fold)**	**Physiological effect**	**Positive effect (Growth, compensation point)**	**References**
PEPC[b] *Z. maize*	Tobacco	*Nicotiana cab*	2.2	Higher PEPC activity in leaves, lesser activity of rubisco, lesser photosynthetic rate	Slower growth	Hudspeth et al., (1992)
PEPC[b] *Z. maize*	Rice	*Z. maize*	110	Reduced O_2 inhibition of photosynthesis and photosynthetic rate	No effect	Ku et al., (1999)
PEPC[b] *Corynebacterium gene*	Potato	*35SS (CaMV)*	5.4	Acceleration stomatal opening	Slower growth	Gehlen et al., (1996)
PEPC[b] *Z. maize*	Potato	*35SS (CaMV)*	2.4	Chlorophyll content lower	Slower growth	Kogami et al., (1994)
PEPC[b] *S. tuberosum*	Potato	*35SS (CaMV)*	2.8	Stimulation of NADP-ME, Increased carbon flow to amino acid.	compression of internode	Häusler et al., (2001)
NADP-MDH[b] *(S. vulgare)*	Tobacco	*35SS (CaMV)*	3	Higher malate	Not determined	Gallardo et al., (1995)
AspAT[b]	Tobacco	*35SS (CaMV)*	3.1	PEPC and mAspAT increased	Not determined	Sentoku et al., (2000)
NADP-Me *F. pringlei*	Potato	*35SS (CaMV)*	7.1	Reduced electron requirement for fixation of CO_2	Not determined	Lipka et al., (1999)
NADP-Me[c] *O. sativa*)	Rice	*Rice cab*	5	No effect	No effect	Tsuchida et al., (2001)
NADP-Me[c] *Z.* maize	Rice	*Rice cab*	30	Chlorosis, lower CO_2 assimilation	Inhibition	Tsuchida et al., (2001)
NADP-ME[c]	Rice	*Rice cab*	70	Less PSII activity, lesser chlorophyll content & abnormal chloroplast	inhibition	Takeuchi et al., (2000)
PEP-CK[c] (*U. panicoides*)	Rice	*PEPC (Z. maize)*	0.5[d]	Change in carbon flow in mesophyll cells	No effect	Suzuki et al., (2000)
PPDK[b] (*Z. mays*)	Arabidopsis	RbcS (*A.thaliana*)	2.4	No influence on photosynthetic parameters	Not determined	Ishimaru et al., (1997)
PPDK[b] (*Z. mays*)	Arabidopsis	35SS (CaMV)	4	No influence on photosynthetic parameters	Not determined	Ishimaru et al., (1997)
PPDK[b] (*Z. mays*)	potato	Enhanced 35SS (CaMV)	5.4	Lesser pyruvate More malate	No effect	Ishimaru et al., (1998)

PPDK[b] (*Z. mays*)	Rice	Rice cab	5	Supression of photosynthesis,Photores-piration increases	No effect	Fukayama et. al.,(2003)
PPDK [b] (*Z. mays*)	Rice	Maize intact	40	Increased respiration, change in stomatal movement, photosynthesis decrease	No effect	Fukayama et. al., (2000)
PEPCK (*S. meliloti*)	Tobacco	35SS (CaMV)	35[d]	No effect	No effect	Häusler et al., (2001)

(Matsuoka et al., 2001)

a- Highest activity in primary transgenic plants.
b- Mesophyllic C_4 enzymes.
c- C_4 Enzyme from bundle sheath cells.
d- Determined enzyme activity in isolated chloroplast.

1.8 Increasing regenerative capacity of the Calvin cycle

Improvement of the photorespiration cycle is not just about increasing CO_2 fixation but should also aim to increase both nitrogen use efficiency and water use efficiency while maintaining high productivity. Author C. A. Raines (2011) explained, in C_3 cycle, the different phases are depending on the characteristics of enzymes like enzymes of the regenerative phase in the cycle could possible to target in determining the rate of photosynthesis. Eight enzymes are involved in the regeneration of the CO_2 acceptor RuBP (Figure 1.8).

Enzyme Sedoheptulose-1,7-bisphosphatase (SBPase), Transketolase (TK) und Aldolase probably the targets for improving C_3 cycle flux (Harrison *et al*., 1998; Haake *et al*., 1998; Henkes *et al*., 2001; Raines, 2003). Certainly, overexpression of either a bifunctional SBPase/FBPase from cyanobacteria or plant SBPase in tobacco plants resulted in increased photosynthetic CO_2 fixation and growth upto 30% and also shows larger leaf surface and higher growth rates during the early development stage. In apposite to the tobacco increasing the SBPase activity in rice did not show any higher biomass or photosynthesis. However, if the plants were exposed to heat or salt stress conditions, photosynthesis rates in the transgenic plants with increased SBPase plant were higher compare to wild type plants. So this might be concluded that increasing photosynthesis and biomass by manipulation of SBPase is likely to be dependent not only on species but also on growth conditions (Feng et al., 2007a; Miyagawa et al., 2001; Lefebvre et al., 2005). Increase in photosynthesis could be applied to an increase in the capacity to regenerate the CO_2 acceptor molecule RuBP, observed after analysis of these plants in CO_2 response curve. Overexpression of TK with SBpase or without shows stunted and chlorotic phenotype. This chlorotic phenotype could be increasing TK activity and

influence the balance of export of carbon from the C_3 cycle. This concluded that reduction of TK activity related with the decrease in carbon flow from the C_3 cycle to the shikimate pathway (Henkes et al., 2001; Raines, 2011).

Therfore, most of these observations help to assimilate possible goal for CO_2 concentarion and also acknowledge flux from the Calvin cycle. However, making multigene pathways could support the regenerative phase enzymes for getting more clear idea of regenerative capacity of C_3 cycle or altering the photorespiration could improve the suitable environment for Calvin cycle.

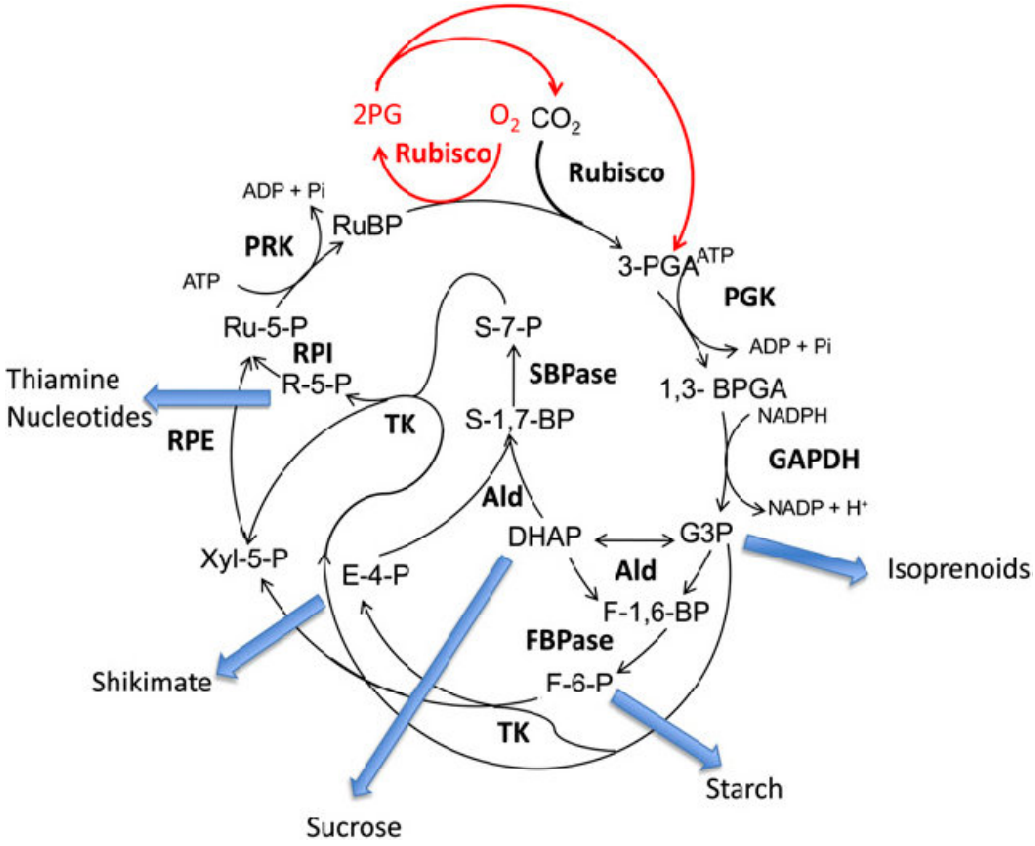

Figure 1.8: Regenerative enzymes in Calvin cycle
The carboxylation reaction catalyzed by Rubisco fixes CO_2 into the acceptor molecule RuBP forming 3-PGA. The reductive phase of the cycle follows with two reactions catalyzed by 3-PGA kinase (PGK) and GAPDH, producing G-3-P. The G-3-P enters the regenerative phase catalyzed by aldolase (Ald) and either FBPase or SBPase, producing Fru-6-P (F-6-P) and sedoheptulose-7-P (S-7-P). Fru-6-P and sedoheptulose-7-P are then utilized in reactions catalyzed by TK, R-5-P isomerase (RPI), ribulose-5-P (Ru-5-P) and epimerase (RPE) and producing Ru-5-P. The final step converts Ru-5-P to RuBP, catalyzed by PRK. The oxygenation reaction of Rubisco fixes O_2 into the acceptor molecule RuBP, forming PGA and 2-phosphoglycolate (2PG) and the process of photorespiration (shown in red) releases CO_2 and PGA. The five export points from the pathway are shown with blue arrows (Raines, 2011).

1.9 Expression of bacterial glycolate pathway in C_3 plants

Glycolate is the primary product of the oxygenase activity of Rubisco and many bacteria and algae have been investigated for the metabolism of glycolate. The metabolic pathway of glycolate from *E. coli* was described earlier in detail (Kornberg and Sadler, 1961; Hansen and Hayashi, 1962; Lord, 1972; Pellicer et al., 1996). *E. coli* adapted to grow on glycolate as sole carbon source. The metabolism of glycolate in *E. coli* is done by an oxidation reaction of glycolate catalyzed by glycolate dehydrogenase (GO), a multi protein complex that is capable to oxidize glycolate to form glyoxylate in an oxygen independent manner so this enzyme is also called as glycolate dehydrogenase (GDH). Glycolate dehydrogenase has three subunits that are encoded by three different open reading frames called glcD, glcE and glcF which are located in the glc operon of *E. coli* (Lord, 1972; Pellicer et al., 1996). In the next stage glyoxalate is metabolized by two divergent condensation reactions. In one reaction glyoxalate condenses with an acetyl group provided by acetyl coenzyme A and forms malate after catalyzing by malate synthase. The other reaction condenses two molecules of glyoxylate catalyzed by glyoxalate carboligase (GCL) and forms tartronic semialdehyde and CO_2 (Chang et al., 1993). Tartronic semialdehyde is reduced to glycerate by tartronic semialdehyde reductase (TSR) and subsequently phosphorylated to glycerate-3-phosphate by glycerate kinase (Gotto and Kornberg, 1961). A similar pathway as a photo respiratory cycle is found in some green algae and cyanobacteria (Nelson and Tolbert, 1970; Ramazanov and Cardenas, 1992). In this case, glycolate oxidation is catalyzed by glycolate dehydrogenase which is located in the mitochondria.

The further metabolism of glycolate seems to be like the same way as in the peroxisomes of higher plants (Stabenau et al., 1984; Igamberdiev and Lea, 2002). Installed glycolate oxidising pathway from *E. coli* in the chloroplast of *Arabidopsis thaliana* can increase the efficiency of photosynthesis and biomass production (Kebeish et al., 2007; Leegood, 2007). This pathway was aiming to suppress the photorespiration for improving the CO_2 fixation in the C_3 plant for higher biomass. The pathway includes three enzymes GDH, GCL, and TSR in the chloroplast for the metabolism of glycolate formed by the oxygenase activity of Rubisco to the glycerate (Fig. 1.9). This pathway bypasses the whole wasteful pathway of photorespiration in some percentage by avoiding the channel of metabolites through the mitochondria to peroxisome. The CO_2 is released at the time of ligation of two

molecules of glyoxylate catalyzed by GCL to form tartronic semialdehyde. This adds to the benefit of increasing the concentration of CO_2 in the vicinity of Rubisco, resulting in a reduction of oxygenase activity and hence photorespiration.

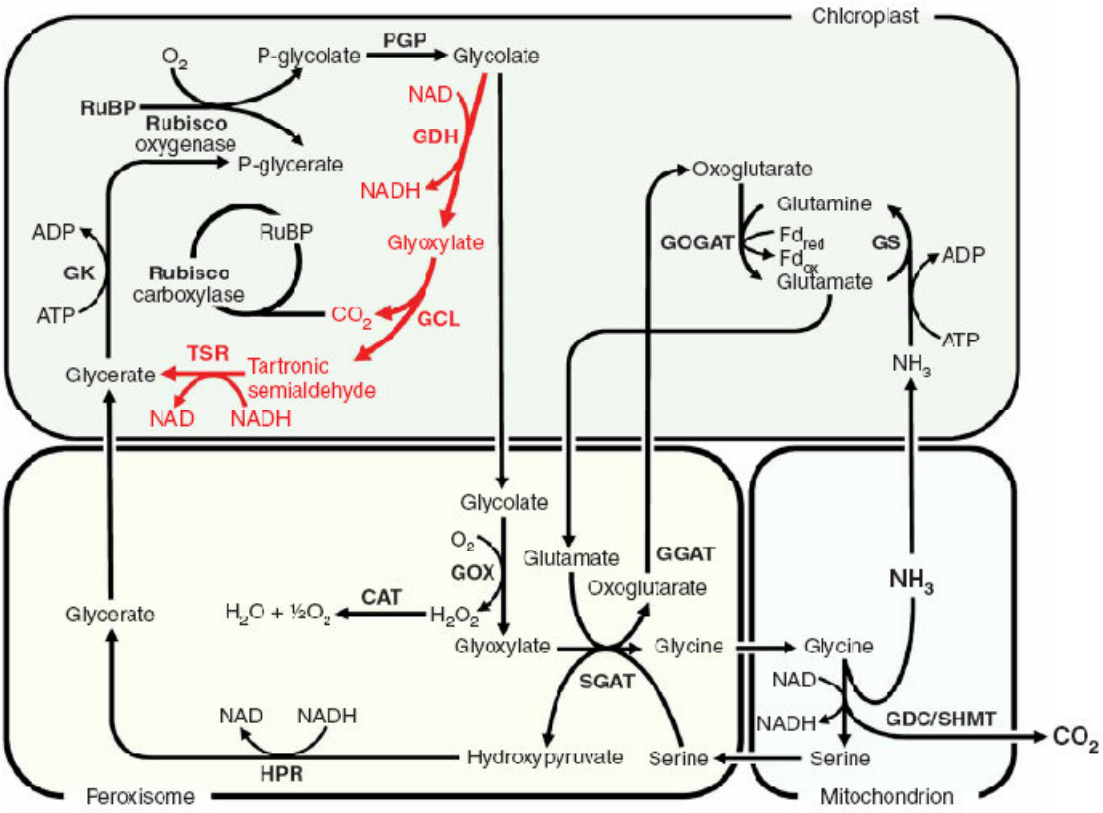

Figure 1.9: Representation of the photo respiratory pathway (black) in C_3 plants and the proposed pathway (red) for the conversion of glycolate to glycerate
PGP = phosphoglycolate phosphate; GDH = glycolate dehydrogenase; cTP-AtGDH = *A. thaliana* glycolate dehydrogenase fused to a chloroplast transit peptide (cTP); GCL = glyoxylate carboxyligase; TSR = tartonic semialdehyde reductase; GK = glycerate kinase (photo respiratory enzyme described in Introdution chapter 1.3 (Kebeish et al., 2007).

The oxygenase reaction of Rubisco results in the formation of P-glycerate and P-glycolate. Phosphoglycolate forms glycolate after being dephosphorylated by PGP. Glycolate is oxidized by GDH to form glyoxylate. Two molecules of glyoxylate are condensed by GCL forming tartronic semialdehyde and CO_2 released in the chloroplast. Tartronic semialdehyde is then reduced by TSR forming glycerate. Glycerate is phosphorylated by GK to form P-glycerate that is used directly for carbohydrate biosynthesis by the Calvin cycle. This approach to bypass photorespiration by introducing the *E. coli* glycolate pathway gives big potential advantages; first to reduce the photorespiration CO_2 loss by modifying the metabolic pathways of the products resulting from the oxygenase reaction

of Rubisco but release the CO_2 in the chloroplast, and the second advantage being that the bacterial pathway does not release NH_3, which reduce the consumption of energy for the metabolism of NH_3 and most important, this pathway does not consume ATP like C_4 pathway where ATP is used for regeneration of CO_2 acceptor molecule PEP.

1.10 The aim of the present study

An objective of this work was to optimize the CO_2 fixation in C_3 plants. Manipulation of the C_3 cycle offers an opportunity to increase photosynthesis and yield. Because most of our important crops, such as rice, wheat, soybean or potato are classified as C_3 plants and the first product of atmospheric CO_2 fixation is the 3-phosphoglycerate (3PGA), which is formed in the Calvin-Benson cycle by only one CO_2 acceptor molecule Rubisco in the chloroplast stroma. However, at the active site of Rubisco CO_2 and O_2 compete each other for fixation (Chen and Spreitzer, 1992; Jordan and Ogren, 1984) which results in a loss of up to 50% of the carbon because metabolisation of phosphoglycolate, the byproduct of oxygenase reaction loose CO_2, ammonia and ATP for the regeneration of 3-phosphoglycerate in the notorious process photorespiration. In the present work, our aim is to get higher concentration of CO_2 around the vicinity to Rubisco for higher photosynthesis and higher photosynthesis might results into more biomass in C_3 plant. Two different approaches are used in this study for the suppression of photorespiration. In one approach installed the "Single cell C_4 mechanism like *Hydrilla verticilliata*" into the tobacco and in the another approach installed the multigene pathway for the bypass the photorespiration activity in higher amount in the transgenic C_3 plant with already installed *E. coli* glycolate pathway. Both pathways intend to inhibit the oxygenase activity and increase the concentration of CO_2 in the environment of Rubisco. To achieve our aim for these both multigenes metabolic pathways used the MultiRound Gateway technology which simultaneously cloned the multiple DNA fragments (Expression cassette) in a versatile format for the transformation into the plant genome.

2 Materials and Methods

2.1 Materials

2.1.1 Chemicals and consumables

The chemicals used throughout the work were purchased from the following companies: Amersham Pharmacia Biotech (Freiburg), BioRad Laboratories GmbH (München), Calbiochem (Bad Soden), Carl Roth GmbH (Karlsruhe), Eurogentec (Cologne), Hartmann Analytic (Braunschweig), Invitek (Berlin, Germany), Duchefa Biochemie (Haarlem, Netherlands), Invitrogen (Leck, Netherlands), KMF Laborchemie Handels GmbH (St. Augustin), Kodak (Stuttgart), Macherey-Nagel (Düren), MBI Fermentas (St. Leon-Rot), Metabion (Planegg-Martinsried), Molecular Probes (Leiden, Netherlands), New England BioLabs (Frankfurt), Novagen (Darmstadt), Pharmacia (Freiburg), Promega (Madison, USA), QIAGEN (Hilden), Roche Applied Science (Mannheim), Röhm (Darmstadt), Sigma (Taufkirchen), Serva (Heidelberg) Sigma ARK (Taufkirchen).

The consumables were obtained from: Agilent technologies, Applied Biosystems (Darmstadt), Biometra (Göttingen), BioRad Laboratories GmbH (München), Eppendorf (Hamburg), Fuji (Düsseldorf), GGA GmbH (Moers, Germany), Gibco BRL (Eggenstein), Greiner (Solingen), Hanna Instrument (Kehl, Germany), Heraeus (Osterode), Hewlett Packard (Germany), Herolab (Wiesloch) Kodak (Stuttgart), Kontron Instruments (München), Labomedic (Bonn), Leica (Heidelberg), LI-COR® Biosciences (Lincoln, USA), Merck (Darmstadt), Millipore (Eschborn), MWG Biotech (München), Pharmacia (Freiburg), Raytest (Berlin, Germany), Serva (Heidelberg), Schott Glaswerke (Mainz), Sorvall (Bad Homburg), Wissenschaftliche Technische Werkstätten (Weilheim), Whatman (Maidstone, UK).

2.1.2 Instruments

Instruments used in this study are listed in Table 2.1

Table 2.1: Used equipments and Accessories

Electroporater:
Gene pulserTM BioRad Laboratories Gmbh (Munich)

Photodocumentation:
Herolab UVT-20M Herolab (Wiesloch)
Gelelectrophoresis Appratus:
Agarose gel electrophoresis accessories Mechanical workshop of the Institute for BiologyI RWTH Aachen
pH-Meter :
Mechanical workshop, Weilheim
Photometer:
SmartSpec plus Spectrophotometer BioRad Laboratories GmbH (Munich)
Disposable cuvette Sarstedt (Nürnbrecht)
Cuvettes: Quartz glass cuvettes Hellma (Müllheim)
Real-Time-PCR System:
ABI Prism® 7300 Applied Biosystem (Darmstadt)
ABI Prism® 7300 SDS Software Applied Biosystem (Darmstadt)
Thermocycler and Thermoblock:
Biometra T personal Biometra (Göttingen)
MWG Primus 96 plus MWG Biotech (Munich)
PeqLab Primus 96 plus PeqLab (Erlangen)
GeneAmp®PCR System9700 Applied Biosystems (Darmstadt)
Centrifuge and Rotor:
Biofuge fresco Heraeus (Osterode)
Megafuge 3.0R Heraeus (Osterode)
Mikro 22 Hettich (Tuttlingen)
Sorvall RC 5 B Plus Sorvall (Bad Hamburg)
Rotar HFA 22.50 Heraeus (Osterode)
Optima L-100XP Beckman-Coulter (Fullerton, USA)
Rotor SW 41 Ti Beckman-Coulter (Fullerton, USA)
SpeedVac Eppendorf concentrator plus (Hamburg Germany)
Photosynthesis measurement:
Licor Li 6400 Licor Bioscience (Lincoln, USA)
Elisa Reader:
BioTek ELx808 BioTek (Vermont, USA)
Microscope:
Leica TCS SP Leica (Wetzlar)

2.1.3 Solutions, buffers and media

Most of the buffers, media and solutions were prepared as described in Sambrook and Russel, 2002 unless supplied with the kits. The pH for buffers was adjusted with 1M, 5M

and 10M NaOH and 1M and 5M KOH or 37 % HCl V/V. Sterilization of all solutions, buffers and media was achieved by autoclaving (20 min; 120°C, 1 bar) or, for thermolabile solutions, by filtration through 0.2 µm filters. Heat-sensitive components, such as antibiotics, were prepared as stock solutions, and added to the medium/buffer after cooling to 50°C. Buffers and media are listed in appropriate methods.

2.1.4 Different size markers for gel electrophoresis

The different size markers are used in this work as follows:

Table 2.2: Different size markers for gelelctrophoresis

Name	Company
λ-DNA/*Pst*I	MBI Fermentas (St. Leon-Rot)
1000 bp Marker	MBI Fermentas (St. Leon-Rot)
100 bp Marker	MBI Fermentas (St. Leon-Rot)
50 bp marker	MBI Fermentas (St. Leon-Rot)

2.1.5 Used kits

Throughout this work some reaction kits were used from various manufacturers. The exact names, manufacturers and purpose are shown in Table 2.3.

Table 2.3: Used Reaction kits

Company	Purpose
Invisorb® Spin PCRapace Kit Invitek (Berlin)	Purification of PCR and Restriction product
Invisorb® Spin PCRapace Kit Invitek (Berlin)	Purification of nucleic acid from agarose gel
QIAEX II® Gel Extraction Kit QIAGEN (Hilden)	Purification of nucleic acid from agarose gel
NucleoSpin® Plasmid-Kit Macherey-Nagel (Duren)	Plasmid Isolation
TOPO TA Cloning® Kit Invitrogen Topocloning of PCR (Leck NL)	Topo-cloning
Gateway®LRClonase®II Invitrogen(LeckNL)	MultiRoung Gateway cloning
Platinum®SYBR®Green Invitrogen qPCR Supermix-UDG with Rox (Leck, NL)	Real-Time PCR

2.1.6 Enzymes

Table 2.4: Enzymes used throughout the work

Name	Comapany
AntarcticPhosphtase	New England Biolabs (Frankfurt)
GoTaq-Polymerase	Promega (Mannheim)
Phire-Polymerase	Finnzymes/Fisher Scientific (Schwerte)
Phusion-Polymerase	Finnzymes/Fisher Scientific (Schwerte)
T4 DNA–Ligase	MBI Fermentas (St. Leon-Rot)
T4 DNA–Polymerase	MBI Fermentas (St. Leon-Rot)
Deoxyribonuclease I, RNAse free	MBI Fermentas (St. Leon-Rot)
Moloney Murine Leukemia Virus	Promega (Mannheim)
Reverse Transcriptase (M-MLV-RT)	MBI Fermentas (St. Leon-Rot)
Restriction enzymes	New England Biolabs (Frankfurt)

2.1.7 Synthetic oligonucleotide

The following primers (from Sigma and Metabion) were used for cloning, sequencing, multiplex PCR and qPCR of the genes required for the establishment of the novel pathways.

Table 2.5: Synthetic Oligonucleotide

3628_ME_FX2	ACGCGTTAGGTGCATGTTCTCATCCTACGCACTCG
3629_ME_RX2	TCTAGACTACCTGTAGCTGCGGTAGAC
3630_ME_F_NcoI	GCTACCATGGTAGGTGCATGTTCTCATCCTACGCACTCG
3811_MLE_F_DTOPO	CACCATGAAGGATGTAAGATTGCCAACACT
3812_MLE_R_DTOPO	GCCTAGTTTTTCGGCTTTAACTGTATTG
3813_pepc$_4$ nhei	ACTGGTGCTAGCTTAACCAGTGTTCTGCATGCCAGCAGCAATAC
3814_171_PPS_SEQ_F	CCTCCGATCACTCCAAAG
3815_171_PPS_SEQ_R	TTGTAGAGAGAGACTGGTGATTTTTG
3816_171_seq_pps_2	GCGAAATGAACCGCATCGAAC
3817_171_seq_pps_3	TCATTTCGCTGATGTCATGG
3818_171_pepc_seq_2	CGATAAGGCTCATGCGGAGGAATTTGC

3819_171_pepc_seq_3	GAGCCTTATCGAGTTGTACTTG
3862_MLUI_F_ANTI	CGAGCACGCGTATGAAGGATGTAAGATTGCCAACACTATT TGAA
3863_XBAI_ANTI_R	GACAGTCTAGATTAGCCTAGTTTTTCGGCTTTAACTGTA
3864_ASCI_PPS	ATCGGGCGCGCCCGGGGATTTATTTTATTTCTTC
3865_Fw1_PPS	GGAGTGTGAAGCAGTGAAACGTGTG
3866_Rev1_PPS	TGGACGGGATTTCACACATCATGATG
3867_Fw2_PPS	CGTGCATAAACCGACACTGGCGG
3868_Rev2_PPS	GCAGGAACAGCGTGACATCTTCTC
3869_Rev3_PPS	GTTCTCGCCACGTTTCAGCCCCT
3937_CCA1_MP_TP_NCOI_ R	GAGCCCATGGGGATCCCACTAAGCTCCTCTAC
3938_CCA1_MP_TP_ASCI_ F	CGACGGCGCGCCAAGCTTCTTCTCGGCATGGAAC
3939_L700_MLUI_5U	GACGACGCGTCTTTTTCTTCTTTTGCTCTCACTACTTAGTAT G
3940_L700_ASCI_3´	GCAGGGCGCGCCAATTCCCAAGTTTTTTTGTTGTTTCTATC
3951_cca1_n_F2	TCTTAAATTCGTCCCGCCAATCTGTCCC
3952_cca1_n_R1	ACGTGGCGGACGTAGAGACGATCTTGGAG
3953_cca1_n_F1	GTGTGAGAATAGCGCGTGTAG
3980_me_Gbanii_s	AGCAGGGGCCCTATATCAGCTGGTACATTGCCGTAG
3981_me_Gmlui_s	GACAACGCGTGCGATCGCTACGTACCTGCAGTACAAG
3982_me_sapi_s	ACGGGCTCTTCGGCGATCGCTACGTACCTGCAGTACAA
3983_me_bamh1_eco31i_r	AGCGAGGTCTCGGATCCTCGTGGCGCGCCGCGGACTCTAG ATTAG
3984_MLE_BAMH1_R_M	GACACGGATCCTTGCGGACTCTAGATTAGCCTAGTTTTTC
3985_MLE_mlu_m_F	GACGAACGCGTCGTATGAAGGATGTAAGATTGCCAACACT
3986_PEP_ECORI_M_F	ACGACGAATTCTCCTCCTAAGTATCTAAACCATGGGCAAC
3987_PEP_BAMHI_M_R	ACGAAGGATCCCCTTATTTCTTCAGTTCAGCCAGGCTTA
3988_LDHa_mlui_F_M1	GCACGACGCGTATGGCAACCCTCAAGGACCAGCTGAT
3989_LDHa_bamhi_m2_R	ACGACGGATCCACTCTAGAACTGCAGCTCCTTCTGGATT
3990_pps_eco31i_oh	AACTGAGGTCTCCCATGTCCAACAATGGCTCGTCACCGCTG GTG
3991_PEPC_MLUI_M_R	ACGCGTTAGCTTAACCAGTGTTCTGCATGCCAGCAGCAAT
3992_PEPC_BCLI_MF	CGCTTTGTTCCTGCGGTTATCAAC
3993_PEPC_BCLI_MR	CAATTGGTTAATCACCGCAGGAACAAAGCGATC
3994_PEPC_MLUI_M_R	ACGCGTTAGCTTAACCAGTGTTCTGCATGCCAGCAGCAAT
3995_pTRAK_MDH5	CCTCCACGCCCAAATTAATG
3996_MLE_BAMHI_R	GACGGATCCTTTGCGGACTCTAGATTAGCCTAGTTTTTC

3980_me_Gbanii_s	AGCAGGGGCCCTATATCAGCTGGTACATTGCCGTAG
3981_me_Gmlui_s	GACAACGCGTGCGATCGCTACGTACCTGCAGTACAAG
3982_me_sapi_s	ACGGGCTCTTCGGCGATCGCTACGTACCTGCAGTACAA
3983_me_bamh1_eco31i_Mr	AGCGAGGTCTCGGATCCTCGTGGCGCGCCGCGGACTCTAG ATTAG
3984_MLE_BAMH1_R_M	GACACGGATCCTTGCGGACTCTAGATTAGCCTAGTTTTTC
3985_MLE_mlu_m_F	GACGAACGCGTCGTATGAAGGATGTAAGATTGCCAACACT
3986_PEP_ECORI_M_F	ACGACGAATTCTCCTCCTAAGTATCTAAACCATGGGCAAC
3987_PEP_BAMHI_M_R	ACGAAGGATCCCCTTATTTCTTCAGTTCAGCCAGGCTTA
4012_ldhb_mlui_f_m	GCAGAACGCGTAAGAGTAAAGAAGAACACCATGGCAACC CTTAAG
4013_ldhb_eco31i_r_m	GCAGCGGTCTCGGATCCTTTTTGCGGACTCTAGATCACAGG
4031_eco31i_Ubi_m_R	AGCGAGGTCTCGGATCCGTTGCGGACTCTAGATTAGATGG AGGTACGG
4032_MLE_mlu_m_T	GACGAACGCGTCGATGAAGGATGTAAGATTGCCAACACT
4038_se hypepc F	AGGAGAACTCCACCTACACCACAAG
4039_se hypepc R	CGGAAGATCCGGACCAAACAATG
4104_mle_325_asci	CGCGGGGCGCGCCCGGTCC
4105_mle_325_acc651	GCAGAGGTACCGCCGCCCGGTCACTG
4106_me_bsai_asci	GCAGAGGTCTCGCGCGCCCGTACCTGCAGTACAAG
4107_me_SalI	GCAGAGTCGACTTGGGCGCGGGGCGCGTACATC
4108_ldha_asci_325	GCAGAGGCGCGCCCGGTCCAAAGACCAGAGG
4109_ldha_acc651_325	GCAGAGGTACCCGGCCGGCCGCCCGGTC
4110_ldhb_new_asci	CGCGGGGCGCGCCAAATTC
4111_ldhb_sali_324	GCAGAGTCGACGCCGCCCGGTCACTGGATTTTGG
4163 3´UTR_Ldha_Seq	TTGGCCGGTATATTCGGACG
4164_seq_spect_325_F	TAGATGGCCGCCATAGTGACTG
4165_seq_spec_325_R	ACTGGGCCGGCCAGCGCTGGTAC
4370_att_pps_R	GGTTAAGCCTGGCTGAACTGAAG
4371_att_mdh_F	ACGAGCACGCGCATTGGTTCCTTC
4372_att_mdh_R	GAGAAGACGCTTGCTTACTCA
4373_att_ldha_F	ATCCAGAAGGAGCTGCAGTTCTAGAG
4374_att_ldhb_R	TCCTTAAGGGTTGCCATGGTGTTC
4375_att_ldha_R	AGAAGATTCACAATCAGCTGGTCCTTGAG
4376_att_ldhb_F	AAAGACCTCAAGGACCTGTGATCTA
4377_att_pepc_F	CTGCTGGCATGCAGAACAC

4378_att_pepc_R	ACGAGATTGTCGTCCTCCGACACCTTC
4379_att_me_R	GGTGGCAACAGCTGCTGAGGACATTACTGAAG
4380_att_me_F	CTACCGCCGTACCTCCATCTAATC
4381_att_MLE_F	GCCGAAAAACTAGGCTAATC
4396_pps_F_ Eco311_acc651	GCAGAGGTCTCGGTACCCGGGGCGCGTACATCTTG
4397_pps_R_BsaI_AscI	GGAGAGGTCTCGGCGCGCCAGTTCTAGAGCGGCCGCTGGC
4398_pps_R_ newI_AscI	GGAGAGGTCTCGCGCGCCAGTTCTAGAGCGGCCGCTGGC
4413_mls1_mlui_MMPIM	GCAGAACGCGTAATGAGTCAAACCATAACCCAGAGCCGTT TAC
4414_mls1_Xbai_MMPIM	ACGACTCTAGATTAATGACTTTCTTTTTCGCGTAAAC
4415_ENO_Mlui_MMPIM	GACAGACGCGTAATGTCCAAAATCGTAAAAATCATCGGTC GTGAA
4416_ENO_Xbi_MMPIM	ACGAGTCTAGATTATGCCTGGCCTTTGATCTCTT
4421_MUTASE_MluI	GCAGAACGCGTAATGGCTGTAACTAAGCTGGTTC
4422_MUTASE_XbaI	AGCAGTCTAGATTACTTCGCTTTACCCTGGTTTG
4441_PPS_100_F	CATCCGCGAAGCCTATGCAC
4442_PPS_100_R	GGTTTCCTGCTGACCGGCAAAAG
4443_MDH_F	CAGCGTGGTGCTGCAATCA
4444_MDH_R	CATCAATCGGGAGGCCTTG
4445_Ldhb_F	CTGCCGTCCCGAACAACAAG
4446_ldhb_R	TCCACTTCCAATCACGCGGTGCTTAG
4447_Ldha_F	GATGCACCCGCCTAAGGTTC
4448_Ldha_R	GGTTGCAATCTGGATTCA
4449_PEPC_F	TCCGGAGTTGGAATATGGACGGATG
4450_PEPC_R	CCTTATTCTCTTCAATGTGTAAGCTTGGCAAGCATTC
4451_ME_F	CAGGTTCAGCGGGATGCG
4452_ME_R	GCGCGGGAGACTTTCTGAATATC
4453_Mle_F_M	TTAGGTATTAGACTCGGTTATTC
4454_Mle_R_M	ACCGCCAAAACCAAGGCCAAAGAT
4681_Eno_M_F	CAGCTGCTCCGTCAGGTGCTTCTA
4682_Eno_M_R	TGATCTGGCCTGCAGCAGTACC
4683_malate sy_F	ACGCCAGGCGTGTAATAACGGTTCG
4684_malate sy_R	CGCGTAATGAGTCAAACCATAAC
4685_Mutase_M_F	TTGAAATTCTCGTCGAACTC
4686_Mutase_M_R	TGTCTGAGAAAGGCGTAAGC

4687_Npt_M_F	ATGCGCTGCGAATCGGGAGCGGCGATAC
4688_Npt_M_R	TCGATGCAGGCATGATTGAACAAGATGGA
4689_PPS_M_F	GCCTCCCTGGGTGAAATGATTACT
4690_PPS_M_R	TTCTGTTGCATCTCCACAGCCCACTA
4717_ME2RTF_neu	TGGCTGCTCAAGTAACTGAGGAAC
4718_ME2RTR_neu	GAGACGTGTTGCCACAACAAG
4719_pepc_RTn_F	GGGATCCATACCTGAAAC
4720_pepc_RTn_R	CCCTGGGTCCCTTATTCTC
4721_ldha_RTn_F	ACCACCTGCTTGTGAAC
4722_ldha_RTn_R	ATGGCGACTCCAGTGTGCCTGTG
4723_Mutase_RT_F	TCCGCCGGAACTGACTAAAG
4724_Mutase_RT_R	GGTCAATGGTCAGCGCCAGGCTTTC
4725_Npt_RT_F	GCTTGCCGAATATCATGGTG
4726_Npt_RT_R	AGCAATATCACGGGTAGCC
4727_Enolase_RT_F	GCTCCGTCAGGTGCTTCTAC
4728_Enolase_RT_R	CGCAGCAACAGCTTTGGTTAC
4729_MS_RT_F	CCCTTCTGGCTGTACATGTC
4730_MS_RT_R	ACGAGCGTAATAACGTGCTTTCCGGTCTG
4731_PPS_RT_F	CCGGTCAGCAGGAAACCTTCCTC
4732_PPS_RT_R	GGTGCACACGATAAGAGATGG
4733_ME_RT_F	CCGGAAGTGGTCGAAACCATCGAAG
4734_ME_RT_R	CTGGATGTTACGCAGGTAGATGTG
4735_pps_RT_NF	GCCACCGCAGAAGATATG
4736_pps_RT_NR	GCGCGATCGTTAAACAGAG
4737_pepc_RT_NF	GCCACAACAGCCATTTCATCC
4738_pepc_RT_NR	GGGAAGAGCGCTTGTGCTTCAGGAC
4739_Mdh_RT_NF	ACCACGCTGTTGGACAGTTG
4740_Mdh_RT_NR	AACCATGCCACAGTGAAG
4741_MleN_RT_NF	GGCGGTCTGCTTGAGAAAC
4742_MleN_RT_NR	ATCGCACAGCCGAAGATGTTTG
4743_ldha_RT_NF	GCTTGTGCCATCAGTATC
4744_ldha_RT_NR	CCATCATCTCGCCCTTG
4745_ldhb_RT_NF	AAGCTCATCAGCCAGAGAC
4746_ldhb_RT_NR	TGCCGTCCCGAACAACAAG

4774_Rubisco Ls_F	TGGCAGCATTCCGAGTAAC
4775_Rubisco Ls_R	GATCAAGGCTGGTAAGTCCATC

2.1.8 DNA plasmids and vectors

Genes involved in these novel pathways: Hydrilla mimic pathway (HC_4l) and MMPEM pathway- PEPC, Mle, PPS, MDH, Mutase, Enolase, Malate synthase were cloned into pTRA_K_RbcS1_CTP, pTRA_K_RbcS1_CTP-SBPase, pTRA_K_Cm-RbcS-P_Cm-cTP_gcvT_3'g7, pTRA_K_LeRbcS_3´g7, pTRA_K_35SS vectors. Plant vectors for PEPC, NAD-ME, Mle, NAD-Mdh, PEPS, LdhA, and LdhB, Mutase, Enolase, Malate synthase were cloned in donar vectors (entry vector) using the cassette of promoter gene and polyadelynation for gateway recombination. LdhA and LdhB gene cloned by Alexander Heil Biology I (RWTH Aachen) and cloned into pTRA-K-rbcS1-CTP, pTRA-K-35SS plant vector respectively. The cloning of the gateway vectors were shown in 2.1.8.1, 2.1.8.2 and 2.1.8.3.

2.1.8.1 Entry plasmids for gateway recombination

The regions with the attachment sites (L1/2/3/4/R1/2/3/4) were synthesized by the EUROFINS Medigenomix (Ebersberg) in the pBS SK(+)_G325A, pBS SK(+)_G325B, pBS SK(+)_G324A and pBS SK(+)_G324B plasmid and this work done by Matthias Buntru (Bio1 RWTH Aachen).

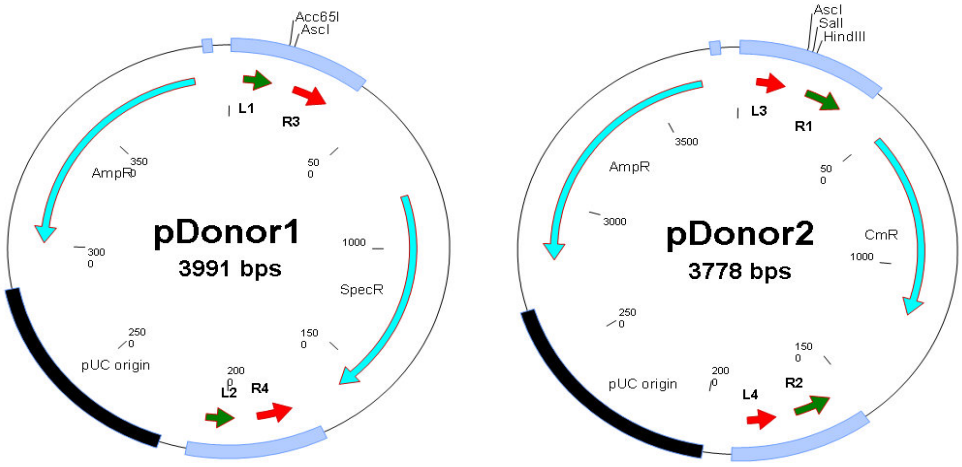

Figure 2.1: Entry vectors for gateway recombination

L12R34_A/B and L34R12_A/B: synthesized regions with the attachment sites L1/2/3/4 /R1/2/3/4; AmpR = β-Lactam antibiotics gene (bla) as a selection marker in *E. coli*; CmR = Chloramphenicol Acetyltransferase gene (cat) as a selection marker in *E. coli*; SpecR = Spectinomycin/streptomycin-Nucleotidyltransferase gene (aadA) as a selection marker in *E. coli*; pUC origin = Replication origin in *E. coli* for vector; lacZ = α-fragment of β-galactosidase; I SceI and PI-SceI = recognition sequences for homing endonuclease; MCSI and MCSII = Multiple cloning sites; iMCSI = inverted MCSI and vector named as pUC324_CmR and pUC325_SpecR respectively.

2.1.8.2 Destination vector for gateway recombination

Destination vector was constructed to have capacity for carrying multiple genes and can transform *Agrobacterium*. Basic vector provided by (Xue-chen Wang University Japan) and internal changes ccdB CmR made by Matthias Buntru (Bio1 RWTH Aachen) and RIKEN BioResource Center, Tsukuba, Japan.

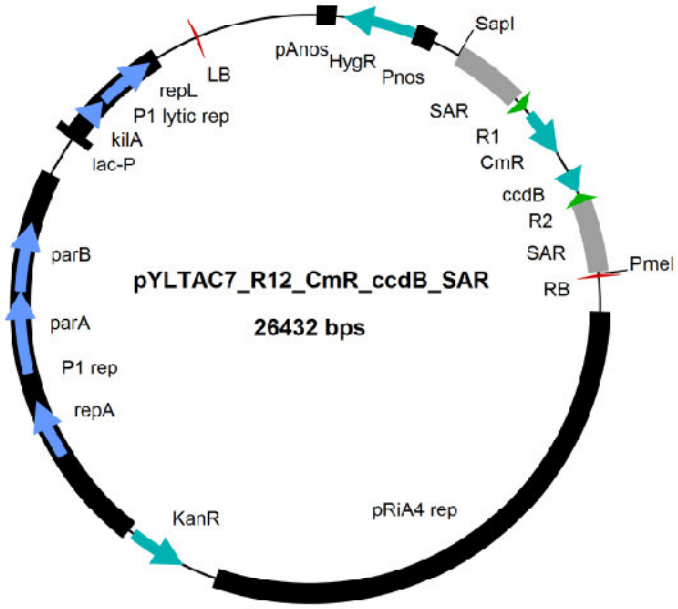

Figure 2.2: Destination Vector for gateway recombination
R1 and R2 = Attachment sites; AmpR = (β-Lactamase gene (bla)) as a selection marker in bacteria (β-Lactam antibiotics resistance to ampicillin); ccdB = lethal gene for negative selection for *E. coli*; pUC origin = *E. coli* Replication origin for vector; RK2 origin = Replication origin for *Agrobacterium* in the vector; SAR = Scaffold attachment region; LB/RB = left/right border of Nopalin TI plasmid pTiT37; pRiA4 repA = "single-copy" replication origin from *A. rhizogenes* for replication of Agrobacterium in the vector; P1 rep = "single-copy" replication origin of phage P1 for replication of the vector in *E. coli*; P1 lytic rep = inducible lytic Replicon phage P1 for replication of the vector in *E. coli* with higher copy numbers; Lac-P = Lactose promoter; KanR = Neomycin-phosphotransferase gene (nptII) as a selection marker in bacteria (Aminoglycoside mediated antibiotics such as kanamycin resistance); HygR = Hygromycin B phosphotransferase gene (hph) as a selection marker in transgenic plants; Pnos = Promoter of Nopalin synthase gene from *A. tumefaciens*; pAnos = Polyadenylation /Terminations sequence of Nopalin synthase gene from *A. tumefaciens.*

2.1.8.3 Plant vectors and gateway entry vectors

Gateway entry vectors were created after cloning the gene expression cassette in to the plant vector. Expression cassette for entry vector was isolated from plant vector. Basic cloning statergy for cloning of the genes from both pathways (HC_4l and MMPEM) was similar except different restriction enzymes used for each entry vector due to different restriction enzyme sequences in each gene sequences.

Phospho*enol*pyruvate synthase gene was isolated from *E. coli* and digested with enzyme EcoRI and BamHI and ligated over vector pTRAK_CmRbcSP_CmcTP_gcvT_3'g7. Mle (Malate-Lactate antiporter) gene was isolated from bacteria *Bacillus subtilis* and cloned into the vector pTRA-K-rbcS1-cTP-SBPase using restriction enzyme MluI and XbaI. Malate dehydrogenase was isolated from *Z. maize* and cloned into plant expression vector pTRAK_LeRbcS-P_LecTP_gcvP_3'g7 using enzyme BsaI and XbaI. Genes involved in the novel pathways PEPC, Mle, PPS, MDH, Mutase, Enolase, Malatesynthase were cloned into pTRA-K-rbcS1-CTP, pTRA-K-rbcS1-CTP-SBPase, pTRAK_CmRbcS-P_CmcTP_gcvT_3'g7 respectively. LdhA and LdhB genes were cloned into pTRA-K-35SS, pTRA-K-rbcS1-CTP of the vector respectively. All these plant vectors for genes PEPC, NAD-ME, Mle, NAD-Mdh, PPS, LdhA, and LdhB, Mutase, Enolase, Malate synthase, were cloned first in plant vector. Later cassette of promoter gene and polyadelynation cloned into donor vectors (entry vector) for the MultiRound gateway recombination. The donar vector pUC324_CmR and pUC325_SpecR were used for cloning the cassette. Cloning techniques were similar for each entry vector only two different sets of restriction enzymes were used for specific entry vector. PCR product of the expression cassete (promoter, gene and polyadenylation) was amplified with resrtriction sites from respective plant vector and ligated over the digested empty entry vector with respective enzymes. PEP synthase gene cassette was isolated using the primer 3888_PPS_SalI and 3889_PPS_StuI and ligated over the digested vector pUC325_SpecR with enzymes SalI and StuI (Fig. 2.3 and 2.4). HvPEPC entry vector was created by using plant vector pTRA_K_AtRbcS_HvPEPC digested with AscI and FseI and ligated over digested pUC325_SpecR vector with enzymes AscI and FseI (Fig. 2.9 and 2.10). MleN (Malate-Lactate antiporter) expression casstte was isolated from the plant vector pTRA_K_Pssu_Ara_cTP_MleN and foe PCR primers 4104 and 4105 were used and ligated over pUC325_SpecR and vectors were digested with enzymes AscI and Acc651 (Fig. 2.7 and 2.8). Malate dehydrogenase (MDH) gene cassette amplified from plant

vector pTRA_K_LeRbcS_mdh5_3´g7 using primers 4112 and 4113 and ligated over vector pUC324_CmR (Fig. 2.5 and 2.6). LdhA gene entry vector was created by using pTRA_K_35SS_LdhA plant vector and amplified expression cassete by using primers 4108 and 4109 and ligated over digested vector pUC325_SpecR with enzyme AscI and Acc651 (Fig. 2.11 and 2.12). Gateway entry vectors for malic enzyme and pep synthase with transit peptide provided by Matthias Buntru (RWTH Aachen Biology I). LdhB expression cassette was isolated using primers 4110 and 4111 from plant vector pTRA_K_RbcS_LdhB and ligated in vector pUC324_CmR (Fig. 2.13 and 2.14).

2.1.8.4 Plant vectors and entry vector for pYLTAC7_*Hydrilla* pathway

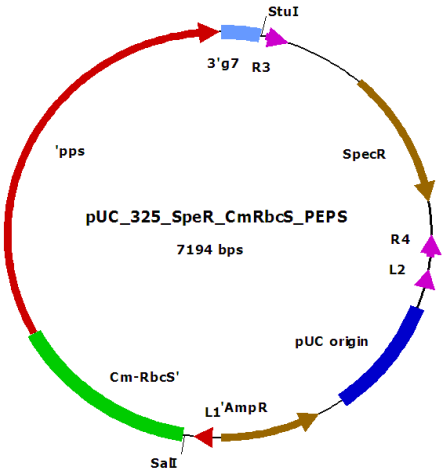

Figure 2.3: Plant vector: phospho*enol* pyruvate synthase

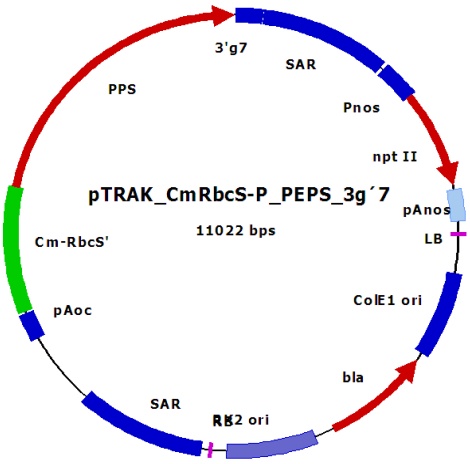

Figure 2.4: Entry vector: phospho*enol*pyruvate synthase

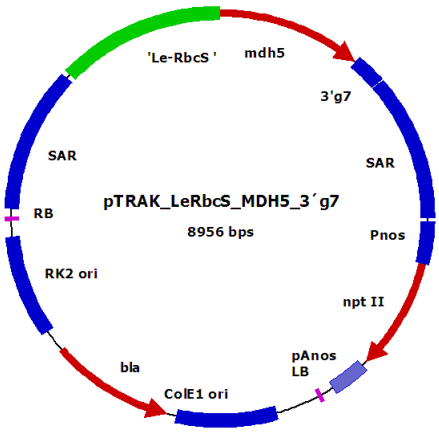

Figure 2.5: Plant vector: malate dehydrogenase

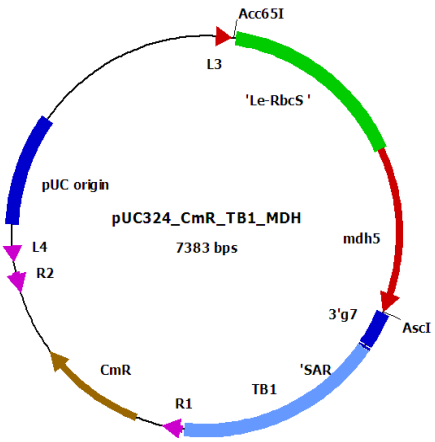

Figure 2.6: Entry vector: malate dehydrogenase

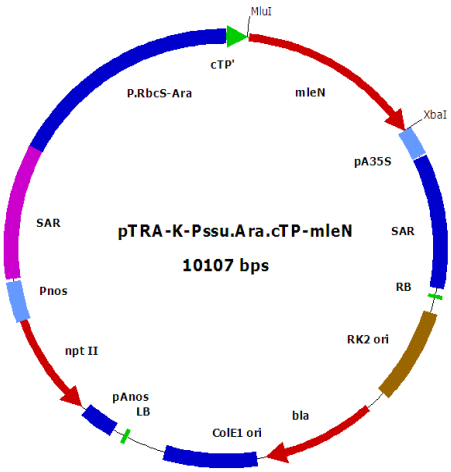

Figure 2.7: Plant vector: malate/lactate antiporter

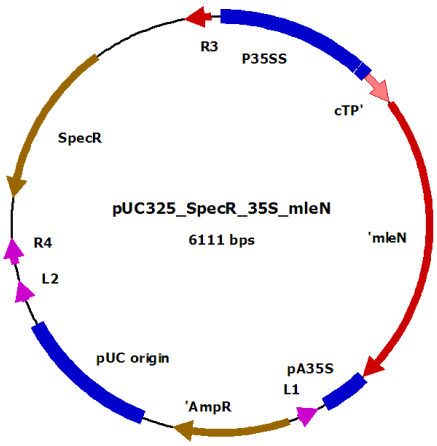

Figure 2.8: Entry vector: malate/lactate antiporter

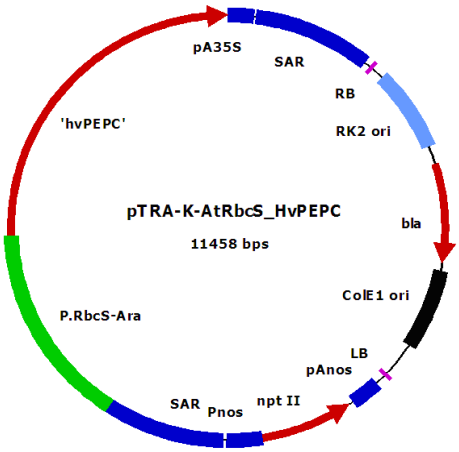

Figure 2.9: Plant vector: phospho*enol*pyruvate carboxylase

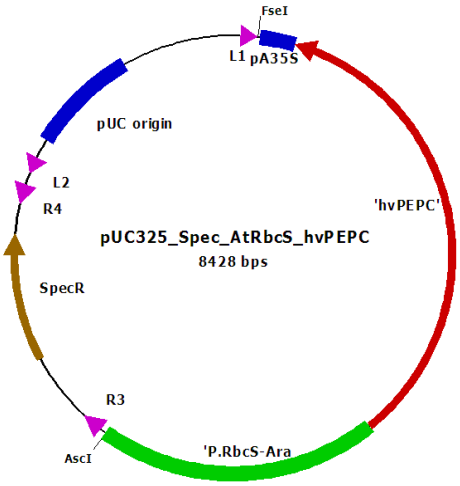

Figure 2.10: Entry vector: phospho*enol*pyruvate carboxylase

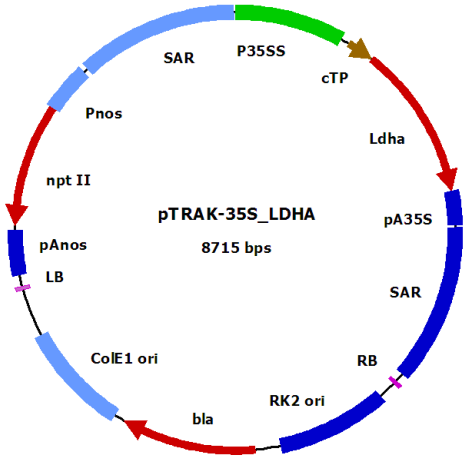

Figure 2.11: Plant vector: lactate dehydrogenase A

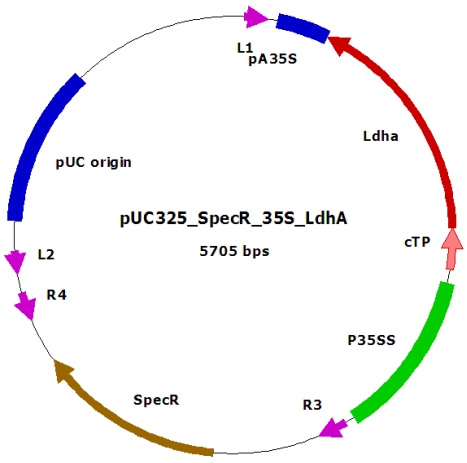

Figure 2.12: Entry vector: lacate dehydrogenase A

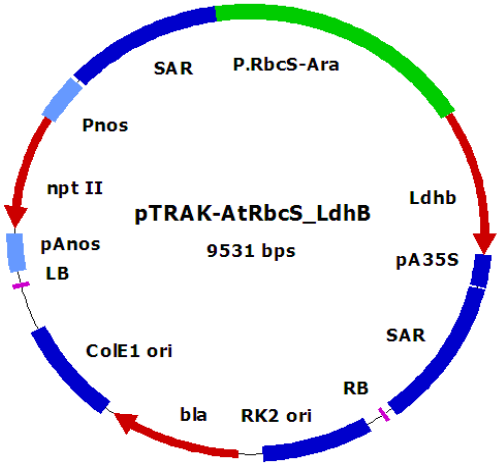

Figure 2.13: Plant vector: lactate-dehydrogenase B

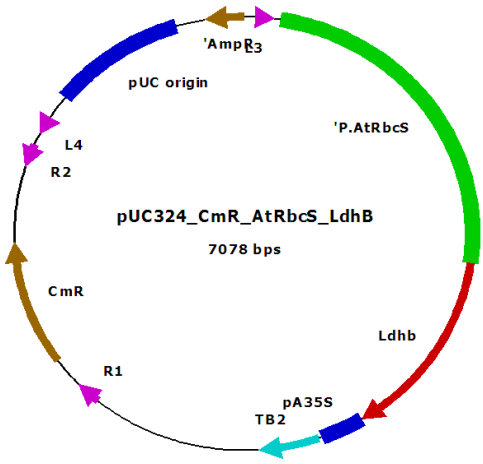

Figure 2.14: Entry vector: lactate-dehydrogenase B

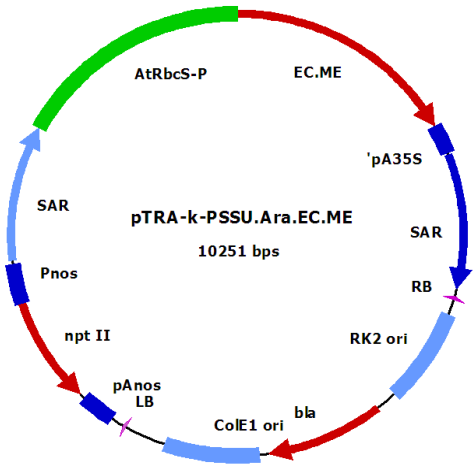

Figure 2.15: Plant vector: NAD-malic enzyme

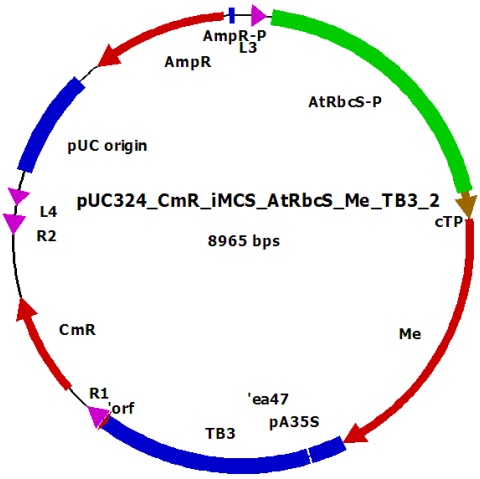

Figure 2.16: Entry vector: NAD-malic enzyme

Sourse of the genes and promoters explained above from fig. 2.3, to fig. 2.16

Figure 2.3: pTRAK_CmRbcS-P_PEPS_3g´7: PEPS = Phospho*enol*pyruvate synthase isolated from *E. coli* under the control of *Chrysanthemum* Rubisco promoter; 3g´7 = polyadenylation termination isolated from gene 7 of *A. tumefaciens*. Figure 2.4: pUC325_ SpecR_CmRbcS: PEPS = phosphor-*enol*pyruvate synthase gene in spectinomycin resistance entry vector. Figure 2.5: pTRA-k-LeRbcS-MDH-3g´7: MDH = NAD dependent malate dehydrogenase isolated from *Z. maize* with promoter from *Solanum lycopersicum* (Tomato) and with transcription blocker. Figure 2.6: pUC-324_CmR_TB1_MDH: malate dehaydrogenase gene in chloramphenicol resistance entry vector. Figure 2.7: pTRAK_K_35S_MleN: MleN = Malate lactate antiporter isolated from *Bacillus subtilis* under the control of 35SS promoter. Figure 2.8: pUC324_SpecR_35S_mleN = malate-lactate antiporter gene in spectinomycin resistance vector; Figure 2.9: pTRAK_PSSU_Ara_PEPC: PEPC = isolated from *H. verticillata* with promoter from *Arabidopsis* Rubisco; Figure 2.10: pUC_SpecR_AtRbcs_HvPEPC: phospho*enol*pyruvate carboxylase gene in spectinomycin entry vector; Figure 2.11: pTRA_K_35S_LDHA: LDHA = lactate dehydrogenaseA isolated from mouse liver with 35SS promoter; Figure 2.12: pUC_SpecR_35S_LDHA: Lactate dehydrogenase gene in spectinomycin resistance entry vector; Figure 2.13: pTRA_K_AtRbcS_LDHB: LDHB = lactate dehydrogenase gene isolated from rat heart with promoter from *Arabidopsis* Rubisco and transcription blocker; Figure 2.14: pUC324_CmR_AtRbcS_LdhB: Lactate dehydrogenase B gene in chloramphenicol resistance entry vector; Figure 2.15: pTRA_K_PSSU_Ara_ECME: NAD-ME- malic enzyme gene isolated from *E. coli* under control of *Arabidopsis* Rubisco promoter; Figure 2.16: pUC_324_ CmR_AtRbcS_ME_TB$_3$: Malic enzyme gene in pUC325_ChloR vector with transcription blocker (TB3).

2.1.8.5 Destination vector with *Hydrilla* pathway (HC_4l) genes

The plasmid pYLTAC7_C_4_*Hydrilla* (Fig. 2.17) is obtained after MultiRound Gateway. In the table 2.6 shown the gateway entry vectors (genes from HC_4l) which were cloned into destination vector pYLTAC7_R12_CmR ccdB_SAR.

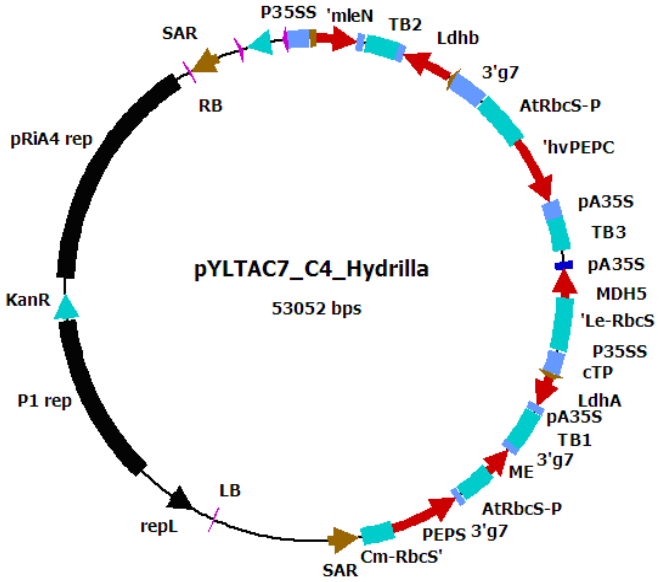

Figure 2.17: Vector pYLTAC7_C_4 *Hydrilla* after recombination
MleN = Malate lactate antiporter isolated from *Bacillus subtilis* under the control of 35SS promoter; LDH-B = Lactate dehydrogenase B isolated from rat heart with *Arabidopsis* rubisco promoter and transcription blocker; PEPC = phosphor-*enol*pyruvate carboxylase isolated from *H. verticillata* under *Arabidopsis* Rubisco promoter; NAD-MDH = dependent malate dehydrogenase isolated from *Z. maize* with promoter from *Solanum lycopersicum* and transcription blocker; LDHA-A = Lactae dehydrogenase A mouse liver with 35SS promoter; NAD-ME = malic enzyme genes isolated from *E. coli* with *Arabidopsis* rubisco promoter; PEPS = Phospho*enol*pyruvate synthase isolated from *E. coli* with *Chrysanthemum* rubisco promoter.

Table 2.6: Destination vector pYLTAC7_C_4_*Hydrilla* and Gateway entry Vectors

I. pYLTAC7_C_4_Hydrilla	
i)	pUC325_SpecR_CmRbcS_PEPS
ii)	pUC324_CmR_TB1_MDH
iii)	pUC325_SpecR_35S_LDHA
iv)	pUC324_CmR_AtRbcS_LDHB
v)	pUC325_SpecR_AtRbcS_hvPEPC
vi)	pUC324_CmR_iMCS_AtRbcS_ME_TB3_cTP
vii)	p UC325_SpecR_35S_mleN

2.1.8.6 Plant vectors and Gateway entry vectors for pYLTAC7_MMPEM pathway

Genes from MMPEM pathway malate synthase, mutase, and enolase were isolated from *E. coli* and appropriate sequences were copied from (NCBI) and cloned in to the vectors pTRA_k_35SS_cTP, pTRA-K-rbcS1-CTP and using restriction sites MluI and XbaI. Mutase, Malate synthase were used in pUC325_SpecR vector and using primers 4541_Mutase_AscI and 4542_Mutase_Acc651 for cloning of Mutase gene (Fig. 2.20 and 2.21) and 4670_MS_1 and 4671_MS_2 for cloning of malate synthase gene (Fig. 2.22 and 2.23). For enolase used entry vector pUC324_CmR_TB2 using primes 4727_Enolase_F and 4728_Enolase_R (Fig. 2.24 and 2.25) and Npt gene cloned for the neomycin phosphotransferase type II that confers resistance to aminoglycoside antibiotics (i.e. kanamycin and neomycin) and was used for selection of transgenic plants because GTDEF plants carries hygromycin resistance gene. Therfore it was better to select MMPEM plants on kanamycin resistance gene. It was possible to transfer MMPEM pathway into the chloroplast of GTDEF plants because of different selection marker. Npt gene was cloned into the entry vector pUC325_SpecR. Figs 2.18 to fig. 2.25 have been shown the all plant vectors and gateway entry vectors used in MMPEM pathway.

Table 2.7: Abbrevation used for vectors from fig. 2.18 to 2.25

pA35SS	Polyadenylation /Termination sequence from CaMV
bla	ß-lactamase gene for selection in bacteria (ampicillin/carbenicillin resistance).
Hv pepc	The coding sequence for phospho*enol*pyruvate carboxylase
ColE1 ori	Replication origin for vectors in *E. coli.*
LB and RB	Left and right border sequences of Nopalin-Ti-plasmids pTiT37
Npt	Neomycin phosphotransferase type that confers resistance to aminoglycoside antibiotics (i. e. kanamycin and neomycin) and was used for selection of transgenic plants in axenic culture.
PAnos	Polyadenylation of Nopaline synthetase gene from *A. tumefaciens.*
Pnos	Promoter of Nopaline synthase gene from *A. tumefaciens.*
P. RbcS. Ara	Promoter from Arabidopsis rubisco
RK2 ori	Replication origin for vectors in *A. tumefaciens.*
SAR	Scaffold Attachment Region from the tobacco RB7 gene (gi U67919).
pUC origin	Replication origin for vector in *E. coli*
p35SSS	Promoter sequence from Cauliflower mosaic virus
pA35SS	Polyadenylation/Termination sequence of the Cauliflower mosaic virus
KanR	Neomycin phosphotransferase gene (nptII)

CmR	Chloramphenicol Acetyltransferase gene (cat) as a selction marker in *E. coli*
SpecR	Spectinomycin/streptomycin-Nucleotidyltransferase gene (aadA) as selection marker in *E. coli.*
TB1/2/3	AT rich sequences from lambda phage as a transcription blocker
Cab7-cTP	Transit peptide of the chlorophyll a/b binding protein 7.
TB1/2/3	AT rich sequence from lambda phage and used as a transcrption blocker
3´g7	Polyadenylation termination from gene7 from *A. tumefaciens*
CHS	5' Untranslated region of chalcone synthase
pAocs	Polyadenylation termination of the Octopin synthase gene from *A. tumefaciens*
CmRbcS-P/ CmRbcS-cTP	Promoter sequence or transit peptide of the small subunit of RUBISCO from *Chrysanthemum*
AtRbcS-P/ AtRbcS-cTP	Promoter sequence or transit peptide of the small subunit of RUBISCO from *A. thaliana*
LeRbcS-P/ LeRbcS-cTP:	Promoter sequence or transit peptide of the small subunit of RUBISCO from *S. lycopersicum*

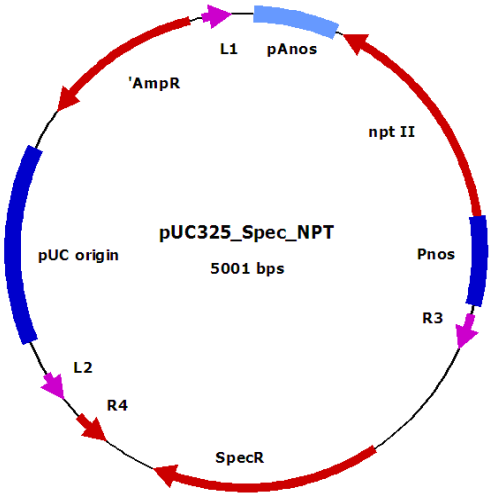

Figure 2.18: Entry vetor: neomycin phosphotransferase

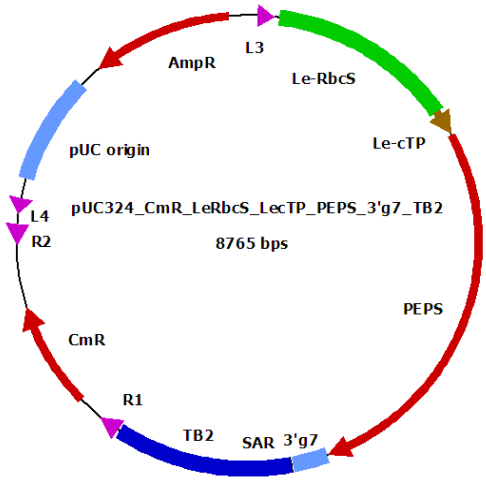

Figure 2.19: Entry vector: phospho*enol* pyruvate synthase

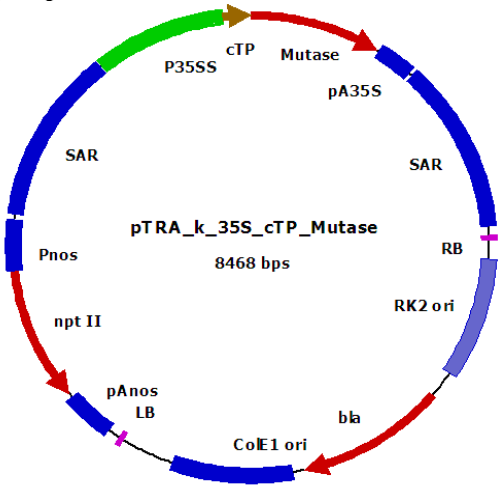

Figure 2.20: Plant vector: mutase

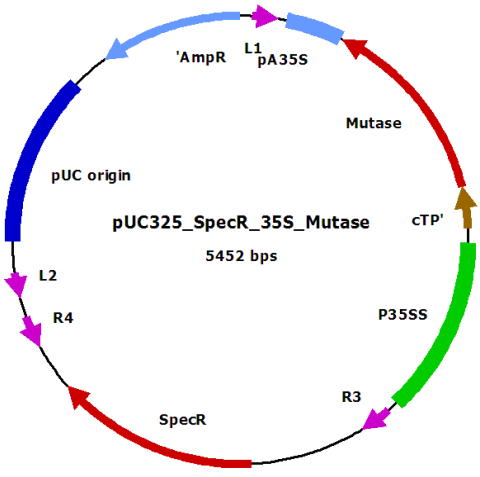

Figure 2.21: Entry vector: mutase

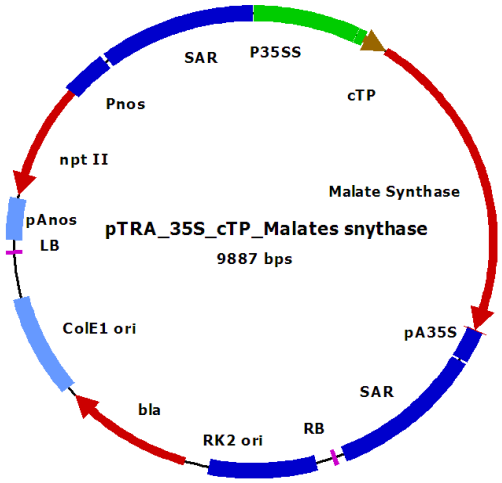

Figure 2.22: Plant vector: malate synthase

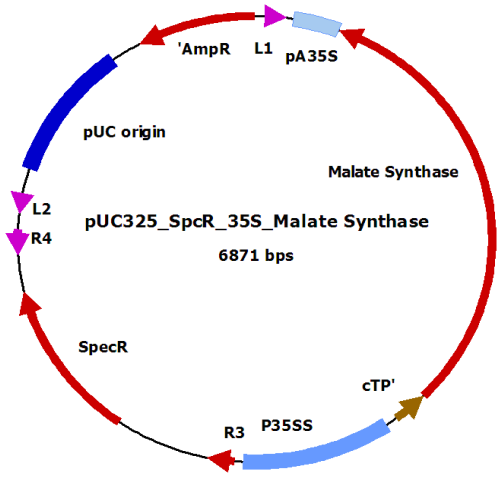

Figure 2.23: Entry vector: malate synthase

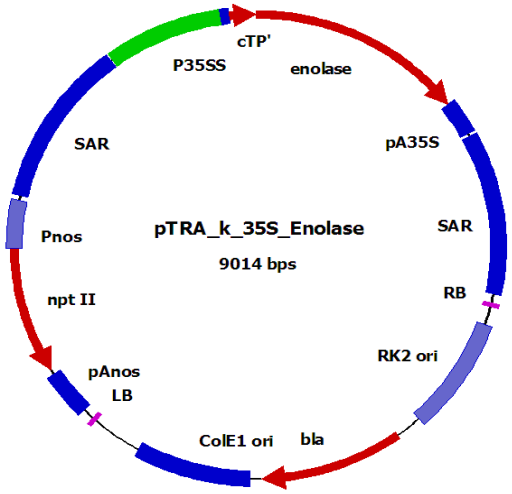

Figure 2.24: Plant vector: enolase

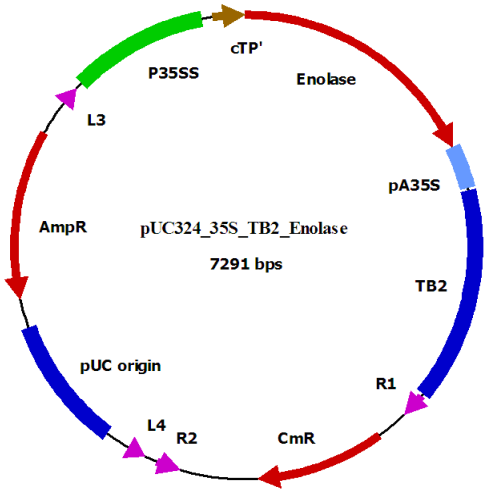

Figure 2.25: Entry vector: enolase

2.1.8.7 Destination vector with MMPEM pathway genes

Vector pYLTAC7_MMPEM (Fig. 2.26) was obtained after the MultiRound Gateway recombination. Table 2.8 shows the gateway entry vectors which were cloned into the empty destination vector pYLTAC7_R12_CmR ccdB_SAR.

Table 2.8: Destination vector pYLTAC7_MMPEM and gateway entry vectors

II. pYLTAC7_MMPEM	
i)	pUC324_CmR_LeRbcS_LeCTP_PEPS_3g´7
ii)	pUC325_SpecR_NPT
iii)	pUC325_SpecR_35S_Mutase_TB2
iv)	pUC325_SpecR_35S_Malate synthase

v)	pUC324_CmR_Enolase_TB1
vi)	pUC324_CmR_i MCS_AtRbcS_ME_TB3

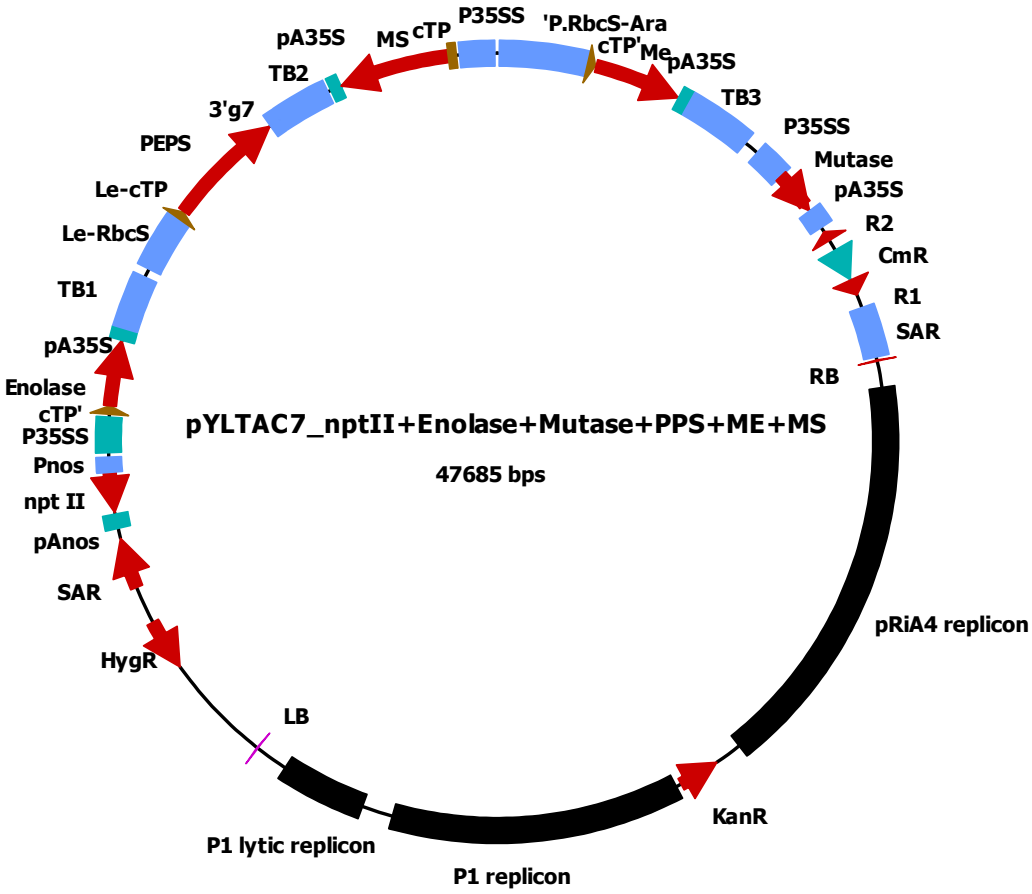

Figure 2.26: Plasmid pYLTAC7_MMPEM after recombination
Destination vector with gene expression cassettes after recombination phospho*enol*pyruvate synthase gene isolated from *E. coli* with promoter from *Solanum lycopersicum* (Tomato); Mutase gene isolated from *E. coli* and this under control of 35SS promoter and used transcription blocker; Malate synthase gene isolated from *E. coli* and was under the control of 35SS promoter; Enolase gene isolated from *E. coli* under the control 35SS promoter; Malic enzyme isolated from *E. coli* and promoter from *Arbidopsis* Rubisco; LB/RB = left/right border of Nopalin TI plasmid pTiT37; pRiA4 rep = "single-copy" replication origin from *A. rhizogenes* for replication of Agrobacterium in the vector; P1 rep = "single-copy" replication origin of phage P1 for replication of the vector in *E. coli*; P1 lytic rep = inducible lytic Replicon phage P1 for replication of the vector in *E. coli* with higher copy numbers; KanR = Neomycin-phosphotransferase gene (nptII) as a selection marker in bacteria (Aminoglycoside mediated antibiotics such as kanamycin resistance); HygR = Hygromycin B phosphotransferase gene (hph) as a selection marker in transgenic plants; Pnos = Promoter of Nopalin synthase gene from *A. tumefaciens*; pAnos = Polyadenylation /Terminations sequence of Nopalin synthase gene from *A. tumefaciens.*

2.1.9 Plant materials

Model plant *Nicotiana tabacum* cv. Petit Havana SR1 used throughout the study.

Non sterile plant culture: First seeds were sown in the soil (soil type-VM, Werkverband, Sintal-Josaa) and after 2 weeks seeds were germinated. Small individual germinated plantlets were transferred into the small pots (soil ED 73). The ages of the plants were calculatee after the germination of seeds.

For sterile culture: Seeds were surface sterile with 70% ethanol solution with agitation for 2 min. Later with 96% ethanol and agitation with 1 min. then transported in to the weck glasses on MS medium (Table 2.9).

The cultivation conditions: Long day: 16 hours light, 8 hours dark, where transgenic plants received photosynthetic photon flux density: PAR- Photosynthetically active radiation) approx. 160 µmol photons/m^2 and s^{-1}. Day temperature in long day room was 26°C and the night temperature was approx. 20°C for the transgenic *N .tabacum* plants

Table 2.9: Murashige and Skoog (MS) Medium

component	Endconcentration
MS-Salt with MES and Vitamins	4.4 g/l
Sucrose	20 g/l
Thiamin-HCl	0.2 mg/l
Plant agar	0.8% (w/v)
pH 5.8 adjusted with NaOH	

2.1.10 Bacteria

2.1.10.1 *Escherichia coli* cultures

Chemical transformations: The *E. coli* strain DH5α was used for the propagation and isolation of plasmids with f-endA1 glnV44 thi-1 recA1 relA1 gyrA96 deoR nupG Φ80dlacZΔM15 Δ (lacZYA-argF) U169, hsdR17 (rK-_mK^+) used mcrA λ.

Electroporation: The *E. coli* strain TOP10 with f-mcr Δ(mrr-hsdRMS-mcrBC) φ80lacZΔM15 ΔlacX74 nupG recA1 araD139 Δ(ara-leu) 7697 galE15 galK16 rpsL (Str^R). This bacterial strain possesses a modified recombination system (*rec*A1), which results in

reduced recombination probability, and lacks endonuclease (*end*A1). It was therefore used in the cloning experiments. Cultures of *E. coli* DH5α or TOP10 were grown in LB medium and on LB Plates (Table 2.10). The appropriate antibiotics have been added to the selection and kept overnight for growing at 37°C.

Table 2.10: Luria Bertani (LB) Medium

Components	Endconcentration
Yeast extract	0.5% (w/v)
NaCl	1% (w/v)
Trypton	1% (w/v)
Agar	1.5% (w/v)

2.1.10.2 *Agrobacterium tumefaciens* culture

In the transient and stable transformation of *N. tabacum* GV3101 and AGL1 *Agrobacterium* strains were used. GV3101 is the Ti plasmid pMP90RK, which contains *vir* region and the genes for the two resistances gentamycin and kanamycin. GV3101 strain of *Agrobacterium* was used for the transformation of plasmids with resistance to carbenicillin; AGL1 was used for the plasmids with kanamycin resistance. AGL1 strain of *Agrobacterium* carries the hypervirulent Ti plasmid pTiBo542. Chromosomal encoded AGL1 for resistance to rifampicin and carbenicillin. GV3101 was cultured in YEB medium (Table 2.11) and AGL1 was cultured in LB medium (Table 2.10).

Table 2.11: YEB Medium

Components	Endconcentration
Nutrient Broth	0.8% (w/v)
Yeast extract	0.1% (w/v)
Sucrose	1.5% (w/v)
$MgSO_4$	2 mM
Agar	1.5% (w/v)
pH 7.4 adjust with NaOH	

2.1.11 Used internet softwares and computer programs

The Internet software, online programs and computer programme used in this work are specified in Table 2.12. All Internet adresses and software updated from the year 2012 versions.

Table 2.12: Used computer programs

Name	Comapany	Purpose
SECentral CloneManager© 9.10	Scientific and Educational Software	Primer design, display cloning Steps, repesentation and simulation of plasmid
Chromas© 2.31	Technelysium Pvt. Ltd	Processing of sequence data
Oligonucleotide Properties Calculator	http://www.basic.northwestern.edu/biotools/oligocalc. html	Primer design
National Center for Biotechnology Information (NCBI)	http://www. ncbi.nlm.nih. gov/	Analysis of sequences
NCBI Entrey PubMed	http://www. ncbi. nlm. nih. gov/	Literature search

2.2 Methods

2.2.1 Molecular biological methods

The molecular biological techniques used in the present study are based on the methods described by Sambrook *et al.,* (1989). The use of restriction endonucleases and DNA-modifying enzymes were according to the manufacturer's manual.

2.2.1.1 Isolation of plasmid DNA from *E. coli*

The isolation of plasmid DNA was done by a plasmid minipreparation kit from Macherey nagel GmbH and Co. KG. NucleoSpin Plasmid column kits were used for small size plasmid according to the manufacturer's manual but for larger size gateway plasmid (30-40 kb) used boiling minipreparation method which showed more favourable results. This method described by Holmes and Quigley (1981) was routinely applied for rapid preparation of plasmid DNA for restriction analyses. It is suitable for the isolation of bigger plasmid from transformed *E. coli*.

- A single bacterial colony was grown in 5 ml of LB liquid medium containing appropriate antibiotics at 37°C overnight.
- 2 ml culture was transferred to an Eppendorf tube and cells were harvested by centrifugation (13000 rpm, 1 min on Biofuge A).
- Pellet was resuspended in 110 µl of buffer PI (Table 2.21)
- Buffer PII (Table 2.22) added for lysis the cells because of buffer containing SDS and incubate 5 min. at room temperature.
- After addition of buffer PIII (Table 2.23) resulted into neutralization of lysate which separate the chromosomal DNA and cell debris in precipitate.
- After incubation for 5 min in ice centrifuge the sample at 14000 x g for 10 min at 4°C and supernatant transferred into new tube.
- RNA contaminations have been removed by the addition of 4 µl RNAse (10 µg/ml) and incubate at 37°C for 15 min.
- Then solutions precipitates with addition of 1 vol. isopropanol and gently mixes and centrifuge with 14000 g for 15 min at 4°C and later incubate 5 min in ice.
- The supernatant was discarded and pellet washed with 500 µl 70% ethanol and removed complete ethanol traces. Reaction vessel washed again with 500 µl 70% ethanol and dried the pellet of nucleic acids at 37°C to remove the remaining traces of ethanol and resuspended in 50-100 µl H_2O.

Table 2.21: Buffer PI for plasmid isolation

Component	End concentration
Tris-HCl pH 8	25 mM
Glucose	50 mM
EDTA	10 mM

Table 2.22: Buffer PII for plasmid isolation

Components	End concentration
Tris-HCl pH 8	25 mM
NaOH	200 mM
SDS	1% w/v

Table 2.23: Buffer PIII for Plasmid isolation

Components	End concentration
Potassium acetate	3 M
Amino acids	1.8 M

2.2.1.2 Combined isolation of DNA and RNA

20-30 mg of leaf materials were harvested and frozen into liquid nitrogen in 2 ml eppi filled with small glass beads. Leaves were grinded in the eppi with the help glass beads in the thick cardboard box. In the homogenized leaf material added 500 µl of DNA-RNA extraction buffer (table 2.24). Later sample were vortexed 1 min and kept for shaking at room temperature followed centrifugation ~15 min at 14000 g at RT for 10 min. After centrifugation it showed the separate phases and from upper phase transfers 300 µl of supernatant into new eppi. The sample were precipitated with1/10 volume of 3M sodium acetate (pH 5.2) and 2 volume of 96% ethanol (v/v) then again centrifuge for 20 min. 14000 g at 4°C. The supernatant were discarded and pellet was washed with 70% ethanol (v/v) and removed the traces of ethanol from eppi by centrifugation for 10 min. Finally the pellet was resusupended in 200 µl H_2O.

Table 2.24: DNA/RNA Extraction buffer

Components	End Concentration
Tris-HCl pH 7.6	0.05 M
SDS	0.5 % (v/v)

2.2.1.3 Agarose gel electrophoresis

Nucleic acids were seperated by using agarose gel in pressence of elctric field. Agarose is a polymer of glycosidically linked by D-galactose and 3,6-anhydro-L-galacto-pyranose. Nucleic acids are negatively charged by phosphates and separated on the agarose gel because of cathode (-) and anode (+). The speed depends on molecular weight and structure of nucleic acids, the pore size of the matrix, as well as the applied voltage and the ionic strength of the buffer.

The agarose gelelctrophoresis was carried out for checking the concentration of DNA-RNA (2.2.1.2), control check the PCR products (2.2.1.6), and for checking the fragments after digestion with restriction enzymes. DNA fragments were separated on an agarose gel with an appropriate concentration 0.8-2% depending on the fragment sizes by electrophoresis. Ethidium bromide 0.25 µg/ml was used in gel and running buffer (1 × TAE) to make DNA visible under UV light. Lambda DNA of known concentration

digested with *Pst*I or 1kb DNA ladder served as a DNA size marker. Documentation of the gel was photographed under the UV light transilluminator (λ = 302 nm) through an orange filter after electrophoresis.

Table 2.25: 50 xTris-Acetate EDTA buffer (TAE)

Components	End concentration
Tris, pH 8.0	2 M
Glacial actic acid	5% (v/v)
EDTA pH 8.0	50 mM

2.2.1.4 Purification of DNA fragments from agarose gel

The Invisorb® Spin DNA Extraction kit was used for the purification of DNA fragments from agarose and protocol used according to manufacturer's specifications of spin DNA extraction Kit (Invitek, Berlin).

2.2.1.5 Sequencing of DNA

The method used for the sequencing of double stranded plasmid DNA is based on the dideoxynuleotide chain termination method (Sanger *et al.,* 1977).
This was performed by Raphael Soeur, Jost Muth and colleagues in the Institute for Molecular Biotechnology (RWTH Aachen). The sequencing reactions were applied on Biosystems 3700 DNA analyzer and "big-dye ™ cycle sequencing terminator". In above table shows the stdanderd mixture for DNA to be sequence.

Plasmid DNA (approx. 140/160 ng/kb plasmid)

Primer	20 pmol
DH_2O up to	30 µl

2.2.1.6 Polymerase chain reaction (PCR)

Polymerase chain reaction (PCR) is a method for enzymatic amplification and modification of a target DNA sequence flanked by two known sequences (Saiki *et al.,* 1988). Two synthetic oligonucleotides complementary to the (+) and (−) strands respectively of the sequence were used as a primers. After heat denaturation of the target DNA, these primers bind to the opposite strands of DNA. New (−) and (+) strands fragments are then synthesized across the region between these primers by the catalysis of a thermostable Taq-DNA-polymerase. The newly formed DNA strands are the templates for the PCR primers. Repeating the cycles of denaturation, primer annealing, and extension results is an exponential accumulation of the target DNA fragment. The reaction conditions (e.g. template concentration, annealing temperature and extension duration) were optimized for the individual experiments on the basis of standard protocol shown in Table 2.26. Depending on the intended use different polymerases were employed (Table 2.27). Phusion polymerase was used solation of DNA fragments from genomic DNA by amplification of a specific region of DNA.

The colony PCR was performed by GoTaq polymerase (*E. coli*) and Phire polymerase (*A. tumefaciens*). Phire polymerase was used for the analysis of isolated DNA from transgenic plants by PCR. The multiplex PCR was used for the checking of transgenic *N. tobacum* plants in DNA level. The post annealing temperature was calculated by using SECentral CloneManager. Time of the elongation phase focused on the size of the DNA fragment to amplify. Typical thermal cycler programs for the employed polymerases are shown in Table 2.28 and Table 2.29.

Table 2.26: Standard PCR protocol for Taq Polymerase

Components	End Concentration
PCR-Puffer	1x
dNTP-Mix	200 µM
Primer 1	0.2 µM
Primer 2	0.2 µM
DNA-Polymerase	0.02 U/µl
Template	0.2 pg - 2 ng/µl
H_2O	Add upto 25 µl

Table 2.27: Standard PCR Program for Phusion Polymerase

Steps	Temp.	Time	
1	98°C	2 min	
2	98°C	10 sec	35x
3	60-72°C	20 sec	
4	72°C	15-30 s/kb	
5	72°C	10 min	
6	4°C	∞	

Table 2.28: Standard PCR Program for GoTaq Polymerase

Steps	Temperature	Time	
1	95°C	2 min	
2	95°C	30 sec	35x
3	55-65°C	30 sec	
4	72°C	1 min/kb	
5	72°C	5 min	
6	4°C	∞	

Table 2.29: Standard-PCR-Program for Phire Polymerase

Steps	Temperature	Time	
1	98°C	2 min	
2	98°C	10 sec	35x
3	60-72°C	10 sec	
4	72°C	15-30 s/kb	
5	72°C	1 min	
6	4°C	∞	

2.2.1.7 Purification of PCR products

The purification of PCR products was performed using the PCR Purification Kit Invisorb® Spin PCRapid Kit (Invitek, Berlin). DNA molecules were binds on an anion-exchange resin matrix (silica gel) due to its polyanionic character in high concentrations of chaotropic salts. Proteins were not affected by washing the silica gel with appropriate buffers. The PCR fragments are eluted, from column with lower ion strength buffer while small oligonucleotides (primers) and dNTPs were bounded to the column. Purification of PCR products was carried out by instruction manual.

2.2.1.8 Multiplex PCR

In this type of PCR, it is possible to amplify more than one DNA fragment using more than one primer pairs in the same PCR reaction mixture. In this study, the multiplex PCR was used for checking the transgenic *N. tabacum* plants on DNA level. Four multiplex PCR system used in this study for the constructs pYLATC7_Hydrilla and GTDEF+MMPEM. Primers were designed for gene sequences which can bind inside the genes and should yields single right product. In the destination vector primers can bind on various places of homozygous sequences from same promoter and PA and can produce false multiple PCR products. Therfore, it was better option that to design primers can bind inside the gene sequence. The reaction conditions (e.g. template concentration, annealing temperature and extension duration) were optimized for the individual experiments.

2.2.1.9 First strand cDNA synthesis from RNA

Isolated total RNA samples from transgenic *N. tobacum* plants were digested with DNAse enzyme to remove the genomic DNA. One unit of the DNAse enzyme with buffer (Table 2.30) was added to 5 µl of the isolated RNA and then the reaction mixture was incubated at 37°C for 10-15 min. The DNAse activity in the reaction mixture was stopped by incubating the sample at 65°C for 15 min. 1 µl sample was visualized on 1% (w/v) agarose gel containing ethidium bromide to check whether the genomic DNA was digested or not and to be sure that the RNA was not affected. After that the cDNA (Table 2.31) was synthesized as follows: 2 µl from the isolated RNA sample (about 100-800 ng) were mixed to 10 µl bidest H_2O and 1 µl oligo (dT) 18 primer (10 pmol/µl). The reaction mixture was incubated 5 min at 65°C, cooled and 2 µl dNTPs, 4 µl MMLV-RT buffer (5 x reverse transcriptase buffer) and 1.5 units of reverse transcriptase enzyme (MMLV-RT) were added. Then the reaction mixture was incubated for 40 min at 37°C. Later the enzyme activity was stopped at 65°C by incubation for 15 min. For negative samples, the sample without reverse transcriptase was not added, i. e. in the negative samples, no cDNA should be synthesized but conditions are otherwise identical. The synthesized cDNA was used as a template for qRT-PCR amplification.

Table 2.30: DNAse Digestion

Component	End Concentration
DNAse I	1 U
DNAse buffer I	1x
RNA	1-5 µg
H_2O	Add up to 20 µl

Table 2.31: Reverse Transcription

Components	End concentration
dNTP-Mix	20 nmol
MMLV-buffer	1x
MMLV-RT	200 U
H_2O	Add up to7 µl

2.2.1.10 RNA analysis with RT-PCR

The quantitative or Real Time PCR is used not only for the amplification of specific fragments of DNA but also for the quantitative analysis of the resulting products in each cycle throughout the amplification reaction. In this type of PCR, SYBR Green I is used to give the fluorescence signals that indicate the formation of double stranded DNA and as a result the amount of double stranded PCR product can be measured each cycle by this fluorescence. If fluorescence is plotted against cycle number, the accumulation of PCR

products can be visualized on a curve. The melting temperature curves, which are formed as a result of plotting the first deviation of the fluorescence against temperature help in the identification of the products in addition to other functions (Meuer *et al.,* 2001). The ABI-7000 (Applied Biosystems) was used for amplification of about 300 bps from the first strand cDNA that was synthesized from the isolated RNA from the transgenic plants. By this, it was possible to check the expression of the transgenes at the RNA level. The instructions in the qPCR™ Core Kit for SYBR® Green I (Invitrogen, Carlsbad, United States) were followed using reading frame specific forward and reverse primers. The resulting products from the qRT PCR were visualized on 2% (w/v) agarose gel containing ethidium bromide.

2.2.1.11 Restriction Digestion of DNA

The analysis of cloned plasmids requires the cleavage of DNA using restriction enzymes for the production of certain DNA fragments. One unit of the enzyme with 1 µg DNA and the corresponding buffer (1x) has been mixed and incubated for at least 45 min at 37°C. An inactivation done by heating to the specific inactivating temperature mention in the manufacturer's manual of specific restriction enzyme.
Cutting efficiency of PCR products at DNA ends were digested with enzymes should be precise. The efficiency can be viewed for restriction enzymes shown in http:// http://www.fermentas.com/techinfo/re/restrdigpcrii.htm (St. Leon-Rot).

2.2.1.12 Dephosphorylation of DNA 5´-ends

Phosphatase catalyzes the removal of 5´-phosphate groups from DNA and RNA. Since the phosphatase treated fragments lack the 5´-phosphoryl termini required for ligases, so they cannot self ligate. This characteristic was used to decrease the vector background in cloning strategies. A standard approach for the dephosphorylation is shown in Table 2.32. Incubation condition for 5' overhangs was 15 min. at 37°C or for "blunt ends" and 3'-overhangs was 60 min. Then, the enzyme was inactivated by incubation at 65°C for 5 min.

Table 2.32: Standard chart for the Dephospho-phorylation of DNA-5´prime

Components	End concentration
DNA	1-5 µg
Antarctic Buffer	1x
Antarctic Phosphatase	5 U
H_2O	Add up to 20 µl

2.2.1.13 "Blunting" of DNA 5 '- or 3'-overhanging ends

At the time of cloning, if the fragment ends of the DNA for ligations were not compatible then blunting of the overhangs was performed and for this purpose T4 DNA polymerase was used. T4 DNA catalyzes the synthesis of DNA in the 5´→ 3´ direction in the presence of template and primer. This enzyme also has a 3´→ 5´ exonuclease activity which is much more active than that found in DNA polymerase I (*E. coli*). Unlike *E. coli* DNA polymerase I, T4 DNA Polymerase does not have a 5´→ 3´ exonuclease function. The reactions condition were incubated for 15 min at 12°C and inactivate the enzyme at 75°C for 10 min. Table 2.33 shows the standard protocol for blunting of DNA.

Table 2.33: Standard chart for the Blunting of DNA ends

Components	End concentration
DNA	1 µg
dNTP	2 mM
T4-DNA-Polymerase	1 U
H_2O	Add up to 20 µl

2.2.1.14 Ligations reaction

Ligation were performed as follows (Table 2.34) and mixture incubated overnight at 16°C. Ligase and the ligation buffers were transferred on silica column (Invisorb® spin PCRapace Kit, Invitek, Berlin).

Table 2.34: Ligations protocol

Components	End concentration
Vector: Insert	1:6
T4 Ligase	5U
T4Ligase-buffer	1x
H_2O	add up to10 µl

2.2.1.15 TOPO TA cloning

Cloning in topovector was done by according to the manufacture manual TOPO TA cloning kits.

2.2.1.16 Gateway cloning

Gateway cloning technology is based on the site-specific recombination system used by lambda phage integrate its DNA in the *E. coli* chromosome. In which, used specific recombination sites called *att*P in lambda phage and *att*B in *E. coli*. The integration process (lysogeny) is catalyzed by 2 enzymes: the lambdaphage encoded protein Int (Integrase) and the *E. coli* protein IHF (Integration Host Factor). Upon integration, the recombination between *att*B (25 bp) and *att*P (243 bp) sites generate *att*L (100 bp) and *att*R (168 bp) sites that flank the integrated lambdaphage DNA.

The gateway reactions are in vitro versions of the integration and excision reactions. To make the reactions two directional, slightly different and specific site were developed, att1 and att2 for each recombination site. These sites react very specifically compatible with each other. For instance in the LR Reaction attL1 only reacts with attR1 resulting in attB1 and attP1, and attL2 only with attR2 giving attB2 and attP2. The reverse reaction (BP Reaction) shows the same specificity. Gateway system was commercially developed by Invitrogen (leak, NL). The gateway cloning was performed with the gateway LR Clonase II according to the manufacturer instruction. A standard chart is shown in Table 2.35. Equimolar amounts of entry clone and destination vector were used for the reaction.

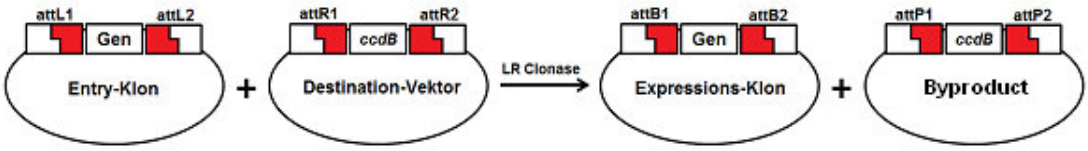

Figure 2.27: Gateway LR reaction
Gateway LR reaction: Gene of interest in entry vector (flanked by attL sites) is transferred into a destination vector (attR sites). The reaction of the attL sites with the attR sites exchange to attB and byproduct with attP sites. The lethal ccdB gene for a negative selection against the unwanted byproduct.

Table 2.35: Standard chart for gateway Recombination

Components	Recombination	Control
Entry-Vector	50 ng	50 ng
Destination-Vector	200 - 400 ng	200 - 400 ng
TE-Puffer pH 8,0	ad 4 µl	ad 5 µl
LR Clonase	1 µl	
Incubation at 25°C für 2 - 4 hours		
Proteinase K	1 µl	1 µl
Incubation at 37°C for 10 min		

2.2.1 Analysis of plant growth

i) Plant growth analysis

Plant growth was analysed by measuring three growth parameters.

1. Plant height was measured from the surface of soil to the uppermost leaf. The measurement was performed several times during the whole experimental period.
2. Leaf number was counted from the 6-8 weeks old plants several plants and several lines.
3. Stalk diameter was measured at the position approx. 1 cm above the base of leaf stalk of the 7th leaf on a certain day.
4. Fresh weight of the above-ground plant part was measured just before the end of experiment.
5. Formation of flowers and fruits was observed during the whole experimental period. At the end of experiment, the fruits maturating degree on each plant was determined. In the T_0 generation for HC_4l transgenic lines showed earlier formation of flowers and fruits than

the control lines. The growth rate (increase in height per day) and the average length of internode were calculated for each plant.

ii) Determination of the leaf area

For the determination of leaf area, length and width of the leaves were measured.
Leaf area was determined using following formula (Provided by Research Center Jülich, IGB2).

Formula: $A = 3{,}73 \times (L \times W/100) + 0{,}011 \times (L \times W/100)^2$

Leaf area: (A), length: (L) and width: (W) of the leaf.

2.2.2 Microbiological Method

2.2.2.1 Transformation of competent *E. coli* (DH5α) by heat-shock

As soon as the competent cells were thawed, plasmid DNA (up to 10 to 100 ng) or 1-3 µl from the ligation products were mixed gently with the competent cells and then incubated on ice for 30 min. The cells were incubated at 42°C for 90 seconds and placed directly on ice for 2 min. Later 1 ml of LB medium was added immediately on heat shocked bacteria in the tube. The transformed cells were incubated at 37°C for 45 min with continuous shaking (200 x g). Transformed cells were plated onto LB agar plates supplemented with appropriate antibiotics and incubated at 37°C overnight.

2.2.2.2 Preparation of electro competent *E. coli* cells

Electro competent *E. coli* cells (TOP10) were preculture from one individual colony from LB plate. Single colony was inoculated in 5 ml LB medium with 20 mg/l of streptomycin and stirred on a rotary shaker at 37°C overnight. 500 ml LB medium was inoculated with 5 ml overnight culture and stirred on a rotary shaker at 37°C until OD_{600} of 0.8-1.0 was reached. The main culture was incubated on ice for 20 min and then centrifuged at 4500 rpm for 10 min at 4°C. The supernatant was discarded and pellet washed with 10% glycerol successively with 500 ml, 300 ml and 30 ml. Finally the pellet was suspended in

1 ml of 10% glycerol from which 50 µl each aliquot were frozen in liquid nitrogen and then store at -80°C for the transformation.

2.2.2.3 Transformation of electro competent *E. coli* cells

Electrocompetent cells (100 µl) were thawed on ice before the electroporation. 10 to 100 ng of plasmid was added on cell mix and incubated on ice for 5 min. Later cell mix were transferred in to the prechilled electroporation cuvette and assembled into a safety chamber (Electroporator). Then trigger the pulse (2.5 kV) less than 30 sec. Then cells were resuspended in 1 ml of LB medium in a 2 ml eppendorf tube and stirred on shaker at 37°C for 45-60 min for the regeneration. Later cells were place on an appropriate antibotic LB plate and incubate overnight at 37°C.

2.2.2.4 Preparation of electro competent *Agrobacterium* cells

For the preparations of electrocompetent *Agrobacterium* cells, first the single cell was preculture in LB/YEB medium overnight. LB medium used for the prepartion of electrocompetant AGL1 strain and YEB medium used for the preparation of GV3101 strain. Individual colonies were inoculated in 50 ml medium for incubation at 28°C for one day. Second day 50 ml pre culture was transferred into 250 ml medium as a main culture. It was incubated for another day at 28°C. The culture was centrifuged for 4000 rpm for 20 min at 4°C and discarded the supernatant. The pellet was successively washed with 240 ml, 120 ml and twice 80 ml sterile H_2O. Then pellet was washed again with 40 ml of 10% glycerol and resuspend in 600 µl 10% glycerol. 50 µl each aliquot were frozen first in liquid nitrogen and then store at -80°C for the transformation.

2.2.2.5 Transformation of electrocompetent *Agrobacterium* cells

0.2-1.0 µg of plasmid DNA was added in the thawn aliquot of *Agrobacterium* electro-competent cells and incubated in ice for 3 min. The cell-DNA mixture was transferred into a prechilled electroporation cuvette (0.2 cm) and assembled into a safety chamber

(electroporator). After application of the pulse (25μF/2.5kV/200Ω), the cells were diluted in 1 ml of YEB mediumin a 2 ml eppendorf tube and incubated on rotary shaker at 28°C for 2 to 3 hours for regeneration. Finally, 1-10 μl of the cells were plated on YEB or LB plates containing appropriate antibiotics and incubated at 28°C for at least 3 days.

2.2.2.6 Transient transformation of *Nicotiana tabacum*

Agrobacterium colonies were checked by PCR for each gene for the HC_4l and MMPEM pathway. Positive *Agrobacterium* colonies were used for the plant transformation. In the transient transformation, first main culture were inoculated with postive *Agrobacterium* colonies in LB medium and incubated at 28°C overnight. Over the next day cells were centrifuge and resuspended the pellets in an infiltration media until the 0.8-1 at OD_{600}. In the transformation method, 2 ml syringe with agrobacterium suspension was used. Lower surface of the leaf were scratched and squeezed with gentle pressure and push the agrobacterium suspension into the the intracellular space of the leaf. Transformed plants were incubated at 23-25°C overnight in the dark then again incubated at 23-25°C and 16 hours of light period for 1-2 days. After two days of incubation transformed leaves used for the RNA isolation (Material and Methods 2.2.1.2).

2.2.2.7 Stable transformation of *Nicotiana tabacum*

Stable transformation of *Nicotiana tabacum* was performed by the mediation of *Agrobacterium*. Protocol was based on the "leaf disc" transformation method described by Horsch *et al.,* (1985), De Block (1988) and Dietze *et al.,* (1995).

Agrobacterium positive colonies were plated on LB (AGL1) or YEB agar plates (GV3101). These plated agrobacterium were incubated for at least three days. After incubation, the cells were scraped with a spatula from the plates and resuspended in 200 ml of YEB induction medium (Table 2.36). The main culture (200 ml of YEB) was incubated overnight at 28°C on shaker and reaching an OD_{600}. 0.5-1. After centrifugation at 4800 rpm at 4°C for 20 min resulting pellet was resuspended in an infiltration media (Table 2.37) until the final OD_{600} 1.0. The resulted infiltration media used for the leaf disc transformation. Sterile leaves of the *Nicotiana tabacum* (plantlets from the weckglass)

were cuted into small pieces with the scalpel (approx. 0.5-1 cm²). Leaf discs were incubated in to the *Agrobacterium* suspension around 10 minutes at room temperature. Then the incubated leaf pieces were put on wet whatmann filterpaper in the petri plates and sealed with parafilm. Later petri plates with leaf discs were incubated at 23-25°C for 2 days in the dark room. After 2 days the leaf discs were washed with sterile water with 200 mg/ml cefotaxime, and put on to the MSII plates (Table 2.38), for the callus formation at 23-25°C at 16 hour light period. Every 2-3 weeks calli have been transform on fresh MSII plates. After 4-5 weeks regenrated shoots were cut off from the calli and transformed on the root induction MSIII medium (Table 2.39). Rooted plantlets were transferred to soil and grown in greenhouse.

Table 2.36: YEB Induction medium (pH 5.6)

Components	End concentration
Nutrient Broth	0.8 % (w/v)
Yeast extract	0.1 % (w/v)
Sucrose	0.5 % (w/v)
$MgSO_4$	2 mM
MES pH 5,6	10 mM
Acetosyringone	20 µM
Carbenicillin	50 mg/l
Kanamycin	15 mg/l

Table 2.37: Infiltrations medium (pH 5.6)

Components	End concentration
Sucrose	2% (w/v)
MS-Salt (Basal Salt Mixture)	0.43% (w/v)
MES pH 5,6	10 mM
Acetosyringone	200 µM

Table 2.38: MSII Medium with Plant agar

Components	End concentration
MS-Medium with Plant agar	4.4 g/l
BAP (6-Benzyl-aminopurin)	1 mg/l
NAA 1-Naphthalene-acetic acid	0.1 mg/l
Hygromycin/Kanamycin	50/100 mg/l
Cefotaxim	200 mg/l

Table 2.39: MSIII Medium

Components	End concentration
MS-Medium with Plant agar	4.4g/l
Hygromycin/Kanamycin	50/100 mg/l
Cefotaxim	200 mg/l

2.2.3 Biochemical Methods

2.2.3.1 Determination of protein concentration

Proteins were determined according to the method described by Bradford (1976). This test is based on a binding of the dye Coomassie brilliant blue G-250 to proteins in acid solution. Leaf extract with 300 µl of Bradford reagent at absorbance at 595 nm showed the protein concentration in the solution. After 15 min of incubation at room temperatue, the extinction coefficient at 595 nm was measured against blank reagent prepared from 2 µl of the appropriate buffer and 300 µl of Bradford reagent. Bovine serum albumin (pH 7.0, SERVA) was used as standard in a range between 1 and 10 µg.

Table 2.40: Bradford Reagent

Components	End Concentration
Coomassie brilliant blue G-250	100 mg/L
Ethanol (96%)	50 ml/L
H_3PO_4 (85%)	100 ml/L
H_2O	add 1L

2.2.3.2 Determination of enzyme activities

The determination of enzyme activities were based on extinction change of samples by NADH/NADPH oxidation or NAD/NADP reduction with spectral colorimetry ELISA reader and measuresd the enzymes dependent on NAD(H) or NADP(H). The activity of the enzyme measured is a direct the extinction reduction per unit of time. Specific enzyme activity in mU per mg protein was measured shown formula above.

$$\text{Specific activity } \left(\frac{\text{mU}}{\text{mg}}\right) = \frac{\Delta E \cdot VK \cdot 1000}{Vp \cdot Cp \cdot \varepsilon \cdot d}$$

Formula 2.7: Calculation of the Specific enzyme activity
Abbrevation: **Δ**E: maximum absorbance change per min, VK: Volume of the reaction mixture (0.3 ml), Vp: Volume of the sample (0.015 or 0.030 ml)**,** Cp: Protein concentration in extract (mg/ml), ε: molar extinction coefficient (NADH/NADPH = 6220 or 6310 l mol^{-1} cm^{-1})**,** d: thickness of the cuvette (0.8 cm).

2.2.3.2.1 Hydrilla PEP carboxylase (PEPC) activity measurements

Phospho*enol*pyruvate (PEP) is catalyzed by phospho*enol*pyruvate carboxylase and it is converted into oxaloacetate (OAA). In the presence of malate dehydrogenase (MDH), OAA is further reduced to malate while NADH is oxidized into NAD^+. The decline of the optical density of NADH was measured at 340 nm on spectrophotometer. It was directly proportional to the consumption of PEP. One unit (U) enzyme activity is defined as the amount of PEPC oxidizing 1 µmol of NADH per minute at 25°C. The specific activity of PEPC is defined as U per mg protein. The reaction was started by the addition of 10 µl leaf extract and later added 290 µl of reaction mixtures and reaction mixtures omitting PEP served as a control. The decline in NADH was calculated from the linear part of the curve during the first minutes. The values for protein samples were corrected by subtracting non-specific NADH turnover in controls. HvPEPC Reaction buffer was followed according to Jiao and Chollet 1988, and further modified according to Magnin et al. 1997.

Table 2.41: HvPEPC Reaction mixture

HvPEPC Reaction mixture	End concentration	
Hepes-KOH	1000	mM
$MgCl_2\,6H_2O$	1000	mM
$NaHCO_3$	1000	mM
DTT	1000	mM
NADH	20	mM
MDH	12000	U/ml
PEP	100	mM
H_2O	upto 1	L

Reaction 2.1: Reaction for the measurement of PEPC

PEP + HCO_3^- < (**PEPC**) > OAA + P
OAA + NADH < (**MDH**) > Malate + NAD

2.2.3.2.2 NAD-malic enzyme (ME) activity measurements

NAD dependent malate enzyme (EC 1.1.1.38) catalyzes the decarboxylation of malate to pyruvate while NAD is reduced to NADH. The measurement of malic enzyme activity was described by Bologna et al. (2007). Aspartate acts as an activator for the enzyms. The reaction was started by the addition of 10 µl leaf extract on plate well and later added 290 µl of reaction mixtures (Table 2.42). Reaction mixture omitting malate served as controls (table 2.42). The absorbance change was measured for 30 min at 30°C.

Reaction 2.2: Reaction for the measurement of malic enzyme

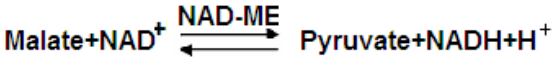

Table 2.42: NAD-ME Reaction mixture

NAD-ME Reaction mixture	End concentration
Tris-HCl	50 mM
$MnCl_2$	10 mM
NAD	0.5 mM
Aspartate	2 mM
Malate	10 mM

2.2.3.2.3 NAD-dependent malate dehydrogenase (MDH) activity measurement

The NAD-dependent Malate dehydrogenase (EC 1.1.1.37) catalyzes the reversible reduction of the OAA to malate while NADH is oxidized into NAD^+. The measurement of enzyme activity was followed according to Sutherland and McAllister-Henn (1985). EDTA was used to sequester metal ions in aqueous solution. Bivalent cations (Mg^{2+}, Mn^{2+}) required for MDH as a cofactor. The reaction was started by the addition of 15 µl leaf extract and later added 285 µl of reaction mixtures (Table 2.43). The absorbance change was measured at 30°C for 30 min.

Reaction 2.3 Reaction for the measurement of malate dehydogenase

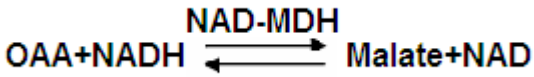

Table 2.43: NAD-MDH Reaction mixture

NAD-MDH Reaction mixture	End concentration	
Hepes-KOH	1000	mM
NADH	100	mM
EDTA	500	mM
DTT	1000	mM
OAA	100	mM
H_2O	up to	1 L

2.2.3.2.4 PEP synthase (PEPS) activity measurement

Phospho*enol*pyruvate synthase (PEPS; EC 2.7.9.2) catalyzes the synthesis of phospho*enol*pyruvate from pyruvate and ATP in the presence of divalent metal ion (Mg^{+2}) by the following reversible reaction (Berman and Cohn, 1970; Cooper and Kornberg, 1965). The PEPS (EC 2.7.9.2) was assayed spectrophotometrically in which the pyruvate dependent production of PEP was linked to NADH oxidation via PEP carboxylase and malate dehydrogenase. The reaction was started by the addition of 15 µl leaf extract on plate well and later added 285 µl of reaction mixtures (Table 2.44). Reaction mixture omitting pyruvate or ATP served as a control. Sample without ATP was measured befor the samples with ATP.

Table 2.44: The PEPS Reaction mixture

PEPS Reaction mixture	End concentration	
Tris-HCl 8.0	1000	mM
$MgCl_2$	1000	mM
DTT	1000	mM
$NaHCO_3$	1000	mM
Pyruvate	1000	mM
Glc6P	100	mM
NADH	20	mM
PEPC	10	U/ml
MDH	12000	U/ml

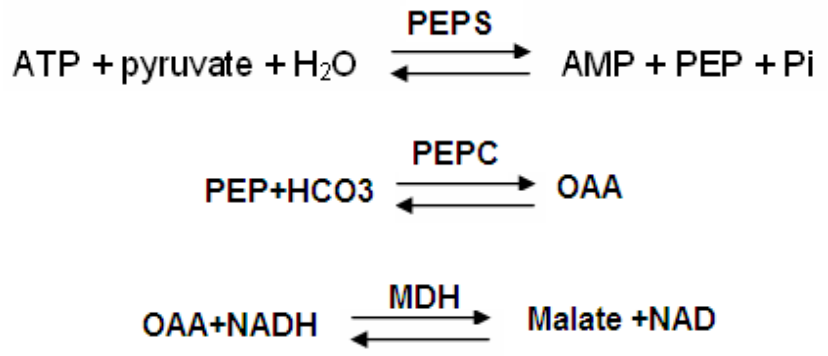

Reaction 2.4: Measurement of PEPS activity

2.2.3.4 Extraction of soluble and insoluble metabolites from *N. tobacum* leaves

The soluble and insoluble metabolites were extracted from the leaf discs of *N. tobacum* according to (Stitt *et al.,* 1989). One leaf discs (each 2 cm^2) per plant were used for this purpose. The plant leaf discs were harvested in 2 ml eppendorf tubes and immersed immediately in liquid nitrogen. 1 ml of 80% (v/v) hot ethanol was added to the leaf discs. Samples were incubated 15 min at 90°C in a heating block. The leaf discs were then transferred into a new 2 ml eppendorf tube containing 1 ml hot 80% (v/v) ethanol and incubated as before. The extracted leaf discs were then transferred into a new 2 ml eppendorf tube and later used measurement for starch content. Ethanol was evaporated either by incubation in a heating block at 90°C or dried in a speedvac. The pellet was then resuspended in 500 µl bidest. H_2O and then spun down. Supernatent was collected and used for the determination of soluble sugars as glucose and fructose. For extraction of starch, 250 µl of 2 M KOH was added to the extracted leaf discs (as described above). The leaf discs were then homogenized and 250 µl of 2 M KOH was added. The samples were then incubated at 95°C for 45 min. The samples were the centrifuged and 400 µl from the supernatant were transferred into a new 2 ml eppendorf tube. 900 µl of 1 M acetic acid were then added in order to have a pH of 4.8. Samples were then either stored at -20°C or used directly for measuring the starch content. The glucose, fructose, starch and sucrose contents were estimated enzymatically as described by (Stitt *et al.,* 1989). The enzymatic assay tests were performed in 96 well microtiter plates and the OD_{340} change was measured via microplate spectrophotometer (BioTek ELx808 BioTek Vermont, USA), (2.1.2).

I) Determination of glucose and fructose content

Glucose and fructose were extracted as described above (2.2.3.4) and were estimated enzymatically as follows: 20 µl from the previously extracted soluble metabolites were transferred into the well of a microtiter plate. In each well were added 180 µl of the glucose/fructose reaction buffer (2.45). The basic extinction (λ = 340) was measured at 30°C (blank; E0). Then 2 µl of HK/G6PDH (0.7 unit hexokinase/glucose-6-phosphate dehydrogenase) were added. The microtiter plate was then incubated for 15 min at 37°C and the basic extinction E1 (λ = 340) was recorded. Later 2.5 µl of PGI (1.75 units; phosphogluco-isomerase) were added to the tested samples. The plate was further incubated for 15 min at 37°C and the basic extinction E2 (λ = 340) was recorded.

Table 2.45: Glucose/Fructose Reaction buffer

Components	End concentration
Triethanolamine pH 7.6	150 mM
NADP	0.25 mM
$MgCl_2$	5 mM
ATP	2.5 mM

II) Determination of starch content

For determination of starch contents, 100 µl from the extract (insoluble metabolites 2.2.3.4) were mixed with 400 µl of sodium acetate (pH 4.8). Then 1 unit of amyloglucosidase and 2 units of α-amylase were added to the assay mixture. Samples were then incubated 15 h at 50°C. During this incubation starch was converted into glucose equivalents. Samples were then spun down and 20 µl of the supernatants were used for measuring glucose equivalents.

III) Determination of sucrose content

For estimation of sucrose contents, 100 µl from the soluble metabolite extract (2.2.3.4) were mixed with 100 µl of 100 mM citrate-NaOH buffer (Table 2.46). 2 µl of invertase (2 units) added and the samples were then incubated at 37°C for 1 h. 20 µl from this mixture were used for the determination of glucose equivalents as described above.

Table 2.46: Citrate NaOH Puffer

Components	End concentration
Citrat-NaOH pH 4.6	100 mM

$$\text{Sucrose} \xrightarrow{\text{Invertase}} \text{Glucose} + \text{Fructose}$$

$$\text{Glucose} + \text{ATP} \xrightarrow{\text{HK}} \text{Glucose-6-phosphate}$$

$$\text{Glucose-6-phosphat} + \text{NADP}^+ \xrightarrow{\text{G6P-DH}} \text{6-Phosphogluconat} + \text{NADPH}^+ + \text{H}^+$$

Reaction 2.5: Reaction for the measurement of Sucrose

The amounts of glucose, fructose, sucrose, and starch were estimated from the following equation:

$$c(mol/g) = \frac{\Delta E \cdot V_K \cdot V_E}{V_P \cdot A \cdot \varepsilon \cdot d}$$

- $\Delta E_{340} = E_{end} - E_{blank}$
- V_K (L): Volume of the reaction mix (here, 0.0002 L)
- V_E (L): Volume of the metabolite extracts (here, 0.0005 L)
- V_P (L): Volume of metabolite sample in the reaction mix (here, 0.0002 L)
- *A* (m^2): the total area of leaf discs used (here, 0.0003 m^2)
- ε (L x mol^{-1} x cm^{-1}): molar extinction coefficient
- $NADP_+$/NADPH: 6310 L x mol_{-1} x cm_{-1}
- NAD_+/NADH: 6220 L x mol_{-1} x cm_{-1}
- d (Cocciolone *et al*) : the microtiter plate well length (here, 0.6 cm)

IV Determination of malate content

The rate of NAD dependent OAA (oxaloacetate formation is monitered by a coupled NAD reduction via MDH (malate dehydrogenase). GOT (glutamate oxaloacetate-transaminase) remove OAA permenantly out, so that the malate content detect quantitatively 10 µl extract were mixed with 190 µl malate reaction buffer (Table 2.47) in an ELISA plate and the measured basic extiction E_0 at 340 nm and 30°C. After adding 24 U MDH incubates in ELISA reder until a constant value is achived E1. The measurement is based on the specified reaction 2.6.

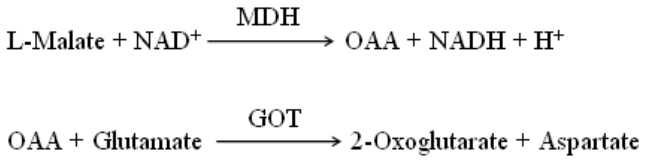

Reaction 2.6: Schematic reaction for malate measurement

Table 2.47: Malate reaction buffer

Components	End concentration
GlyGly-Puffer pH 10,0	1x
NAD	3.5 mM
GOT	1 U/ml

Table 2.48: GlyGlyBuffer

Components	End concentration
Glycylglycin	600 mM
L-Glutamat	100 mM
pH 10.0	

2.2.3.5 Ammonia release assay

The ammonia release assay was performed as described by Gaunt *et al.,* (1998). Leaf disc from *N. tobacum* plants (8 mg each) were harvested and placed in well of a microtiter plate containing 200 µl of incubation medium (Table 2.49). As a blank, 4 wells containing only incubation medium were used. The tested samples were incubated under 100 PAR light intensity for 6 h at 26°C. 20 µl incubated medium from well were transferred into a new microtiter plate containing 100 µl of reagent I (Table 2.50). Samples were mixed and 100 µl of reagent II (2.51) were added. Samples were then incubated at 37°C in dark for 15 min. The samples were then incubated at room temperature for further 15 min. The presence of ammonium ions in the tested samples resulted in an emerald green to dark blue colour which was quantified by measuring the basic extinction at 655 nm in microtiter plate in spectrophotometer (spectra max 340 ELISA Reader, USA) compared to a set of ammonium standards.

Table 2.49: Ammonia release assay Incubations medium

Component	Final concentration
Potassium phosphate buffer pH 5.8	50 mM
Sucrose	2 %
Tween20	0.1 %
2,4 Dichlorophenoxyacetic acid	0.1 mg/l
Phosphinotricin	25 mg/l

Table 2.50: Ammonia release assay reagent I

Component	Final concentration
Sodium salicylate	0.21 M
Trisodium citrate	0.085 mol/l
Sodium tartrate	25 g/l
Sodium nitroprusside	0.4 mM

Table 2.51: Ammonia release assay reagent II

Component	Final concentration
NaOH	0.75 mol/L
Sodium dichloro isocyanurate	2.3 mM

2.2.3.6 Analysis of metabolites by gas chromatography and mass spectroscopy (GC-MS)

The gas chromatography mass spectrometry is a coupled procedure for the regulation of gases and volatile substances. First a temporal separation of the compounds is reached by the gas chromatography. The mass spectrometer serves then for the detection of the components and permits additionally their identification on the basis of their mass spectrum. GC-MS sample analysed by Prof. Dr. Christoph Peterhänsel (Institute of Botany, Hannover).

I. Gas chromatography

Separation of substances in gas chromatography takes place on the basis of their molecular characteristics such as mass and polarity. Once the specimen injected into the injector port of the GC-MS instrument, it vaporizes immediately and then carried by a carrier gas through a capillary column to the detector port of the machine.

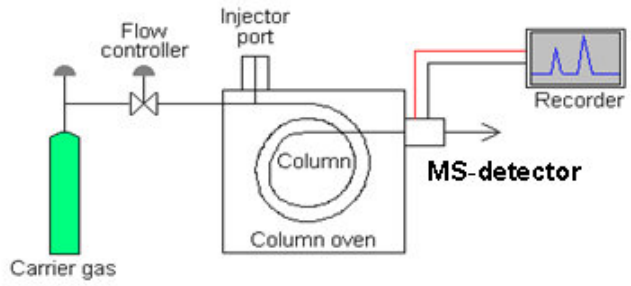

Figure 2.28: Diagrammatic representation of the GC-MS system

The carrier gas is usually an inert gas (as Helium). The column is a metal tube, often packed with a sand-like material (modified polysiloxan) to promote maximum separation.

As the sample moves through the column, the different molecular characteristics determine how each substance in the sample interacts with the column surface. The column allows the various substances to partition themselves. The time elapsed between injection and elution is called the retention time.

The retention time can help to differentiate between some compounds. The separated substancs move to the end of the column into the detector port of the GC machine. Each component produces a specific spectral peak that is recorded electronically (see figure 2.28). The GC-MS machine is working with a standerd temperature program throughout the separating process in Table 2.52.

Table 2.52: The GC-MS machine temperature program

Injector:	250°C
Detector:	280°C
Starting temperature:	70°C, 5 min
Heating level:	5°C/min
Ending temperature:	300°C, 1 min

Table 2.53: Chemicals for GC

Chemicals	Company	O. No.
Water Rotisolv ultra	Roth	HN43.1
Chloroform Rotisolv HPLC	Roth	7331.2
Ethanol	Roth	9065
Ethyl acetat	Sigma	650528
n-Hexan	Sigma	34859
Methoxyamin-Hydrochlorid	Aldrich	226904
Pyridine	Sigma	270407
Adonitol (Ribitol)	Fluka	2240
N-Methyl-N-trimethylsilytrifluoracetamid	Sigma	69479

Table 2.54: Used chemicals in GC-MS (FAMES)

FAMES	Company	O. No.	C No.	Mol. wt.
Methyl octanoate (caprylate)	Aldrich	260673	C9	158.24
Methyl pelargonate (nonanoate)	Aldrich	76368	C10	172.26
Methyl caprate (decanoate)	Aldrich	21479	C11	158.24

Methyl laurate	Aldrich	234591	C13	214.34
Methyl myristate	Sigma	M3378	C15	242.4
Methyl palmitate (hexadecanoate)	Sigma	P5177	C17	270.45
Methyl stearate	Sigma	S5376	C19	298.5
Methyl arachidate (eicosanoate)	Sigma	A3881	C21	326.56
Methyl behenate (docosanoate)	Sigma	B3271	C23	354.61
Lignoric acid Methylester (tetracosanoate)	VWR	SAFF87115	C25	382.66
Methyl hexacosanoate	Sigma	H6389	C27	410.72
Methyl octacosanoate	Fluka	74701	C29	438.77
Triacontanoic Acid Methyl Ester	Ultra	FLSA-030	C31	466.82

II. Mass Spectrometry (MS)

The used mass spectrometer is involved in the GC-MS unit as a detector. This mass spectrometer formed of an ionization source, a molecule accelerator, and a detector. Once the sample left the GC-column, it enters the ionization chamber where a beam of electrons is accelerated with a high voltage. The sample molecules are shattered into well-defined fragments upon collision with the high voltage electrons. Each fragment is charged and travels to the accelerator as an individual particle. In the acceleration chamber the charged particle's velocity increases due to the influence of an accelerating voltage. The charged particles travel in a curved path towards the detector. When an individual charged particle collides with the detector surface, several electrons (also charged particles) emit from the detector surface. These electrons accelerate towards a second surface, generating more electrons, which bombard another surface. Each electron carries a charge. Eventually, multiple collisions with multiple surfaces generate thousands of electrons which emit from the last surface. The result is an amplification of the original charge through a cascade of electrons arriving at the collector. At this point the instrument measures the charge and records the fragment mass as the mass is proportional to the detected charge. The MS unit produces the output by drawing an array of peaks, the "mass spectrum" (m/z). Each peak represents a value for a fragment mass. Peak's height increases with the number of fragments detected with one particular mass. In the current study, two different modes of the MS-scanning were used; Scan-mode and Single-Ion-Monitoring mode (SIM-mode). In the Scan-mode, the mass spectra (m/z) for all substances present in the tested sample are quantified. This type of scanning is used for qualification and quantification of all the

sample components. This will result in an increase in the background as well as in the quantification results.

III. Preparation, derivatisation and injection of samples

In the current study, the amounts of the Glucose, fructose, amino acids, and organic acids in the leaves of *N. tobacum* were quantified. The samples were prepared according to Roessner et al., (2000). 50 mg of leaves from *N. tobacum* plants were harvested and freezed immediately in liquid nitrogen. The frozen leaves were ground in liquid nitrogen to a fine powder with a mortar. 1000 µl precold extraction buffer (Methanol/$CHCl_3$/H_2O as a ratio 1/ 2.5/1) was added. This extraction buffer contains 0.2 mg 13C6 sorbitol per ml as an internal standard. Samples were vortexed and shaked for 6 min at 4°C. Transferred 500 µl of supernatant in a new eppendorf tube and then added 250 µl ultrapure H_2O then samples were vortexed vigorously. The samples were then centrifuged (14000 g) for 2 min. 220 µl from the polar phase were taken and allowed to dry in the vaccuspeed. After the samples were completely dried, added methoxyamination reagent then 30 mg/ml pyridine was added at 40°C and incubated 90 min. In order to completely dissolving the dried pellets, the samples were incubated 1 h at 37°C. Because the volatility of amino acids is normally small and the separation of substance in GC-MS occurred only in its gaseous phase, it was necessary to derivatize the samples before injecting it into the GC-MS system.

IV. Data interpretation

The quantification analysis was done using the 'HP chemstation'software as well as the agilent technologies software provided with the GC-MS system. The maximum spectra, peak area and retention time were quantified via the auto integration function of involved in this software. The real amounts of the single substances were calculated based on weight of the plant material and corrected by 13C sorbitol concentration in each experiment.

Table 2.55: Injection method for GC

Back Inlet Type	Gerstel
Carrier Gas	Helium
Back Inlet Mode	Splitless
Column 2/Back Inlet	
Rate (ml/min)	Initial
Target Flow	2 ml/Min.
Back Inlet Septum Purge	3 ml/Min.
Back inlet Purge Time	60 sec.
Back Inlet Purge Flow	20 ml/Min.
Back Inlet Total Flow	22 ml/Min.
Back Inlet Temp.	Initial 200°C 1 min.
	600°C 320°C 1 min.
Back Inlet Gas Server Flow	15 ml/Min.
Back Inlet Gas Server Time	5 ml/Min.
Oven temp.	Initial 85°C 2 Min.
	15°C/Min. 330°C 6 Min.
Transfer Line	250°C

Table 2.56: Injection-Method with Gerstel MPS

MPS	Liquid	
	Syringe 10 µl	
	Inf. Volume	1,0 µl
	Inj. Speed	100 µl/s
	Fill Volume	3 µl
	Fill Strokes f. Sample	3 µl/s
	Fill Speed	1 µl/s
	Eject Speed	30 µl/s
	Inj. Penetration	30 mm
System	Runtime	25 Min.
	GC Cool down time	10 Min.
	Cryo Timeout	60 Min.
CIS	Heater Mode	Standard
	Initial Temp.	200
	Equilibr. Time	0.05
	Initial Time	1
Ramp 1	Rate CIS	10
	End Temp.	320
	Hold Time	1

Table 2.57: Rinse setting

Rinse Settings		preclean	postclean
1.Wash 2	Ethylacetat	1	2
2.Wash 1	Hexan	1	2
Sample		1	
Fill speed	5µl/s		
Eject speed	50 µl/s		

Table 2.58: MS method

MS-Method	
Acquisition delay	225 sec.
Start Mass	70
End Mass	600
Acquisition Rate	20
Detector Voltage	1550
Electron Energy	-70
Mass Defect Mode	manual
	Verify offset before collecting Data
Start of Run	225 s Filament Off
	225 s End off run Filament On
Source	250°C

2.2.3.7 Measurement of photosynthetic parameters

All gas-exchange and fluorescence measurements were carried out using the LI-COR® photosynthesis portable measuring device version 5, (Lincoln, NE) (2.1.3). A leaf chamber fluorometer (LCF) together with an infrared gas analyzer (IRGA) was provided with the measuring device. The measurements were performed according to Lipka et al., 1999 and Pinelli and Loreto, 2003.

I Measurement of the CO_2 compensation point

The rates of CO_2 assimilation (A) and transpiration (E) as well as the intercellular CO_2 concentrations (Ci) were calculated automatically by the software provided in the measuring device. The measurement of the CO_2 compensation point was at temperature 27°C, and flow rate was 100 µmol s^{-1} and a photon flux density (PFD) of 1000 µmol photon m^{-2} s^{-1} and blue light set at 10% and the humidity was about 70%. After an adaptation period about 30 min until the stomatal conductivity had a constant value. The A/Ci-curve was estimated by measuring the assimilation rates (A) at different CO_2 concentrations (Ca) (40, 60, 80, 100, 150, 200, 250, 300, 350 and 400 ppm).

II The post illumination burst (PIB)

The post illumination burst (PIB) was measured according to Atkin et al., (1998) where the plants were adapted dark overnight then plant leaf was placed in the measuring device under a photorespiratory conditions (i. e. 1000 µmol photon m^{-2} s^{-1}, 100 ppm CO_2). The plant leaf was left to be adapted to the measuring environment for 10 min. The plant leaf was allowed to achieve a steady-state rate of photosynthesis then it was suddenly darkened. As a result, a momentary rapid outburst of CO_2 was recorded before the leaf achieved a steady-state dark respiration (Rn). The difference between this CO_2 burst and Rn equals PIB. The assimilation rates were recorded continuously through out the measurements using a timed lamp automatic program as shown in Table 2.59.

Table 2.59: The PIB measuring protocol

Time	PAR	Ca	Measuring intervals
180 sec	1000 µmol m^{-2} s^{-1}	100 ppm	2 sec
600 sec	0 µmol m^{-2} s^{-1}	100 ppm	2 sec
180 sec	1000 µmol m^{-2} s^{-1}	100 ppm	2 sec

3 Results

3.1 Project A

3.1.1 Establishment a novel pathway in C_3 plants for assimilation of CO_2 under in vicinity of rubisco

Ribulose-1,5-bisphosphate carboxylase oxygenas (Rubisco) is a bifunctional enzyme. It catalyses the addition of CO_2 to ribulose-1,5-bisphosphate (RuBP) through the photosynthetic carbon reduction cycle in two molecules of 3-phosphglyecerate (3PGA), which are then metabolized to triose phosphate. It also catalyzes the addition of O_2 to RuBP to produce 3-PGA and 2-phosphoglycolate. The 2-phosphoglycolate which is the potent inhibitor of chloroplastic function (Anderson, 1971) is metabolized in three compartments of the leaf cell such as the chloroplast, the peroxisome and the mitochondria. The metabolic process of 2-phosphoglycolate involves several enzymatic reactions and transport processes (Leegood et al., 1995). The 2-phospogycolate is subsequently recycled back to 3PGA and this process is called photorespiration.

Photorespiration is an energy consuming process (e.g. ATP, NH_3, and CO_2). The process of photorespiration diminishes the efficiency of CO_2 assimilation and the yield of C_3 crop plants. Due to the presence of O_2 at the site of Rubisco, the competitive inhibition of CO_2 fixation can be reduced by almost 50% in ambient air and high temperature (Chen and Spreitzer., 1992; Jordan and Ogren., 1984). On the other hand C_4 plants possess a CO_2 concentrating mechanism by which CO_2 is ligated to PEP by phospho*enol*pyruvate carboxylase and a C_4 compound, oxaloacetate is formed. This C_4 acid is reduced to malate, which is then transported to the bundle sheath cells (Kranz anatomy) decarboxylated again and CO_2 is formed to ribulose-1,5-bisphosphate. In the bundle sheath cells no oxygenase reduction can be measured. However, segregation of mesophyll cells and bundle sheath cells is not necessary for a CO_2 concentrating mechanism. Some submerged living aquatic species like *Hydrilla verticilliata* can induce a C_4 like CO_2 concentrating mechanism in single cell type when CO_2 concentration becomes lesser. *Hydrilla verticilliata* is a single cell type C_4 species which induces the C_3 to a C_4 type CO_2 fixation system in single cell when the surrounding CO_2 concentration becomes limited. In the present study it was attempted to mimic the '*Hydrilla* C_4 like single cell' (HC_4l)

mechanism in tobacco plants. A novel pathway was created, in which oxaloactate which is formed in the cytoplasm by PEP-carboxylase is transported to the chloroplast, reduced to malate which is decarboxylated to CO_2 and pyruvate is formed in the vicinity of Rubisco. This results in a higher concentration of CO_2 at the site of Rubisco which increases the rate of photosynthesis. As a result, of increased photosynthesis the increased biomass of the C_3 study plant was aimed.

This pathway includes six active enzymes and one antiporter all together seven genes which have to be transformed into *Nicotiana tabacum* plant. For the transformation of the complete pathway into the plants a multigene construct had to be created which carries seven transgenes (promoter, structural gene, polyadenylation cassette). The large plasmid was constructed by the MultiRound Gateway technology.

3.1.2 Construction of Multigene pathway in a single vector

The principle of gateway recombinational cloning is this system takes the advantage of the site specific recombination reactions enabling the bactriophage lambda (λ) to integrate and excise itself in and out of the bacterial chromosome (Katzen, 2007). Gateway protocols rely essentially on the BP and LR clonase reactions (Hartley et al., 2000). In the present work the LR reaction was used for the cloning of multiple genes. Entry clones and destination vector are the key substrates in this reaction and catalyzed by the LR clonase II enzyme. This mix consists of integrase, integration host factor and the phage excisionase. Gateway LR clonase II mix catalyzes in vitro recombination between entry clone (attL) and an destination vector containing attachment R and create an expression clone containing a attB sites (Karimi et al., 2007). The multiple rounds of gene recombination by LR reaction called as 'MultiRound Gateway'. The establishment of the MultiRound gateway method for the multigene pathway was essential for the achievement of our aim for the transformation of multiple genes in a single event. In this system the vectors were used according to Chen et al., 2006; Liu *et al.,* 1999 and internal changes made by Matthias Buntru (BioI RWTH Aachen). The gateway entry vectors and destination vector were design to carry large complex DNA fragments and which can shuttle through the *E. coli* and *A. tumefaciens*.

3.1.3 Construction of the Gateway Entry Vectors

The attachment sites sequences used throughout the work for the gateway Entry Vectors were from Chen *et al*. (Chen et al., 2006; Wang et al., 1998) as shown in fig. 3.1.

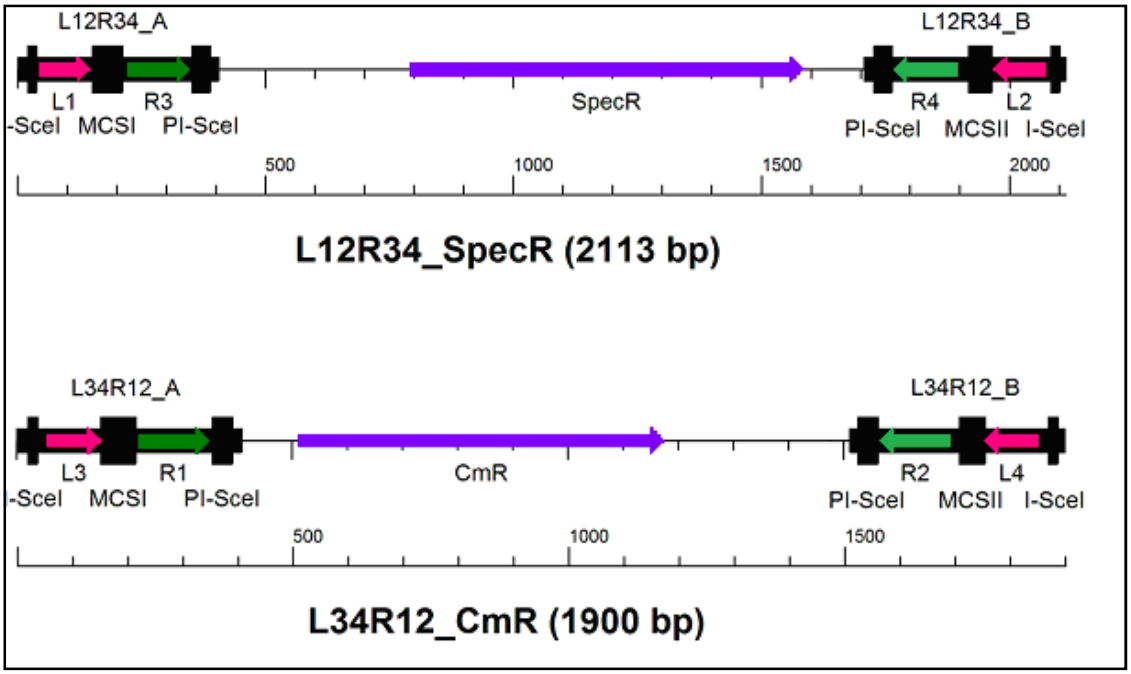

Figure 3.1: Gateway Entry Vectors with attachment regions for MultiRound Gateway recombination
L12-34 and R12-34 multiple cloning sites (MCSI and MCSII), recognition sequence of homing endonuclease I SceI and PI-SceI are in black colour, two selection markers SpecR and CmR are used for the selection after successful recombination.

The key of the recombination, a first multiple cloning site (MCSI) is in between the attachment sites L1, R3 and L2, R4 (Material and Methods 2.1.8.1) used for the integration of the expression cassette which allowed to recombination into the destination vector. The second multiple cloning site (MCSII) is in between R1 and L3, L4 and R2, and which allows to integration of second fragment. The two restriction sequences from homing endonuclease PmeI and SceI are used for recombination event for the linearization of the entry vector. The use of homing endonuclease has the advantage that they are extremely rare in natural sequences. The linearization of gateway entry vectors was done to prevent the cotransformation of entry vector and destination vector in the same *E. coli* cell.

3.1.4 Construction of the destination vector

The destination vector for MultiRound Gateway recombination was created for several requirements of the transformation in the *agrobacterium* and plants like:
i) it should be compatible to the entry vector,
ii) it must be able to carry stable large DNA fragments in *E. coli* and *A. tumefaciens*,
iii) it must have the Cis element sequences, the LB (left border) and RB (right border) for the agrobacterium mediated transformation in plants, which should signals at the beginning and at the end of the T-DNA for the vir proteins and are therefore essential for the transformation, iv) the gateway destination vector should have the SAR region which ensures the stable expression of transgenes transferred to the host,
v) Two selection markers CmR ccdB is the potent inhibitor to *E. coli*. and used for the selection of recombination in the destination vector.
The assembled destination TAC vector (transformation-competent artificial chromosome) named as the pYLTAC7 (Material and Methods 2.1.8.2) with all of necessities discussed above. This vector also includes the P1 replicon and the lytic P1 replicon from the P1 phage replication in *E. coli*. The vector possesses an origin of replication, the lytic replicon which is the under control of the lac promoter in order to get a to higher copy numbers. The vector has the origin of replication for replication in *Agrobacterium tumefaciens* of Ri plasmid of *A. rhizogenes* (root inducing). It also contains the Cis elements LB and RB and a hygromycin resistance gene for the selection of transgenic plants. The SAR element cloned into the pYLTAC7 has been isolated from another destination vector (Liu *et al.,* 1999; Early et al., 2006). Details about the destination vector are shown in the materials and methods (2.1.8.2).

3.1.5 MultiRound Gateway recombination

This system is based on multiple rounds of recombination of two components (entry vector which is also called donor vector and destination vector) which is called a MultiRound Gateway recombination. Three important vectors were used for the MultiRoundGateway recombination pYLTAC7_R12_CmR_ccdB_SAR (destination vector) pUC325_SpecR and pUC324_CmR (gateway entry vectors). Transgenes

delivered sequentially into gateway compatible destination vector through the alternate use of entry vector by LR reaction. Gateway entry vectors were constructed by using the gene cassette from the plant vectors for the *Hydrilla* mimic pathway (HC_4l). Multiple rounds of the LR recombination reactions (7 recombination events) were performed, to transfer DNA fragment (gene cassette) from entry clones to the destination vector. LR recombination was done according to manual instructions (Invitrogen, CA) with some small changes e.g. extending the incubation time because of the larger size of the plasmid (Material and Methods 2.2.1.16).

First two rounds of recombination had shown in figure 3.1.1. The first round of LR recombination was performed between pYLTAC7_R12_CmR_ccdB_SAR and pUC324_SpecR_Mle (linearized by PmeI for avoiding the formation of wrong clones due to the co-transformation of entry and destination vector).

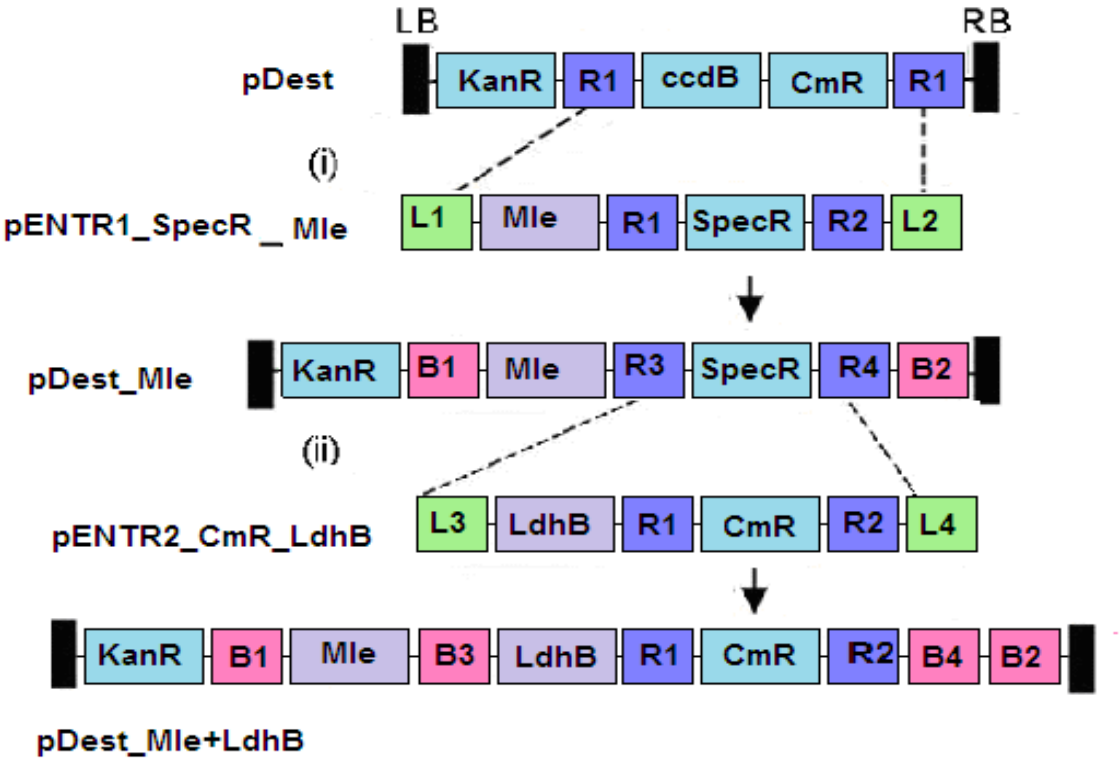

Figure 3.1.1: Multiple Rounds of LR recombination reaction
Two rounds of reaction are shown above. Genes Mle (malate lactate antiporter and LdhB (lactate dehydrogenase) used for showing the two recombination events. pUC325_SpecR_Mle used as an entry vector and with destination vector perform first LR recombination. pUC324_CmR_LdhB used as a second entry vector and performed a second LR recombination. The pYLTAC7_R12_CmR_ccdB_SAR used as a destination vector for carrying multiple gene fragments.

In this round of LR recombination pYLTAC7 (destination vector) was leads to the change in resistance marker CmR to SpecR and also integrates Mle gene cassette with the attachments sites R3-4. The resulted byproduct CmR ccdB did not survive in TOP 10 cells due to the presence of ccdB gene (toxic to *E. coli*). Some of the transformants were carried only parental vectors (destination vector, entry vector). Different byproducts after the recombination did not survive because of the double selection spectinomycin and kanamycin antibiotics. The resultant right transformant pYLTAC7_Mle were survived on selection plate. The second round of recombination was in between entry vector pUC324_Ldhb and destination vector pYLTAC7_Mle with attachment sites R3-4. In this round SpecR replaced back to CmR from the entry vector pUC324_Ldhb. The expected recombinants were selected on kanamycin and chloramphenicol antibiotic and the wrong clone means pYLTAC7_Mle did not survived on this selection. After second round of recombination destination vector received two genes Mle and LdhB. After the recombination, vector called pYLTAC7_Mle_Ldhb, after the alternate repetitions of the process described above with the additional targeted genes (Entry vector). The recombination conducted in seven round of LR reaction and resulted in a "Destination vector" (pYLATAC7_Mle, LdhB, HvPEPC, MDH, LdhA, NAD-ME, PEPS) (Material and Method 2.2.8.5) carrying with seven functional fragments. After each LR recombination reaction constructs confirmed by restriction digestion (Results Fig. 3.1.5) and PCR. Enzymes AscI and BamHI were used for the restriction digestion (Result Fig. 3.1.5).

3.1.6 Novel biochemical pathway like single cell *Hydrilla verticilliata* plants, aiming to increase CO_2 concentration in the chloroplast of C_3 plant

Our long term attempt is to introduce a single-cell C_4 like pathway into C_3 plants in which the CO_2 captures and release event occurs in the mesophyll cells, in the similar way like the well-known aquatic plant *Hydrilla verticillata*. The present pathway mimics the *Hydrilla* like single cell C_4 photosynthetic (HC_4l) pathway and creates one unique approach for the fixation of CO_2 in a single cell of C_3 plants. This pathway shows the important implications for the multiple genes channel for the carbon in single cell from cytoplasm to chloroplast. The new C_4 pathway involves main steps like: initial fixation of

CO_2 by phospho*enol*pyruvate carboxylase (PEPC) to form C_4 acid ii) decarboxylation of C_4 acid to release CO_2 at the site of the Rubisco (Calvin cycle) and iii) regeneration of the primary CO_2 acceptor phospho*enol*pyruvate (PEP) by phospho*enol*pyruvate synthase with the use of one ATP. In the C_4 plants initial fixation of CO_2 (PEP-carboxylase) and decarboxylation of malate (release of CO_2) both events happens in physically separated compartments the bundle sheath cell (BSCs) and the mesophyll cell (MCs) (Hatch, 1987). The C_4 type photosynthesis in the *Hydrilla verticillata* has been found in a single cell without any compartmentation (Bowes et al., 2001). It is a facultative C_4 plant that shifts from C_3 to C_4 photosynthesis at low CO_2 concentartion without undergoing any structural modification of its leaf cells. Genes involved during the shift of C_4 photosynthesis, encoding the C_4 specific isoenzyme of PEPC, PPDK and NADP malic enzyme. The expression of all genes is upregulated (Rao et, al., 2006). In our attempt a single cell C_4 like pathway has to be introduced into C_3 host possessing 6 enzymes and one antiporter to test the hypothesis whether CO_2 concentration will increase and suppress the photorespiration. *Hydrillia verticilliata* mimic C_4 state pathway with modification had shown in the figure 3.1.2. The key steps within this pathway are the carboxylation of PEP by PEPC in the cystol and decarboxylation of the resultant C_4 acid malate inside the chloroplast.

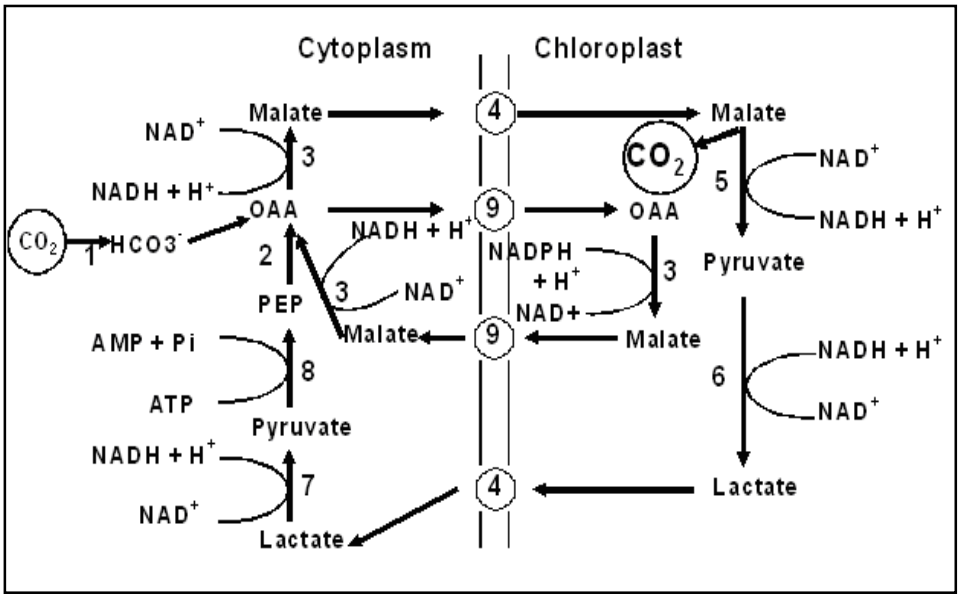

Figure 3.1.2: Schematic representation of modified C_4 pathway in *Hydrilla verticillata* (HC_4l)
CO_2 from ambient air is converted into to HCO_3^- by (1) Carbonanhydrase (endogen). HCO_3^- forms in the cystol of the mesophyll cells and fixed by the oxygen insensitive (2) Phospho*enol*pyruvate carboxylase (PEPC) and convert into OAA. Oxaloacetate is reduced by (3) NAD^+ dependent malate dehydrogenase (MDH), and resultant malate exported to the chloroplast by (4) Malate lactate antiporter (Mle). Malate is decarboxylated by (5) NAD-Malic enzyme (ME). Malate decarboxylation forms pyruvate and which is

reduced by (6) Lactate dehydrogenase A (LdhA), and forms a lactate. Lactate is exported to the cytoplasm and it oxidized to pyruvate by (7) Lactate dehydrogenase B (LdhB). Finally PEP is regenerated by pyruvate and catalyzed by (8) Phospho*enol*pyruvate synthase (PEPS). (9) Malate-OAA antiporter (endogen).

The CO_2 from ambient air is converted into to HCO_3^- by carbonic anhydrase (Endogene) in the cystol of the mesophyll cells and fixed by the oxygen insensitive PEPC (2) (Isolated from *Hydrilla verticillata* leaf) the resultant oxaloacetate is imported into the stroma of the mesophyll chloroplast and reduced by NAD^+ dependent malate dehydrogenase (3) into malate. Malate/lactate antiporter (4) imports malate into the chloroplast and exports lactate into the cytoplasm. Redox equivalent needed in the cytoplasm is transported from the chloroplast to the cytoplasm by a counter exchange mechanism catalyzed by malate/OAA transporter (endogen). The import of OAA has not been a subject of debate, since OAA is actively taken up by the chloroplast via the 'malate valve' which functions in transferring reducing equivalents from the chloroplast stroma to the cystol (Scheibe, 2004). In the modified Hydrilla pathway, malate produced from OAA, is decarboxylated in the chloroplast by NAD dependent ME in order to increase CO_2 concentration in the vicinity of the Rubisco. Pyruvate is the product of malate decarboxylation and it is reduced to lactate by LDH A. Lactate is exported to the cytoplasm and is oxidized to pyruvate by lactate dehydrogenase B. Primary inorganic carbon acceptor PEP is regenerated by PEP synthase and the cycle continue for the fixation of CO_2. This is the primary idea of a pathway to getting increased CO_2 concentration under the proximity of Rubisco.

3.1.7 Construction of gateway plasmids containing genes used for the modified Hydrilla C_4 pathway (HC_4l)

The idea behind to use the gateway technology was to put all genes together from the novel pathway pYLTAC7_Hy (HC_4l) in one event for the agrobacterium plant transformation. All genes from novel pathway to transform into the model plant were difficult by classical cloning and transformation rate was also very low by other multiple gene transformation techniques. In the past the transformation of multiple gene was done by different techniques e.g. repeated crossing, gene stacking, gene pyramiding (Ashikari and Matsuoka, 2006), co transformation (Agarwal et al., 2005; Zhu et al., 2008). Gateway recombination is an ideal technique as compared to the other techniques mention above for transformation of multiple genes. In this work used Multi- round Gateway Technology

was efficiently worked for the transformation of multigene pathways. In figure 3.1.3 shows the arrangement of genes used for the recombination in the gateway vector.

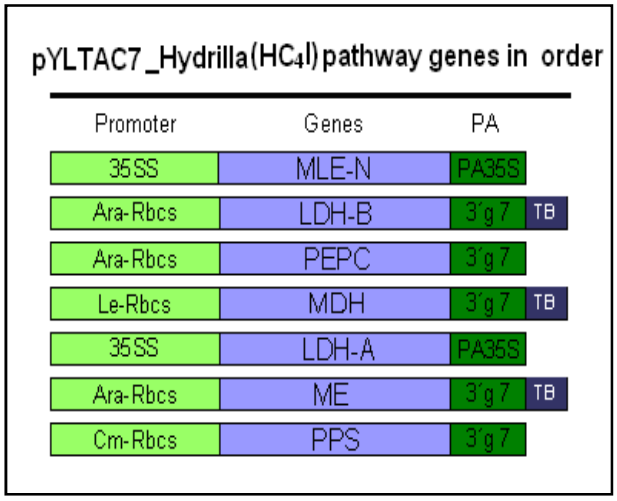

Figure 3.1.3: Schematic diagram shows the arrangement of genes in destination vector
Genes for HC_4l pathway = violet color; promoters = light green ; Polyadenylation sites = dark green; purple color = transcription blockers MleN = Malate lactate antiporter with 35SS promoter; LDH-B = Lactate dehydrogenase B with promoter *Arabidopsis* Rubisco and transcription blocker; PEPC = phospho*enol*pyruvate carboxylase with promoter from *Arabidopsis* Rubisco; MDH-NAD = dependent malate dehydrogenase under the control of *Solanum lycopersicum* promoter with transcription_blocker; LDHA-A = Lactae dehydrogenase A with promoter 35SS; NAD-ME = dependent malic enzyme under the control of *Arabidopsis* Rubisco promoter; PPS = Phospho*enol*pyruvate synthase under the control of *Chrysanthemum* Rubisco promoter.

In HC_4l pathway we tried to use different promoters because as our previous experiences were showed that if promoter used more than three times it could create a silencing effect. In order to avoid silencing effect we were used different promoters for the genes from the pathway. Seven different promoters were not in our collection so we used four different promoters in this pathway in order to recombinate seven genes. Expression cassette from the plant vector was created first to perform the MultiRound Gateway technology. In the figure 3.1.3 had shown the order of genes and promoter used in the gateway recombination. In table 3.1.1 had shown the source of the genes which were used in the HC_4l pathway. Construction of gateway entry vectors and destination vector describe in material and methods (2.1.8.3 and 2.1.8.4). Hydrilla imitated pathway (HC_4l) genes were constructed in a single vector with promoter and polyadenylation cassette. The vector named as pYLTAC7_Hydrilla has been built by MultiRound Gateway recombination into

destination vector pYLTAC7_R12_ CmR_ ccdB_SAR. Construction of gateway entry vectors in order to recombinate into destination vector were described in Material and Methods (2.2.8.4).

Table 3.1.1: Genes and the source of the genes with promoters

No.	Source organism	Genes	Promoter
1	*Bacillus subtilis*	Mle-malate lactate antiporter	35SS
2	Rat Heart	LDH-B-Lacatedehydrogenase	Ara. RbcS
3	*Hydrilla*	PEPC-phospho*enol*pyruvate carboxylase	Ara. RbcS
4	*Maize*	PPS-phospho*enol*pyruvate synthase	Cm. Rbcs
5	Mouse liver	LDH-A-lactate dehydrogenase	35SS
6	*E. coli*	ME-malic enzyme	Ara. Rbcs
7	*E. coli*	MDH-malate dehydrogenase	Le. RbcS

Table 3.1: In above table shown the organism source for the isolation of coding sequence of genes for HC4l pathway; 1MleN = malate lactate antiporter isolated from *Bacillus subtilitis* with transit peptide and promoter 35SS; 2 LDHB = lactate dehydrogenase derived from rat heart and promoter used for this gene from *Arabidopsis* Rubisco; 3 PEPC = phosphoenolpyruvate carboxylase from *Hydrilla verticillata* (photosynthetic PEPC) under the control of *Arabidopsis* Rubisco promoter; 4 MDH = malate dehydrogenase from Z. *mays* and promoter from *Solanum lycopersicum*; 5 LDH-A = lactate dehydrogenase from mouse liver and promoter 35SS; 6 ME = malic enzyme-NAD-dependent from *E. coli* and promoter from *Arabidopsis* Rubisco with transit peptide; 7 PPS = phospho*enol*pyruvate synthase isolate from *E. coli* and cloned with promoter Rubisco *Chrysanthemum indicum*.

The position of the promoter from the entry vector into the destination was important at the time of recombination like the orientation of the expression cassette for recombination. Padidam and Cao, (2001) demonstrated that when two genes are cloned head to tail (→ →) the expression of the downstream gene is reduced by 80% compared to the upstream gene. When two genes are cloned together tail to tail (→ ←) the expression of the upstream gene is reduced by 53% through the expression of the downstream gene. If the orientation of the genes is head to head (← →) no interference of the expression is observed. When the orientation of the gene expression cassette was head to tail and tail to tail used transcription blocker to prevent transcription interference for avoiding silencing. Transcription blocker is an AT rich sequence from lambda phage. In order to avoid recombination of homologous sequences adjacent to each other (some of the genes posses same promoters) a spacer region of about 1 kb was used, so could avoid an unwanted intramolecular recombination. In figure 3.1.3 had shown the arrangement of the gene expression cassette cloned into the destination vector. In figure 3.1.4 had shown the

control restriction digestion of destination vector with the genes after each successful recombination of six genes. The seventh recombination construct of all genes was checked by PCR and by restriction digestion with two different enzymes (see fig. 3.1.5).

Figure 3.1.4: control restriction digestion of destination vector carrying each additional gene after recombination

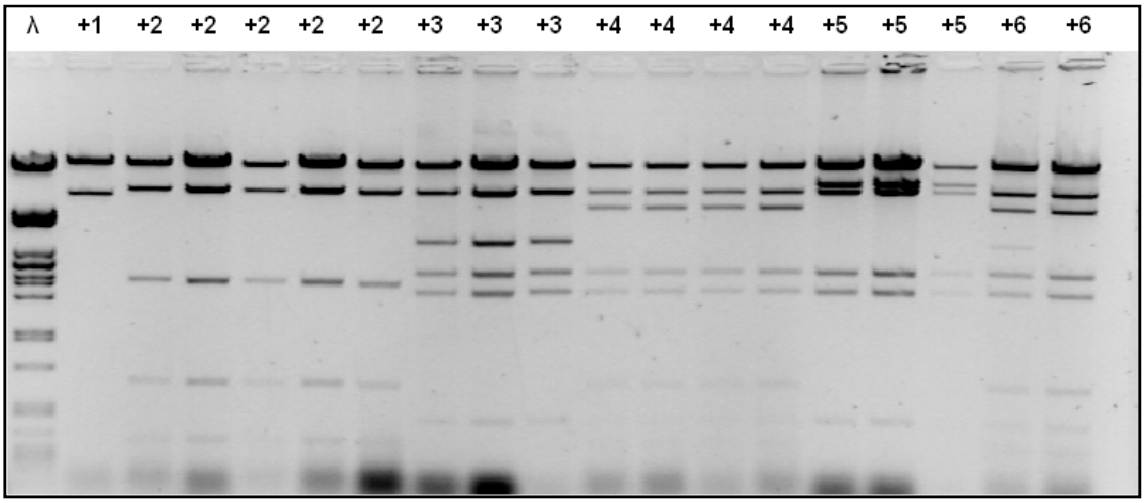

Figure 3.1.4: Verification by restriction digestion for pYLATC7_C4 Hydrilla (HC4l) vector (6 genes) Restriction digestion of successful recombination for every additional gene into the destination vector and shows six round of recombination until six genes recombinate into destination vector used 1% agarose gel. λ PstI Lambda marker; +1 = Destination vector and gene (Mle); (1st lane in digestion after λ marker); +2 = Destination vector and genes (Mle, Ldha); +3 = Destination vector and genes (Mle, Ldha, PEPC); +4 = Destination vector and genes (Mle, Ldha, PEPC, Mdh); +5 = Destination vector and genes (Mle, Ldha, PEPC, Mdh, Ldha); +6 = Destination vector and genes (Mle, Ldha, PEPC, Mdh, Ldha, Me). The expected sizes of the fragments are given in Table 3.1.2.

Table 3.1.2: Control digestion of additional genes after recombination in destination vector pYLTAC7_Hydrilla (HC_4l)

+1	+2	+3	+4	+5	+6
21696	21827	22138	22036	22124	26358
7558	8323	8323	8323	9459	8354
	2126	3531	5993	8323	5904
	703	2390	2390	2390	3531
	304	1926	1926	1926	2390
		472	703	472	1926
			472		703

In table 3.1.2 had shown the destination vector after every additional gene recombination digested with enzyme *BamHI*. Fragment size shows the each additional gene in destination vector from, started from 1st gene with in destination vector until recombination with 6th

gene. Seventh gene was confirmed by restriction digestion with two different restriction enzymes individually had shown in fig. 3.1.5.

Figure 3.1.5: control restriction digestion of destination vector carrying seven genes

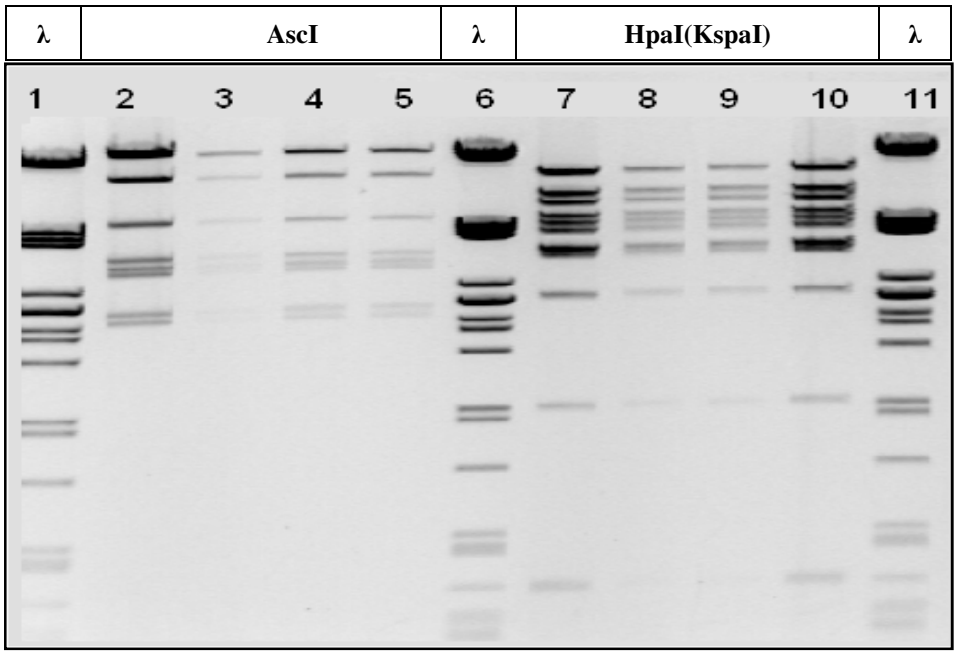

Figure 3.1.5: Destination vector with seven genes restriction digestion
15 µl digested reaction mixtures was analysed on 1% agarose gel. Destination vector carrying seven genes digested with two different restriction enzymes AscI and KspI; Lane 1, 6 and 11 = λ PstI marker; Lane 2, 3, 4, 5 = Destination vector with seven genes digested with AscI; Lane 7, 8, 9, 10 = Destination vector digested with KspI (SacII). In table 3.1.3 had shown the fragment size of the digested vector.

Table 3.1.3: Fragment size of digested destination vector with seven genes digested with AscI and KspI (HpaI) enzymes

KspI	9687	7020	6456	5350	4934	4644	3819	3811	3732	2540	1190	348	348
AscI	23993	9094	5513	3700	3419	3264	2512	2223	87	85			

3.1.8 Big size destination vector transformation in *A. tumefaciens*

The destination vector with all seven genes is named pYLTAC7_C_4_Hydrilla using the initials of destination vector and C_4 *Hydrilla* imitated pathway. *Agrobacterium* strain AGL1 was used for the transformation of big size (35 kb) vector pYLTAC7_C_4_Hydrilla into the plants. This strain carries the hyper virulent, attenuated tumor inducing plasmid pTiBo542. The T region has been deleted from the original plasmid for the optimal transformation in the dicotyledonous plants. *Agrobacterium* AGL1 carries on insertion

mutation in its recA general recombination gene which stabilizes the recombinant plasmids (GR Lazo et al., 1991). It was decided to use AGL1 strain for its optimal characteristics suitable for the gateway plasmid. The pYLTAC7_C_4_hydrilla and the pYLTAC7_empty vector as a control were transformed by the electroporation (Material and Methods 2.2.2.5) into *agrobacterium* strain AGL1 and incubated at 28°C, 4 hours for the regenration. Then the bacteria were plated on LB plates containing the antibiotics carbenicillin (100 mg/l), rifamicin (25 mg/l), kanamycin (15 mg/l). These mention concentrations of antibiotics were favorable for *Agrobacterium* carrying the destination vector. After 4 days of incubation in 28°C small colonies have been seen on plates and these colonies were checked by multiplex PCR for every gene with different primes because only few colonies carries desired set of the genes (+7). Positive colonies were checked for all seven genes by PCR and ~ 25 colonies were checked for every gene from the pathway and new master plate was created. Single positive colony from the master plate plated on new LB plates and used for the stable transformation in *Nicotina tabacum*.

3.1.9 Transient expression of Hydrilla pathway (HC_4l) in tobacco

Transient expression was carried out before the stable transformation of tobacco to check weather all seven genes from plasmid pYLTAC7_C_4_hydrilla vector in tobacco was expressed. Transient expression was conducted like explained in materials and methods 2.2.2.6. The plants were incubated for 12 hours in the dark room and then illuminated with light, Incubation conditions: 16 hours light with about 160 PAR (photosynthetic active radiation) and 8 hours of darkness. Later infiltrated leaves were used for the RNA isolation (Material and Methods 2.2.1.2) and cDNA was made (Material and Methods 2.2.1.9). The expression of the transgenes in relation to the Actin2 gene was then determined by real time PCR (Igarashi et al., 2003). The results of the real time PCR prove that all seven transegens from the gateway plasmid are expressed. However the expression of transformed genes was heterologous.

Even the genes with the same promoter show variable expression like PEPC, Ec-ME and LDHB all of which were made under the control of light inducible AtRbcs. The PEPS gene was under the control of the light inducible CmRbcs promoter and shows the highest expression ~ 6 times higher than the endogenous Actin2 gene. PEPC shows the lowest

expression ~ 0.9 times than actin 2 genes. LDHA and Mle genes were under the control of the constitutive promoter 35SS shows an expression 1.5 to 2.0 times higher than the actin 2 genes. Gene MDH was under the control of the light inducible LeRbcs promoter shows 1.5 times higher expression than the control. Therefore *Agrobacterium* transformation of the big size gateway vector was possible and it proved that all the promoters used in this pathway are able to control of gene expression in tobacco.

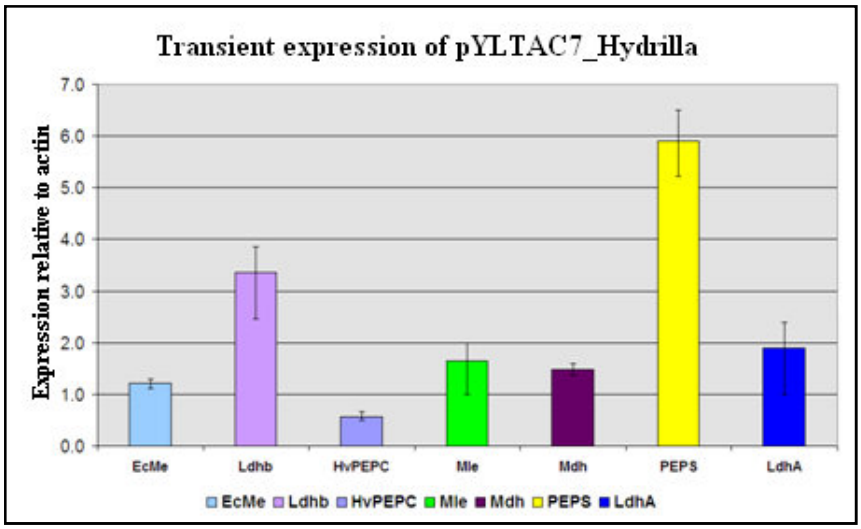

Figure 3.1.6: Transient expression of pYLTAC7_Hydrilla (HC_4l) gateway vector in Tobacco
The results above show the all seven gene expression with vector pYLTAC7_Hydrilla. The expression of the different transgene was determined by real time PCR and relative to the expression of endogenous Actin2 gene. EcMe = *E. coli* malic enzyme; LdhB = Lactate dehydrogenase B; HvPEPC = Hydrilla phospho*enol*pyruvate carboxylase; Mle = Malate lactate antiporter gene; Mdh = Malate dehydrogenase; PEPS = phospho*enol*pyruvate synthase; LdhA = lactate dehydrogenase A. Each data point is based on the measurement of three different samples. The error bars indicate standard error.

3.1.10 Stable expression of C_4 genes in tobacco (T_0 generation)

The stable transformation of tobacco with the gateway vector, which encodes hydrilla imitated C_4 like pathway followed according to De Block (1988) and Dietze et al., (1995) detail procedure in (Material and methods 2.2.2.7).

The RNA level of different transgenes has been tested by real time PCR (Material and methods 2.2.1.10). The different transgenes in different preparation of RNA expression is normalized with the help of the endogenous Actin2 transaction script (Igarashi et al., 2003). We found 20% of the plants expressing all seven genes in the T_0 generation. Expression of the transgenes depends on the position within the chromosome. If the

foreign DNA integrates close to a transcriptional activating element a high expression rate might be possible. Some of the foreign genes seem not to be expressed in all times. This might be due to the methylation or post transcriptional gene silencing (De la Riva et al., 1998).

The expression of HvPEPC, Mdh, Mle, EcMe, Ldhb, Ldha, and PEPS in *planta* was tested on the RNA level using real Time RT-PCR. In fig. 3.1.7 had shown the expression of all seven genes in plant no. 4, 5 and 10 although expression was variable. About 150 plants were tested in the T_0 generation for all seven genes mention above. Only 29 lines showed expression of all seven genes and all 29 plants shows varying expression levels of transformed genes. All seven genes expressed plant shows the early formation of reproductive organs and some of the plants show a slightly different phenotype but no stunting growth has been seen in lines expressing all seven genes. The expression level of HvPEPC was always very low (0.5-2 times compared with the actin 2 genes). PEPS and Mle genes shows higher expression level in most of the plants, 10 to 20 times higher than actin 2. The expression level relative to the actin gene as follows NAD-Me +3 to 8 times; Ldhb +16 times; LdhA +2 to 4 times. Seeds from the lines 4, 5, 10, 12, 49, 50, 71, 139, 141, 171 expressing all 7 genes from T_0 generation were passes for the T_1 generation and chose few lines with overexpressed some other combination of genes.

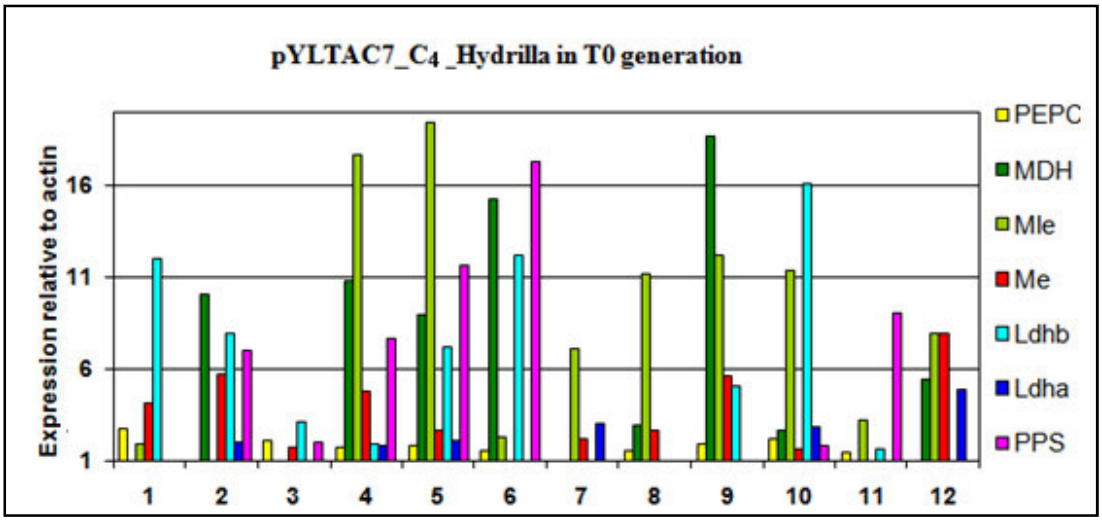

Figure 3.1.7: Stable expressions of pYLTAC7_C_4 Hydrilla (HC4l) genes in tobacco plants in T_0 generation

Expression of mRNA was measured by Real-Time RT-PCR and calculated in arbitrary units. Each value is the relative accumulation of the respective RNA compared to the Actin 2 levels measured in the preparation from 4 weeks old plants. EcMe = *E. coli* malic enzyme; LdhB = Lactate dehydrogenase B; HvPEPC = Hydrilla phospho*enol*pyruvate carboxylase; Mle = Malate lactate antiporter gene; Mdh = Malate dehydrogenase; PEPS = phospho*enol*pyruvate synthase; LdhA = lactate dehydrogenase A.

Plants from the T_0 generation were not used for the enzymatic assay and for measurement of different parameters (CO_2 compensation point, post illumination burst, production of glucose, etc.). The plants are strongly influenced by the hormones (BAP, NAA) which have to be added to the cells for regeneration at the the time of stable transformation. This effect was proved by the plant material from T_0 generation used for isolating probes for GC-MS (Gas chromatography and Mass spectroscopy, material and methods 2.2.3.6) and the samples run on GC/MS shows very unusual chromatograms (Personal communication Prof. Dr. C. Peterhansel). Therefore it was decided to analyzed most of the parameters for transgenes in the T_1 generation to avoid the effect of hormones used at the time of stable transformation.

3.1.11 Stable expression of PEPC, MDH, Mle, EcME, LDHA, LDHB, and PPS genes in tobacco (T_1 generation)

In order to analyse important parameters of the metabolism of the transgenic plants possessing the C_4 hydrilla imitated pathway (HC4l), plants from the T_1 generation were used. Two weeks old plants were harvested in order to measure the expression rate of the recombinant genes. This was done by RT-PCR. The samples were taken after 4 hour exposure to light and different primer pairs used for seven genes. After 4 weeks again the same plant lines was used for checking the expression of genes (PEPC, MDH, Mle, EcME, LDHA, LDHB, and PPS) whether age can differentiate the expression of genes. In this case we found out there was difference seen on the expression of genes from the same plant line checked before.

In line no. 10 around 4 plants were azygote and other six plants shows expression relatively homozygous. This clearly indicates that seven genes integrated in one chromosome. While in line 4 only 3 plants showed the expression out of 12 plants and other plants were azygote (Data not shown here). From line 5 had seen the relatively homozygous expression and only one plant seems to be azygote (figure 3.1.8). In most of the transgenic lines the expression of the PEPC gene was relatively less in T_0 generation and the similarly seen lesser expression in T_1 generation. Mle and PPS genes show higher expression in most of the plants. Many plant lines expressed these both genes but

expression of other genes showed in few lines. This might related to the position of genes in the vector or the influence of promoter on the expression of genes.

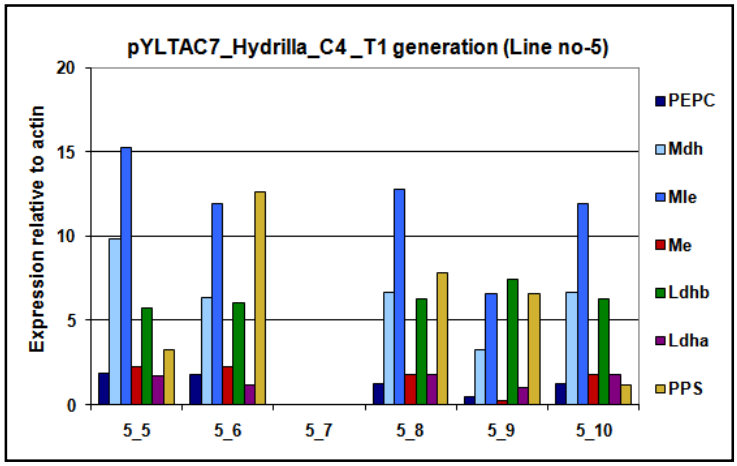

Figure 3.1.8: Stable expressions of pYLTAC7_C_4 *Hydrilla* genes in tobacco plants in T_1 generation
The result above shows all seven gene expression in T_1 generation from pYLTAC7_Hydrilla. The expression of the different transgene was determined by real time PCR and relative to the expression of endogenous Actin2 gene. The samples were taken from two week old plants after four hours of exposure to light. EcMe = *E. coli* malic enzyme; LdhB = Lactate dehydrogenase B; HvPEPC = Hydrilla phosphor-*enol*pyruvate carboxylase; Mle = Malate lactate antiporter gene; Mdh = Malate dehydrogenase; PEPS = phospho*enol*pyruvate synthase; LdhA = lactate dehydrogenase A.

3.1.12 Enzyme activities and transcription level of a C_4 hydrilla like pathway in transgenic tobacco plants

At different stages of development, plants show different cellular metabolic properties and this directly affects transcription and translation of many genes and their mRNAs. In order to avoid the influence of the stage of development on metabolism, probes for all enyzmes measured were taken from the same lines. Samples were taken from 4 week old plants. The C_4 enzyme activity was measured from the same line in T_1 generation. The plant line with pYLTAC7_empty was used as a negative control. The extraction protocol was followed for different enzymes activities explained in material and methods (2.2.3.2). Specific as well as relative activity of the enzymes shown in figures above for PEPS, NAD-ME, NAD-MDH and LDH from the 34 tested plants. The enzyme activities of most of the lines were higher than the endogenous enzymes activity. Maximum activity for PEPC in line no. 5_16 was observed 2.9. Enzyme activity for PEPC in most of the plants was in between 1.5 to 2.9; however the activities were relatively low probably due to the cosuppression or (HdGS) homology dependent gene silencing (Meyer and Saedler, 1996).

It explained, if the gene is higher homology to endogenous gene it works better if the homology of both genes lesser than 80% (Thierry and Vaucheret, 1996).

In our previous work PEPC gene was used from the *Solanum tuberosum*. It was 87% similar to the endogenous and show lesser enzyme activity (Matthias Buntru PhD thesis). In this pathway PEPC gene was from the *Hydrilla verticilliata* and the homology with endogenous is around ~73%. The enzyme activity of *Hydrilla verticilliata* gene (HvPEPC) was higher than the enzyme activity of PEPC from *Solanum tuberosum*. The HvPEPC gene was under the control of AtRbcS promoter but, it might show higher activity if it would under the control of 35SS promoter because stPEPC show better activity under the control of 35SS promoter (Thomas Rademacher PhD thesis, Bio1).

In the table 3.1.4 had shown the relative activity of enzyme in T_1 generation from selected transgenic crops which express all seven genes and shown the relative expression of genes Mle and ldhb and Ldha against Actin2. These results lead to the conclusion that the novel pathway enzymes are active in tobacco.

Table 3.1.4: Relative expression and relative activity of transgenes in T_1 generation

Transgenes	**Relative activity**					**Relative Expression**		
pYLTAC7_Hy	PEPC	PPS	NAD-ME	NAD-MDH	LDH	Mle	LHDA	LDHB
No.5	2.9	15.51	4.5	2.5	15.6	15.9	2.5	6.91
No.10	2.8	16	3.2	4.5	14.3	16.12	1.6	7.91

In order to access the extent of increase in enzyme activity in individual transformants their relative activities were calculated by dividing their specific enzyme activity by that control plant. Relative activity of PEP synthase was in between 6 to 16 and highest relative activity was in line no. 4-16 was 15.51 (fig. 3.1.9). The specific activity of HvPEPC was about 25 to 45 mU/mg protein and for the control plant specific activity was 10 mU/mg proteins. The specific activity of PEP synthase was in between 60 to 115 mU/mg proteins and endogenous activity was 5mU/mg protein (Fig. 3.1.10). The relative activity for NAD-ME and NAD-MDH for pYLTAC7_Hydrilla transformant was 4.5 and 2.5 respectively (Fig. 3.1.11). NAD-MDH activity and NAD-ME activities were quite high, because the endogenous activities were also high, Endogenous activity: NAD-ME 100-200 mU/mg protein and NAD-MDH 100-150 mU/mg protein (Fig. 3.1.12). In our previous experiments relative activity of NAD-ME was higher (Matthias Buntru Phd thesis BioI) and it showed chlorosis in the plants (maximum relative activity over 200).

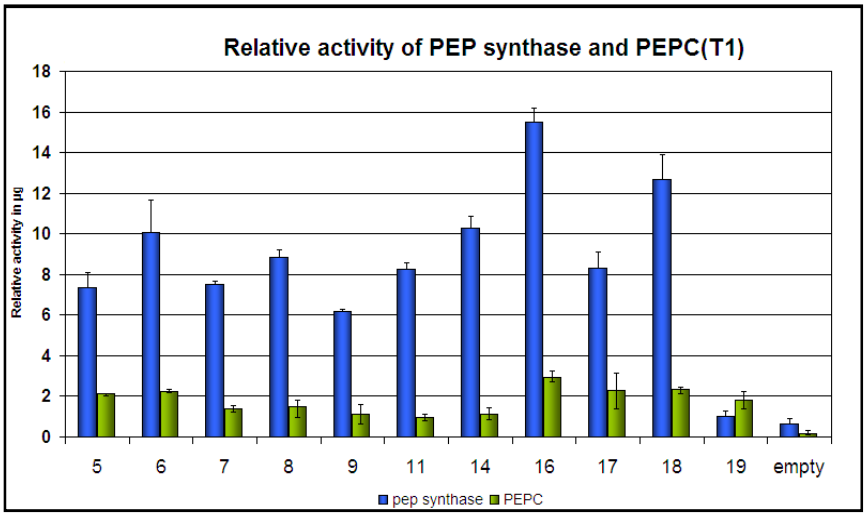

Figure 3.1.9: Relative activity (µg)of phospho*enol*pyruvate synthase and phospho*enol*pyruvate carboxylase in T_1 generation

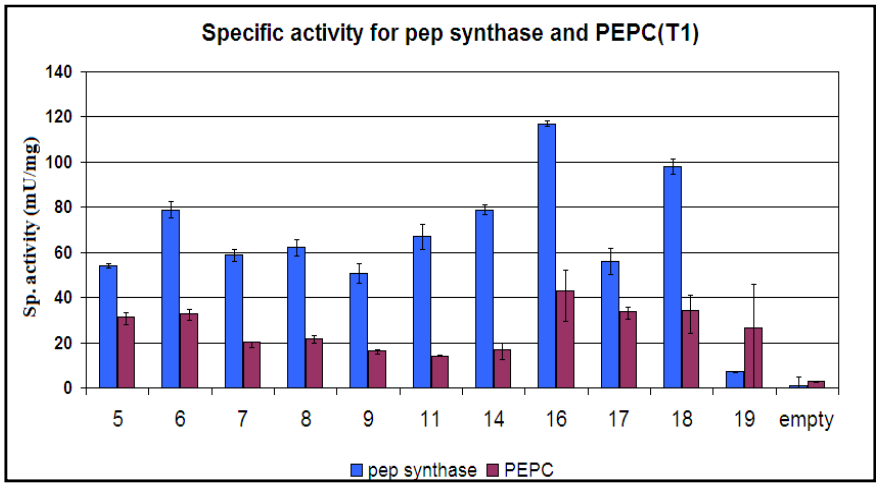

Figure 3.1.10: Specific activities (mU/mg) of phospho*enol*pyruvate synthase and phospho*enol*pyruvate carboxylase in T_1 generation

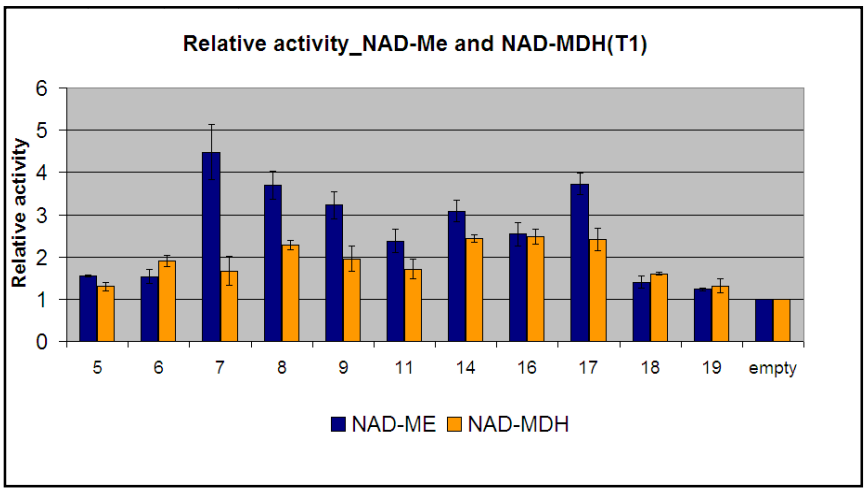

Figure 3.1.11: Relative activity (µg) of NAD dependent malic enzyme and NAD dependent malate dehydrogenase in T_1 generation

In the transgenics of pYLTAC7_Hydrilla relative activity was not high enough to form the chlorosis on the leaves of the plants. The enzyme activity of LDH individually was not measured in this study (in cytoplasm and chloroplast). But, the enzyme activity of LDH (see fig. 3.1.13) was measured from the total crude plant leaf extract in the reaction buffer.

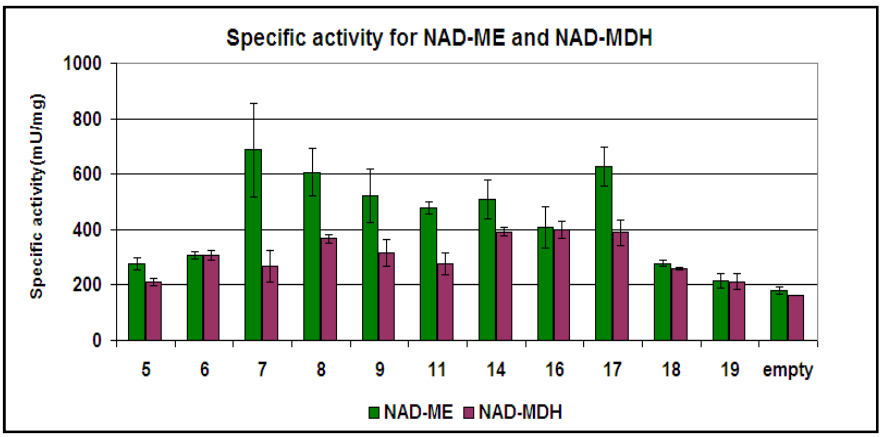

Figure 3.1.12: Specific activity (mU/mg) of NAD dependent Malic enzyme and NAD dependent Malate dehydrogenase in T_1 generation

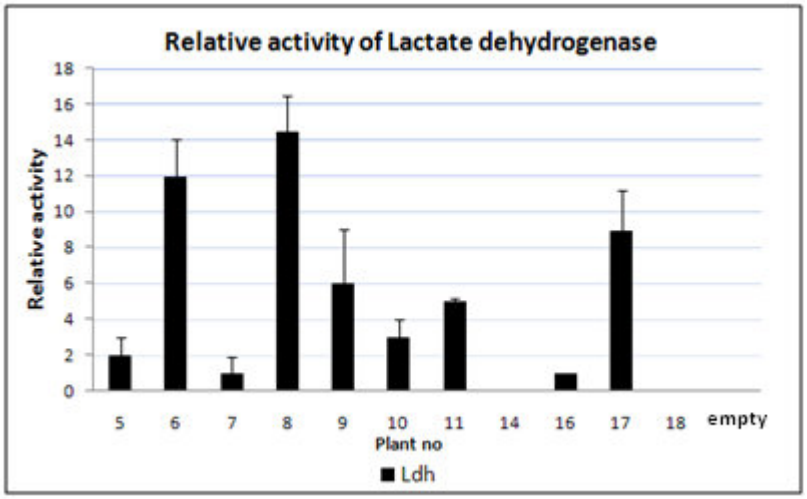

Figure 3.1.13: Relative activity (µg) of Lactate dehydrogenase in T_1

3.1.13 Phenotypic effects of the C_4 Hydrilla pathway on transgenic tobacco plant

We evaluated the effect of foreign enzymes after introducing in tobacco plant. Foreign enzymes may alter many physiological parameters, such as: the activities of endogenous enzymes, content of primary and secondary metabolites, photosynthetic parameters, delay or early formation of reproductive organs and growth rate etc. Leaf shape of the transgenic

plants was pointed towards the end and conical as compared with the control plats but the total leaf area of transgenic plant was lesser than the control plant. In the fig. 3.1.14 had shown the different type of phenotype from transgenes carrying different combinations of genes. Plants with overexpressed PEPC, Mle, ME, PEPS genes showed some positive effects like slightly more leaf area than the control plants and the transgenic plants with seven genes (pYLTAC7_Hydrilla) and difference in average internode show slightly higher length in which plant expressed +4 genes. So it was concluded that the expression level was might correlated with the phenotype effect (Rafijul Bari, PhD thesis, Bio1). The expression of all seven genes HvPEPC, Mdh, Mle, EcMe, LDHA, LDHB, and PEPS was not observed any positive effect on C_3 plants. The higher expression of HvPEPC, Mle, EcMe, and PPS showed slightly higher length than the control plants. Therefore, it might conclude that the lines with malate-lactate antiporter and three other genes (Mle, ME, PEPS) overexpression shows slightly higher leaf size (total leaf area) and length (Materials and Methods 2.3.3.3). Malate lactate antiporter could be better option to export malate into the chloroplast in higher level and continue the small cycle with malic enzyme and PEP synthase.

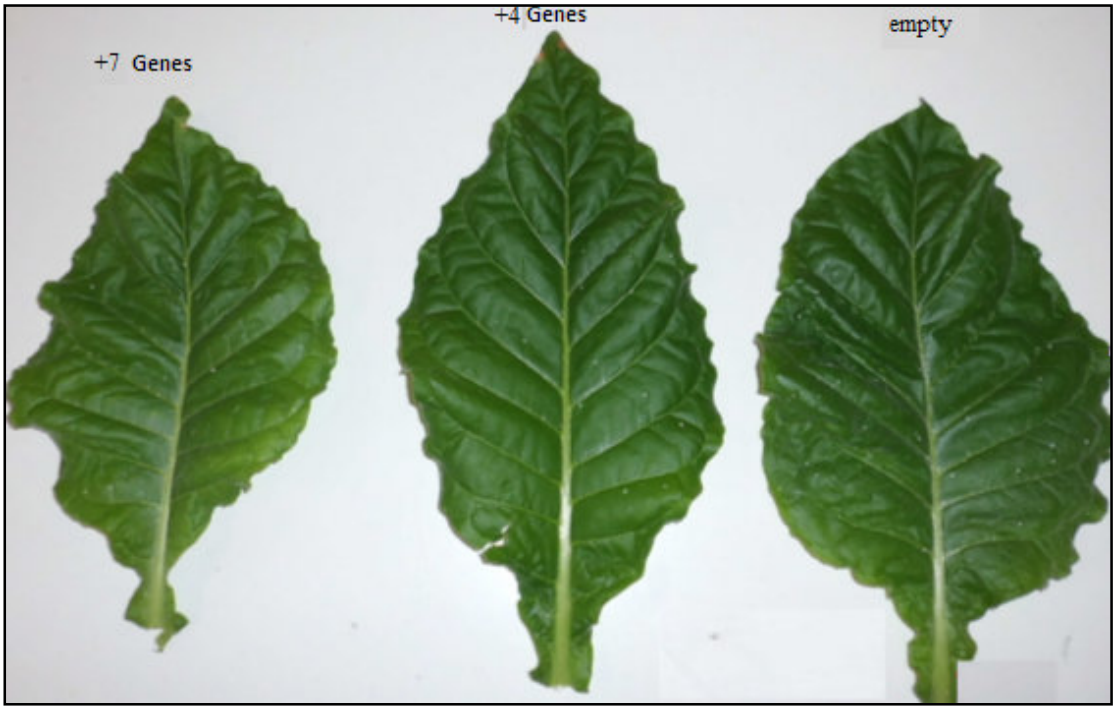

Figure 3.1.14: Phenotypic effects of the HC_4l pathway genes on transgenic tobacco plant
In fig. above shown the 5 week old plant leaves were cutted from the upper 4th position of the plant in T_1 generation. **+**4 genes = Overexpressed HvPEPC, Mle, NAD-ME and PEPS; +7 genes = HvPEPC, NAD-MDH, NAD-ME, Mle, LdhA, LdhB and PEPS (HC_4l); Empty = control plants transformed with empty vector.

Plants with PEPC, malic enzyme, malate-lactate antiporter and PEP synthase shows faster growth rate the plant with complete pYLATC7_Hydrilla pathway. Some lines with +4 genes (PEPC, Mle, ME, PPS) were showed slightly longer internodes than the control ~ 2 to 3 percentages but not very astonished effect on *Nicotiana tabacum* plants.
Introduced foreign C_4 enzymes with one antiporter possibly balance the energy consumption in the chloroplast after introduction of forigen C_4 enzymes in the C_3 plant. Therefore, it may be simply concluded that balancing the energy in chloroplast showed some extent good indicator for increasing the photosynthesis in C_3 plants.

3.1.14 Measurement of ammonia release during photorespiration

In the photorespiratory pathway ammonia is released during the conversion of two glycine molecule to one serine in the mitochondria. The released ammonia is refixed by the GS-GOGAT cycle (Introduction 1.3.1) Tachibana et al., (1986); Wild and Ziegler, (1989) have shown that phosphinotricin (herbicide) which is a glutamate analog and inhibits glutamine synthase activity irreversibly and consequently ammonia accumulates inside the plant leaf tissues after treatment with phosphinotricin. De block (1995) developed an assay in which leaf tissues incubated in a medium with phosphinotricin will not be able to assimilate ammonium. The accumulating ammonia in the leaf tissues diffuses into the surrounding medium where a colorometric reaction shows the concentration of ammonium. This assay clearly shows: The higher the concentration of ammonium in the medium after treatment with phosphinotricin the higher the photorespiration and vice versa and lower the concentration of ammonia the lower the photorespiration.
Therefore ammonia is the marker component for photorespiration and it was positive test for the amount of ammonia released from the leaf tissues of the transgenic plants.
The results shown in figure 3.1.15 could be summerised as follows: Plants with the higher expression of the C_4 genes PEPC, Mle, ME and PEPS shows lower accumulation of NH_3 than the control lines and lines with a higher expression of all seven genes. This might demonstrate that plants which express PEPC, Mle, ME and PEPS have an increased positive impact compared with lines expressing all seven genes.

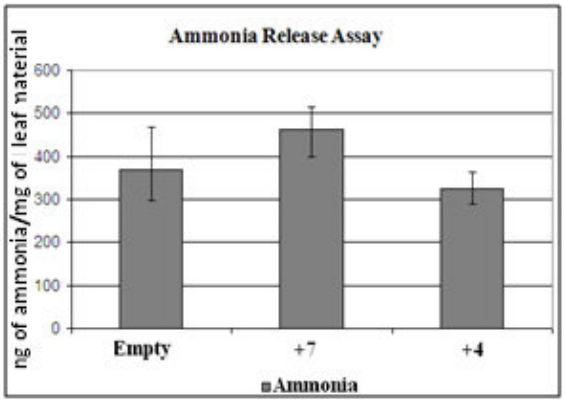

Figure 3.1.15: Ammonia release assay from the transgenic plant
Ammonia released bioassay was performed using 6 week old plant and 5 mg each leaf tissues. X axis= ng of ammonia/mg of leaf material. Each data point shows the amount of ammonia released and based on three independent experiments. A vertical bar shows standard deviation. Abbreviations: Empty = Transgenic plants containing empty plasmid as a control; +7 = Transgenic plants containing all seven genes from the *Hydrilla* pathway (HC_4l); +4 = over expression of PEPC, Mle, ME and PPS in transgenic plants.

3.1.15 Concentration of Malate in C_4 Hydrilla Transgenic plants (T_1 generation)

Malate has a vital role in most plant organelles. Malate is involved in many physiological functions, such as: It provides NADH for nitrate reduction, provision of carbon skeletons and NADPH and for fatty acid biosynthesis, stomatal movement by regulation of osmotic pressure, control of cellular pH, redox homeostasis, transport and exchange of reduced equivalent between cellular compartments (Lance and Rustin, 1984,). Malate synthesis during the light period involves PEPC and MDH. In 2002 Rademacher et al., showed that transgenic potato plants with modified PEPC from *Solanum tuberosum* showed higher concentration of malate than control plant. Hence the plant lines which expressed the decarboxylating enzyme NAD-ME could reduce the concentration of malate.

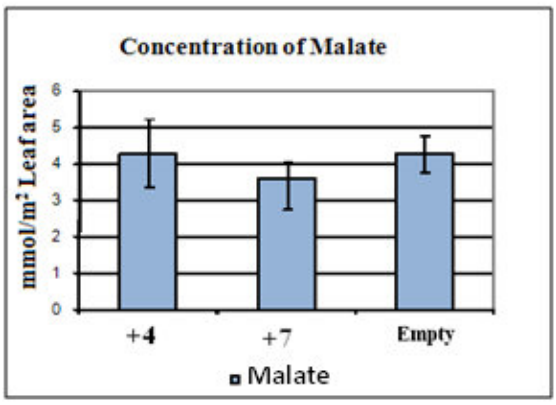

Figure 3.1.16: Concentration of malate in the transgenic plants
4 weeks old plants used for this assay. +7= concentration of malate in pYLTAC7_Hydrilla (HC_4l) pathway plants and +4 = plants over expressed PEPC, Mle, ME, PEPS; empty = empty plasmid carrying plants. In fig. explained decarboxylating enzyme worked well in the transgenic plants with complete hydrilla pathway +7 (HC_4l) and showed lesser malate content as compared with overexpressed +4 (PEPC, Mle, ME, PPS) genes plants and empty plasmid carrying-plants.

Both transgenic lines (HC_4l expressing 7 genes and plant with overexpressd 4 genes) express the NAD-ME gene. The malate concentration of the control plants and the lines

expressing 4 genes are almost identical. The lines with 7 genes were showed a decreased malate concentration as compared to the other lines (Figure 3.1.16).

3.1.16 Determintaion of glucose, fructose, sucrose and starch by enzymatically

Soluble metabolites (glucose, fructose, sucrose) and insoluble metabolites (starch) are the end product of photosynthesis. The comparison between the plants which over expressed PEPC, MLE, ME, PPS genes and HC_4l pathway (seven genes) has shown in fig. 3.1.17. Which showed the lesser concentration of soluble and insoluble metabolites in C_4 hydrilla pathway plants than the four genes overexpressed transgenic plants.

The total soluble (glucose, fructose, sucrose) and insoluble (starch) metabolites were extracted from plant leaf tissues and quantified enzymatically (material and methods 2.2.3.4). Plants with the complete C_4 *hydrilla* imitated pathway (HC_4l) showed lesser soluble and insoluble metabolites than azygote plants. Plant lines expressing 4 genes (PEPC, Mle, ME, PEPS) showed a higher accumulation of glucose, fructose, sucrose and starch compared with plants expressing all 7 genes. It can be concluded that the higher expression of C_4 genes and antiporter changes basic metabolic pathways of the tested plants.

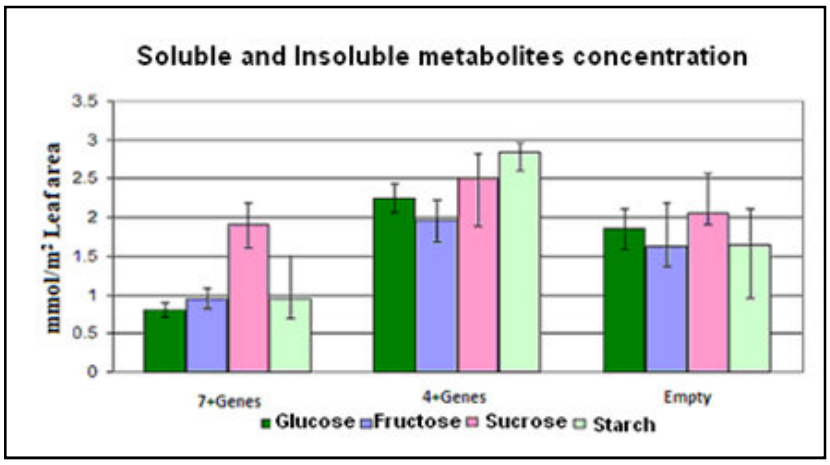

Figure 3.1.17: Soluble and insoluble metabolites measured from transgenic plants
Relative content of soluble (glucose, fructose and sucrose) and insoluble (starch) metabolites measured from 5 weeks old different transgenic *Nicotiana tabacum* plants. Each data point shows the average of metabolites measured from 4 sister plants and is based on at least three independent experiments. Vertical bars show standard deviation, green bar show = Glucose content; blue bar = Fructose content; pink bar = sucrose content; light green bar = starch content; 7+genes = complete pathway with all seven genes (HC_4l) PEPC, MDH, Mle, EcMe, Ldha, Ldhb, PPS; 4+genes = overexpressed PEPC, Mle, ME, PPS and for control used empty plasmid plants.

3.1.17 Determination of metabolites by GC-MS

Introduction of foreign pathway in the endogenous metabolism of C_3 plants affect the total metabolic performance. Initial or end products of the endogenous pathways shows variations. Other end product from photosynthesis from this work was not shown here because higher fluctuation on GC-MS chromatograms and only glucose, fructose and sucrose shows stable values for HC_4l pathway plant lines. In the above fig. 3.1.18 showed the concentration of glucose, fructose and sucrose.

In this study the GC-MS method was used to estimate the concentration of most of the photosynthetic and Calvin Benson cycle related compounds. This could give a confirmation for the increased in the concentration of glucose and sucrose of the plant line overexpress 4 genes PEPC, Mle, ME and PPS as compared with pYLTAC7_hydrilla pathway (HC4l) and azygote plants. Figure 3.1.18 showed the relative glucose, fructose and sucrose concentration.

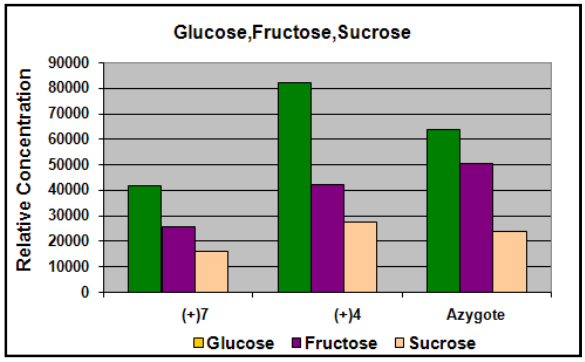

Figure 3.1.18: Glucose, fructose and sucrose by GC-MS
Probes isolated from 3 weeks old plants and independent preparation of polar phase performed in two times for getting similar effect. (+) 7 = Plants expressing complete HC_4l pathway = HvPEPC, NAD-MDH, NAD-ME, Mle, LdhA, LdhB and PEPS; (+) 4 = Plant overexpressing 4 genes PEPC, Mle, NAD-ME, PEPS in transgenic plants.

3.1.18 Photosynthetic performance of transgenic plants

Overexpression of different gene combination and novel pathway genes which might have an impact on transgenic plants should change their photosynthetic performance. Therefore, the post illumination burst (PIB) and the apparent CO_2 compensation point (Γ) were measured.

i) Postillumination burst (PIB) as a marker for the rate of photorespiration.

Postillumination burst means that if a C_3 plant is exposed to sudden darkness after a period of illumination (that time plant achieve steady state of photosynthesis), a momentary rapid outburst of CO_2 occurs before the plant reaches steady state dark respiration (Rn).

This CO_2 outburst shows the amount of CO_2 delivered in plant mitochondria at the time of photorespiration (Atkin et al., 1998; Bulley and Tregunna, 1971). So, PIB measurement from transgenic and azygote plants give an idea of the effect of the line expressing 4 genes (PEPC, Mle, ME) and antiporter as compared to the pYLATC7_Hydrilla novel pathway transformed into the host plants.

Transgenic line overexpress +4 (PEPC, Mle, ME, PEPS) genes shows lesser PIB values as comapared with +7 genes and azygote plant line. These results shows the overexpression of +4 genes mention above in *N. tobacum* plants responsible for the reduction in the photorespiration CO_2 release in the mitochondria.

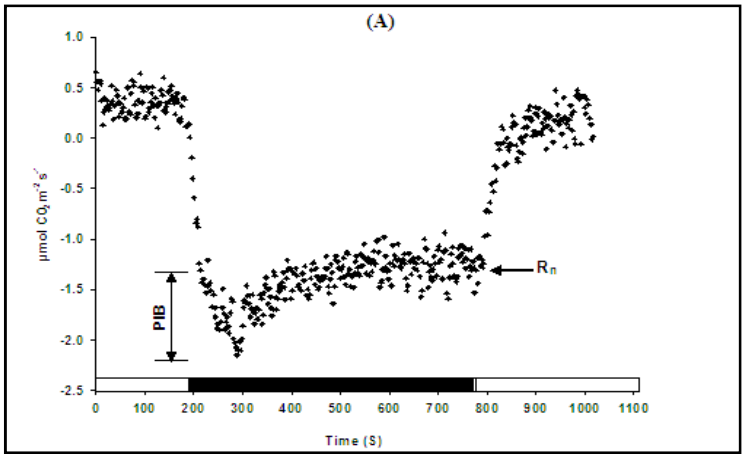

Figure 3.1.19A: Post illumination burst
Time course of net CO_2 exchange from a *Nicotina tobacum* plant leaf under 1000 µmol photons m^{-2} s^{-1} and 100 ppm CO_2 and the different postillumination bursts measured from ayzgote and different transgenic plants In figure 3.1.19 A: PIB = Postillumination burst and Rn = plant dark respiration; white horizontal bar = light on and black horizontal bars = light off.

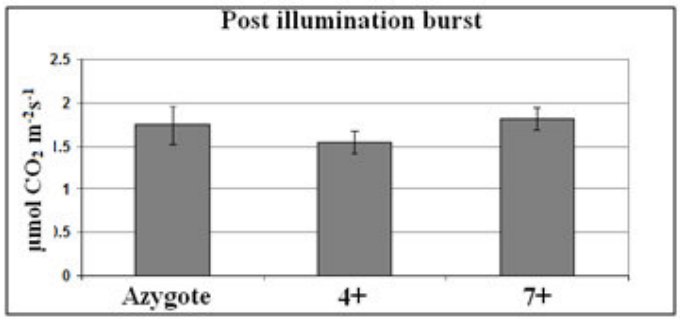

Figure 3.1.19B: Post illumination burst
Each value shows the PIB and is based on at three independent measurements of four independent plants for each line. Vertical bars show standard error. +4 = Transgenic plants overexpressed 4 genes (PEPC, Mle, ME, PEPS) and plants expressed with seven genes a Hydrilla pathway (HC_4l) as +7 (PEPC, MDH, Mle, ME, LdhA, LdhB, PEPS) and for control used azygote plant.

ii) Determination of the apparent CO_2 compensation point (Γ)

At the apparent CO_2 compensation point, the amount of CO_2 fixation by a plant equals the amount of CO_2 released from the plant by photorespiration and respiration. The compensation point was measured from Azygote plants as well as from plants transgenic for +4 (HvPEPC, Mle, NAD-ME, PPS) by measuring their photosynthesis from different leaf internal CO_2 concentrations and it is called A/Ci curve as described in the (Materials and Methods 2.2.3.7). Figure 3.21 shows the different A/Ci curves that were measured from the indicated genotypes. Γ was calculated as the crossing point between the measured A/Ci curve and the X axis.

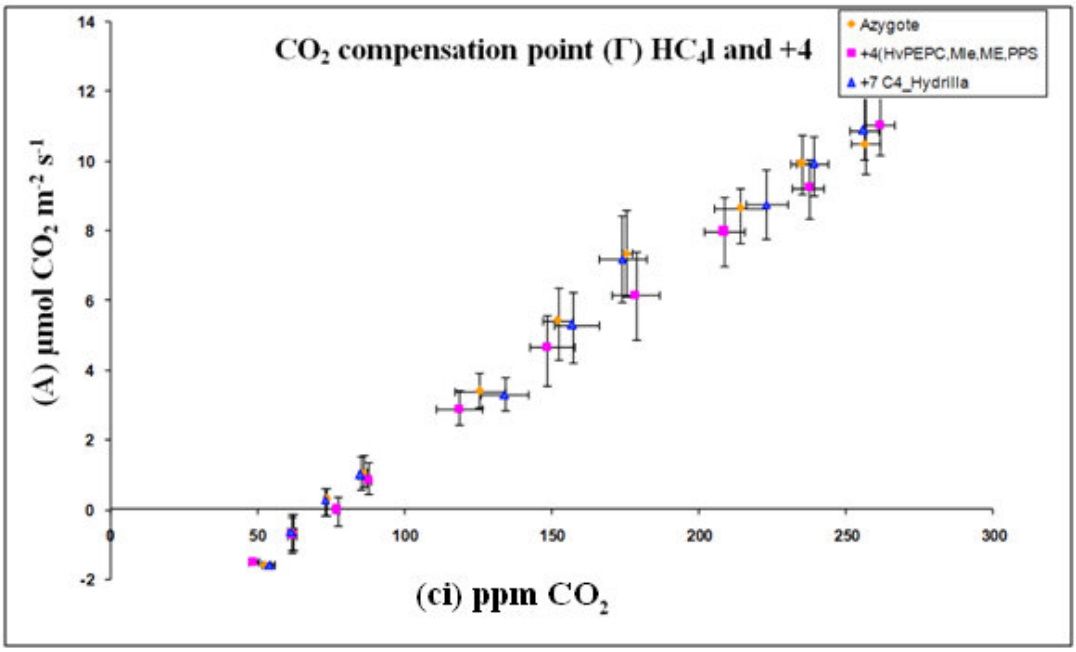

Figure 3.1.20: A/Ci-curve from azygote and transgenic plants
Different A/Ci-curves measured from 9-10 weeks old Azygote, +4, +7 plants under illumination of 1000 µmol photons m^{-2} s^{-1} and different external CO_2 concentrations (Ca) (350, 300, 250, 200, 150, 100, 80, 60 and 40 ppm CO_2). Each value represents the assimilation rate and is based on at least 4 independent measurements from 4 sister plants for each line. Vertical and horizontal bars show standard error. (A) = Assimilation rate; (Ci) = internal CO_2 concentration in leaf intercellular spaces; +4 genes (pink) = PEPC, Mle, NAD-ME, PEPS; +7 (blue) genes plants expressing all 7 genes from the C_4_hydrilla imitated pathway(HC_4l), Azygote plants (orange).

The apparent CO_2 compensation points for all the tested plants are listed in Table 3.1.5. C_4 Hydrilla plants (HC_4l) observed the highest values of apparent CO_2 compensation point compared to the other tested plants. Plants transgenic higher expressed +4 genes (PEPC, Mle, NAD-ME, PEPS) have more or less similar values. Azygote plants have a slightly lower Γ compared to the other tested plants. Based on this result, it can be concluded that

the tested transgenic plants have similar rates of photosynthesis compared to their azygote counterparts.

Table 3.1.5: CO_2 Compensation point for different transgenes

Plant	Apparent CO_2 compensation point (Γ)
Azygote	70.38 ± 2.45 ppm CO_2
+4	69.74 ± 2.34 ppm CO_2
+7	73.06 ± 3.36 ppm CO_2

3.1.19 What is the influence of the novel pathway on plant growth?

Transgenic plants should inherit maximum available "HC_4l pathway" genes from their parents and thus have complete cycle of CO_2 concentration mechanism and other could have parts of them. It is quite possible that certain combination of enzyme could render either positive or negative effect on plant growth. As some of the genotypes like overexpressed four genes (PEPC, Mle, NAD-ME, PEPS) observed a faster growth as compared to the azygote plant, this effect was quantified by determining the leaf area (Material and Methods 2.2.1) of plants every week after sowing. In order to evaluate the effect of the novel pathway on the growth of the transgenic plants, the plant leaf area was measured from all transgenic lines HC_4l (+7: PEPC, MDH, Mle, ME, LdhA, LdhB, PEPS) parallel with azygote plants. Leaf area measurements showed that plants transgenic +7 have similar values of leaf area compared to azygote plants. Plants transgenic for higher expressed +4 (HvPEPC, Mle, NAD-Me, PEPS) genes developed a slightly bigger leaf area (Fig. 3.1.14) in some lines with higher expression of PEPS (Difference was very less so data not shown here). Therefore it may be concluded that expression of the complete pYLATC7_hydrilla pathway (HC_4l) results has no effect on complete biomass of the plant and as well as no effect seen on the photosynthetic performance of the transgenic plants as compared to the control plant.

3.2 Project B

3.2.1 A novel biochemical pathway aiming to increase CO_2 concentration in the chloroplasts of transgenic GTDEF plants

In the present study, it was tried to introduce a new biochemical pathway into transgenic GTDEF (introduction 1.8) plants to metabolized glyoxalate by using five different genes from *E. coli* for the formation of 3-phosphoglycerate.

In a previous work of our group, introduction of chloroplastic GTDEF pathway in *Arabidopsis* plants shows promising results by higher photosynthetic rate and suppression of photorespiration by increasing the CO_2 concentration at the vicinity of rubisco (Kebeish et al., 2007). The GTDEF pathway was established in the plant chloroplast for two benefits: Metabolism of glyoxylate produced inside the chloroplast before entering into the photorespiratory pathway and CO_2 released inside the chloroplast in the vicinity of the rubisco which can refix the oxidized carbon. GTDEF pathway resembles to the bacterial glycerate pathway for the metabolism of glycolate. In the GTDEF pathway glyoxylate is formed from glycolate by the glycolate dehydrogenase (GDH). In our new (MMPEM pathway) malate synthase is the first enzyme which converts glyoxylate to malate after catalyzing the condensation reaction between glyoxylate and acetyl-CoA. Malate is decarboxylated by NAD dependent malic enzyme and forms pyruvate which is then converted into phospho*enol*pyruvate. The phospho*enol*pyruvate is formed to 2-phosphoglycerate by the enzyme enolase. Finally 2-phosphoglycerate is converted in to 3-phosphoglycerate by phosphoglycerate mutase.

The aim of this pathway was to increase the CO_2 concentration in the chloroplast of the GTDEF plants. The GTDEF transgenic plants already fix CO_2 in higher amounts than the wild type plants. Using the new MMPEM pathway in the chloroplast of GTDEF plants can fix more CO_2. It also metabolizes glyoxalate in higher amount than the GTDEF pathway alone. The result of this strategy could be an increased production of biomass compared to GTDEF plants. Therefore introducing the new pathway into the chloroplast was beneficial for transgenic GTDEF plants. The GTDEF plants already showed higher biomass in our previous work, bypassing the photorespiration in C_3 plants (Arabidopsis) improved to lower the CO_2 compensation point (Γ). It was around 66.80 compared to compensation point 77.70 of the wild type plants. It showed ~30% increased of glucose, sucrose and starch (Kebeish et al., 2007). Hence, the expression of the MMPEM pathway

genes inside the chloroplast of GTDEF plants could reduce of photorespiratory flow in higher amount and in turn an increase in the CO_2 concentration under the vicinity of Rubisco.

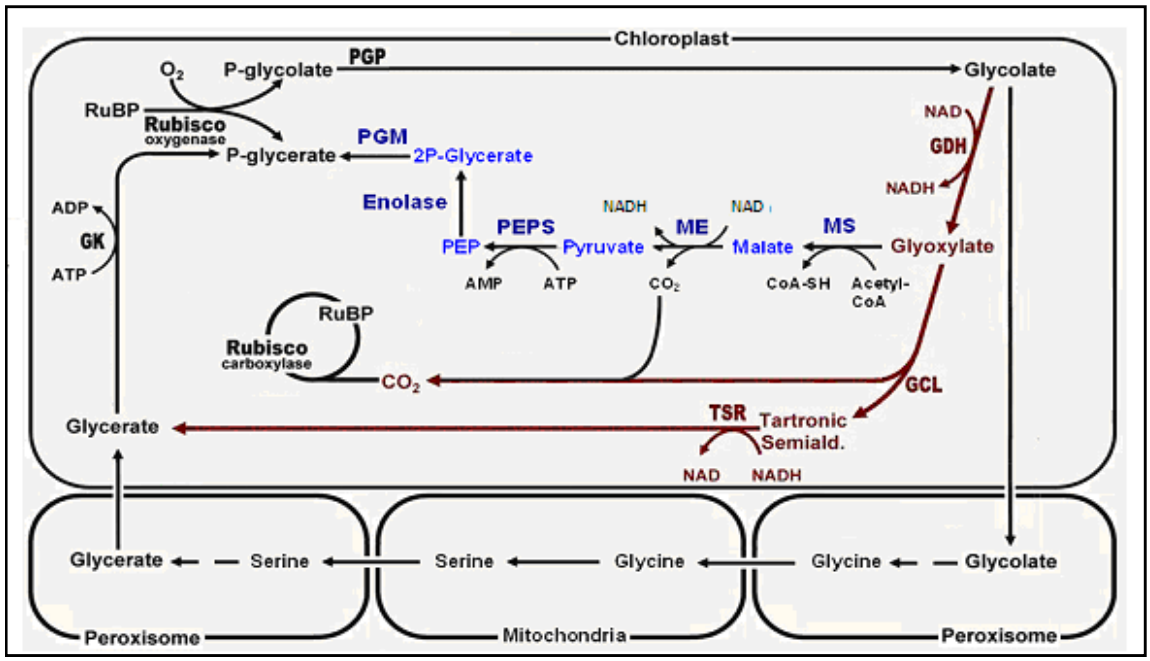

Figure 3.2.1: Representation of the photorespiratory pathway (black) in C_3 plants and the proposed pathway (red) for the conversion of glycolate to glycerate. New improved pathway (Blue)
The oxygenase reaction of Rubisco results in the formation of P-glycerate and P-glycolate. P-glycolate is dephosphorylated by PGP forming glycolate that is oxidized by GDH to form glyoxylate. Two molecules of glyoxylate are condensed by GCL forming tartronic semialdehyde and CO_2 is released in the chloroplast. Tartronic semialdehyde is then reduced by TSR forming glycerate. Glycerate is phosphorylated by GK to form P-glycerate that is used directly for carbohydrate biosynthesis through the Calvin Benson cycle. Again blue pathway from glyoxalate converts malate with the help of malate synthase. In this reaction malate synthase uses acetyl CoA and convert to CoA. Malate decorboxylate by malic enzyme forms pyruvate. PEP regenerated by pep synthase consumes ATP for regeneration of PEP. PEP converted to 2PG catalysed by enolase. PGM transfer phosphate group from 2PGM to 3PGM. PGP = phosphoglycolate phosphatase; GDH = glycolate dehydrogenase; cTP-AtGDH = *A. thaliana* glycolate dehydrogenase fused to a chloroplast targeting peptide (cTP); GCL = glyoxylate carboxyligase; TSR = tartronic semialdehyde reductase; GK = glycerate kinase; MS = malate synthase; ME = Malic enzyme; PEPS = phspho*enol*pyruvate synthase; PEP = phospho*enol* pyruvate; PGM = phosphoglycerate mutase; the photorespiratory enzymes are described in chapter. For the sake of clarity not all cofactor are shown.

3.2.2 Construction of pathway by MultiRound Gateway technology into single destination vector

The pYLTAC7_MMPEM pathway was transformed into the *N. tabacum* by *Agrobacterium* using a gateway single vector which was constructed by MultiRound Gateway technology. The *Agrobactrium* transformation with single vector (five genes)

could give higher transformation rate than the transformation with multiple single gene vectos. The construction of the multigene single vector mention in gateway technology (results 3.1.5). Recombinations of gateway vector (linearised gateway entry vectors) construct the way to avoid the silencing due to the orientation of promoter and polyadenylation cassette (Padidam and Cao *et al.,* 2001). If the orientation of the expression cassette was head to tail (←←) used the transcription blocker, which is an AT reach sequence from lambda phage DNA for avoiding the transcription interference.

In figure 3.2.2 showed the arrangement of expression cassette with five genes from the MMPEM pathway. In this pathway decided to use multiple times 35SS promoter, because in our first pathway pYLATC7_Hydrilla used four different promoters still HvPEPC and LdhA genes showed silencing effect in some lines. In this pathway 35SS promoter used for three genes and for one gene used At-RbcS promoter.

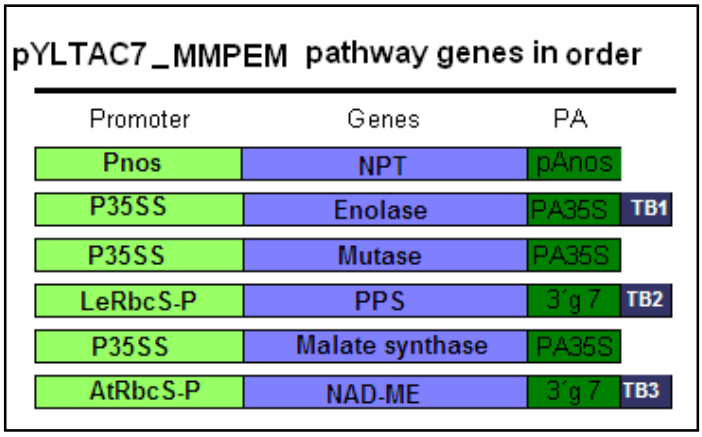

Figure 3.2.2: The arrangement of expression cassette with five genes
Genes and promoter form the MMPEM pathway: Light green box = promoter; purple colour box = genes from the pathway; dark green box PA = Polyadenylation; NPT = Neomycin phosphotransferase with Pnos = Promoter of nopaline synthase gene from *A. tumefaciens*; Enolase gene isolated from *E. coli* with 35SS promoter; Mutase gene isolated from *E. coli* with 35SS promoter; PPS = phospho*enol*pyruvate synthase gene isolated from *E. coli* with promoter from *Solanum lycopersicum* rubisco; Malate synthase gene isolated from *E. coli* with 35SS promoter; NAD-ME = malic enzyme gene isolated from *E. coli* with *Arabidopsis* rubisco promoter.

3.2.3 Analysis of agrobacterium and transgenic plants on DNA level

In order to check each gene (Enolase, Mutase, PPS, Malate synthase, NAD-ME, NPT) transform into *Agrobacterium* from the novel pathway, a multiplex PCR system was optimized for this purpose. Multiplex PCR analysis was undertaken for 10 different

agrobacterium colonies and 10 different transgenic plants DNA after transformation. In first approach used three different pair of primers for Me, PEPS, Enolase in the second approach used 2 different primer pairs for mutase and npt. Malate synthase gene checked individual by PCR. Each gene checked for individual colony of *Agrobacterium*, for testing the transgenic plants on the DNA level for each gene the same primer system used for the multiplex PCR.

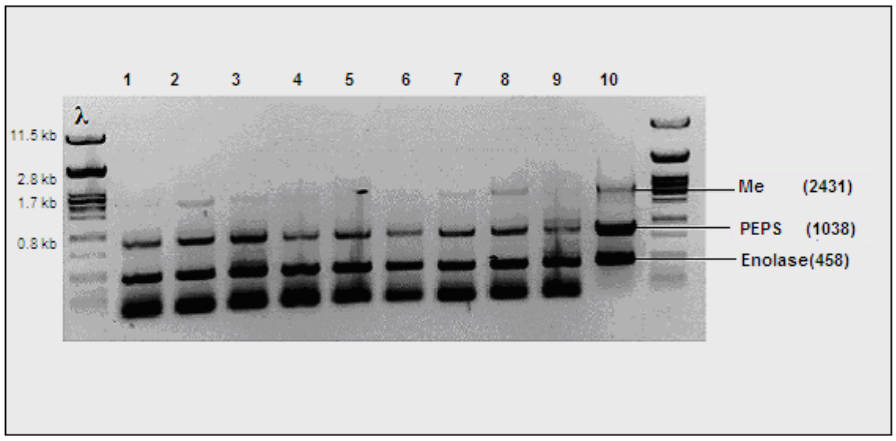

Figure 3.2.3: Multiplex PCR for Me, PPS and Enolase

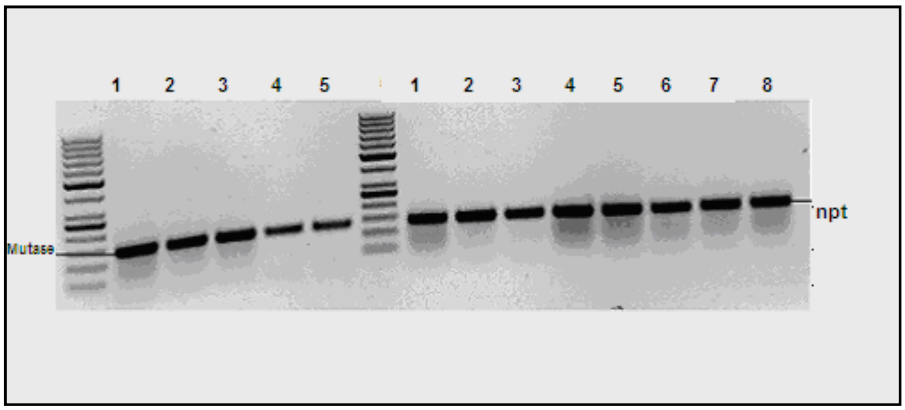

Figure 3.2.4: Multiplex PCR for Mutase and npt

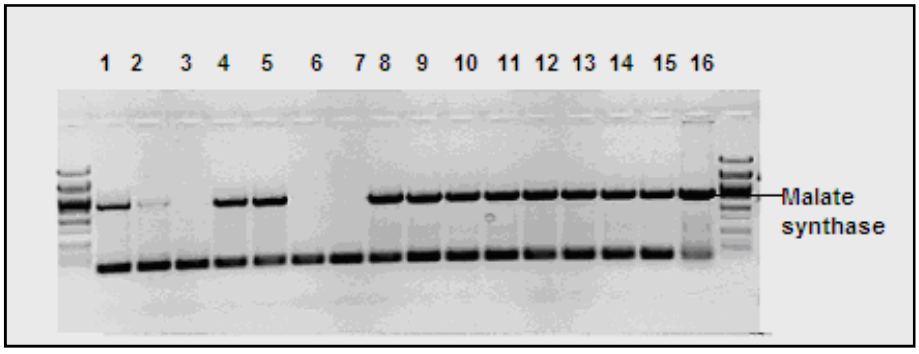

Figure 3.2.5: Control PCR for malate synthase

Figure 3.2.3 and 3.2.4: 15µl PCR reaction mixture for each agrobacterium colony and each plant DNA was analysed on 1% agarose gel. Results of the PCR from the different *A. tumefaciens* colonies and each gene checked for individual colony for ME, PEPS, Enolase, Mutase and npt genes respectively. Three primer pair used for the ME (2431 bp), PEPS (1038 bp) and Enolase (458bp) and lambda marker used for the gel picture. For Mutase and npt PCR two primer pairs and 100 bp markers have been used for the gel picture. **Figure 3.2.5:** malate synthase gene checked by PCR and 100 bp marker used for gel picture.

3.2.4 Transient expression of GTDEF+MMPEM pathway

Transient expression was carried out whether five genes from the construct pYLTAC7_MMPEM can express all five genes in the transgenic GTDEF tobacco plants. Transient expression was performed according to chapter material and methods 2.2.2.6. Plant growth conditions are described in results (3.1.9).

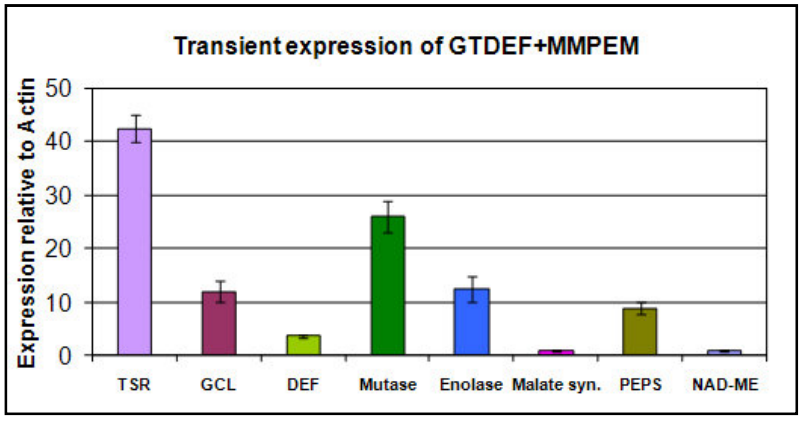

Figure 3.2.6: Transient expression of pYLTAC7_MMPEM gateway vector in transgenic GTDEF Tobacco plants. The above results shows the difference in expression level of transformed genes in tobacco. All eight gene expression of vector pYLTAC7_MMPEM in GTDEF transgenic plants: TSR = tartronic semialdehyde reductase; *GCL* = glyoxylate carboxyligase; DEF = *E. coli* glycolate dehydrogenase enzyme is formed from three different polypeptides that are encoded by three different open reading frames named *glc*D, *glc*E and *glc*F; PEPS = phospho*enol*pyruvate synthase; NAD-ME = NAD dependent malic enzyme. The expression of the different transgene was determined by Real time PCR and relative to the expression of endogenous Actin 2 gene. Each data point is based on at least three independent preparations. The error bars indicate standard error.

In GTDEF pathway all promoter were similar 35SS and in MMPEM pathway genes were under the control of 35SS and LeRbcs, At-RbcS promoter (see fig. 3.2.2). The results from the Real Time PCR showed that all five genes from the new construct are expressed in transgenic GTDEF plants but, TSR, Mutase GCL, genes showed higher expression than the other genes from the pathway.

The relative expression of malic enzyme was very low around 0.90 to 1 times relative to actin. A very high expression was measured with the tartronic semialdehyde reductase (TSR) gene which was around 50 times higher relative to actin. The TSR gene is stably integrated into the plant genome and its expression is not transient.

3.2.5 Stable expression of the genes of the MMPEM pathway in the chloroplast of transgenic GTDEF tobacco plants (T_0 generation)

The stable transformation performed like described by De block *et al.,* (1988) and Dietze *et al.,* (1995). The expression of the different transgenes RNA-level has been tested by Real time PCR. The different transgenes in different preparation of RNA expression is normalized with the help of the endogenous Actin2. The expression of five MMPEM genes in the GTDEF plants has been checked for 56 plants. It has been shown that 16 plants expressed all MMPEM and GCL, TSR and DEF genes. Although expression was heterogeneous and this depends on variable factors (Results 3.1.10). The transformation rate with the MMPEM pathway was 10% higher compared with the pYLTAC7_Hydrilla pathway transformed plant. The expression of NAD-ME, PPS, Mutase, Malate Synthase and Enolase in *planta* was tested on the RNA level using RT-PCR (Material and Methods 2.2.1.10).

In fig. 3.2.7 shows the expression of all five genes and expression of three GTDEF genes. GTDEF genes are constitutively expressed and show higher expression rate compared with the MMPEM genes expression in transgenic tobacco plants. Highest relative expression was observed for the TSR gene (69 times higher than Actin). The lowest expression was measured by the malic enzyme (around 0.9 to 1.9 times than Actin). The data in figure 3.2.7 shows a very heterogeneous rate of the expression. Enolase 14 ± 0.6, Malate synthase 1.4 ± 0.46, Mutase 60 ± 2.42, DEF 2 ± 2, TSR70 ± 4.34, GCL 16 ± 3.56, PPS 60 ± 2.4. Expression of TSR and Mutase was mostly higher in many plants than other genes. Expression of with all eight genes showed in line 7, 10, 13, and 33 which were passes in the T_1 generation to test other parameter for the evaluation of the GTDEF+MMPEM pathway.

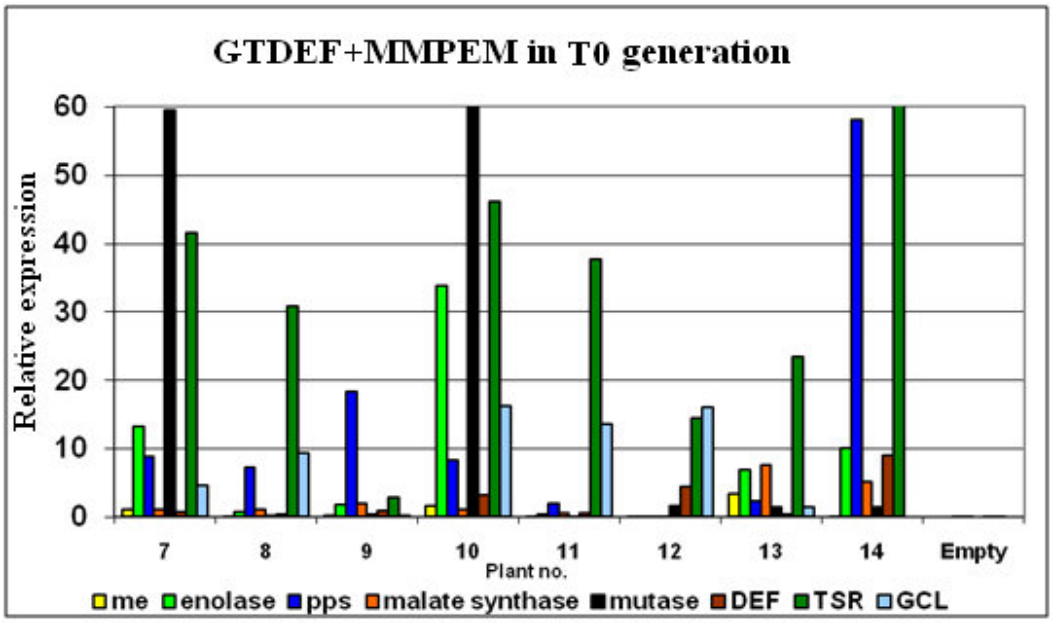

Figure 3.2.7: Expression of genes measured by Real-Time PCR
Values calculated by arbitrary units. Each value is the relative accumulation of the respective RNA compared to the Actin 2 levels measured in the preparation from 4 weeks old plants after about 4 hour exposure to light. Empty = transgenic plants carrying empty plasmid in T_0 generation. TSR = tartronic semialdehyde reductase; *GCL* = glyoxylate carboxyligase; DEF = *E. coli* glycolate dehydrogenase enzyme is formed from three different polypeptides that are encoded by three different open reading frames named *glc*D, *glc*E and *glc*F; PPS = phospho*enol*pyruvate synthase; ME = NAD dependent malic enzyme.

3.2.6 Stable expression of Enolase, Malate synthase, Mutase, NAD-ME, PPS, DEF, TSR, GCL in T_1 generation

Various biochemical parameters of transgenic *N. tabacum* plants possessing the GTDEF plants the MMPEM pathway were tested in the T_1 generation. Three weeks old plants were harvested to measure the expression of foreign genes by RT-PCR (Material and methods 2.2.1.10). The samples were taken after 4 hours of exposure to light. All eight genes were tested in the T_1 generation. The expression patterns are shown in fig. 3.2.8 from plant line 7. Twelve plants were checked for the expression data from the line 7 and it shows 8 plants were expressed all genes and 3 plants were azygote. Line 10 and 14 were showed the expression of eight gens in only 4 and 3 plants respectively out of 10 plants for each line. The expression of TSR, mutase and enolase was high compared to all other genes from th pathway shown in figure 3.2.8. The relative expression of NAD-ME and malate synthase was least, 1.2 to 1.3 respectively compared to the actin gene.

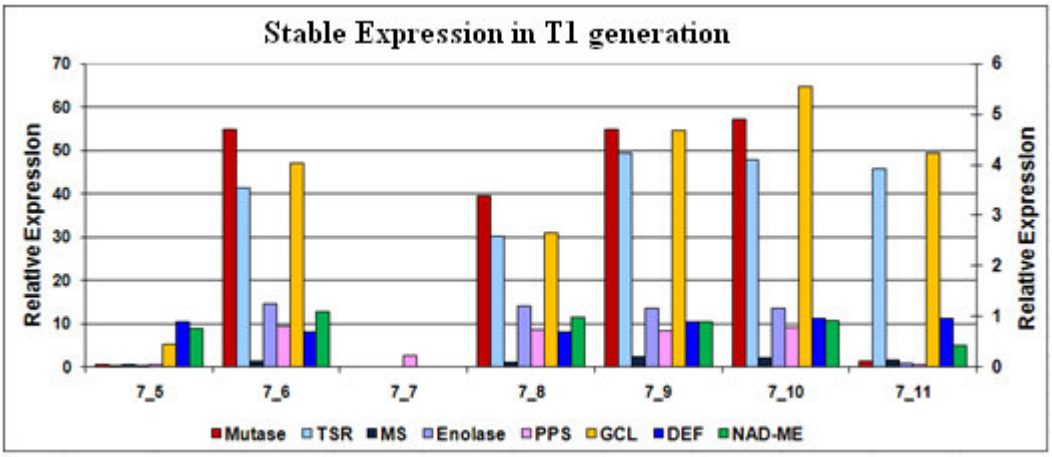

Figure 3.2.8: Stable expression of genes measured by Real Time PCR
Data calculated in arbitrary units. Each value is the relative accumulation of the respective RNA compared to the Actin 2 levels measured in the preparation from 4 weeks old plants. Each data point is based on at least three independent RNA preparations. TSR = tartronic semialdehyde reductase; GCL = glyoxylate carboxyligase DEF = *E. coli* glycolate dehydrogenase enzyme is formed from three different polypeptides that are encoded by three different open reading frames named glcD, glcE and *glc*F; PPS = phospho*enol*pyruvate synthase; ME = NAD dependent malic enzyme.

3.2.7 Determination of the MMPEM pathway activities and evaluation of the transcription levels in transgenic GTDEF tobacco plants

Samples were taken from 5 weeks old plants from the the T_1 generation. The relative enzyme activities were calculated to determine the increase of the enzyme activities of individual transformants. NAD-ME and PEP synthase activity (Material and Methods 2.2.3.1) determined in this part of the study.

Transgenic plants from line 7 and 10 (T_1 generation) shows the maximum relative activity of PEP synthase and NAD-malic enzyme in the table (3.2.1) and the maximum relative expression of GCL, TSR, DEF, Enolase, Mutase and malate synthase.

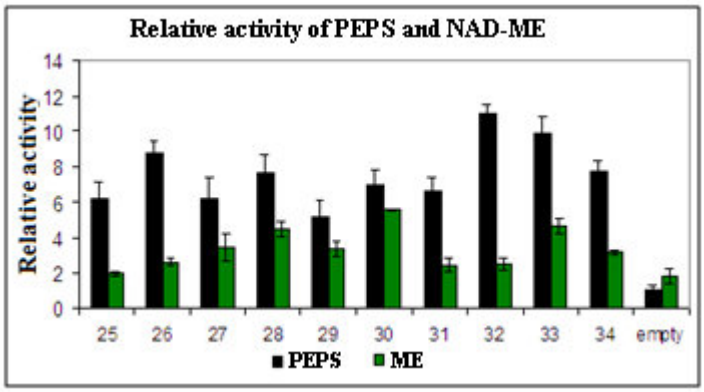

Figure 3.2.9: Relative activity of NAD-ME and PEPS synthase

Extracts isolated from 6 weeks old empty vector plants as well as from plants transgenic for GTDEF+MMPEM were tested: PPS = phosphor-*enol*pyruvate synthase and ME = malic enzyme activity (Material and Methods 2.2.3.2). Each data point is based on at least three independent experiments. Vertical bars show standard deviations. Black bars = PPS; green bars = malic enzyme; empty = Plant carrying empty vector used as control.

Table 3.2.1: Relative expression and relative activity of transgenes in T_1 generation

Transgenes	Relative activity		Expression relative to actin					
GTDEF + MMPEM	PEPS	NAD-ME	GCL	TSR	DEF	Enolase	Mutase	Malate synthase
No. 7	10.93	1.3	5.49	41.47	1.1	14.13	54.81	1.4
No. 10	6.91	1.4	16.24	46.2	3.26	33.65	82	1.6

3.2.8 Determination of metabolites by GC-MS

In this study the GC-MS method was used for most of the photosynthetic and Calvin Benson cycle related compounds. This could give a primary idea about introduction of MMPEM genes into the chloroplast of GTDEF plants increase the rate of photosynthesis and ultimately the slightly higher concentration of glucose, fructose and sucrose as compare to only MMPEM and GTDEF pathways (Fig.3.2.10A).

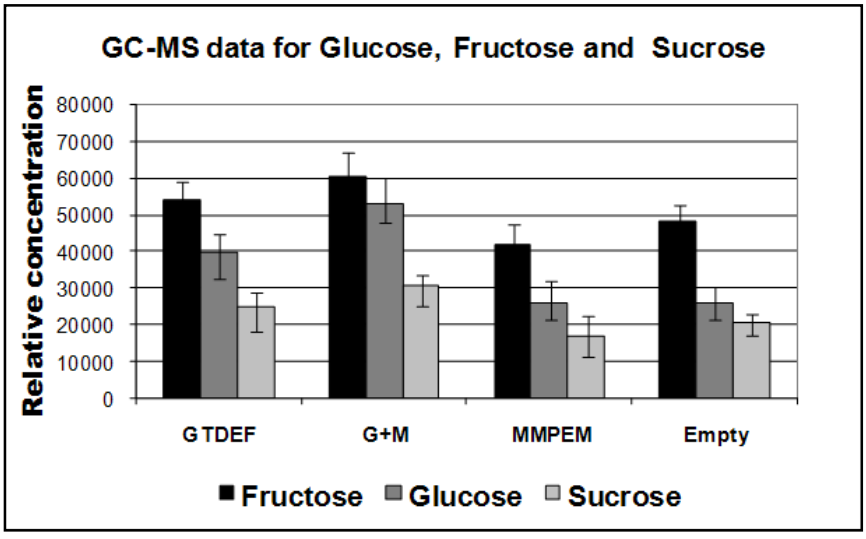

Figure 3.2.10A: Relative concentration of Glucose, Fructose and Sucrose by GC-MS
Probes isolated from 3 weeks old plants and independent preparation of polar phase performed three times for getting similar effect. G+M = Plant expressing GTDEF and MMPEM pathway; GTDEF = plant expressing *Ec*GDH, GCL, TSR; TSR = tartronic semialdehyde reductase; GCL = glyoxylate carboxyligase; DEF = *E. coli* glycolate dehydrogenase. This enzyme is formed from three different polypeptides that are encoded

by three different open reading frames named *glc*D, *glc*E and *glc*F; MMPEM = plant expressing Mutase, Enolase, Malate synthase, EcME, PEPS; PEPS = phospho*enol*-pyruvate synthase and ME = malic enzyme. Vertical bars show standard deviations.

Amino acids: Impact of MMPEM+GTDEF pathway genes on concentration of amino acids was measured by GC/MS because serine, glycine is the important amino acids for to check the activity of photorespiration (Introduction 1.3.1). GTDEF+MMPEM and GTDEF transgenic plants showed lesser serine concentration as compared with the MMPEM and control plant lines so possibly lesser photorespiration in these transgenic lines. But the concentration of glycine not showed any difference in these transgenic plant lines as compared with the control lines. Other checked amino acids like threonine, proline and alanine amino acid were showed similar concentration in GTDEF and GTDEF+MMPEM transgenic plants (Fig. 3.2.10 B). Other metabolites from transgenic lines were showed very inconsistent values therefore not showed in this study.

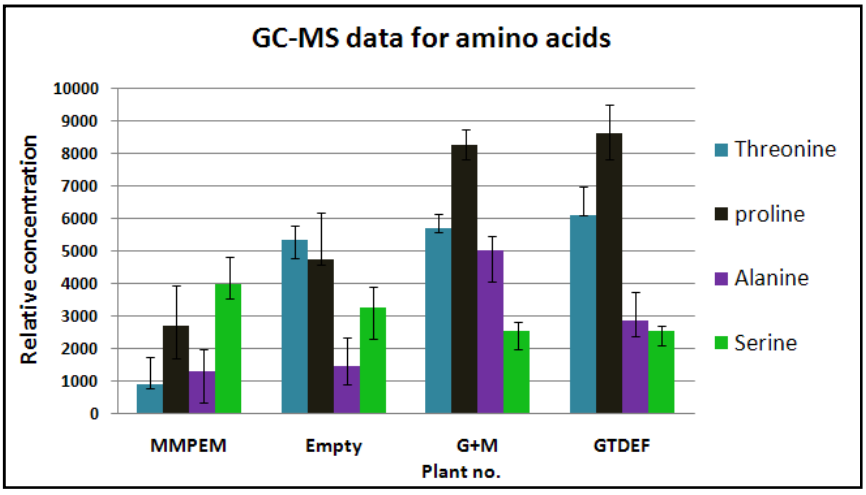

Figure 3.2.10B: Relative concentration of amino acid by GC-MS
Probes isolated from 3 week old plants and independent preparation of polar phase performed two times for getting similar effect. Concentration of threonine, proline, alanine and serine were showed in MMPEM, GTDEF+MMPEM, and GTDEF plants as compared with the empty as a control.

3.2.9 Phenotype effect of MMPEM and GTDEF pathway on transgenic tobacco plant

Established GTDEF pathway has been known for higher biomass and lesser compensation point in the model species *Arbidopsis* (Kebeish *et al*., 2003). This pathway proposed to

reduce the photorespiratory losses. In our new strategy for MMPEM pathway in the chloroplast of GTDEF plants tried to reduce more amount of photorespitatory fluxes than mere GTDEF plants.

By this strategy, we observed GTDEF and MMPEM plants line which accumulated more biomass as compared with the solely GTDEF plant lines. The growth rate of MMPEM+GTDEF plants was faster than the control lines and other transgenic plants (MMPEM, GTDEF). Transformed plants with only the MMPEM pathway did not showed any improvement as compared with the control plant lines. Expression of the only MMPEM pathway in chloroplast showed slight variation in leaf anatomy like pointed blade like leaves. The expression of MMPEM pathway in chloroplast of GTDEF pathway does not induce any harmful effects in the transgenic plants but slightly enhance plant growth. In figure 3.2.11 has shown the same age plants of GTDEF+MMPEM seen higher length and leaf area than other three phenotypes MMPEM and GTDEF plants and wild type plant.

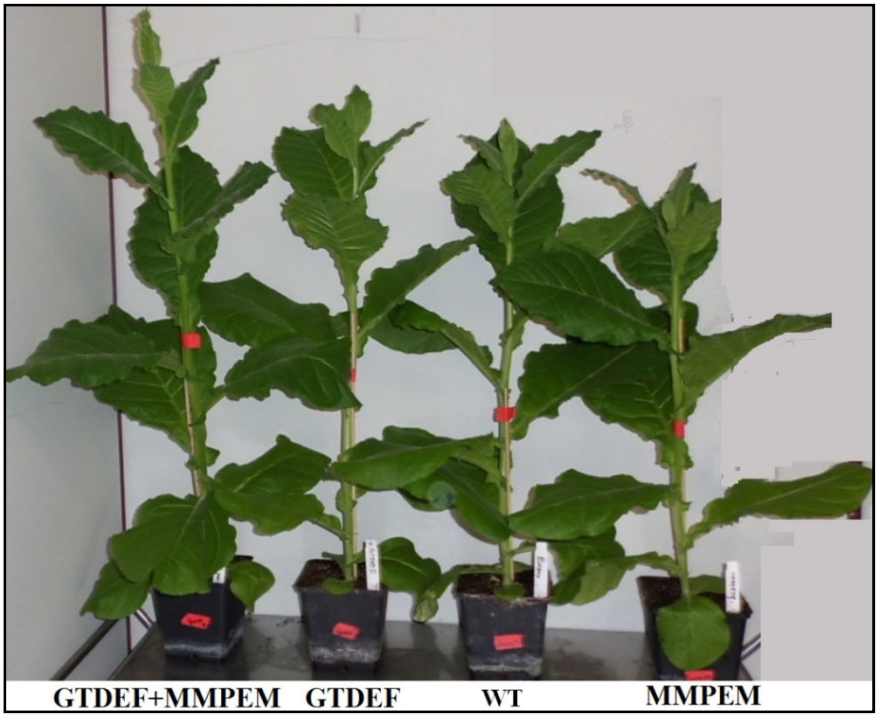

Figure 3.2.11: Phenotypic effect of MMPEM, GTDEF, GTDEF+MMPEM and wild type plants

In above fig. phenotypes of 7-8 weeks old MMPEM, GTDEF, GTDEF+MMPEM and azygote transgenic plants compared to wild type plants. GTDEF+MMPEM = Transgenic plants carrying GCL, TSR, DEF, Mutase, Enolase, Malic enzyme, PEP synthase and Malate synthase genes; GTDEF = Plant carrying GCL, TSR, DEF genes; MMPEM = Plant carrying Mutase, Enolase, Malic enzyme, PEP synthase and Malate synthase genes; Wild type plants used as a control.

3.2.10 Effect of the novel pathway on the plant leaf area and the height of the plant

I. Measurement of the plant leaf area

Quantification of the effect of the MMPEM+GTDEF plants investigate by determining the leaf area in cm^2 and height of the plants at the age of 8 weeks after sowing. In order to evaluate the influence of novel pathway on the growth of the transgenic plants, the plant leaf area was measured from GTDEF, GTDEF+MMPEM, MMPEM and parallel with empty plasmid possessing plants. Leaf area measurement showed that GTDEF plants have higher leaf area as compared to empty plasmid plants. It also revealed that GTDEF+MMPEM have even higher leaf area than transgenic plants expressing individual GTDEF and MMPEM pathway (Fig. 3.2.12). The expression of GTDEF genes inside the plant (*Arabidopsis*) chloroplast showed higher leaf area and as our previous experiences (Kebeish et al., 2007). In this new dual pathway experiment (GTDEF+MMPEM) shows: The leaf area increases when expressing the MMPEM pathway genes inside the chloroplast of GTDEF plants. Transgene for alone MMPEM pathway showed lesser leaf area as compared to other transgenic plants (empty, GTDEF and GTDEF+MMPEM pathway). This can also add to the positive impacts of the GTDEF+MMPEM pathways in the transgenic plants.

II Measurement of the height and diameter

The height and the diameter of the stem measured from 8 week old plants growing under ambient condition as shown in fig. 3.2.12. A plant transgenic for MMPEM and empty plasmid possessing plants showed similar height and diameter (Material and Methods 2.2.3.3). On the other hand, GTDEF+MMPEM plants showed higher length as compared with GTDEF and wild type plants shown in fig. 3.2.12. Although GTDEF+MMPEM and GTDEF plants shows similar stalk diameter (thickness of the stem) as compared to the empty plasmid plants. The stalk is one of the metabolic sink organ of tobacco plants, and the increases in its length and thickness depends on the supply of sucrose by source leaves. In this case we found out higher concentration of sucrose in GTDEF+MMPEM plants but still did not show any improvement in stalk thickness. Genotype of chloroplastic expression of both pathways together GTDEF and MMPEM show bigger leaf area as well as higher length of the plant as compared to the empty, MMPEM alone and GTDEF pathway plants.

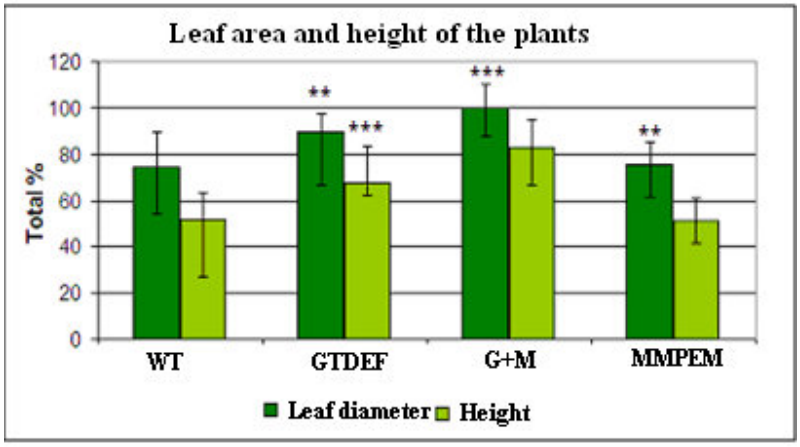

Figure 3.2.12: Leaf area and height of the plants
Relative values of plant leaf diameter measured from 6 weeks old wild type and all generated transgenic lines growing under long day conditions (8 h light, 16 h dark) in percentage. The tested plant seeds (T_0 generation) were sowed in a soil and later planted individual plant in a pot and directly transported in a long day room. Plants were checked for every gene by PCR and Real time PCR Plants transgenic for each transgenic line. Finally, the plant leaf area was determined from each genotype by this formula A = 3.73 x (L x W/100) + 0,011 x (L xW/100)² Leaf area (A), length (L) and width (W) of the leaf. Each value represents the average of leaf area measured from at least 5 sister plants for each line. Leaf surface area (leaf diameter) calculated by formula material and methods (2.2.1.17) and leaf diameter in cm^2 and plant height calculate in cm and converted into the percentage to check the actual differentiation in each genotype. GTDEF+MMPEM = Transgenic plants carrying GCL, TSR, DEF, Mutase, Enolase, Malic enzyme, PEP synthase and Malate synthase genes; GTDEF = Plant carrying GCL, TSR, DEF genes; MMPEM = Plant carrying Mutase, Enolase, Malic enzyme, PEP synthase and Malate synthase gene. *, **, and *** denote deviations from the wild types with $P<0.1$, $P<0.05$ and $P<0.001$, respectively.

3.2.11 Measurement of the total fresh and dry weight of the transgenic plants

C_4 plants are superior to C_3 plants in apparent photosynthesis rates due to diminished photorespiration (3.2.12). Therefore, they have higher rate of fresh and dry matter production. In this approach, the total fresh and dry weight of the different transgenic plants was measured. Plants were allowed to grow for 8 weeks from the seedling stage under ambient conditions. Transgenic plants were harvested at this time point of 8 weeks and total fresh and dry weight were calculated. Plants were measured in two generations and average of the total weights calculated for the results. The aim was to calculate the effect of GTDEF+MMPEM on the total biomass of the plant. Two generations of plants created to checked plants grown in winter time in the green house and summer time in the green house. In both cases light intensity and temperature was similar in the green house but summer time grown transgenic plants shows higher biomass and faster growth as

compared to azygote. Winter time grown transgenic plants were shown slower growth rate and lesser biomass as compared to summer time grown plants. The reason might be the direct sunlight on the plants gives positive impact on the transgenic plants by increasing the leaf size. Measurement of total fresh and weight was done repeatedly.

Plants transgenic for GTDEF+MMPEM showed an increased fresh weight as compared with lines possessing only GTDEF, MMPEM and wild type plants (see figure 3.2.13). For the measurement of the dry weight 8 weeks old transgenic plants were harvested. They were kept in oven for 2 days on 100 degree centigrade to remove the water content. The wild type and plants possessing the MMPEM pathway alone showed the same results. In figure 3.2.13 showed higher dry weight in plants with GTDEF pathways but even higher dry weight in plants with GTDEF+MMPEM plants. The total fresh and dry weight of GTDEF and GTDEF+MMPEM plants were 10 to 20% higher compared to the control.

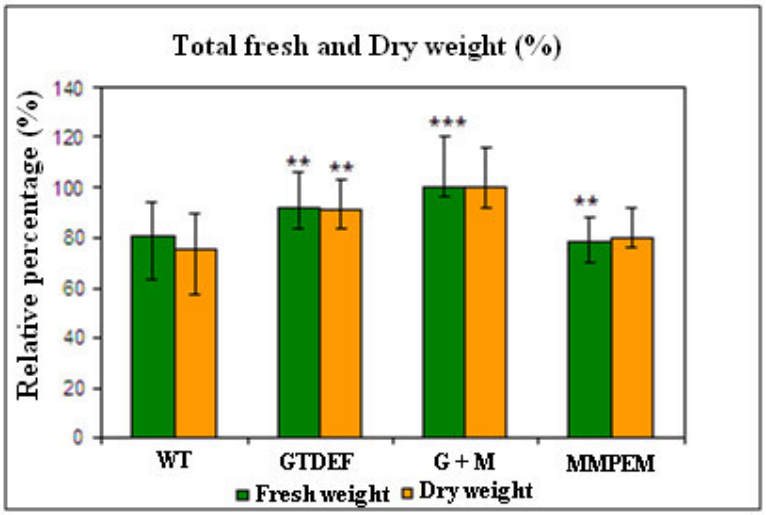

Figure 3.2.13: Total dry and fresh weight of transgenic plants
Relative changes in the percentage of total fresh and dry weight measured from 8 and 9 weeks old wild type and different transgenic plants growing under long day conditions (8 h light, 16 h dark). The tested plants were allowed to grow for 8 weeks under long day growth conditions. All genotypes were allowed to grow in the same chamber and similar conditions (level of water, light conditions, soil type and temperature) optimized for each genotype. At this time point, the fresh and dry weight was determined from all genotypes. The total fresh and dry weight measurements were repeated three times for two generations. Each value represents the average of changes in plant fresh and dry weight measured from at least 6 sister plants for each line. The total average calculated in percentage and highest weight of the transgenic plant considered 100%. GTDEF = plants expressing *GDH*, *GCL* and *TSR*; MMPEM = plants expressing malate synthase, mutase, enolase, ME and PEPS; G+M = plant expressing GCL, TSR, GDH, expressing malate synthase, mutase, enolase, ME and PEPS. *, **, and *** denote deviations from the wild types with $P<0.1$, $P<0.05$ and $P<0.001$, respectively.

Our presented result shows the expression of the novel MMPEM pathway in the chloroplast of GTDEF plants has a positive impact on the plant growth. Azygote and MMPEM lines showed the same results in many parameters. The reason is: in MMPEM plants no glyoxalate is produced by the glycolate dehydrogenase. Therefore the MMPEM pathway has no substrate for continuation of the pathway in the chloroplast.
Parameters like lesser compensation point than other genotype, post illumination burst, biochemical analysis, and total biomass measurement showed in this study. Concerning all these results, transfer of the novel MMPEM pathway in transgenic GTDEF leads to decrease their photorespiratory flow and increase the total plant productivity.

3.2.12 Photosynthetic performance of transgenic plants

In the chapters above the possible impact of the novel pathway on the plant metabolism was measured. In this chapter the impact of the expression of the genes of the novel pathway on the photosynthesis performance was checked. Therefore, the post illumination burst (PIB) and the apparent CO_2 compensation point (Γ) were measured.

3.2.12.1 The postillumination burst (PIB) as a marker for the rate of photo-respiration

Postillumination burst means: If a C_3 plant is exposed to sudden darkness after a period of illumination (where the plant achieves steady state rates of photosynthesis), a momentary rapid outburst of CO_2 occurs before the plant reaches steady state dark respiration (Rn). This CO_2 outburst shows the amount of CO_2 delivered in plant mitochondria at the time of photorespiration (Atkin et al., 1998; Bulley and Tregunna, 1971). Depends on this criteria, it was decided to determine the postillumination burst (PIB) from transgenic as well as azygote plants as a measure for the photorespiratory flow in these plants. PIB was measured using LI-COR 6400F, a portable photosynthesis measuring device (2.1.2). The post illumination burst calculated as shown in fig. 3.2.14 (B). Difference between the maximum CO_2 release after 20-120 second from the switching off the light and the amount of CO_2 release during steady state dark respiration (Rn) is called Post illumination burst. Plant transgenic for GTDEF+MMPEM plants show decrease in the amount of CO_2

release at the time of photorespiration as shown PIB values in fig. 3.2.14B compared to their wild type *Nicotiana tabacum* plants.

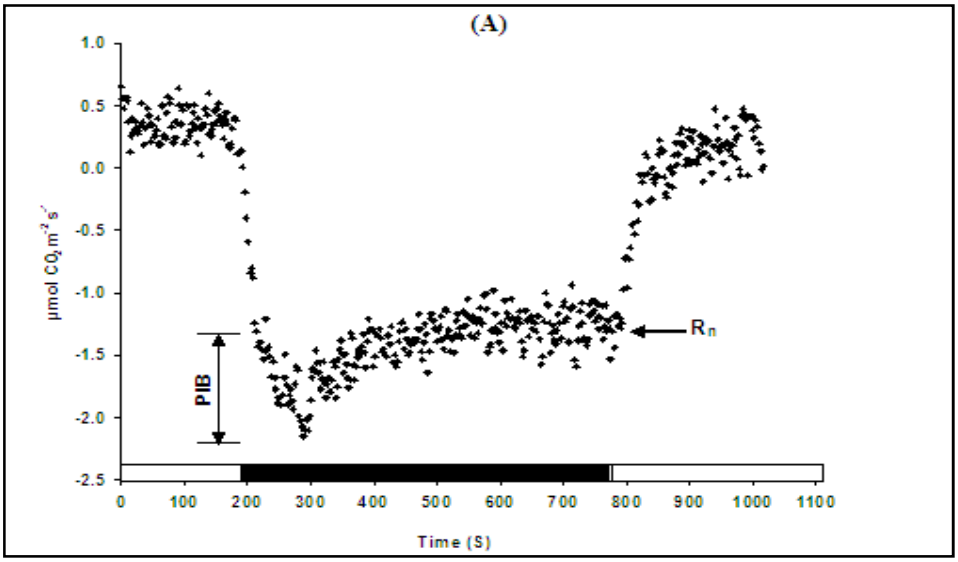

Figure 3.2.14A: Postillumination burst from transgenic plants.
Shown are a time course of net CO_2 exchange from a *Nicotina tobacum* plant leaf under 1000 µmol photons m^{-2} s^{-1} and 100 ppm CO_2 and the different postillumination bursts measured from ayzgote and different transgenic plants. In figure 3.2.14A: PIB = Postillumination burst; Rn = plant dark respiration; white horizontal bar = light on; black horizontal bars = light off.

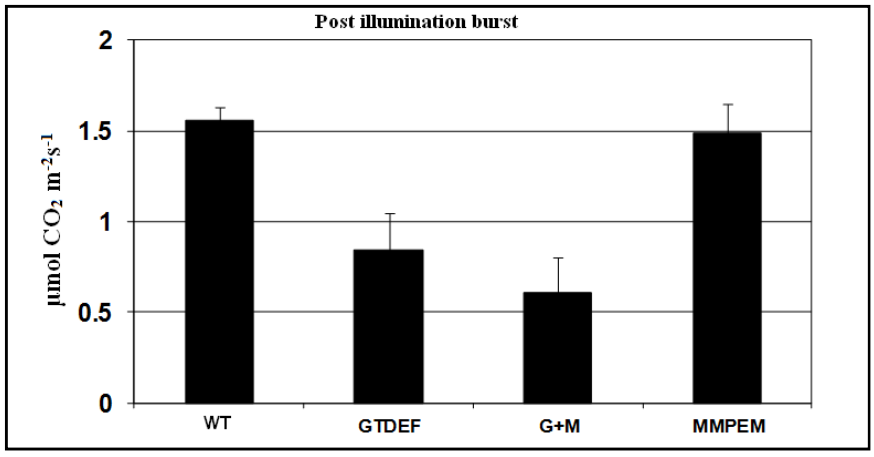

Figure 3.2.14B: Postillumination burst from transgenic plants
In figure B: Each value shows the different PIB for the WT, GTDEF; GTDEF+MMPEM and MMPEM plants. PIB and is based on three independent measurements of four sister plants for each line. GTDEF = plants expressing GCL, TSR and EcGDH; G+M (GTDEF+MMPEM) = plant expressing GCL, TSR and EcGDH, Mutase, Enolase, Malate synthase, Malic enzyme and PEP synthase; MMPEM = plant expressing Mutase, Enolase, Malate synthase, Malic enzyme, and PEP synthase. A vertical bar shows the standard error.

This decrease in PIB is observed by the expression of MMPEM pathway genes in the chloroplast of GTDEF plants. These results shows the expression of GTDEF pathway

genes in *N. tobacum* plants responsible for the reduction in the photorespiration CO_2 release in the mitochondria but even further decrease the CO_2 release in the mitochondria if, MMPEM pathway gene express in the chloroplast of transgenic GTDEF plants. This shows the MMPEM pathway together with GTDEF plants added significant effect to reduction of photorespiration as compared with only GTDEF and MMPEM plants.

3.2.12.2 Determination of the apparent CO_2 compensation point (Γ*) of the transgenic plants

At the apparent CO_2 compensation point, the amount of CO_2 fixation by a plant equals the amount of CO_2 released from the plant by photorespiration and respiration (Atkin *et al.,* 1998; Laisk, 1977; Laisk *et al.,* 1984).

The compensation point Γ was measured GTDEF+MMPEM, GTDEF, WT and MMPEM plants by measuring their photosynthetic rates (A) at different leaf internal CO_2 concentrations (Ci) (is called A/Ci- curve) as described in the materials and methods chapter 2.2.3.7. The CO_2 compensation point (Γ) gives an idea about the amount of CO_2 released in plant mitocondria during the photorespiratory pathway and amount of CO_2 concentration in the vicinity of Rubisco at a given Ci. As described above the A/Ci curves were determined by GTDEF, G+M, MMPEM and control plants (wild type and empty plasmid carrying plants) from the T_1 generation (Figure 3.2.15).

Γ was calculated as the crossing point between the measured A/Ci-curve and the X-axis. The apparent CO_2 compensation point of each plant tested has been shown in table 3.2.2. WT plants and lines possessing the MMPEM (in this pathway no gloxylate is made in the chloroplast) shows a similar CO_2 comensation point. This represents, that the MMPEM pathway alone is not beneficial for the CO_2 fixation reaction in C_3 plant *N. tabacum.* Lines expressing the GTDEF together with the MMPEM pathway shows the lowest value of Γ, even lower than GTDEF lines (Table 3.2.2).

Therefore it can be concluded that the MMPEM pathway has a positive impact on the CO_2 fixation in C_3 plants, if glycolate is produced in the chloroplast by the glycolate dehydrogenase. The result showed the expression of the MMPEM pathway genes inside the GTDEF plant chloroplast results in a reduction of photorespiratory flow and in turn an increase in CO_2 concentration in the vicinity of Rubisco.

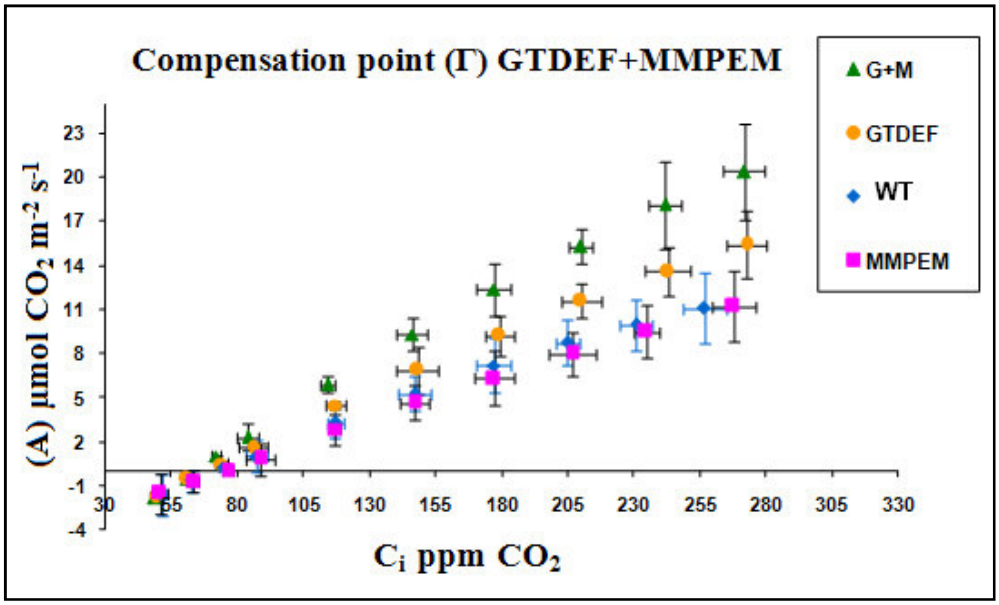

Figure 3.2.15: A/Ci-curve from WT and transgenic plants
Different A/Ci-curves measured from 6-8 weeks old wild type, GTDEF, MMPEM and GTDEF+MMPEM plants under illumination 1000 µmol photons m^{-2} s^{-1} and different external CO_2 concentration (Ca. = 400, 350, 300, 250, 200, 150, 100, 80, 65 and 45 ppm CO_2). Each value represents the assimilation rate is based on at 4 independent measurements from 6 sister plants for each line. Vertical and horizontal bars shows standard errors (A) = Assimilation rate; (Ci) = internal CO_2 concentration in the leaf intercellular spaces; G + M = Plant expressing GTDEF and MMPEM pathway genes; GTDEF = plant expressing *Ec*GDH, *GCL*, *TSR*; MMPEM = plant expressing Mutase, Enolase, Malate synthase, EcME, PEPS.

Table 3.2.2: The apparent CO_2 compensation point (Γ) of WT and transgenic plants

Plant	**Apparent CO_2 compensation point (Γ)**
WT	72.65 ± 2.14 ppm CO_2
MMPEM	73.72 ± 2.45 ppm CO_2
GTDEF	64.88 ± 2.88 ppm CO_2
GTDEF+MMPEM	60.89 ± 3.96 ppm CO_2

Table 3.2.2: shows the apparent CO_2 compensation points measured from 6-8 weeks old WT and different transgenic plants. GTDEF = plant expressing *Ec*GDH, *GCL*, *TSR*; MMPEM = plant expressing Mutase, Enolase, Malate synthase, EcME, PEPS; GTDEF+MMPEM = Plant expressing GTDEF and MMPEM pathway genes.

4 Discussion

4.1 Bi-functionality of Rubisco

As has been described in the chapter introduction, the enzyme ribulose 1,5-bisphosphate carboxylase (Rubisco) Rubisco; EC 4.1.1.39 is a bifunctional enzyme. In addition to its carboxylation function, it can also catalyze O_2 fixation (Bowes et al., 1971). CO_2 and O_2 are mutually competitive at the same large subunit active site of Rubisco. Rubisco favors CO_2 (K_m = 10 μM) over O_2 (K_m = 200 μM) by a factor of up to 100, but the concentration of O_2 (around 21%) in the atmosphere is much higher than that of CO_2 (0.038%). As a result one molecule of O_2 is fixed by Rubisco for every three molecule of CO_2 (Sharkey, 2001). Rubisco possesses two activities: the carboxylation and the oxygenase reaction. Carboxylation of RuBP forming two phosphoglyceric acid (PGA) molecules which are directly used for the biosynthesis of carbohydrates as well as for the regeneration of ribulose-1,5-bisphosphate in a reaction sequence requiring ATP and NADPH (Calvin) and the oxygenation of RuBP, producing one 2-phosphoglycolate and one phosphoglycerate. Phosphoglycolate has no known metabolic purpose and in higher concentration it is toxic for the plant (Anderson, 1971). Plants metabolize phosphoglycolate to phosphoglycerate in side reaction sequences that occur in the chloroplast, peroxisome and mitochondria, with the release of CO_2 and ammonia in the mitochondria (Andrews and Lorimer, 1987; Leegood et al., 1995). The photorespiratory pathway in plants requires large machinery consisting of 16 enzymes and more than 6 translocators (Douce and Neuburger, 1999). CO_2 release during the photorespiratory pathway results in the loss of one quarter of the carbon in the form of phosphoglycolate (Leegood et al., 1995). Although photorespiration seems to be deleterious, but it helps C_3 plants in two ways: Firstly, photorespiration supplies C_3 plants with the two amino acids glycine and serine for protein synthesis (Sharkey, 2001). Secondly, C_3 plants are protected against high irradiances because of photorespiration (Kozaki and Takeba, 1996). However, for these functions C_3 plants have other mechanisms which are a better option than photorespiration. In the first case, capacity for starch and sucrose synthesis exceeds the capacity for glycine and serine synthesis. In the second case, spend of excess light by a mechanism involving zeaxanthin can spend much more energy than can photorespiration in most leaves (Sharkey, 2001). While these two functions of photorespiration may be useful to the plant, the overall effect of photorespiration is harmful. The study of photorespiration on Barely, (Wingler et al.,

1997) and Arabidopsis (Beckmann et al., 1997) shows, that growth of both photorespiratory mutant, is not affected under high CO_2 concentration (where no or little photorespiration and no enhanced photosynthesis is observed). By growing both mutant under lower CO_2 concentration (high photorespiratory rates), the plant growth was stunting or the plants died. The previous results supported the argument that partial suppression of photorespiration in C_3 plants may not be harmful for C_3 plant growth. Slight increase in the performance for photosynthesis of some crops species have been observed already when the external CO_2 concentration is doubled under greenhouse condition (Arp et al., 1998; Kimball, 1983) but this approach is variable species to species. The CO_2 enrichment in green house on tobacco lowers the photosynthsis. The statement behind that plant might lack the ability to acclimatise high level of CO_2 (Makino *et al*., 1999).

4.2 C_4 syndrome in C_3 plants

Photorespiration lowers the photosynthetic efficiency particularly in C_3 plants and to overcome this cope nature evolved the alternative mode of evolution "C_4 photosynthesis" response to prehistoric advent of atmospheric conditions that allowed for significant oxygenase activity and photorespiration (Ehleringer et al., 1991; Sage et al., 1999). C_4 plants can reach this through its carbon concentration mechanism leading to efficient suppression of the oxygenase reaction and shows one up to ten times higher CO_2 concentration in the bundle sheath cells when compared to the surrounding air. This strategy has been developed about 10 million year ago by a nature where C_4 plants were retested by evolution. This strategy has been successful in many plant species, in higher plants and in microalgae (an effective CO_2 concentration mechanism has been found in several microalgae).

The C_4 pathway acts to concentrate CO_2 at the site of the reactions of the C_3 pathway, and thus inhibit photorespiration (Hatch, 1987). Since, the discovery of CO_2 conentration mechanism in C_4 photosynthesis and its agronomic advantages, the transfer of C_4 traits in C_3 plants has been one strategy to improve the photosynthetic performance in C_3 plant. The C_4 pathway involves three steps that have been described in chapter (Introduction 1.4) and the separation between bundle sheath cell and mesophyll cell gives maximum advantage to diffusion of CO_2 at the site of Rubisco and at these two sites shows structural

and biochemically different chloroplast. The molecular basis for such differentiation of chloroplast is not yet fully understood (Edword at al., 2004).

The CO_2 fixation reaction in C_3 crop plants (rice, wheat barely potato or sugar beets) and their production of biomass could be improved enzymatically, if the oxygenation reaction could be reduced, and the carboxylation reaction could be improved, instead. Many attempts have been made to mutagenesis the Rubisco in order to reduce the oxygenase and increase the carboxylation reaction. All these experiments failed more or less. It seems not to be possible to obtain a Rubisco complex which can distinguish between O_2 and CO_2, just by some point mutations.

The transfer of C_4 plants traits into C_3 plants has long been a strategy for improving the photosynthetic performance of C_3 plant because C_4 plants have up to 10 fold higher apparent CO_2 assimilation rates than the most productive C_3 plants. This requires higher fluxes of metabolic intermediates across the chloroplast envelope membrane of C_4 plants in comparison with those of C_3 plants. The fluxes are metabolites involved in the biochemical inorganic carbon pump of C_4 plants, such as malate, pyruvate, oxaloacetate, and phospho*enol*pyruvate must be higher in C_4 plants because they exceed the apparent rate of photosynthetic CO_2 assimilation, whereas they represents relatively minor fluxes in C_3 plants. C_4 photosynthesis allows a fast biomass accumulation with high nitrogen and water use efficiency and is the desired trait to increase crop productivity (Leegood and Edward, 1996; Sage, 2004).

The C_4 CO_2 fixation mechanism is very complex. C_4 plants, e.g. maize, posses two major cell types which are important for CO_2 fixation, the mesophyll and the bundle sheath cells. They contain two types of chloroplast, possessing different sets of enzymes. Although the C_4 syndrome has been developed in many plant species it is believed, that many genes are involved in the differentiation process for the formation of classical C_4 syndrome. Only a few of the C_4 related genes are known. Therefore it is nowadays not possible to transfer a classical C_4 syndrome to C_3 plants.

C_4 photosynthesis has been found in some aquatic plants where it shows no compartmentation for the concentration of CO_2 but it is accomplished in a single cell (Bowes et al., 2002). *Hydrilla verticilliata* (L.f) Royle has been best documented. *Hydrilla verticilliata* which belongs to the angiosperm and lives submerged in warm shallow lakes in tropical region. During the cooler seasons the plant fixes CO_2 according to the C_3 cycle. During the summer the water temperature increases and the CO_2 and HCO_3^- concentration

drop dramatically. *H. verticillata* changes CO_2 fixing from a normal C_3 to a specific C_4 type mechanism. Within a few days the expression of the following enzyme is increased by factor of 4 to 8: PEPC, ME, Pyruvate-Pi-Dikinase, and PEP-translocator. The CO_2 compensation point decreases from 60 PPM to about 15 PPM. The angiosperm Hydrilla verticilliata possesses a mimic C_4 like (HC_4l) CO_2 fixation mechanism. The CO_2 concentration mechanism and CO_2 fixation are located in a single cell. The HC_4l seems to be less complex than the classical C_4 mechanism e.g. in marine plant. Several strategies have been tested in our group to transfer the hydrilla C_4l mechanism into either potato or tobacco plants (Gehlen et al., 1996; Hudspeth et al., 1992; Ishimaru et al., 1997; Kogami et al., 1994; Ku et al.,1999; Suzuki et al., 2000; Takeuchi et al., 2000; Häusler et al., 1999). Several interesting results have been obtained from these experiments, but it was not able to demonstrate a decrease of the CO_2 compensation point and an oxygen inhibition or an increase in CO_2 fixation and biomass production. e.g. the attempts made to express two C_4 enzymes PEPC and PEP-CK (Suzuki at al., 2006) and five Enzymes PEPC, PPDK, or PEP synthase, PEP-CK, NADP-malate dehydrogenase, NADP-ME (Häusler et al., 2002), the basic steps identified in these pathways are the carboxylation of PEP by PEPC in the cystol and decarboxylation of resultant C_4 acid inside the chloroplast and this cycle is created without any modification of intracellular metabolite transport, and this pathway involves import of OAA and transport of PEP from chloroplast. Since OAA is actively taken up by the chloroplast via the malate valve, which functions in transferring reducing equivalents from the chloroplast stroma to the cystol (Scheibe, 2004).

4.3 The optimized Hydrilla (HC_4l) pathways

Plants possess a dicarboxylate (malate, oxaloacetate) translocator (antiporter) in the inner membrane of the chloroplast envelop. This transporter system has two functions:
One is transportation of light generated ATP from the chloroplast into the cytoplasm via the 3PGA (3-phospho-glyceric acid)/DiHOAcP (Dihydroxy-acetone-phosphate) shuttle (Godwin, Mercer., 1986). Second is export of reduction equivalent from the chloroplast stroma to the cytoplasm ($2H^+ + 2e^-$ from photosynthesis). Therefore, it is necessary that an adequate concentration of malate/oxaloacetate is present in the cytoplasm and in the stroma. In the first attempt to establish the HC_4l pathway in crop plants (potato, *N. tabacum*) a relatively simple hydrilla mimic pathway was used as shown in fig. 4.1. The

following genes see fig. 4.1 were transformed and overexpressed in potato plants: no. 2, 4, 5, 6, 7, 8 all enzyme activities have been found in C_3 cells (Häusler et al., 2001). The activity of the cystolic carbonic anhydrase (Anderson and Beardall., 1996) has been described, but it turns to be much lower than the one in the chloroplast. The corresponding enzymes of all genes transformed to the potato cells were active.

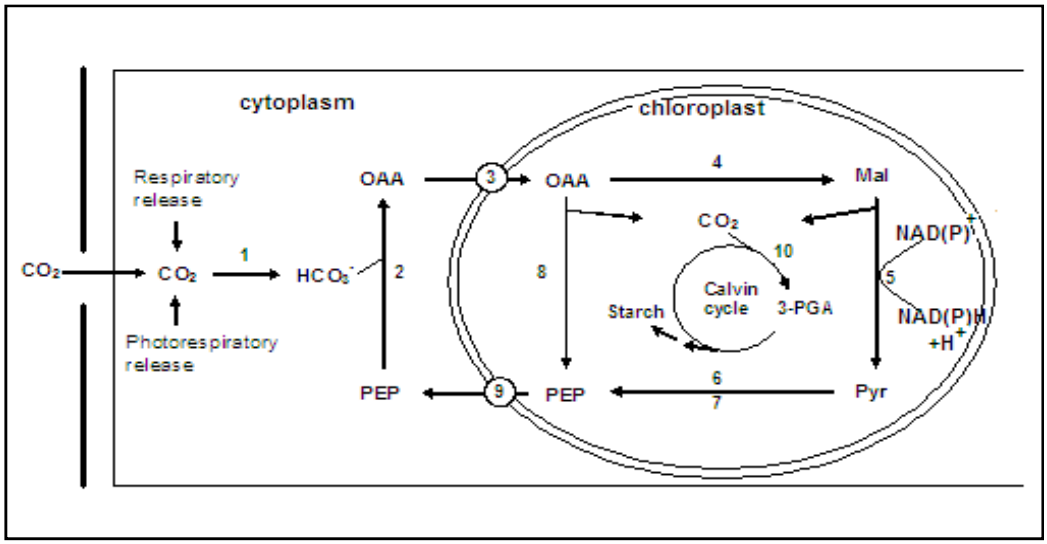

Figure 4.1: Hydrilla pathway transferred to potato cells
In fig. above used abbrevation: PEP = phospho*enol*pyruvate; OAA = oxaloacetate; Mal = malate; Pyr = pyruvate; 1 = Carbonic anhydrase (CA); 2 = PEP carboxylase (PC); 3 = OAA translocator; 4 = NADP-malate dehydrogenase (NADP-MDH); 5 = NADP-malic enzyme (ME); 6 = Pyruvate-orthophosphate dikinase (PPDK); 7 = PEP synthase (PEPS); 8 = PEP carboxykinase (CK); 9 = PEP/phosphate translocator (PT).

Measurement of various physiological parameters from this pathway showed that the photosynthetic effect observed in Hydrilla (*Hydrilla verticilliata* CO_2 compensation point 15 ppm) could not be transferred to potato plants. Therefore in this pathway has not seen any increase in biomass. Instead a relatively high percentage of small and chlorotic transgenic plants could be seen. These phenotypes corresponded with high activities of the malic enzyme or the PEP carboxylase.

The explanation of this observation might be that the concentration of malate or PEP could be too low, if the activities of the enzymes mentioned are too high. If malate is decarboxylated too much in the chloroplast the export of ATP and reduction equivalent to the cytoplasm is too low. This could be the reason for the chlorotic phenotype observed if the malic enzyme activity is high. It seems that, within these experiments the enzymatic activities of some enzymes could not be regulated in a suitable manner. In our previous study, in which OAA/Malate antiporter used for the transport of malate in chloroplast it

showed, if too much malate is decarboxylated in the chloroplast by the malic enzyme, the export of reduction equivalent and ATP to the cytoplasm cannot function efficiently. This might be the explanation for the chlorotic and stunted phenotype if the activity of the malic enzyme is too high. Stunted phenotypes could also be seen, if the expression and the enzymatic activity of the PEP carboxylase were high, i.e. 4 to 6 times higher than the endogenous PEPC (Thomas Rademacher thesis Bio I RWTH; Maurino et al., 2010). This data seems to indicate that the regulation of gene expression (The genes were ligated behind a constitutive promoter 35SS) and the enzymatic activities were not suitable for the heterologous host. Some groups have claimed that overproduction of the maize PEPC enhanced photosynthesis and increased crop yields of transgenic rice plants (Jiao et al., 2002; Bandyopadhyay et al., 2007). In order to overcome the putative problems, that not enough ATP and reduction equivalent could be exported from the chloroplast to the cytoplasm.

In the second attempt, it was decided to transfer an optimized Hydrilla C_4 pathway (HC_4l) into tobacco cells. This pathway is shown in fig. 4.2 (Result. 3.1.6).

In the scope of this study, we mimic hydrilla pathway for CO_2 concentration mechanism in *Nicotina tabacum*. We introduced a modified Hydrilla C_4 state pathway for better photosynthetic performance. Pathway involved multiple C_4 genes had successfully transformed using MultiRound gateway technology. Pathway involved the C_4 genes PEPC, NAD-MDH, NAD-ME and Mle (Malate-Lactate antiporter), LdhA, LdhB have been successfully overproduced in tobacco leaves.

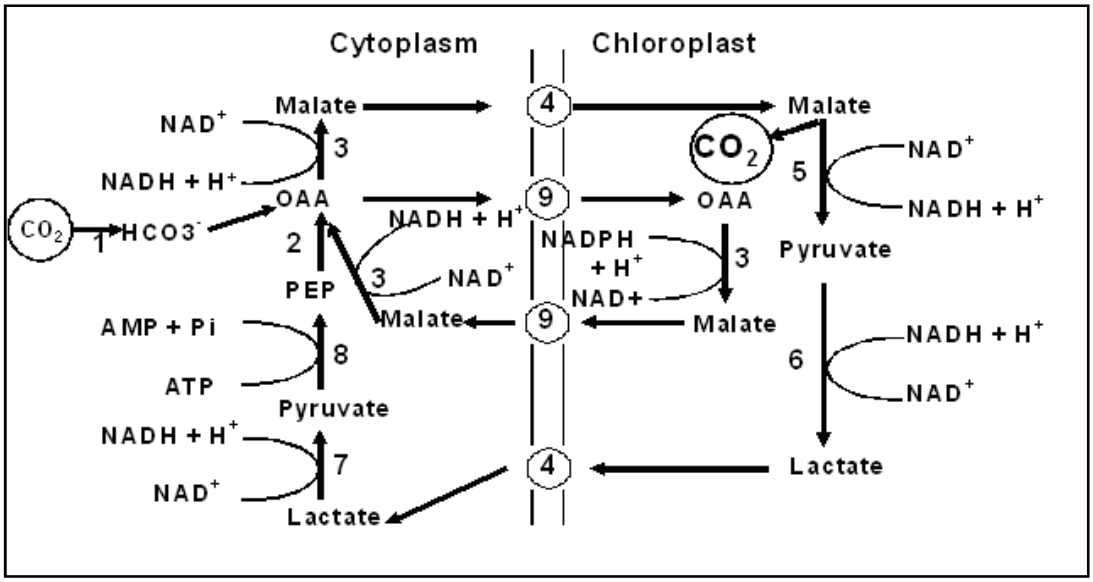

Figure 4.2 (3.1.2): Representation of modified and optimized *Hydrilla* C_4 like pathway (HC_4l)

CO_2 from ambient air converted into to HCO_3^- by (1) Carbonanhydrase (endogen). HCO_3^- forms in the cystol of the mesophyll cells fixed by the oxygen insensitive (2) Phospho*enol*pyruvate carboxylase (PEPC) and convert into OAA. Oxaloacetate is reduced by (3) NAD^+ dependent malate dehydrogenase (MDH), and resulatant malate exporeted to the chloroplast by (4) Malate lactate antiporter (Mle) and Malate decarboxylate by (5) NAD-Malic enzyme (ME). Malate decarboxylation forms pyruvate and which is reduced by (6) Lactate dehydrogenase A (LdhA) and forms lactate. Lactate exported to the cytoplasm and is oxidized to pyruvate by (7) Lactate dehydrogenasem B (LdhB). Finally PEP regenerated bypyruvate and catalyzed by (8) Phospho*enol*pyruvate synthase (PEPS). (9) Malate-OAA antiporter (endogen).

We integrated the following genes into host DNA by the gateway technology: i) Malate dehydrogenase (3) (foreign enzyme in the cytoplasm: NAD^+ dependent, endogenous enzyme in the chloroplast: $NADP^+$ dependent). ii) Malate/lactate antiporter (4); iii) NAD malic enzyme from *E. coli* (5); iv) Lactate dehydrogenase A (6) (in the chloroplast), NAD^+ dependent; v) Lacate dehydrogenase B (7) (in the cytoplasm); vi) PEP synthase (8) (from *E. coli*). Antiporter (4) can import malate into chloroplast, where it can be decarboxylated (to pyruvate which can be further reduced to lactate) and exports lactate (which is then oxidized to pyruvate, recarboxylated to OAA and reduced to malate).The endogenous OAA/malate antiporter should not be depleted for one of their substrates (malate, by the malic enzyme) which interrupt the exchange. Malate should be always present, either it is formed by the malate dehydrogenase from OAA (3) or, if decarboxylated (malic enzyme) it is resynthesized via pyruvate, lactate and PEP by the PEP-carboxylase. Reduction equivalent (e^-, H^+) can also be exported to the cytoplasm by the malate/lactate antiporter system.

By this pathway important knowledge has been gained about the transformation of multiple genes in the C_3 plants by gateway technology and the effect of combination or individual genes overexpression in the plants. A relatively low activity of carbonic anhydrase (1) has been found in the cytoplasm of C_3 cells; although its function is not clear (Hatch and Burnell et al., 1990; Utsunomiya and Muto 1990; von Caemmerer et al., 1997). The pH in the cytoplasm has been measured. It varies between 7 and 7.2. At this pH and at the equilibrium of the following reaction $CO_2 + H_2O$ –slow→ H_2CO_3 – fast→$HCO_3^- + H^+$, 80% of the CO_2 molecule exists as HCO_3^-. This equilibrium might not be reached in the cytoplasm because CO_2 diffuses to the chloroplast membrane and can enter in the stroma, but at least part of the CO_2 will be present as HCO_3^-. This molecule is one of the substrates for the PEP-carboxylase (2) which forms oxaloacetate (PEP + HCO_3^- ⇌ oxaloacetate + Pi). As has been described in the chapter results, regenerated plants were analyzed in detail and physiological, photosynthetic and biochemical (metabolic compound) parameters were measured.

Increase in the activity of PEPC might elevate cystolic PEP consumption and OAA productions, which may in turn, stimulate glycolysis as well as restrict the formation of flavanoids. NAD-ME catalyses the decarboxylation of strongly acidic malate formed from NAD-MDH or endogenous NADP-MDH which might attenuate the increases in the content of organic acids caused by elevated PEPC activities. Phosphoenolpyruvate synthase (PEPS) in the transgenic plants may enhance the conversion rate of pyruvate to phosphoenolpyruvate (PEP). Higher activity of malate lactate antiporter might increase the malate concentration in the chloroplast of transgenic plants. Lactate is recycled back to the cystol which might enhance the pyruvate concentration the substrate for the PEP synthase. This could increase the sustainability of "C4 cycle". The release of CO_2 could be increased due to the novel pathway at the site of Rubisco and might improve photosynthesis. These changes in photosynthetic characteristics may effect the growth and reproduction of these plants. The different physiological parameters checked in this study whether novel pathway could really beneficial for transgenic tobacco as refer to faster growth and higher biomass. The plant with pYLTAC7_Hydrilla shows similar growth curve compared with control plants. Some of the observations made like formation of reproductive organs were earlier in the transgenes of pYLTAC7_Hydrilla than in control plant lines. It might conclude that some of the genes induce the flow of the auxin at the direction of the site of apical meristem or genes might interferes the PIN transporter which takes part in the transportation of auxin (Forestan and Varroto., 2011). However enhancement of photosynthesis can not be seen after introduction of mimic hydrilla pathway in C_3 plants but some unexpected finding are made that have important implication for the activity of C_4 enzymes in C_3 plants. Overproduction of C_4 gene PEPC under the control of AtRbcS promoter, Mle-Malate-Lactate antiporter under the control of 35SS promoter, NAD-ME under the control of AtRbcS promoter and PEP synthase under the control of CmRbcs promoter. These set of genes show some positive impact on plant by observing some results from the measurement of ammonia release assay. The plants with higher expression of C_4 genes (PEPC, Mle, ME, PPS) shows lesser amount of ammonia accumulated in transgenic plants (explanation in details later part of the discussion) as compared with the transgenic plants with all seven genes (mimic pathway) and control plants. However the expression of individual C_4 gene, or the other genes from the pathway not showed any astonished difference than control plants. As predicted, almost no stunted or chlorotic phenotype could be observed in these experiments. This

was positive, but the CO_2 compensation point, the ammonia release, the CO_2 assimilation, the biomass production and starch synthesis were similar or even unfavorable compared to the plants possessing empty vector or wild type. This point will be discussed in the next chapter.

4 gene experiment (PEPC, Mle, NAD^+-ME, PEPS)

During the transformation and regeneration process, plant have been discovered, in which only four of the transformed genes have been overexpressed: i) PEP carboxylase (2); ii) Malate/Lactate antiporter (4); iii) NAD dependent Malic enzyme (5); v) PEP synthase (8). Assumed biochemical pathway can be seen in fig. 4.3. In these plants, CO_2 which enters the cell can react with H_2O and forms HCO_3^- or it diffuses directly into the chloroplast stroma. The PEPC enzyme then can form OAA using the substrate PEP (which is formed by the PEP synthase from *E. coli* (8)) and HCO_3^- (CO_2). OAA can enter the chloroplast, using the Malate/OAA antiporter (9), or it is reduced by the endogenous malate dehydrogenase located in the cytoplasm. The activity of the cytoplasmic MDH is 1.5 to 4.5 times higher than the entire endogenous MDH (MDH cytoplasm + MDH chloroplast). In the chloroplast oxaloacetate (OAA) is reduced to malate by the malate dehydrogenase. The elevation of the MDH activity is essential for the restoration/enhancement of photosynthesis. Because the overproduction of MDH is necessary for direct uptake of OAA into the chloroplast and also for the decarboxylation reaction of overproduced ME (Taniguchi *et al.,* 2008).

But this is not the case in the overproduction of NAD-MDH from *Z. mays* in the tobacco with the combination of other genes that we used in this study. We checked every possible combination with NAD-MDH and it did not show any improvement in CO_2 fixation capability in tobacco. The possibility might be that the expression of PEPC was too low for the production of OAA and not enough OAA in cytoplasm for the reduction by NAD-MDH for the production of enough malate to be transported into the chloroplast. NADP-MDH activity not significantly rises in *Hydrilla verticilliata* when it switches from C_3 state to C_4 state. Endogenous NAD-MDH activity is high enough because multiple forms of MDH are involved in different metabolic pathways and are located in different compartments. In plants, three NAD-dependent MDH types are located in the mitochondria, the microbodies, the cytoplasm and an NADP-dependent type in the chloroplast (Poeydomenge et al., 1995). The endogenous chloroplastic NAD-MDH could

play role to equilibrium in reducing equivalent in the dark because it is active in dark (Berkemeyer at al., 1998) on the other hand NADP-malate dehydrogenase is regulated indirectly by light via the thioredoxin system (Furbank *et al.,* 2000) which can be transported back to the cytoplasm (translocator (9)) where it can be oxidised to OAA (export of reduction equivalent). Alternatively, malate formed in the cytoplasm (3) might

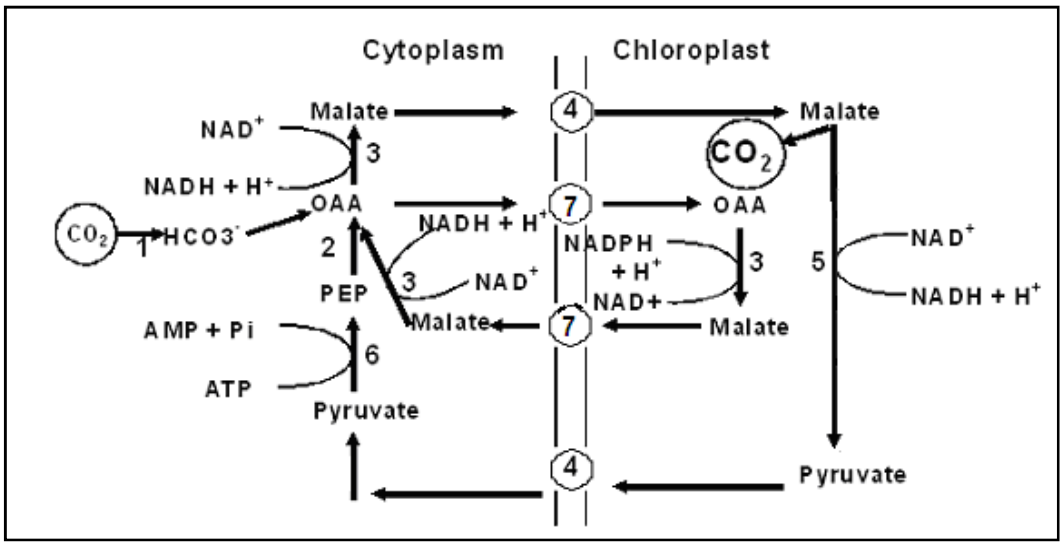

Figure 4.3: Overexpressed C_4 enzymes and antiporter cycle assumption
CO_2 from ambient air is converted into to HCO_3^- by carbonic anhydrase (1) Carbonanhydrase (endogen). HCO_3^- in the cystol of the mesophyll cells and fixed by the oxygen insensitive (2) PEPC Phospho*enol*pyruvate carboxylase (PEPC) and forms OAA. Oxaloacetate is reduced by (3) NAD^+ dependent malate dehydrogenase (MDH) (endogen). Resulatant malate is export to the chloroplast by (4) Malate lactate antiporter (Mle), where malate is decarboxylated by (5) NAD-Malic enzyme (ME) (endogen). Malate decarboxylation forms pyruvate and PEP is regenerated by (8) Phospho*enol*pyruvate synthase (PEPS). (9) Malate-OAA antiporter (endogen).

enter the chloroplast using the malate/lactate antiporter, if the pyruvate can be reduced to lactate in the chloroplast. This reaction is not very likely because to our knowledge, no lactate dehydrogenase has been described in chloroplast under aerobic conditions. Under anaerobic condition pyruvate can be reduced to lcatate in plants using NADH as cofactor (Dashek V.W et al., 2006). The NAD-ME localized in the mitochondria and involved in together with anapleuratic PEPC provides a carbon skeleton for the synthesis of amino acids (Douce and Neuburger, 1989). In addition, it plays a role in the metabolism of carbon and nitrogen (Tronconi *et al*., 2008). In this study, we used NAD-ME from *E. coli* (*SfcA*, EC 1.1.1.38) for the NAD-dependendent decarboxylation of malate in the chloroplast. It works at a broad pH and shows 90% activity at optimum pH at 7.5 and pH 8.5 (Yamaguchi *et al.*, 1973; Bologna *et al.*, 2007). The optimal activity for the plant NAD-ME can be measured in acidic range at pH 6.5-7.0. So, increasing the pH, activity of

enzyme decreases highly (Hatch *et al.*, 1974; Grover *et al.*, 1981; Willeford and Wedding, 1987). For example the NAD-ME from *Hydrilla* shows its activity at pH 7.2 and shows, only 2% of its activity at pH 8.3 (Magnin et al., 1997). Bologna et al (2007) explained the coenzyme of malic enzyme in details, coenzyme SfcA clearly preferred NAD^+ over $NADP^+$ and shows 100-times-higher catalytic efficiency with NAD^+ over $NADP^+$.The coenzyme SfcA can decarboxylate malate but also decarboxylate OAA at acidic pH, when comparing forward and reverse reactions (malate oxidative decarboxylation and reductive pyruvate carboxylation, respectively) SfcA catalyzed the carboxylation reaction at rates nearly 30 times lower than those for decarboxylation (Bologna *et al.*, 2007).

Generally bundle sheath cell chloroplast of C_4 plant of NADP-ME type (subgroup: Introduction C_4 pathway) lack photosystem II and hence the capacity for non cyclic electron transport NADPH formed by NADP-ME is utilized for the reduction of 50% of 3 PGA formed by Rubisco. The residual 3-PGA is exported by C_4 type TPT (triose phosphate translocater) and is transferred to the mesophyll chloroplasts and imported into the stroma via TPT and reduced to triose phosphates. The carbon acceptor PEP is regenerated by PPDK. The PPi released by this reaction is cleaved by pyrophosphtase and AMP converted to ADP by adenylate kinase (Hausler *et al.,* 2002). Malate formed in the cytoplasm could also use malate/OAA antiporter to enter the chloroplast, where it can be decarboxylated to pyruvate. In the chloroplast pathways have been described by which pyruvate can be formed to 3-PGA. This can be transporter to the cytoplasm by the 3-PGA/Pi antiporter. In the cytoplasm pyruvate can be formed from 3-PGA by enzymes involved in the glycolytic pathway: phosphoglycerate phosphomutase, (EC 5.4.2.1); enolase, (EC 4.2.1.11); pyruvate kinase (EC 2.7.1.40); and a spontaneous reaction which forms pyruvate from enolpyruvic acid. One molecule ATP is formed in the course of this pathway; the reaction step from PEP to *enol*pyruvate. PEP formed in the cytoplasm from 3-PGA can be used by the PEPC to catalyse the OAA Malate formation (substrate is HCO_3^-). The biochemical reaction mentioned in this chapter might open the possibility to form a cyclic pathway, starting with PEP and HCO_3^-. It is not possible in this thesis to compile all the biochemical pathways within the cell, which are affected by the overproduction of OAA/malate by the transformation of C_3 plants with the genes: PEPC; malate/lactate antiporter; malic enzyme; PEPsynthase, but the results indicate that the transformed genes might optimize CO_2 fixation and biomass production, although to a small extend.

The second possibility might be when the expression of higher PPDK plants shows amount of Glu (glutamic acid) was higher than the control plants (Sheriff et al., 1998) and author explained that supply of additional alpha-ketoglutarate which is generated from citrate and is the condensation product of acetyl-CoA and OAA. Anaplerotically OAA is generated from pyruvate. Thus additional pyruvate as well as additional PEP is needed to drive the increase in Glu (Sheriff et al., 1998). Data observed in the transformant with the overexpression of PEPS together with other three genes plant show slightly better photosynthesis.

The small assumed cycle of PEPC, Mle (malate-lactae antiporter), PEPS and NAD-ME could create its own dependent machinery so; it did not harm the other mechanisms in the plant cell. Other genes from the HC_4l pathway (NAD-MDH, LDHB, and LDHA) can create deleterious effect on the whole machinery in the photosynthesis dependent electron transport system. This might be the reason plants did not show any positive effect or higher growth when the transfer of complete *Hydrilla* pathway (HC_4l) into the C_3 plants. The explanation of the multiple gene transformation in plants author David Kramer (2011) explains, the light reaction involve highly reactive species and if not controlled properly can produce deleterious reactive oxygen species. The synthesis of ATP and NADPH in linear electron flow (LFF) is tightly coupled, i.e. one cannot occur without the other. Author also explains if, the substrate for the ATP synthase (ADP, Pi) is limited, then builds the proton motive force (pmf) and inhibits electron transfer to NADP (+) and the same way, if NADP (+) is limiting, photosynthetic electron carriers become reduced, slowing electron transfer and associated proton translocation, so limiting ATP synthesis. Linear electron flow form fixed ratio of ATP/NADPH and each metabolic pathway directly powered by photosynthesis consumes different fixed ratio of ATP/NADPH. However, these fluxes through these pathway is variable in different physiological conditions and in different species, so transformation of *Hydrilla* pathway (C_4l) could create mismatch and arise in the production and demands for ATP/NADPH. The chloroplasts have very limited pool of ATP and NADPH. Therefore such mismatch could rapidly inhibit photosynthesis and shows chlorotic effect or stunting of growth and necrosis these might the effect of inhibition or disturbance in the photosystem. So, we could create pathways in C_3 plants where the supply of ATP and NADPH in precisely the right proportion to match the consumptions. So the line with overexpression of 4 genes (PEPC, Mle, NAD-ME, PEPS) could be beneficial. These results have to be verified and

optimized. The following results have been obtained by repeating each measurement at least three times: i) Apparent CO_2 compensation point (Γ_*); Azygote = 70 ppm; 4 genes (+4 genes) = 69 ppm; +7 genes = 73 ppm; ii) Starch concentration; +4 genes = 310 mg/g leaf material; +7 genes = 460 mg/g leaf material; empty vector = 370 mg/g leaf material; iv) Sucrose concentration in the leaves; +4 genes = 2.7 mmol/m^2 leaf area; 7 genes = 1.9 mmol/m^2 leaf area; empty vector = 2 mmol/m^2 leaf area; v) Plants expressing 4 genes showed slightly bigger leaves (Several leaves were measured at different age) than plants expressing 7 genes.

We should not over interpret the results obtained with plants overexpressing 4 genes. The effect is relatively small but all measurements were repeated at least 4 times, many plants were tested and all results seem to point in the direction of an optimized CO_2 fixation. The results obtained with all 7 genes are discouraging and should not be repeated. Therefore the experiments should be repeated under optimized conditions but potato plants should be used. These important crops possess a large sink for glucose, the potato tubers. For our experiments it might be great benefit if the host possesses a large sink for starch.

4.4 Summarizing discussion for the optimized Hydrilla pathway (HC_4l)

Higher sweet water plants living submersed (*H. verticillata*) possess a very effective transport system for HCO_3^- from the water to the cells (Schofer, P., Brennicke, A., 2006). These plants also possess a relatively high carbonic anhydrase activity which, because of the high turnover rate, can adjust the equilibrium of HCO_3^-/CO_2 very fast (turnover rate 2 - 4 x 10^6/sec; equilibrium at pH 7.0, HCO_3^-/CO_2 around 4:1). The HCO_3^- uptake mechanism has not been described for *Hydrilla* but it might become established during the (HC_4l) CO_2 fixation period. CO_2 can diffuse into the chloroplasts where it is fixed by the Rubisco. In the chloroplasts the equilibrium of HCO_3^-/CO_2 is 50/1 but, if the Rubisco fixes CO_2, it will be rebuilt by the carbonic anhydrase. It has been mentioned above; *H. verticilliata* can establish a C_4 like CO_2 fixation mechanism, if the HCO_3^-/CO_2 concentration in the water is low. Then HCO_3^- is fixed by the PEP-carboxylase and the OAA produced is transported to the chloroplast. OAA is reduced to malate in the stroma which is decarboxylated to pyruvate and CO_2. CO_2 is fixed by Rubisco and 2 molecule of 3-PGA are formed. Pyruvate is phosphorylated to PEP which is transported to the cytoplasm. The activity of the malic enzyme (decarboxylation of malate) has to be regulated in an ingenious manner,

because not too much malate has to be decarboxylated. If the concentration of malate is too low, not enough reduction equivalents can be transported to the cytoplasm.

Our plan to mimic the HC_4l statergy in C_3 plants were not worked up to now: This might have two reasons: 1 The *H. verticillata* C_4l CO_2 fixation mechanism is in principle not working in C_3 land plants, because the CO_2 but also O_2 concentration are much higher in the air compared to the water (CO_2: air = 0.036%; H_2O = 0.005% O_2; air = 21%; H_2O = 0.0004%). These data indicate that the oxygen inhibition of CO_2 fixation should be higher in terrestrial than in water plants. 2 The *H. verticillata* C_4l CO_2 fixation mechanism might in principle work in terrestrial plants but we were not able to establish the proper regulation of gene expression and enzymatic activity. In any case, more information is needed about the HC_4l CO_2 fixation mechanism of *Hydrilla verticillata.*

4.5 The MMPEM pathway in WT and GTDEF tobacco plants

GTDEF pathway is dealing with the metabolism of glycolate produced in the chloroplast during photorespiration. This pathway showed reduction of photorespiratory CO_2 loss by modifying the metabolic pathways of the products resulting from Rubsico oxygenase activity. We tried to develop new metabolic pathway called MMPEM in the chloroplast of GTDEF plants. The aim of this pathway is to fix higher amount of CO_2 compared to mere GTDEF pathway.

Metabolizing glycolate in the chloroplast via GTDEF and MMPEM pathways will beneficial for C_3 plants in multiple ways. The flow through photorespiration will be decreased to very low levels and thus energy loss during photorespiratory way is avoided. The GTDEF pathway increase the CO_2 concentration at the step, where glycolate is converted to tartronic semialdehyde by glyoxalate carboxyligase and again release the CO_2 in the MMPEM pathway where malate is decraboxylated by malic enzyme and forms pyruvate. At the vicinity of Rubisco, the concentration of CO_2 increases, resulting into a higher rate of photosynthesis and ultimately higher biomass production. Because double amount CO_2 burst in the chloroplast of transgenic crops shows better performance in the photosynthesis. The enzymes involved in this pathway are shown in chapter results 3.2.1. In the GTDEF+MMPEM pathway established plants improves the concentration CO_2 and finally higher biomass production as compare to GTDEF plants.

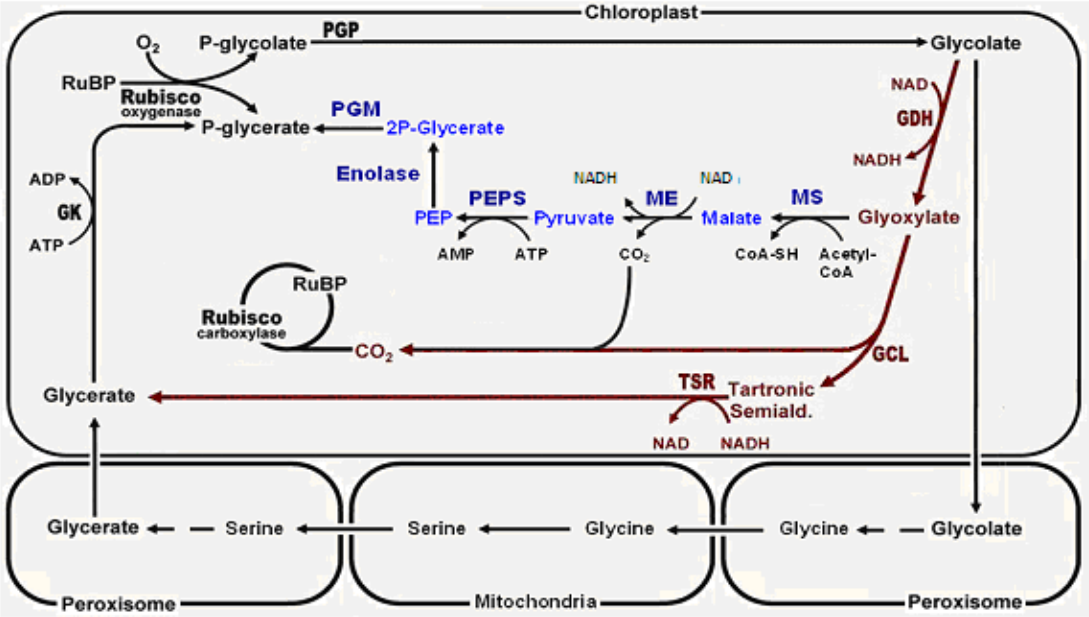

Figure 4.4: Representation of the photorespiratory pathway (black) in C_3 plants and the proposed pathway (red) for the conversion of glycolate to glycerate. New improved pathway (Blue)
The oxygenase reaction of Rubisco results in the formation of P-glycerate and P-glycolate. P-glycolate is dephosphorylated by PGP forming glycolate that is oxidized by GDH to form glyoxylate. Two molecules of glyoxylate are condensed by GCL forming tartronicsemialdehyde and CO_2 is released in the chloroplast. Tartronic semialdehyde is then reduced by TSR forming glycerate. Glycerate is phosphorylated by GK to form P-glycerate that is used directly for carbohydrate biosynthesis through the Benson Calvin cycle. Again blue pathway from glyoxalate form malate with the help of malate synthase. Inthis reaction malate synthase uses acetyl CoA and convert to CoA. Malate decorboxylated by malic enzyme forms pyruvate. PEP regenerated by pep synthase consumes ATP for regeneration of PEP. Pep converted to 2PG caalysed by enolase. PGM transfer phosphate group from 2PGM to 3PGM. **PGP** = phosphoglycolate phosphatase; **GDH** = glycolate dehydrogenase; **cTP-*At*GDH** = *A. thaliana* glycolate dehydrogenase fused to a chloroplast targeting peptide (cTP); **GCL** = glyoxylate carboxyligase; ***TSR*** = tartronic semialdehyde reductase; **GK** = glycerate kinase; **MS =** malate synthase; **ME** = malic enzyme, **PEPS =** phspho*enol*pyruvate synthase; **PEP =** phospho*enol* pyruvate; **PGM** = phosphoglycerate mutase; the photorespiratory enzymes are described in chapter 1.3.1. For the sake of clarity all cofactor not shown.

Detail about enzyme used in MMPEM pathway

Enzymes involved in MMPEM pathway are already available in C_3 plant at very low concentration. MMPEM pathway started from the substrate glyoxylate which is converted from glycolate by glycolate dehydrogenase and glyoxylate converted to malate by malate synthase (EC 2.3.3.9) is an enzyme that catalyzes the chemical reaction:

$$\text{Acetyl-CoA} + H_2O + \text{glyoxylate} \rightleftharpoons \text{(S)-malate} + \text{CoA}$$

The 3 substrates of this enzyme are acetyl-CoA, H_2O, and glyoxylate, whereas its two products are (S)-malate and CoA. Malate synthase catalyse the aldol condensation of glyoxylate with acetyl-CoA to form a malate as part of the second step of the glyoxylate bypass and an alternative to the tricarboxylic acid cycle in bacteria. In the glyoxylate shunt

pathway, the condensation and subsequent hydrolysis of glyoxylate and acetyl-CoA is performed by malate synthase (MS) to produce malate and CoA. Compairing *E. coli* and *Bacillus anthrac* malate synthase showed some interesting findings for the behavior and activity of enzyme. The modes of substrate binding are found in detail in crystallographic and NMR structural studies a catalytic mechanism. Briefly: bound glyoxylate is activated toward nucleophilic attack by salt bridges to an essential Mg^{2+} ion and by hydrogen bonds to the protein backbone and a conserved arginine. An essential aspartic acid residue is accepting a proton from the acetyl-CoA terminal methyl group. The proposed enolate intermediate is stabilized by interaction with the essential arginine. In *E. coli* two forms of malate synthase isoform are found in this study. Isoform A and G of malate synthase from *E. coli* is identical (Lohman, et al., 2008). Isoform A is regulated by fatty acids and acetate and isoform G expression is regulated by presence of glycolate. In this study used isoform G was used (Vanderwinkel and De vlieghere 1968). Isofrom G shows higher identity but found only in bacteria while isoform A shows similar identity and found in plants, fungi and bacteria.

NAD dependent malic enzyme used for the decarboxylation of malate in this pathway. NAD dependent ME is more beneficial for the balance NAD/$NADP^+$ ratio in chloroplast rather than NADP dependent ME. Pyruvate is reduced to phosho*enol*pyruvate (PEP) by phospho*enol*pyruvate synthase from *E. coli* and PEP is catalyzed by enolase (2-phospho-D-glycerate hydrolase; EC 4.2.1.11) and formed 2- phosphoglycerate. It is reversible reaction and works in opposite direction at pH 6.5 . 2-phosphoglycerate is catalyzed by mutase and forms 3-phosphoglycerate. Mutase is an enzyme of the isomerase class that catalyzes the shifting of a functional group from one position to another within the same molecule. In the active site of enzyme contains a phosphohistidine complex formed by phoshphorylation of a specific histidine residue. When 3-phosphoglycerate enters the active site, the phosphohistidine complex is positioned as to facilitate transfer of phosphate from enzyme to substrate C-2 creating a 2,3-bisphosphoglycerate intermediate (MeSH).

The multiple substrates of all pathways are glycolate which is produced by the oxygenase reaction of the Rubisco. The concentration of glycolate must be relatively high in the chloroplast, because about 25% to 30% or even more percentage of the catalytic activity of the Rubisco represents the oxygenase reaction. A common substrate of all pathways is also glyoxylate which, in the case of GTDEF and MMPEM, is formed in the chloroplast

by the glycolate dehydrogenase. In the case of the normal photorespiration, which is also present in GTDEF and MMPEM plants, glyoxylate is formed by the glycolate oxidase in the glyoxysomes. The common end product of all three pathways is glycerate phosphate, which enters the Calvin cycle where glucose and ribulose 1,5 bisphosphate is formed.

The MMPEM pathway integrated into *Nicotiana tabacum* cells possessing photorespiration pathway:

i) WT plants possess the normal photorespiration of C_3 plants; ii) The GTDEF pathway; ii) The MMPEM pathway *Nicotina tabacum* plants have been used, possessing the GTDEF pathway to steady effect of the MMPEM pathway on CO_2 fixation of the Rubisco. It was expected, that the CO_2 fixation improved by the GTDEF pathway. It might be further improved by the MMPEM pathway. Almost all enzymes mentioned in the MMPEM pathway are present in the chloroplast (endogenous) except the PEPS, the gene which has been isolated from *E. coli*. Some of the endogenous MMPEM enzymes show low activities: (Anderson JW., Beardall J 1996; Vooper and Beever 1969). i) MS = 27 µmol $g^{-1}l^{-1}$: The major activity of malate synthase 790 µmol $g^{-1}l^{-1}$ is located in the glyoxysomes of storage tissues of fatty seeds. ii) ME: The gene of this enzyme has been isolated from *E. coli* and integrated in the host DNA. iii) PEPS: The gene has been isolated from *E. coli*. It has been reported that a plant enzyme which also catalyses the formation of PEP from pyruvate, the pyruvate-Pi-dikinase (PPDK) is located in C_3 plant chloroplast although the activity is relatively low (J. Hibberet, 1996). iv) Enolase: This enzyme is involved in the glycolysis in intact chloroplast. **v)** PGM = phosphoglycerate mutase, (85 mmol $min^{-1}mg^{-1}$). By integrating the genes located in a gateway plasmid into the plant genome, the total activity of the enzyme mentioned was increased. GT-DEF *N. tabacum* cells were transformed plants were regenerated, the gene expression analyzed by RT-PCR and by enzymatic activity measured in the T_1 generation (enolase, PEPS, NAD-ME). As has been discussed in the results, a few light inducible promoters (promoter AtRbcS-P for NAD-ME and LeRbcS-P for PEPS) have been used for the concentration of the various genes. This might explain, why the expression of the genes and their appropriate activities vary so much (Fig. 3.2.6 and Fig: 3.2.7) this situation is not satisfying for plant biotechnology. If gene technologists try to incorporate a biosynthetic pathway comprising a few (4 to 10) genes into the plant genome, the enzymatic activities need to the coordinated to obtain an optimal total activity. This cannot be achieved

nowadays, because the expression of the gene is not coordinated (if all genes are located behind the same promoter, silencing will be observed), even in gateway plasmid.

As mentioned before, the enzymatic activities of some enzymes involved in the GTDEF; the GTDEF+MMPEM and the MMPEM pathway have been measured in the T_1 generation. Plants showing highest enzymatic activities have been further analyzed. The data which are important for the decision, whether the CO_2 fixation has been improved in a specific transgenic line is summarized below: The compensation point: Azygote = 100%; MMPEM = 100%; GT-DEF = 87% is -13%; GTDEF+MMPEM = 82 is -18% CO_2 compensation point of MMPEM is identical to the azygote plants. MMPEM lines do not produce glycolate and glyoxalate in the chloroplast. Therefore the MMPEM pathway has no substrate for continuing the whole cycle. In the GTDEF+MMPEM line compensation point (Γ) is reduced by 18%, 5% more than in GTDEF lines. This shows that the MMPEM pathway improves the effect of the GTDEF pathway and works in the same direction. In a set of new experiment the effect of solely the MMPEM (MMPEM+DEF) should be analyzed.

4.6 MMPEM+GTDEF pathway shows positive effect in *N. tabacum*?

Results observed in the GTDEF pathway shows the improvement in photosynthesis. But these results were not steady in the next generation. The results in T_0 generation for GTDEF pathways were showed around 30% more biomass. In T_1 generation GTDEF plants showed around 15% more biomass. So, this data showed transgenic lines in the next generations loosed the capacity of higher photosynthesis phenomenon. These observations were collected by performing the experiments on GTDEF plants on different generation by comparing the controls of GTDEF plants which were propagated vegetatively.

In this study, different parameters for GTDEF+MMPEM plants and different control plants were measured in T_1 generation and some of the plant lines in T_2 generation. Results observed in the T_1 generation showed some promising data but results observed in T_2 generation were not seen similar like T_1 generation but slightly lesser biomass than T_1 generation but higher than the wild type.

The postillumination burst: Azygote 100%; MMPEM = 100%; GT-DEF = 51%; GTDEF+MMPEM = 39%. These experiments also show that the MMPEM pathway has a

positive effect on the CO_2 fixation mechanism in C_3 plants. MMPEM + GTDEF CO_2 compensation point lesser than other counterparts (Results 3.2.12).

Fresh and dry weight: Azygote and MMPEM = 100%; GTDEF = 112%; GTDEF+MMPEM = 125% (Material and methods and Results 3.2.11).

Leaf diameter and length: The analysis of these parameters has been done with older and young leaves of the same plant and with different times of the same plant line (material and methods 2.2.2.17).

Empty_vector and MMPEM leaf diameter = 100% (both lines showed similar results). GTDEF leaf diameter = 120% and height = 153%; GTDEF+MMPEM leaf diameter = 133% and Height = 153% (Result 3.2.10). The results obtained from for fresh and dry weight seems to demonstrate, that the GTDEF pathway improves the biomass production of C_3 plants. The MMPEM pathway boosts the effect of the GTDEF pathway on CO_2 fixation in C_3 plants, presumably by increasing the CO_2 concentration in the chloroplasts (Result 3.2.12).

4.7 MultiRound Gateway technology

One destination vector with two gateway entry vectors is the key to create complex multigene pathways in a single big plasmid. Traditionally, most of the plasmids and families of plasmids that exist today are limited to the expression of single gene. Majority of agronomic traits are quantitative and are controlled polygenetically, rely on complex metabolic and regulatory pathways, which include several genes or gene complexes. The use of such plasmids for the coordinated manipulation of multiple traits presents unique challenge for the plant genetic engineer. There are different ways which can be considered when using single gene vectors for the delivery of multiple genes into plant cells. Some of the approaches used for the transgenic plants with multiple new traits include retransformation (Seitz et al., 2007), stacking of several transgenes (Li *et al*., 2003), co-transformation: delivery of several transgenes in a single transformation and sexual crossings (Zhao at al., 2003). All these different approaches have several disadvantages plenty of time needed for crossing and retransformation. The transgenes derived from different sources integrate at different location in the plant genome and resulted variable expression and likely segregation of the transgenes in the offspring (Dafny-Yelin, 2007).

In contrast, delivering multiple genes by a single vector has many advantages over the use of multiple vectors. In this approach only a single DNA molecule needs to be transferred into the cells therefore fewer plants are generated as compared to the approaches discussed earlier.

For an overall improvement of crops by transferring different metabolic pathways for creating the new acquired environment into the plants by multiple transgenes can be combined in a single plant by genetic crossing of individual transgenic lines similar to gene pyramid strategy used in a conventional breeding (Ashikari and Matsuoka, 2006). Repeated crossing, plants transformed with different vector construct sequentially or co-transformation of vectors in a single transformation event, particle bombardment but all these techniques for creating metabolic pathways in plants with multiple gene have various pros and cons. Crossing and retransformation is very time consuming and co-transformation often leads to integration of multiple copies similar in particle bombardment. Gateway technology is the most potential technique among most of the multiple gene transformation. Transfer of multiple genes located on one vector, created by gateway recombination is a real breakthrough technology and hopes for many pending multigene pathways for development of new era in animal and plant science techniques. In this study, for both approaches (HC_4l and GTDEF+MMPEM) was used gateway technique for the transformation of multigene pathway for the improvement of C_3 crops by concentration of CO_2 at the vicinity of Rubisco.

4.8 Summarizing Discussion

In this PhD thesis two strategies have been followed up to improve the CO_2 fixation in C_3 plants and for both strategies used the MultiRound gateway technology, which is one step ahead for the multigene metabolic pathways transformation into the plants. The first strategy was integration of a modified *H. verticillata* C_4 like (HC_4l) CO_2 fixation pathway. The second strategy was the expression of MMPEM pathway genes in the WT and in GTDEF plants. Up to now attempts failed to improve CO_2 fixation by mutagenesis of the Rubisco. Therefore, it was decided to try and increase the CO_2 concentration inside the chloroplast in the vicinity of the Rubisco. This step could inhibit the oxygenase reaction of the Rubisco and improve carboxylation of ribulose 1,5-bisphosphate.

The *Hydrilla verticillata* imitation strategy (HC_4l) not worked more or less. All genes involved in this pathway have been integrated into the genome of the host plants and all enzymatic activities could be shown but the photosynthetic parameters measured were not convincing.

The MMPEM strategy instead showed more promising results. All data obtained, pointed in the direction of an improved fixation of CO_2 in C_3 plants. All results concerning C_3 photosynthesis have been obtained from the T_1 generation. This is important because the T_0 can show different biochemical characteristics than the T_1 generation. In addition, attention should be paid to the influence of foreign enzyme (MMPEM pathway) on endogenous enzymes of transgenic plants.

4.9 Future work

Hydrilla CO_2 concentration mimic pathway (HC_4l)

HC_4l pathway was good indicator for overexpression of different combination of gene.

As shown in this study, combination of different genes (4 gene = HvPEPC, mleN, NAD-ME, PEPS) makes positive impact on C_3 plants. It will be interesting to check every possible overexpressed combination of genes and measure the impact on photosynthesis.

MultiRound Gateway Technology proves the possibility of transformation of multiple gene metabolic pathways in the plants.

The *H. verticillata* mimic pathway (HC_4l) might decrease the CO_2 compensation point in sweet water plants but not in plants growing in the air; or the regulation of the transcription and the enzymatic activities could not be mimicked in the transgenic lines. In this case check the transgenic line with seven gene and overexpressed four gene (HvPEPC, Mle, ME, PEPS) and repeat the photosynthetic parameters for checking the average in transgenic lines could really show the difference in transgenes (+ 7, + 4 and wt) on beneficial ways. HC_4l pathway could transform into marine plants and might show higher biomass or higher photosynthesis like *Hydrilla verticilliata.* More work has to be done to decide between these two possibilities. This can only be done after collecting more data about the HC_4l, CO_2 fixation mechanism in Hydrilla.

MMPEM and GTDEF pathway

The positive data made it obvious to repeat the experiment and imply more parameters for the confirmation of these results of higher biomass in C_3 plants after bypassing the photorespiration. In the MMPEM pathway, it would be worth to change the promoter for the malate synthase gene which is very less expressed in these plants. Malate synthase is the first gene which started the pathway and uses glyoxalate as a substrate.

Under ambient air conditions, transgenic plants were observed with effect on growth parameters, GTDEF + MMPEM plant shows better performance than GTDEF plants. A GTDEF *Arabidopsis* plants by Kebeish *et al*., (2007) showed different parameters in low CO_2 concentration like glycine serine ratio which is the marker for photorespiration, chlorophyll content and different photosynthesis parameters (Rahad kebeish, PhD thesis Biology I). Therefore, it would be more reasonable to investigate same parameters on transgenic tobacco plants (GTDEF+MMPEM) under such environmental conditions. In addition, attention to be paid on the activity of each enzyme transferred into the plants, because in this study it was not possible to concentrate and to check the activity of each enzyme. Nevertheless, more detailed studies are necessary with optimized experimental conditions and confirmation of higher photosynthesis performance of GTDEF+MMPEM plants.

5 Appendixes

5.1 List of abbreviations

%	Percentage
°C	Degree Celsius
µg	Microgram
µl	Microliter
µmol	Micromol
A	Adenine
A. thaliana	*Arabidopsis thaliana*
A. tumefaciens	*Agrobacterium tumefaciens*
ADP	adenosine diphosphate
Amp	Ampicillin
ATP	Adenosine triphosphate
att	attachment region
B. oleraceae	*Brassica oleraceae*
bla	Beta-Lactamase
bp	Base pair
BSA	Bovine Serum Albumin
C	Cytosine
CA	carbonic anhydrases
Cab	Chlorophyll a/b-Bindeprotein
CAM	Crassulacean acid metabolism
CaMV	Cauliflower Mosaic Virus
Cm	*Crysanthemum*
CO2	Carbon dioxide
dest.	Distilled
DNA	Deoxyribonucleic acid
DNAse	Deoxyribonuclease
dNTP	Deoxyribonucleotide tri phosphate
E. coli	*Escherichia coli*
eGFP	enhanced green fluorescent protein
et al.	*et alia = and others*
EtBr	Ethidium bromide

F. bidentis	*Flaveria bidentis*
F. trinervia	*Flaveria trinervia*
G	Guanine
G3P	Glycerol 3-phosphate
GAPDH	3-phospho glyceraldehydrogenase
GCL	Glyoxylate Carboligase
GDC	Glycine decarboxylase
GDH	Glycolate dehydrogenase
GGAT	Glyoxylate:Glutamate-Aminotransferase
GGT	Glutamate:Glyoxylate-Aminotransferase
GK	Glyceratekinase
*Glc*D	Coding sequence for the D subunit of glycolate dehydrogenase in *E. coli*
*Glc*E	Coding sequence for the E subunit of glycolate dehydrogenase in *E. coli*
*Glc*F	Coding sequence for the F subunit of glycolate dehydrogenase in *E. coli*
GOX	Glycolateoxidase
GS	Glutaminesynthetase
h	hour
H. verticillata	*Hydrilla verticillata*
H^+	Hydrogen ion
H2O	Water
HC_4l	Hydrilla C_4 like
HPR	Hydroxypyruvat reductase
IPTG	Isopropyl-β-D-thiogalactoside
Kan	Kanamycin
kb	Kilobase
KOH	Potassium hydroxide
LB	left border
LB	Luria Bertani (Medium)
M	Mol per Liter (molar)
MDH	Malate Dehydrogenase
$MgCl_2$	Magnesium chloride
min	Minute
ml	Milliliter
mM	Millimolar
mRNA	messenger RNA

MS	Murashige und Skoog (Medium)
N. tabacum	*Nicotiana tabacum*
Na_2HPO_4	Disodium hydrogen phosphate
NaCl	Sodium chloride
NAD^+	Nicotinamide adenine dinucleotide(oxidizing agent)
NADH	Nicotinamide adenine dinucleotide (Reducing agent)
NAD-ME	NAD-dependent malic enzyme
NADPH	Nicotinamide adenine dinucleotide phosphate
NADP-ME	NADP-dependent malic enzyme
NaOH	sodium hydroxide
ng	Nanogramm
NH_3	Ammonia
npt	Neomycin phosphotransferase
O_2	oxygen
OD	Optical Density
ori	origin
P	Promotor
PCR	polymerase chain reaction
PEG	Polyethylenglycol
PEP	Phospho*eno*lpyruvate
PEPC	Phospho*eno*lpyruvate carboxylase
PEPCK	Phospho*enol*pyruvate carboxykinase
PEPS PPS	Phospho*enol*pyruvate synthase
PGP	Phosphoglycolate phosphatase
pH	Hydrogen ion concentration
PIB	Postillumination burst
pmol	Picomol
PPDK	Pyruvate-Orthophosphate-Dikinase
PPT	Phospho*enol*pyruvate/Phosphate-Translocator
PYR	Pyruvate
RB	right border
RbcS	RUBISCO small subunit
rfp	red fluorescence protein
RNA	Ribonucleic acid

RNase	Ribonuclease
rpm	Revolution per minute
RT	Room temperature
RUBISCO	Ribulose-1,5-bisphosphate-Carboxylase/Oxygenase
RuBP	Ribulose-1,5-bisphosphate
RWTH	Rheinisch-Westfälische Technische Hochschule
s	Second
S. cerevisae	*Saccharomyces cerevisae*
S. tuberosum	*Solanum tuberosum*
SAR	scaffold attachment region
SGAT	Serine:Glyoxylate-Aminotransferase
SHMT	Serinehydroxymethyltransferase
spec	Spectinomycin
TAE	Tris-Acetat-EDTA
Taq	*Thermus aquaticus*
TB	Transcription blocker
TBE	Tris-Borate-EDTA
T-DNA	Transfer-DNA
TE Tris EDTA TEMED	N, N, N´, N´-tetramethyl ethylene diamine
Tris	Tris hydroxymethylaminomethane
TSR	Tartronic semialdehyde reductase Reductase
U	Unit
U. panicoides	*Urochloa panicoides*
Ubi	Ubiquitin
UTR	untranslated region
UV	Ultraviolet
v/v	volume/volume
w/v	weight/volume
WT	Wild type

5.2 List of figures

Figure 1.1: The light reaction of photosynthesis 7
Figure 1.2: Schematic representation of the Calvin cycle 9
Figure 1.3: Schematic representations of photorespiration and photo-synthesis 11
Figure 1.4: Representation of the photorespiratory pathway in C_3 plants 12
Figure 1.5: Schematic representations of different types of C_4 photosynthesis 14
Figure 1.6: "Single cell C_4 photosynthesis" in *Hydrilla verticilliata* 16
Figure 1.7: Schematic representation of CAM photosynthesis 18
Figure 1.8: Regenerative enzymes in Calvin cycle 22
Figure 1.9: Representation of the photo respiratory pathway (black) in C_3 plants and the proposed pathway (red) for the conversion of glycolate to glycerate 24
Figure 2.1: Entry plasmids for gateway recombination 35
Figure 2.2: Destination Vector for gateway recombination 36
Figure 2.3: Plant vector: phosphoenol pyruvate synthase 38
Figure 2.4: Entry vector: phospho*enol*pyruvate synthase 38
Figure 2.5: Plant vector: malate dehydrogenase 38
Figure 2.6: Entry vector: malate dehydrogenase 38
Figure 2.7: Plant vector: malate/lactate antiporter 39
Figure 2.8: Entry vector: malate/lactate antiporter 39
Figure 2.9: Plant vector: phosphoenolpyruvate carboxylase 39
Figure 2.10: Entry vector: phospho*enol*pyruvate carboxylase 39
Figure 2.11: Plant vector: lactate dehydrogenase A 39
Figure 2.12: Entry vector: lacate dehydrogenase A 39
Figure 2.13: Plant vector: lactate-dehydrogenase B 40
Figure 2.14: Entry vector: lactate-dehydrogenase B 40
Figure 2.15: Plant vector: NAD-malic enzyme 40
Figure 2.16: Entry vector: NAD-malic enzyme 40
Figure 2.17: Vector pYLTAC7_C_4 Hydrilla after recombination 41
Figure 2.18: Entry vetor: neomycin phosphotransferase 43
Figure 2.19: Entry vector: phospho*enol* pyruvate synthase 43
Figure 2.20: Plant vector: mutase 43
Figure 2.21: Entry vector: mutase 43
Figure 2.22: Plant vector: malate synthase 44

Figure 2.23: Entry vector: malate synthase 44
Figure 2.24: Plant vector: enolase 44
Figure 2.25: Entry vector: enolase 44
Figure 2.26: Plasmid pYLTAC7_MMPEM after recombination 45
Figure 2.27: Gateway LR reaction 58
Figure 2.28: Diagrammatic representation of the GC-MS system 71
Figure 3.1: Gateway Entry Vectors with attachment regions for MultiRound gateway recombination 79
Figure 3.1.1: Multiple Rounds of LR recombination reaction 81
Figure 3.1.2: Schematic representation of modified C_4 pathway in *Hydrilla verticillata* (HC_4l) 83
Figure 3.1.3: Schematic diagram shows the arrangement of genes in destination vector 85
Figure 3.1.4: Verification by restriction digestion for pYLATC7_C4 Hydrilla (HC4l) vector (6 genes) 87
Figure 3.1.5: control restriction digestion of destination vector carrying seven genes 88
Figure 3.1.5: Destination vector with seven genes restriction digestion 88
Figure 3.1.6: Transient expression of pYLTAC7_Hydrilla gateway vector in Tobacco 90
Figure 3.1.7: Stable expressions of pYLTAC7_C4 Hydrilla (HC4l) genes in tobacco plants in T_0 generation 91
Figure 3.1.8: Stable expressions of pYLTAC7_C_4 *Hydrilla* genes in tobacco plants in T_1 generation 93
Figure 3.1.9: Relative activity of phospho*enol*pyruvate synthase and phospho*enol*pyruvate carboxylase 95
Figure 3.1.10: Specific activities of phospho*enol*pyruvate synthase and phospho*enol*-pyruvate carboxylase 95
Figure 3.1.11: Relative activity of NAD dependent malic enzyme and NAD dependent malate dehydrogenase 95
Figure 3.1.12: Specific activity of NAD dependent Malic enzyme and NAD dependent Malate dehydrogenase 96
Figure 3.1.13: Relative activity of Lactate dehydrogenase 96
Figure 3.1.14: Phenotypic effects of the HC_4l pathway genes on transgenic tobacco plant 97
Figure 3.1.15: Ammonia release assay from the transgenic plant 99

Figure 3.1.16: Concentration of malate in the transgenic plants 99
Figure 3.1.17: Soluble and insoluble metabolites measured from transgenic plants..... 100
Figure 3.1.18: Glucose, fructose and sucrose by GC-MS 101
Figure 3.1.19A: Post illumination burst 102
Figure 3.1.19B: Post illumination burst..... 102
Figure 3.1.20: A/Ci-curve from WT and transgenic plants 103
Figure 3.2.1: Representation of the photorespiratory pathway (black) in C_3 plants and the proposed pathway (red) for the conversion of glycolate to glycerate. New improved pathway (Blue)..... 106
Figure 3.2.2: The arrangement of expression cassette with five genes 107
Figure 3.2.3: Multiplex PCR for Me, PPS and Enolase 108
Figure 3.2.4: Multiplex PCR for Mutase and npt 108
Figure 3.2.5: Control PCR for malate synthase..... 108
Figure 3.2.6: Transient expression of pYLTAC7_MMPEM gateway vector in transgenic GTDEF Tobacco plants. 109
Figure 3.2.7: Expression of genes measured by Real-Time PCR..... 111
Figure 3.2.8: Stable expression of genes measured by Real Time PCR..... 112
Figure 3.2.9: Relative activity of NAD-ME and PEPS synthase 112
Figure 3.2.10A: Relative concentration of Glucosse, Fructose and Sucrose by GC-MS. 113
Figure 3.2.10B: Relative concentration of amino acid by GC-MS 114
Figure 3.2.11: Phenotypic effect of MMPEM, GTDEF, GTDEF+MMPEM and wild type plants..... 115
Figure 3.2.12: Leaf area and height of the plants 117
Figure 3.2.13: Total dry and fresh weight of transgenic plants 118
Figure 3.2.14A: Postillumination burst from transgenic plants..... 120
Figure 3.2.14B: Postillumination burst from transgenic plants..... 120
Figure 3.2.15: A/Ci-curve from Azygote and transgenic plants..... 122
Figure 4.1: Hydrilla pathway transferred to potato cells 127
Figure 4.2 (3.1.2): Representation of modified and optimized *Hydrilla* C_4 like pathway (HC_4l)..... 128
Figure 4.3: Overexpressed C_4 enzymes and antiporter cycle assumption 132

Figure 4.4: Representation of the photorespiratory pathway (black) in C_3 plants and the proposed pathway (red) for the conversion of glycolate to glycerate. New improved pathway (Blue) 137

5.3 List of Tables

Table 1: Approaches to expressing C_4 enzymes in C_3 plants.....20
Table 2.1: Used equipments and Accessories 27
Table 2.2: Different size standard for Gelelctrophoresis 29
Table 2.3: Used Reaction kits 29
Table 2.4: Enzymes used throughout the work 30
Table 2.5: Synthetic Oligonucleotide.....30
Table 2.6: Destination vector pYLTAC7_C_4_Hydrilla and Gateway Entry Vectors 41
Table 2.7: Abbrevation used for vectors from fig. 2.18 to 2.25.....42
Table 2.8: Destination vector pYLTAC7_MMPEM 44
Table 2.9: Murashige and Skoog (MS) Medium 46
Table 2.10: Luria Bertani (LB) Medium.....47
Table 2.11: YEB Medium 47
Table 2.12: Used computer programs 48
Table 2.21: Buffer PI for plasmid isolation.....49
Table 2.22: Buffer PII for plasmid isolation 49
Table 2.23: Buffer PIII for Plasmid isolation.....49
Table 2.24: DNA/RNA-Extraction buffer.....50
Table 2.25: 50 xTris-Acetate EDTA buffer (TAE).....51
Table 2.26: Standard PCR protocol for Taq Polymerase 52
Table 2.27: Standard PCR Program for Phusion Polymerase.....52
Table 2.28: Standard PCR Program for GoTaq Polymerase.....53
Table 2.29: Standard-PCR-Program for Phire Polymerase.....53
Table 2.30: DNAse Digestion 54
Table 2.31: Reverse Transcription 54
Table 2.32: Standard chart for the Dephospho-phorylation of DNA-5´prime.....56
Table 2.33: Standard chart for the Blunting of DNA ends 56
Table 2.34: Ligations.....57

Table 2.35: Standard chart for Gateway Recombination..... 58
Table 2.36: YEB-Induction medium (pH 5. 6)..... 62
Table 2.38: MSII Medium with Plant agar..... 62
Table 2.37: Infiltrations medium (pH 5.6) 62
Table 2.39: MSIII Medium..... 62
Table 2.40: Bradford Reagent..... 63
Table 2.41: HvPEPC Reaction mixture..... 64
Table 2.42: NAD-ME Reaction mixture 65
Table 2.43: NAD-MDH Reaction mixture..... 66
Table 2.44: The PEPS Reaction mixture..... 66
Table 2.45: Glucose/Fructose Reaction buffer..... 68
Table 2.46: Citrate NaOH Puffer..... 69
Table 2.47: Malate reaction buffer 70
Table 2.48: GlyGlyBuffer..... 70
Table 2.49: Ammonia release assay Incubations medium..... 70
Table 2.50: Ammonia release assay reagent I 71
Table 2.51: Ammonia release assay reagent lI 71
Table 2.52: The GC-MS machine temperature program..... 72
Table 2.53: Chemicals for GC..... 72
Table 2.54: Used chemicals in GC-MS (FAMES)..... 72
Table 2.55: Injection method for GC..... 75
Table 2.56: Injection-Method with Gerstel MPS 75
Table 2.57: Rinse setting 75
Table 2.58: MS method 75
Table 2.59: The PIB measuring protocol..... 76
Table 3.1.1: Genes and the source of the genes with promoters 86
Table 3.1.2: Control digestion of additional genes after recombination in destination vector pYLTAC7_Hydrilla (HC4l) 87
Table 3.1.3: Fragment size of digested destination vector with seven genes digested with AscI and KspI (HpaI) enzymes..... 88
Table 3.1.4: Relative expression and relative activity of transgenes in T_1 generation..... 94
Table 3.1.5: CO_2 Compensation point for different transgenes..... 104
Table 3.2.1: Relative expression and relative activity of transgenes in T_1 generation..... 113

Table 3.2.2: The apparent CO_2 compensation point (Γ) of WT and transgenic plants 122

6 References

Agarie, S., Miura, A., Sumikura, R., Tsukamoto, S., Nose, A., Arima, S., Matsuoka, M., and Miyao-Tokutomi, M. (2002), 'Overexpression of C_4 PEPC caused O_2-insensitive photosynthesis in transgenic rice plants', *Plant Science, 162* (2), 257-265.

Ainsworth, E. A. and Long, S. P. (2005), 'What have we learned from 15 years of free-air CO_2 enrichment (FACE)? A meta-analytic review of the responses of photosynthesis, canopy properties and plant production to rising CO_2', *New Phytol,* 165 (2), 351-371.

Anderson, L. E. (1971), 'Chloroplast and cytoplasmic enzymes. II. Pea leaf triose phosphate isomerases', *Biochim Biophys Acta*, 235 (1), 237-244.

Anderson, JW., Beardall, J. (1996)**, '**Molecular Activities of Plant Cells: An Introduction to Plant Biochemistry.

Andersson, I. and Taylor, T. C. (2003), 'Structural framework for catalysis and regulation in ribulose-1, 5-bisphosphate carboxylase/oxygenase', *Arch Biochem Biophys,* 414 (2), 130-140.

Andrews, J. T., and Whitney, S. M. (2003), ' Manipulating ribulose bisphosphate carboxylase/oxygenase in the chloroplasts of higher plants', *Arch Biochem Biophys 414*, 159-169.

Andrews, T. J., and Lorimer, G. H. (1987), 'RUBISCO: structure, mechanisms and prospects for improvement', Academic press, New York, *The biochemistry of plants* 10, 131-

Aoyagi, K. and Bassham, J. A. (1984), 'Pyruvate orthophosphate dikinase of C_3 seeds and leaves as compared to the enzyme from maize', *Plant Physiol,* 75 (2), 387-392.

Arp, W. J., Van Mierlo, J. E. M., Berendse, F., and Snijders, W. (1998), 'Interactions between elevated CO_2 concentration, nitrogen and water: Effects on growth and water use of six perennial plant species', *Plant, Cell & Environment 21*, 1-11.

Atkin, O. K., Evans, J. R., and Siebke, K. (1998), 'Relationship between the inhibition of leaf respiration by light and enhancement of leaf dark respiration following light treatment', *Plant Physiol 25*, 437-443.

Ascencio, J. and Bowes, G. (1983), 'Phospho*enol*pyruvate carboxylase in Hydrilla plants with varying CO_2 compensation points', *Photosynth Res,* 4, 151-170.

Ashikari, M., Matsuoka, M. (2006), 'Identification, isolation and pyramiding of quantitative trait loci for rice breeding', *Trends Plant Sci*, 11(7), 344-350.

Ashton, A. R. and Hatch, M. D. (1983), 'Regulation of C_4 photosynthesis: physical and kinetic properties of active (dithiol) and inactive (disulfide) NADP-malate dehydrogenase from Zea mays', *Arch Biochem Biophys,* 227 (2), 406-415.

Ashton, A. R., Burnell, J. N., Furbank, R. T., Jenkins, C. L. D., and Hatch, M. D. (1990), 'Enzymes of C_4 photosynthesis', *Lea PJ, editor. Methods in plant biochemistry,* 3, 39-72.

Ausubel, F. M., Brent, R., and Kingston, R. E. (1994), 'Current Protocols in Molecular Biology', *Wiley Interscience*, *New York.*

Badger, M. R. and Price, G. D. (2003), 'CO_2 concentrating mechanisms in cyanobacteria: molecular components, their diversity and evolution', *J Exp Bot,* 54 (383), 609-622.

Badger, M. R., Price, G. D., Long, B. M., and Woodger, F. J. (2006), 'The environmental plasticity and ecological genomics of the cyanobacterial CO_2 concentrating mechanism', *J Exp Bot,* 57 (2), 249-265.

Bagge, P. and Larsson, C. (1986), 'Biosynthesis of aromatic amino acids by highly purified spinach chloroplasts Compartmentation and regulation of the reactions', *Physiol. Plant.,* 68, 641-647.

Bandyopadhyay, A., Datta, K., Zhang, J., Yang, W., Raychaudhuri, S., Miyao, M., Datta, SK. (2007), 'Enhanced photosynthesis rate in genetically engineered indica rice expressing pepc gene cloned from maize', *Plant Science,*172 (6)1204-1209.

Bari, R., Kebeish, R., Kalamajka, R., Rademacher, T., and Peterhänsel, C. (2004), 'A glycolate dehydrogenase in the mitochondria of *Arabidopsis thaliana*', *J Exp Bot 55*, 623-630.

Beckmann, K., Dzuibany, C., Biehler, K., Fock, H., Hell, R., Migge, A., and Becker, T. W. (1997), 'Photosynthesis and fluorescence quenching, and the mRNA levels of plastidic glutamine synthetase or of mitochondrial serine hydroxymethyltransferase (SHMT) in the leaves of the wild-type and of the SHMT-deficient stm mutant of *Arabidopsis thaliana* in relation to the rate of photorespiration', *Planta 202*, 379-386.

Beckmann, J., Lehr, F., Finazzi, G., Hankammer, B., Posten, C., Wobbe, L., Kruse O. (2009). , 'Improvement of light to biomass conversion by deregulation of light-harvesting protein translation in Chlamydomonas reinhardtii ', *Journal of Biotechnology*, 142,70–77

Berg, J. M., Tymoczko, J. L., Stryer, L. (2002), 'Biochemistry*, 5th edition*

Berkemeyer, M., Scheibe, R., and Ocheretina, O. (1998), 'A novel, non redox regulated NAD-dependent malate dehydrogenase from chloroplasts of Arabidopsis thaliana', *L', J Biol Chem*, 273 (43), 27927-27933.

Bock, R. (2001), 'Transgenic plastids in basic research and plant biotechnology', *J Mol Biol 312*, 425-438.

Bohmert, K., Balbo, I., Kopka, J., Mittendorf, V., Nawrath, C., Poirier, Y., Tischendorf, G., Trethewey, R. N., and Willmitzer, L. (2000), 'TransgenicArabidopsis plants can accumulate polyhydroxybutyrate to up to 4% of their fresh weight', *Planta,* 211 (6), 841-845.

Bologna, F. P., Andreo, C. S., and Drincovich, M. F. (2007), 'Escherichia coli malic enzymes: two isoforms with substantial differences in kinetic properties, metabolic regulation, and structure', *J Bacteriol,* 189 (16), 5937-5946.

Borland, A. M., Hartwell, J., Jenkins, G. I., Wilkins, M. B., and Nimmo, H. G. (1999), 'Metabolite Control Overrides Circadian Regulation of Phospho*enol*pyruvate Carboxylase Kinase and CO_2 Fixation in Crassulacean Acid Metabolism', *Plant Physiol,* 121 (3), 889-896.

Bowes, G. (1996), 'Photosynthetic responses to changing atmospheric carbon dioxide concentration. in advances of photosynthesis, photosynthesis and environment *Baker,NR (ed) Kluwer Academic publisher, Dordrecht, the Netherlands 5*, 387-407.

Bowes, G., Ogren, W. L., and Hageman, R. H. (1971), 'Phosphoglycolate production catalyzed by ribulose diphosphate carboxylase', *Biochem Biophys Res Commun,* 45 (3), 716-722.

Bowes, G., Rao, S. K., Estavillo, G. M., and Reiskind, J. B. (2002), 'C_4 mechanisms in aquatic angiosperms: comparisons with terrestrial C_4 systems', *Functional Plant Biology,* 29, 379–392.

Bowes, G., Rao, S. K., Reiskind, J. B., Estavillo, G. M., and Rao, V. S. (2007), 'Hydrilla: retrofitting a C_3 leaf with a single-cell C_4 NADP-ME system', *Sheehy, J. E., Mitchell, P. L. and Hardy, B. (eds) Charting New Pathways to C_4 rice*, 275-296.

Bradford, M. M. (1976), 'A rapid and sensitive method for the quantitation of microgram quantities of protein utilizing the principle of protein-dye binding', *Anal Biochem,* 72, 248-254.

Brautigam, A., Hoffmann-Benning, S., and Weber, A. P. (2008), 'Comparative proteomics of chloroplast envelopes from C_3 and C_4 plants reveals specific adaptations of the plastid envelope to C_4 photosynthesis and candidate proteins required for maintaining C_4 metabolite fluxes', *Plant Physiol,* 148 (1), 568-579.

Brautigam, A. and Weber, A. P. (2011), 'Do metabolite transport processes limit photosynthesis?', *Plant Physiol,* 155 (1), 43-48.

Bräutigam, A., Kajala, K., Wullenweber, J., Sommer, M., Gagneul, D., Weber, K. L., Carr, K. M., Gowik, U., Mass, J., Lercher, M. J., Westhoff, P., Hibberd, J. M., and Weber, A. P. (2011), 'An mRNA

blueprint for C_4 photosynthesis derived from comparative transcriptomics of closely related C_3 and C_4 species', *Plant Physiol,* 155 (1), 142-156.

Brown, R. H. (1999), 'Agronomic implications of C_4 photosynthesis. In: Sage RF, Monson RK, eds.C_4plant biology. San Diego, CA: *Academic Press, 473–50*

Brooks, A. and Farquhar, G. D. (1985), 'Effect of temperature on the $C0_2$-O_2 specificity of ribulose-1,5-biphosphate carboxylase/oxygenase and the rate of respiration in the light: estimates from gas exchange measurements on spinach', *Planta,* 165, 397-406.

Buchanan, B. B., Gruissem, W., and Jones, R. L. (2000), 'Biochemistry & Molecular Biology of plants', *American Society of Plant Physiologists, Rockville, Maryland*, 625.

Burnell, J. N. and Hatch, M. D. (1985), 'Regulation of C_4 photosynthesis: purification and properties of the protein catalyzing ADP-mediated inactivation and Pi-mediated activation of pyruvate,Pi dikinase', *Arch Biochem Biophys,* 237 (2), 490-503.

Burnell, J. N. (2010), 'Cloning and characterization of Escherichia coli DUF299: a bifunctional ADP-dependent kinase-Pi-dependent pyrophosphorylase from bacteria', *BMC Biochem,* 11, 1.

Calvin, B. (1989), 'Forty years of photosynthesis and related activities', *Photosynth. Reserach,* 21 (1), 3-16.

Carvalho J, Madgwick PJ, Powers SJ, Keys AJ, Lea PJ, Parry MAJ. (2011), 'An engineered pathway for glyoxylate metabolism in tobacco plants aimed to avoid the release of ammonia in photorespiration. *BMC Biotechnology,* 111 (11), 1472-6750.

Carmo-Silva, A.E., Powers, S. J., Keys, A. J., Arrabaca, M.C., Parry, MAJ. (2008), 'Photorespiration in C_4 grasses remains slow under drought conditions', *Plant' Cell and Environment,* 31 (7), 925-940.

Casati, P., Drincovich, M. F., Edwards, G.E., and Andreo, C. S. (1999), 'Malate metabolism by NADP-malic enzyme in plant defense', *Photosyn. Res.,* 61, 99-105.

Chang, Y. Y., Wang, A. Y., and Cronan, J. E., Jr. (1993), 'Molecular cloning, DNA sequencing, and biochemical analyses of Escherichia coli glyoxylate carboligase. An enzyme of the acetohydroxy acid synthase-pyruvate oxidase family', *J Biol Chem,* 268 (6), 3911-3919.

Chastain, C. J., Fries, J. P., Vogel, J. A., Randklev, C. L., Vossen, A. P., Dittmer, S. K., Watkins, E. E., Fiedler, L. J., Wacker, S. A., Meinhover, K. C., Sa-rath, G., and Chollet, R. (2002), 'Pyruvate,orthophosphate dikinase in leaves and chloroplasts of C_3 plants undergoes light-/dark-induced reversible phosphorylation', *Plant Physiol,* 128 (4), 1368-1378.

Chastain, C. J., Fries, J. P., Vogel, J. A., Randklev, C. L., Vossen, A. P., Dittmer, S. K., Watkins, E. E., Fiedler, L. J., Wacker, S. A., Meinhover, K. C., Sa-rath, G., and Chollet, R. (2002), 'Pyruvate,orthophosphate dikinase in leaves and chloroplasts of C_3 plants undergoes light-/dark-induced reversible phos-phorylation', *Plant Physiol,* 128 (4), 1368-1378.

Chen, L., Marmey, P., Taylor, N. J., Brizard, J. P., Espinoza, C., D'Cruz, P., Huet, H., Zhang, S., de Kochko, A., Beachy, R. N., and Fauquet, C. M. (1998), 'Expression and inheritance of multiple transgenes in rice plants', *Nat Biotech-nol,* 16 (11), 1060-1064.

Chen, Q. J., Zhou, H. M., Chen, J., and Wang, X. C. (2006), 'A Gateway based platform for multigene plant transformation', *Plant Mol Biol,* 62 (6), 927-936.

Chen, Q. J., Xie, M., Ma, X. X., Dong, L., Chen, J., and Wang, X. C. (2010), 'MISSA is a highly efficient in vivo DNA assembly method for plant multiple-gene transformation', *Plant Physiol,* 153 (1), 41-51.

Chen, Z., Spreitzer, RJ. (1992), ' How various factors influence the CO,/O, specificity of ribulose-1,5-bisphosphate carboxylase/ oxygenase',.*Photosynth Res*, 31 (2), 157-164

Cheng, J; Baldwin, K; Arthur, A.G; Krulwich,T.M. (1996), 'Na^+/H^+Antiport Activity Conferred by*Bacillus subtilis* tetA(L),a 5´Truncation Product of tetA(L), and Related Plasmid Genes upon *Escherichia coli* ', *Antimicrobial agents and chemo*, 40 (4), 852–857

Cheo, D. L., Titus, S. A., Byrd, D. R., Hartley, J. L., Temple, G. F., and Brasch, M. A. (2004), 'Concerted assembly and cloning of multiple DNA segments using in vitro site-specific recombination: functional analysis of multi-segment ex-pression clones', *Genome Res,* 14 (10B), 2111-2120.

Christou, P. (1997), 'Rice transformation: bombardment', *Plant Mol Biol,* 35 (1-2), 197-203.

Christine A. R. (2011), 'Increasing Photosynthetic Carbon Assimilation in C_3 Plants to Improve Crop Yield: Current and Future Strategies', Plant Physio, 2011(155) 1 36-42

Chuong, S. D., Franceschi, V. R., and Edwards, G. E. (2006), 'The cytoskeleton maintains organelle partitioning required for single-cell C_4 photosynthesis in Chenopodiaceae species', *Plant Cell,* 18 (9), 2207-2223.

Collins, N., and Merrett, M. J. (1975), 'The localization of glycolate pathway enzymes in Euglena', Biochem J *148*, 321-328.

Cooper, R. A. and Kornberg, H. L. (1965), 'Net formation of phospho*enol*pyruvate from pyruvate by Escherichia coli', *Biochim Biophys Acta,* 104 (2), 618-620.

Cooper, R. A. and Kornberg, H. L. (1974), 'Phospho*enol*pyruvate synthetase and pyruvate phosphate dikinase', *P.D. Boyer (Ed.), The Enzymes, Vol. 10 Academic Press, New York, NY*, 631–649.

Conway G. and Toennissen G. (1999), 'Feeding the world in the twenty first century. nature *402*, 55-58.

Cornic, G. and Briantais, J. M. (1991), 'Partitioning of photosynthetic electron flow between CO_2 and O_2 reduction in a C_3 leaf (Phaseolus vulgaris L.) at different CO_2 concentrations and during drought stress', *Planta,* 183, 178–184.

Cushman, J. C. and Bohnert, H. J. (1997), 'Molecular Genetics of Crassulacean Acid Metabolism', *Plant Physiol,* 113 (3), 667-676.

Cushman, J. C. (2001), 'Crassulacean acid metabolism. A plastic photosynthetic adaptation to arid environments', *Plant Physiol,* 127 (4), 1439-1448.

Dafny-Yelin, M. and Tzfira, T. (2007), 'Delivery of multiple transgenes to plant cells', *Plant Physiol,* 145 (4), 1118-1128.

Dai, Z., Ku, M., and Edwards, G. E. (1993), 'C_4 Photosynthesis (The CO_2-Concentrating Mechanism and Photorespiration)', *Plant Physiol,* 103 (1), 83-90.

Daniell, H. and Dhingra, A. (2002), 'Multigene engineering: dawn of an exciting new era inbiotechnology', *Curr Opin Biotechnol,* 13 (2), 136-141.

Dashek, W., and Harrison,M. (2006), 'Plant cell Biology

Davies, D. D. (1986), 'The fine control of cytosolic pH', *Physiol. Plant,* 67, 702–706.

Davis, W. L., and Goodman, D. B. (1992), ' Evidence for the glyoxylate cycle in human liver', Anat Rec *234*, 461-468.

De Block, M. (1988), 'Genotype independent leaf disc transformation of potato (Solanum tuberosum) using Agrobacterium tumefaciens', *Theoretical and Applied Genetics,* 76, 767–774.

De Block, M., De Sonville, A., and Debrouwer, D. (1995), 'The selection mechanism of phosphinothricin is influenced by the metabolic status of the tissue. Planta *197*, 619-626.

De Neve M, De Buck S, Jacobs A, Van Montagu M, Depicker *A* (*1997*), 'T-DNA integration patterns in co-transformed plant cells suggest that T-DNA repeats originate from co-integration of separate T-DNAs', *Plant J* , 11 (1), 15–*29*

Decker, J. P. (1959), 'Comparative responses of carbon dioxide outburst and uptake in tobacco', *Plant Physiol, 34*, 100-102.

Detarsio, E., Alvarez, C. E., Saigo, M., Andreo, C. S., and Drincovich, M. F. (2007), 'Identification of domains involved in tetramerization and malate inhibition of maize C_4-NADP-malic enzyme', *J Biol Chem,* 282 (9), 6053-6060.

Devi, M. T., Rajagopalan, A., and Raghavendra, A. S. (1996), 'Purification and properties of glycolate oxidase from plants with different photosynthetic pathways, distinctness of C_4 enzyme from that of a C_3 species and a C_3–C_4 intermediate', Photosynthesis Research *47*, (3) 231-238.

Dietze, J., Blau, A., and Willmitzer, L. (1995), 'Agrobacterium-mediated transfor-mation of potato (Solanum tuberosum)', *Gene Transfer to Plants XXII. eds Po-trykus, I., Spangenberg, G. (Springer Verlag, Berlin)*, 24–29.

Douce, R., and Neuburger, M. (1989), 'The uniqueness of plant mitochondria', *Annual Review of Plant Physiology and Plant Molecular Biology 40*, 371-414.

Douce, R. and Neuburger, M. (1999), 'Biochemical dissection of photorespiration', *Curr. Opin. Plant Biol.,* 2, 214-222.

Dougherty, W. G., and Parks, T. D. (1995), 'Transgenes and gene suppression: telling us something new?', *Curr Opin Cell Bio, 7* (3), 399-405.

Duff, S. and Chollet, R. (1995), 'In Vivo Regulation of Wheat Leaf Phospho*enol*pyruvate Carboxylase by Reversible Phosphorylation', *Plant Physiol,* 107 (3), 775-782.

Edwards, G. E. and Walker, D. A. (1983), 'C_3, C_4: mechanisms, and cellular and environmental regulation, of photosynthesis', *Oxford: Blackwell Scientific pub-lications*.

Edwards, G. E., Nakamoto, H., Burnell, J. N., and Hatch, M. D. (1985), 'Pyruvate, Pidikinase and NADP-malate dehydrogenase in C_4 photosynthesis. Properties and mechanism of light/dark regulation. ', *Annu. Rev. Plant Physiol.,* 36, 255-286.

Edwards, G. E. and Ku, M. S. B. (1987), 'Biochemistry of C_3-C_4 intermediates', *The Biochemistry of Plants, Vol. 10, M.D. Hatch and N.K. Boardman, eds (New York: Academic Press)*, 275–325.

Edwards, G. E., Franceschi, V. R., and Voznesenskaya, E. V. (2004), 'Single-Cell C4 Photosynthesis versus the Dual-Cell (Kranz) Paradigm', *Annual Reviews in Plant Physiology,*55, 173-196.

Edwards, E. J. and Smit, S. A. (2010), ' Phylogenetic analyses reveal the shady history of C_4 grasses', *Proc Natl Acad Sci U S A, 107, 2532-2537.*

Edwards, G. E., Furbank, R. T., Hatch, M. D., and Osmond, C. B. (2001), ' What does it take to be C_4? Lessons from the evolution of C_4 photosynthesis', *Plant Physiol 125, 46-49.*

Edwards, G. E., Franceschi, V. R., Ku, M. S., Voznesenskaya, E. V., Pyankov, V. I., and Andreo, C. S. (2001), 'Compartmentation of photosynthesis in cells and tissues of C_4 plants', *J Exp Bot,* 52 (356), 577-590

Edwards, G. E., Voznesenskaya, E., Smith, M., Koteyeva, N., Park, Y., Park, J. H., Kiirats, O., Okita, T. W., and Chuong, S. D. X. (2007), 'Breaking the Kranz paradigm in terrestrial C_4 plants: does it hold promise for C_4 rice?', *J. E. Sheehy, P. L. Mitchell, B. Hardy, eds, Charting New Pathways to C_4 Rice. International Rice Research Institute, Makati City, Philippines*, 249–273.

Ehleringer, J.R. (2001), 'Productivity of deserts, *345-362.* In H.A. Mooney and J. Roy (eds.), Primary Productivity in Terrestrial Ecosystems', Academic Press, San Diego

Ehleringer, J. and Bjorkman, O. (1977), 'Quantum Yields for CO_2 Uptake in C_3 and C_4 Plants: Dependence on Temperature, CO_2 and O_2 Concentration', *Plant Physiol.,* 59, 86-90.

Ehleringer, J. and Pearcy, R. W. (1983), 'Variation in Quantum Yield for CO_2 Up take among C_3 and C_4 Plants', *Plant Physiol,* 73 (3), 555-559.

Ehleringer, J. R., Sage, R. F., Flanagan, L. B., and Pearcy, R. W. (1991), 'Climate change and the evolution of C_4 photosynthesis', *Trends Ecol Evol,* 6 (3), 95-99.

Engler, C., Kandzia, R., and Marillonnet, S. (2008), 'A one pot, one step, precision cloning method with high throughput capability', *PLoS One,* 3 (11), e3647.

Estavillo, G. M., Rao, S. K., Reiskind, J. B., and Bowes, G. (2007), 'Characterization of the NADP malic enzyme gene family in the facultative, single-cell C_4 monocot Hydrilla verticillata', *Photosynth Res,* 94 (1), 43-57.

Evans, J. R., and Von Caemmerer, S. (1996), 'Carbon Dioxide Diffusion inside Leaves', Plant Physiol *110*, 339-346.

Fahnenstich, H., Saigo, M., Niessen, M., Zanor, M. I., Andreo, C. S., Fernie, A. R., Drincovich, M. F., Flugge, U. I., and Maurino, V. G. (2007), 'Alteration of organic acid metabolism in Arabidopsis overexpressing the maize C_4 NADP-malic enzyme causes accelerated senescence during extended darkness', *Plant Physiol,* 145 (3), 640-652.

Farquhar, G. D., von Caemmerer, S., and Berry, J. A. (2001), 'Models of photosynthesis', *Plant Physiol,* 125 (1), 42-45.

Feng, L., Wang, K., Li, Y., Tan, Y., Kong, J., Li, H., Li, Y., and Zhu, Y. (2007), 'Overexpression of SBPase enhances photosynthesis against high temperature stress in transgenic rice plants', *Plant Cell Rep,* 26 (9), 1635-1646.

Feng, L. L., Han, Y. J., An, B. G., Yang, J., Yang, G. H., Li, Y. S., and Zhu, Y. G. (2007), 'Overexpression of sedoheptulose-1,7-bisphosphatase enhances photosynthesis and growth under salt stress in transgenic rice plants', *Funct. Plant Biol.,* 34, 822–834.

Fett, T. W. and Coleman, J. R. (1984), 'Characterization and expression of two cDNAs encoding carbonic anhydrase in Arabidopsis thaliana', *Plant Physiol.,* 105, 707-713.

Fischer, K., Kammerer, B., Gutensohn, M., Arbinger, B., Weber, A., Häusler, R. E., and Flügge, U. I. (1997), 'A new class of plastidic phosphate translocators: a putative link between primary and secondary metabolism by the phosphoe-nolpyruvate/ phosphate antiporter ', *Plant Cell,* 9, 453-462.

Flügge, U. I. and Heldt, H. W. (1991), 'Metabolite translocators of the chloroplast envelope', *Annu. Rev. Plant Physiol. Plant Mol. Biol.,* 42, 129-144.

Forestan, C., Varroto, S. (2011)), 'The Role of PIN Auxin Efflux Carriers in polar Auxin Transport and Accumulation and Their Effect on Shaping Maize Development', Mol. Plant., 5, (4) 787–798

Francois, I., Broekaert, W., and Cammue, B. (2002), 'Different approaches for multitransgene stacking in plants', *Plant Sci.,* 163, 281–295.

Frederick, S. E., Gruber, P. J., and Tolbert, N. E. (1973), 'The occurence of glycolate dehydrogenase and glycolate oxidase in green plants: An evolutionary survey', Plant Physiol *52*, 318-323.

Fridlyand, L. E., Backhausen, J. E., and Scheibe, R. (1998), 'Flux control of the malate valve in leaf cells', *Arch Biochem Biophys,* 349 (2), 290-298.

Fukayama, H., Imanari, E., Tsuchida, H., Izui, K., and Matsuoka, M. (2000), 'In vivo activity of maize phospho*enol*pyruvate carboxylase in transgenic rice plants', *Plant Cell Physiol.,* 41, 112.

Fukayama, H., Tsuchida, H., Agarie, S., Nomura, M., Onodera, H., Ono, K., Lee, B. H., Hirose, S., Toki, S., Ku, M. S., Makino, A., Matsuoka, M., and Miyao, M. (2001), 'Significant accumulation of C_4 specific pyruvate, orthophosphate dikinase in a C_3 plant, rice', *Plant Physiol,* 127 (3), 1136-1146.

Fukayama, H., Hatch, M. D., Tamai, T., Tsuchida, H., Sudoh, S., Furbank, R. T., and Miyao, M. (2003), 'Activity regulation and physiological impacts of maize C_4-specific phospho*enol*pyruvate carboxylase overproduced in transgenic rice plants', *Photosynth Res,* 77 (2-3), 227-239.

Furbank, R. T., Jenkins, C. L., and Hatch, M. D. (1989), 'CO_2 Concentrating Mechanism of C_4 Photosynthesis: Permeability of Isolated Bundle Sheath Cells to Inorganic Carbon', *Plant Physiol,* 91 (4), 1364-1371.

Furbank, R.T., Hatch, M.D., and Jenkins, C.L.F. (2000), ' C4 photosynthesis:Mechanism and Regulation. InAdvances in Photosynthesis: 9. Photosynthesis: Physiology and Metabolism. Edited by Leegood, R.C., Sharkey, T.D. and von Caemmerer, S. pp. 435–457. Kluwer Academic Publishers, Dordrecht

Furbank, R. T. (2011), 'Evolution of the C (4) photosynthetic mechanism: are there really three C_4 acid decarboxylation types?', *J Exp Bot,* 62 (9), 3103-3108.

Furumoto, T., Izui, K., Quinn, V., Furbank, R. T., and von Caemmerer, S. (2007), 'Phosphorylation of phospho*enol*pyruvate carboxylase is not essential for high photosynthetic rates in the C_4 species Flaveria bidentis', *Plant Physiol,* 144 (4), 1936-1945.

Gallardo, F., Miginiac-Maslow, M., Sangwan, R. S., Decottignies, P., Keryer, E., Dubois, F., Bismuth, E., Galvez, S., Sangwan-Norreel, B., Gadal, P., and et al. (1995), 'Monocotyledonous C_4 NADP(+)-malate dehydrogenase is efficiently synthesized, targeted to chloroplasts and processed to an active form in transgenic plants of the C_3 dicotyledon tobacco', *Planta,* 197 (2), 324-332.

Gehlen, J., Panstruga, R., Smets, H., Merkelbach, S., Kleines, M., Porsch, P., Fladung, M., Becker, I., Rademacher, T., Hausler, R. E., and Hirsch, H. J. (1996), 'Effects of altered phospho*enol*pyruvate carboxylase activities on transgenic C_3 plant Solanum tuberosum', *Plant Mol Biol,* 32 (5), 831-848.

Gietl, C., Lehnerer, M., and Olsen, O. (1990), 'Mitochondrial malate dehydrogenase from watermelon: sequence of cDNA clones and primary structure of the higher plant precursor protein', *Plant Mol Biol,* 14 (6), 1019-1030.

Gietl, C. (1992), 'Partitioning of malate dehydrogenase isoenzymes into glyoxysomes, mitochondria, and chloroplasts', *Plant Physiol,* 100 (2), 557-559.

Gowik, U. and Westhoff, P. (2011), 'The path from C_3 to C_4 photosynthesis', *Plant Physiol,* 155 (1), 56-63.

Gowik, U., Brautigam, A., Weber, K. L., Weber, A. P., and Westhoff, P. (2011), 'Evolution of C_4 photosynthesis in the genus flaveria: how many and which genes does it take to make C_4?', *Plant Cell,* 23 (6), 2087-2105.

Grover, S. D., Canellas, P. F., and Wedding, R. T. (1981), 'Purification of NAD malic enzyme from potato and investigation of some physical and kinetic properties', *Arch Biochem Biophys,* 209 (2), 396-407.

Haake, V., Zrenner, R., Sonnewald, U., and Stitt, M. (1998), 'A moderate decrease of plastid aldolase activity inhibits photosynthesis, alters the levels of sugars and starch and inhibits growth of potato plants.', *Plant J.,* 14, 147.

Halpin, C., Barakate, A., Askari, B. M., Abbott, J. C., and Ryan, M. D. (2001), 'Enabling technologies for manipulating multiple genes on complex pathways', *Plant Mol Biol,* 47 (1-2), 295-310.

Halpin, C., Boerjan, W. (2003), ' Stacking transgenes in forest trees', *TrendsPlant Sci,* 8 (8), 363–365

Hamilton, C. M., Frary, A., Lewis, C., and Tanksley, S. D. (1996), 'Stable transfer of intact high molecular weight DNA into plant chromosomes', *Proc Natl Acad Sci U S A,* 93 (18), 9975-9979.

Hansen, R. W. and Hayashi, J. A. (1962), 'Glycolate metabolism in Escherichia coli', *J Bacteriol,* 83, 679-687.

Harley, P.C. and Sharkey, T.D. (1991), 'An improved model of C_3 photosynthesis at high CO_2: reversed O_2 sensitivity explained by lack of glycerate reentry into the chloroplast', *Photosynth. Research,* 27, 169-178.

Harrison, E. P., Willingham, N. M., Lloyd, J. C., and Raines, C. A. (1998), 'Reduced sedoheptulose-1,7-bisphosphatase levels in transgenic tobacco lead to decreased photosynthetic capacity and altered carbohydrate accumulation', *Planta,* 204, 27.

Hartley, J. L., Temple, G. F., and Brasch, M. A. (2000), 'DNA cloning using in vitro site-specific recombination', *Genome Res,* 10 (11), 1788-1795.

Hartwell, J., Gill, A., Nimmo, G. A., Wilkins, M. B., Jenkins, G. I., and Nimmo, H. G. (1999), 'Phospho*enol*pyruvate carboxylase kinase is a novel protein kinase regulated at the level of expression', *Plant J,* 20 (3), 333-342.

Hatch, MD., Burnell, JN. (1990), 'Carbonic anhydrase activity in leaves and its role in the first step of C, photosynthesis' *Plant Physiol,* 93 (2), 825-828

Hatch, M. D. and Slack, C. R. (1968), 'A new enzyme for the interconversion of py-ruvate and phosphopyruvate and its role in the C_4 dicarboxylic acid pathway of photosynthesis', *Biochem J,* 106 (1), 141-146.

Hatch, M. D., Mau, S. L., and Kagawa, T. (1974), 'Properties of leaf NAD malic en-zyme from plants with C_4 pathway photosynthesis', *Arch Biochem Biophys,* 165 (1), 188-200.

Hatch, M. D. (1979), 'Regulation of C_4 photosynthesis: factors affecting cold-mediated inactivation and reactivation of pyruvate, Pi dikinase', *Aust. J. Plant Physiol.,* 6, 607-619.

Hatch, M. D., Dröscher, L., Flügge, U. I., and Heldt, H. W. (1984), 'A specific translocator for oxaloacetate in chloroplasts', *FEBS Lett,* 178, 15–19.

Hatch, M. D. (1987), 'C_4 photosynthesis: a unique blend of modified biochemistry, anatomy and ultrastructure', *Biochim. Biophys. Acta,* 895, 81–106.

Hatch, M. D. (1992), 'C_4 Photosynthesis: an Unlikely Process Full of Surprises', *Plant Cell Physiol,* 33, 333-342.

Hatch, M. D. (1997), 'Resolving C_4 photosynthesis: trials, tribulations and other unpublished stories', *Aust. J. Plant Physiol.,* 24, 413–422.

Häusler, R. E., Holtum, J. A., and Latzko, E. (1987), 'CO_2 is the inorganic carbon substrate of NADP malic enzymes from Zea mays and from wheat germ', *Eur J Biochem,* 163 (3), 619-626.

Häusler, R. E., Baur, B., Scharte, J., Teichmann, T., Eicks, M., Fischer, K. L., Flugge, U. I., Schubert, S., Weber, A., and Fischer, K. (2000), 'Plastidic metabolite transporters and their physiological functions in the inducible crassulacean acid metabolism plant Mesembryanthemum crystallinum', *Plant J,* 24 (3), 285-296.

Häusler, R. E., Hirsch, H. J., Kreuzaler, F., and Peterhansel, C. (2002), 'Overexpression of C_4 cycle enzymes in transgenic C_3 plants: a biotechnological approach to improve C_3photosynthesis', *J Exp Bot,* 53 (369), 591-607.

Häusler, R. E., Kleines, M., Uhrig, H., Hirsch, H. J. , and Smets, H. (1999), 'Over-expression of phospho*enol*pyruvate carboxylase from Corynebacterium glutamicum lowers the CO_2 compensation point (T) and enhances dark and light respiration in transgenic potato', *J Exp Bot,* 50, 1231–1242.

Häusler, R. E., Rademacher, T., Li, J., Lipka, V., Fischer, K. L., Schubert, S., Kreuzaler, F., and Hirsch, H. J. (2001), 'Single and double overexpression of C_4 cycle genes had differential effects on the pattern of endogenous enzymes, attenuation of photorespiration and on contents of UV protectants in transgenic potato and tobacco plants', *J Exp Bot,* 52 (362), 1785-1803.

Heldt, H. W. and Rapley, L. (1970), 'Specific transport of inorganic phosphate, 3-phosphoglycerate and dihydroxyacetonephosphate, and of dicarboxylates across the inner membrane of spinach chloroplasts', *FEBS Lett,* 10 (3), 143-148.

Heldt, H. W. (1997), 'Plant Biochemistry & Molecular Biology', *Oxford University Press, New York.*

Henkes, S., Sonnewald, U., Badur, R., Flachmann, R., and Stitt, M. (2001), 'A small decrease of plastid transketolase activity in antisense tobacco transformants has dramatic effects on photosynthesis and phenylpropanoid metabolism', *Plant Cell,* 13 (3), 535-551.

Herrmann, K. M. and Weaver, L. M. (1999), 'The Shikimate Pathway', *Annu Rev Plant Physiol Plant Mol Biol,* 50, 473-503.

Holaday, A. S. and Chollet, R. (1983), 'Photosynthetic/Photorespiratory Carbon Metabolism in the C_3-C_4 Intermediate Species, Moricandia arvensis and Pani-cum milioides', *Plant Physiol,* 73 (3), 740-745.

Holger F, Mariana S, Michaela N, María I. Z, Carlos S. A, Alisdair R. F, María F. D, Ulf-Ingo F, and Verónica G. M. (2007), 'Alteration of Organic Acid Metabolism in Arabidopsis Overexpressing the Maize C_4 NADP-Malic Enzyme Causes Accelerated Senescence during Extended Darkness',*Plant Physiol,145,3 640-652*

Huber, S. C. and Edwards, G. E. (1977), 'Transport in C_4 mesophyll chloroplasts: evidence for an exchange of inorganic phosphate and phospho*enol*pyruvate', *Biochim Biophys Acta,* 462 (3), 603-612.

Hudson, G. S., Evans, J. R., von Caemmerer, S., Arvidsson, Y. B., and Andrews, T. J. (1992), 'Reduction of ribulose-1,5-bisphosphate carboxylase/oxygenase content by antisense RNA reduces photosynthesis in transgenic tobacco plants', *Plant Physiol,* 98 (1), 294-302.

Hudspeth, R. L., Grula, J. W., Dai, Z., Edwards, G. E., and Ku, M. S. (1992), 'Expression of maize phospho*enol*pyruvate carboxylase in transgenic tobacco : effects on biochemistry and physiology', *Plant Physiol,* 98 (2), 458-464.

Huppe, H. C. and Turpin, D. H. (1994), 'Integration of carbon and nitrogen metabolism in plant and algal cells', *Annu. Rev. Plant Physiol. Plant Mol. Biol.,* 45, 577-607.

Igamberdiev, A. U. and Lea, P. J. (2002), 'The role of peroxisomes in the integration of metabolism and evolutionary diversity of photosynthetic organisms', *Phyto-chemistry,* 60 (7), 651-674.

Igarashi, D., Miwa, T., Seki, M., Kobayashi, M., Kato, T., Tabata, S., Shinozaki, K., and Ohsumi, C. (2003), 'Identification of photorespiratory gluta-mate:glyoxylate aminotransferase (GGAT) gene in Arabidopsis', *Plant J,* 33 (6), 975-987.

Ishimaru, K., Ishikawa, I., Matsuoka, M., and Ohsugi, R. (1997), 'Analysis of a C_4 maize pyruvate,orthophosphate dikinase expressed in C_3 transgenic Arabidopsis plants', *Plant Science,* 129, 57-64.

Ishimaru, K., Okawa, Y., Ishige, T., Tobias, D. J., and Ohsugi, R. (1998), 'Elevated pyruvate,orthophosphate dikinase (PPDK) activity alters carbon metabolism in C_3 transgenic potatoes with a C_4 maize PPDK gene', *Physiol. Plant.,* 103, 340- 346.

Jenkins, C. L., Furbank, R. T., and Hatch, M. D. (1989), 'Mechanism of C_4 photosynthesis: a model describing the inorganic carbon pool in bundle sheath cells', *Plant Physiol,* 91 (4), 1372-1381.

Jenkins, C. L., Furbank, R. T., and Hatch, M. D. (1989), 'Inorganic Carbon Diffusion between C_4 Mesophyll and Bundle Sheath Cells: Direct Bundle Sheath CO_2 Assimilation in Intact Leaves in the Presence of an Inhibitor of the C_4 Pathway', *Plant Physiol,* 91 (4), 1356-1363.

Jiao, J. A. and Chollet, R. (1991), 'Posttranslational regulation of phospho*enol*pyruvate carboxylase in c(4) and crassulacean Acid metabolism plants', *Plant Physiol,* 95 (4), 981-985.

Jiao, D., Huang, X., Li, X., Chi, W., Kuang, T., Zhang, Q., Ku, MSB., Cho, D. (2002), 'Photosynthetic characteristics and tolerance to photo-oxidation of transgenic rice expressing C_4 photosynthesis enzymes', *Photosynthesis Research*,72 (1), 85-93.

Jordan, D. B. and Ogren, W. L. (1984), 'The CO_2/O_2 specificity of ribulose 1,5-bisphosphate carboxylase/oxygenase', *Planta,* 161, 308–313.

Jorgensen, R. (1991), 'Silencing of plant genes by homologous transgenes', *Ag-Biotechnol. News Info,* 4, 265N-273N.

Kajala, K., Covshoff, S., Karki, S., Woodfield, H., Tolley, B. J., Dionora, M. J., Mogul, R. T., Mabilangan, A. E., Danila, F. R., Hibberd, J. M., and Quick, W. P. (2011), 'Strategies for engineering a two-celled C_4 photosynthetic pathway into rice', *J Exp Bot,* 62 (9), 3001-3010.

Kanai, R Edwards, G. E. (1999), Biochemistry of C_4 photosynthesis. In: Sage RF, Monson RK, eds. C_4 plant biology. *New York: Academic Press, 49–87.*

Kaplan, A. and Reinhold, L. (1999), 'CO_2 Concentrating Mechanisms in Photosynthetic Microorganisms', *Annu Rev Plant Physiol Plant Mol Biol,* 50, 539-570.

Kebeish, R., Niessen, M., Thiruveedhi, K., Bari, R., Hirsch, H. J., Rosenkranz, R., Stabler, N., Schonfeld, B., Kreuzaler, F., and Peterhansel, C. (2007), 'Chloroplastic photorespiratory bypass increases photosynthesis and biomass pro-duction in Arabidopsis thaliana', *Nat Biotechnol,* 25 (5), 593-599.

Kimball, B. A. (1983). Carbon dioxide and agricultural yield: an assemblage and analysis of 430 prior observations [Effect on crop yields of the increasing global atmospheric carbon dioxide concentration, growth, production includes some woody plants]. *Agronomy Journal [Madison: American Society of Agronomy]* Sept/Oct, 779-788.

Kinney, A. J. (1998), 'Manipulating flux through plant metabolic pathways', *Curr Opin Plant Biol,* 1 (2), 173-178.

Kirschbaum, M. U. (2010), 'Does enhanced photosynthesis enhance growth? Lessons learned from CO_2 enrichment studies', *Plant Physiol,* 155 (1), 117-124.

Kogami, H., Shono, M., Koike, T., Yanagisawa, S., Izui, K., Sentoku, N., Tanifuji, S., Uchimiya, H., and Toki, S. (1994), 'Molecular and physiological evaluation of transgenic tobacco plants expression a maize phospho*enol*pyruvate carboxylase gene under the control of the cauliflower mosaic virus 35S promoter', *Transgenic Res.,* 3, 287–296.

Kohli, A., Leech, M., Vain, P., Laurie, D. A., and Christou, P. (1998), 'Transgene organization in rice engineered through direct DNA transfer supports a two phase integration mechanism mediated by the establishment of integration hot spots', *Proc Natl Acad Sci U S A,* 95 (12), 7203-7208.

Kornberg, H. L. and Sadler, J. R. (1961), 'The metabolism of C2-compounds in micro-organisms. VIII. A dicarboxylic acid cycle as a route for the oxidation of glycollate by Escherichia coli', *Biochem J,* 81, 503-513.

Kozaki, A. and Takeba, G. (1996), 'Photorespiration protects C_3 plants from pho-tooxidation', *Nature,* 384, 557–560.

Kramer, D.M., Evans, J.R., (2011), 'The importance of energy balance in improving photosynthetic productivity', *Plant Physiol*, 155(1), 70-8

Ku, S. B. and Edwards, G. E. (1977), 'Oxygen Inhibition of Photosynthesis: II. Kinetic Characteristics as Affected by Temperature', *Plant Physiol,* 59 (5), 991-999.

Ku, S. B. and Edwards, G. E. (1977), 'Oxygen Inhibition of Photosynthesis: I. Temperature Dependence and Relation to O_2/CO_2 Solubility Ratio', *Plant Phys-iol,* 59 (5), 986-990.

Ku, S. B., Edwards, G. E., and Tanner, C. B. (1977), 'Effects of Light, Carbon Dioxide, and Temperature on Photosynthesis, Oxygen Inhibition of Photosynthesis, and Transpiration in Solanum tuberosum', *Plant Physiol,* 59 (5), 868-872.

Ku, M. S., Wu, J., Dai, Z., Scott, R. A., Chu, C., and Edwards, G. E. (1991), 'Photosynthetic and photorespiratory characteristics of flaveria species', *Plant Physiol,* 96 (2), 518-528.

Ku, M. S., Kano-Murakami, Y., and Matsuoka, M. (1996), 'Evolution and expression of C_4 photosynthesis genes', *Plant Physiol,* 111 (4), 949-957.

Ku, M. S., Agarie, S., Nomura, M., Fukayama, H., Tsuchida, H., Ono, K., Hirose, S., Toki, S., Miyao, M., and Matsuoka, M. (1999), 'High level expression of maize phospho*enol*pyruvate carboxylase in transgenic rice plants', *Nat Bio-technol,* 17 (1), 76-80.

Ku, M. S., Cho, D., Li, X., Jiao, D. M., Pinto, M., Miyao, M., and Matsuoka, M. (2001), 'Introduction of genes encoding C_4 photosynthesis enzymes into rice plants: physiological consequences', *Novartis Found Symp,* 236, 100-111; discussion 111-106.

Kurek, I., Chang, T. K., Bertain, S. M., Madrigal, A., Liu, L., Lassner, M. W., and Zhu, G. (2007), 'Enhanced Thermostability of Arabidopsis Rubisco activase improves photosynthesis and growth rates under moderate heat stress', *Plant Cell,* 19 (10), 3230-3241.

Lai, L. B., Wang, L., and Nelson, T. M. (2002), 'Distinct but conserved functions for two chloroplastic NADP-malic enzyme isoforms in C_3 and C_4 Flaveria species', *Plant Physiol,* 128 (1), 125-139.

Lai, L. B., Tausta, S. L., and Nelson, T. M. (2002), 'Differential regulation of transcripts encoding cytosolic NADP-malic enzyme in C_3 and C_4 Flaveria spe-cies', *Plant Physiol,* 128 (1), 140-149.

Lawlor, D. W. (2001), 'Photosynthesis, 3rd edition, BIOS scientific publishers Ltd.

Lance, C., Rustin, P. (1984), ' The central role of malate in plant metabolism', *Physiol.Veg,*22,625-641

Landy, A. (1989), 'Dynamic, structural, and regulatory aspects of lambda site-specific recombination', *Annu Rev Biochem,* 58, 913-949.

Lawlor, D. W. (2001), 'Photosynthesis, 3rd edition', *BIOS scientific publishers Ltd.*

Leegood, R. C.; Lea, P. J.; Adcock, M. D.; Haeusler, R. E. (1995), 'The regulation and control of photorespiration', *J Exp Bot,* 46, 1397-1414.

Leegood, R. C. (1997), 'The regulation of C_4 photosynthesis', *Advances in Botanical Research,* 26, 251-316.

Leegood, R. C. (2002), 'C_4 photosynthesis: principles of CO_2 concentration and prospects for its introduction into C_3 plants', *J Exp Bot,* 53 (369), 581-590.

Leegood, R. C. (2007), 'A welcome diversion from photorespiration', *Nat Biotechnol,* 25 (5), 539-540.

Leegood, RC., Edwards, EG. (1996), 'Carbon metabolism and photorespiration: temperature dependence in relation to other environmental factors.', In: Baker NR (Ed.) *Photosynthesis and the environment*, 5, 191-221.

Leegood RC, Acheson RM, Técsi LI, Walker RP. (1999), 'The many faceted function of phospho*enol*pyruvate carboxykinase in plants', *Kruger NJ, Hill SA, Ratcliffe RG, eds. Regulation of primary metabolic pathways in plants. Dordrecht: Kluwer Academic Publishers*, 37–51.

Lefebvre, S., Lawson, T., Zakhleniuk, O. V., Lloyd, J. C., Raines, C. A., and Fry-er, M. (2005), 'Increased sedoheptulose-1,7-bisphosphatase activity in transgenic tobacco plants stimulates photosynthesis and growth from an early stage in development', *Plant Physiol,* 138 (1), 451-460.

Leport, L., Kandlbinder, A., Baur, B., and Kaiser, W. M. (1996), 'Diurnal modula-tion of phospho*enol*pyruvate carboxylation in pea leaves and roots as related to tissue malate concentrations and to the nitrogen source', *Planta,* 198, 495–501.

Li, L., Zhou, Y., Cheng, X., Sun, J., Marita, JM., Ralph, J., Chiang, VL. (2003), 'Combinatorial modification of multiple lignin traits in trees through multigene cotransformation', *Proc Natl Acad Sci USA,* 100 (8), 4939–4944.

Lieman-Hurwitz, J., Rachmilevitch, S., Mittler, R., Marcus, Y., and Kaplan, A. (2003), 'Enhanced photosynthesis and growth of transgenic plants that express ictB, a gene involved in HCO3- accumulation in cyanobacteria', *Plant Biotechnol J,* 1 (1), 43-50.

Lin, L., Liu, Y. G., Xu, X., and Li, B. (2003), 'Efficient linking and transfer of multiple genes by a multigene assembly and transformation vector system', *Proc Natl Acad Sci U S A,* 100 (10), 5962-5967.

Lipka, B., Steinmuller, K., Rosche, E., Borsch, D., and Westhoff, P. (1994), 'The C_3 plant Flaveria pringlei contains a plastidic NADP-malic enzyme which is orthologous to the C_4 isoform of the C_4 plant F. trinervia', *Plant Mol Biol,* 26 (6), 1775-1783.

Lipka, V., Häusler, R. E., Rademacher, T., Li, J., Hirsch, H. J., and Kreuzaler, F. (1999), 'Solanum tuberosum double transgenic expressing phospho*enol*pyruvate carboxylase and NADP-malic enzyme display reduced electron requirement for CO_2 fixation', *Plant Sci.,* 144, 93-105.

Liu, Y. G., Shirano, Y., Fukaki, H., Yanai, Y., Tasaka, M., Tabata, S., and Shibata, D. (1999), 'Complementation of plant mutants with large genomic DNA fragments by a transformation-competent artificial chromosome vector accelerates positional cloning', *Proc Natl Acad Sci U S A,* 96 (11), 6535-6540.

Lohman, J.R., Olson, A. C., Remington, J.S. (2008), 'Atomic resolution structures of Escherichia coli and Bacillus anthracis malate synthase A: comparison with isoform G and implications for structure-based drug discovery', *Protein Sci,* 17(11), 1935–1945.

Lord, J. M. (1972), 'Glycolate oxidoreductase in Escherichia coli', *Biochim Biophys Acta,* 267 (2), 227-237.

Ludwig, M., von Caemmerer, S., Dean Price, G., Badger, M. R., and Furbank, R. T. (1998), 'Expression of tobacco carbonic anhydrase in the C_4 dicot flaveria bidentis leads to increased leakiness of the bundle sheath and a defective CO_2-concentrating mechanism', *Plant Physiol,* 117 (3), 1071-1081.

Lyznik, L. A. and Dress, V. (2008), 'Gene targeting for chromosome engineering applications in eukaryotic cells', *Recent Pat Biotechnol,* 2 (2), 94-106.

Magnin, N. C., Cooley, B. A., Reiskind, J. B., and Bowes, G. (1997), 'Regulation and Localization of Key Enzymes during the Induction of KranzLess, C_4-Type Photosynthesis in Hydrilla verticillata', *Plant Physiol,* 115 (4), 1681-1689.

Makino, A. and Mae, T. (1999), 'Photosynthesis and plant growth at elevated levels of CO_2', *Plant Cell Physiol.,* 40, 999–1006.

Matsuoka, M., Tada, Y., Fujimura, T., and Kano-Murakami, Y. (1993), 'Tissue-specific light-regulated expression directed by the promoter of a C_4 gene, maize pyruvate,orthophosphate dikinase, in a C_3 plant, rice', *Proc Natl Acad Sci U S A,* 90 (20), 9586-9590.

Matsuoka, M. (1995), 'The gene for pyruvate, orthophosphate dikinase in C_4 plants: structure, regulation and evolution', *Plant Cell Physiol,* 36 (6), 937-943.

Matsuoka, M., Furbank, R. T., Fukayama, H., and Miyao, M. (2001), 'Molecular Engineering of C_4 Photosynthesis', *Annu Rev Plant Physiol Plant Mol Biol,* 52, 297-314.

Maurino, V. G. and Peterhansel, C. (2010), 'Photorespiration: current status and approaches for metabolic engineering', *Curr Opin Plant Biol,* 13 (3), 249-256.

Meyer, P. and Saedler, H. (1996), 'Homology Dependent Gene Silencing in Plants', *Annu Rev Plant Physiol Plant Mol Biol,* 47, 23-48.

Migge, A., Carryol, E., Kunz, C., Hirel, B., Foch, H., and Becker, T. (1997), 'Expression of the tobacco genes encoding plastidic glutamine synthetase or ferredoxin- dependent glutamate synthase doesn't depend on nitrate reduction and is unaffected by suppression of photorespiration', *J. Exp. Bot.,* 48, 1175-1184.

Miles, B. (2003), ' Photosynthesis', *www.tamu.edu/faculty/bmiles*

Miyagawa, Y., Tamoi, M., Shigeoka, S. (2001), ' Overexpression of a cyanobacterial fructose-1,6-/sedoheptulose-1,7-bisphosphatase in tobacco enhances photosynthesis and growth. Nat Biotechnol, 19 (10), 965–969.

Miyao, M. and Fukayama, H. (2003), 'Metabolic consequences of overproduction of phospho*enol*pyruvate carboxylase in C_3 plants', *Arch Biochem Biophys,* 414 (2), 197-203.

Miyao, M. (2003), 'Molecular evolution and genetic engineering of C_4 photosynthetic enzymes', *J Exp Bot,* 54 (381), 179-189.

Miyao, M., Masumoto, C., Miyazawa, S., and Fukayama, H. (2011), 'Lessons from engineering a single-cell C_4 photosynthetic pathway into rice', *J Exp Bot,* 62 (9), 3021-3029.

Monson, R. K., Moore, B. d., Ku, M. S. B., and Edwards, G. E. (1986), 'Co-function of C_3- and C_4-photosynthetic pathways in C_3, C_4 and C_3-C_4 intermediate Flaveria species', *Planta,* 168, 493-502.

Naqvi, S., Farre, G., Sanahuja, G., Capell, T., Zhu, C., and Christou, P. (2010), 'When more is better: multigene engineering in plants', *Trends Plant Sci,* 15 (1), 48-56.

Nomura, M., Sentoku, N., Nishimura, A., Lin, J. H., Honda, C., Taniguchi, M., Ishida, Y., Ohta, S., Komari, T., Miyao-Tokutomi, M., Kano-Murakami, Y., Tajima, S., Ku, M. S., and Matsuoka, M. (2000), 'The evolution of C_4 plants: acquisition of cis-regulatory sequences in the promoter of C_4-type pyruvate, orthophosphate dikinase gene', *Plant J,* 22 (3), 211-221.

Ogren, W. L. (1984), 'Photrespiration: Pathways, regulation and modification', *Annual Review in Plant Physiology,* 35, 415-442.

O'Leary, M. H., Rife, J. E., and Slater, J. D. (1981), 'Kinetic and isotope effect studies of maize phospho*enol*pyruvate carboxylase', *Biochemistry,* 20 (25), 7308-7314.

Osaki, M. and Shinano, T. (2000), 'Influence of carbon-nitrogen balance on productivity of C_3 plants and effect of high expression of phospho*enol*pyruvate carboxylase in transgenic rice', *Studies in Plant Science,* 7, 177–192.

Osmond, C. B. (1978), 'Crassulacean acid metabolism: a curiosity in context', *Annu. Rev. Plant Physiol.,* 29, 379-414.

Padidam, M. and Cao, Y. (2001), 'Elimination of transcriptional interference between tandem genes in plant cells', *Biotechniques,* 31 (2), 328-330, 332-324.

Park, J., Okita, T. W., and Edwards, G. E. (2010), 'Expression profiling and proteomic analysis of isolated photosynthetic cells of the non-Kranz C_4 species Bienertia sinuspersici', *Funct. Plant Biol.,* 37, 1-13.

Parry, M. A., Andralojc, P. J., Mitchell, R. A., Madgwick, P. J., and Keys, A. J. (2003), 'Manipulation of Rubisco: the amount, activity, function and regulation', *J Exp Bot,* 54 (386), 1321-1333.

Pellicer, M. T., Badia, J., Aguilar, J., and Baldoma, L. (1996), 'glc locus of Escherichia coli: characterization of genes encoding the subunits of glycolate oxidase and the glc regulator protein', *J Bacteriol,* 178 (7), 2051-2059.

Peterhänsel, C., Niessen, M., and Kebeish, R. M. (2008), 'Metabolic engineering towards the enhancement of photosynthesis', *Photochem Photobiol,* 84 (6), 1317-1323.

Peterhänsel, C. (2011), 'Best practice procedures for the establishment of a C_4 cycle in transgenic C_3 plants', *J Exp Bot,* 62 (9), 3011-3019.

Peterhänsel, C. and Maurino, V. G. (2011), 'Photorespiration redesigned', *Plant Physiol,* 155 (1), 49-55.

Poeydomenge, O., Marolda, M., Boudet, AM., Crima-Pettenati, J. (1995), 'Nucleotide Sequence of a cDNA Encoding Mitochondrial Malate Dehydrogenase from Eucalyptus', *Plant Physiol,* 107 (4), 1455-1456

Portis, A. R., Jr. and Parry, M. A. (2007), 'Discoveries in Rubisco (Ribulose 1,5-bisphosphate carboxylase/oxygenase): a historical perspective', *Photosynth Res,* 94 (1), 121-143.

Powles, S. B. (1984), 'Photoinhibition of photosynthesis induced by visible light', *Annu. Rev. Plant Physiol.,* 35, 15-44.

Pracharoenwattana, I., Cornah, J. E., and Smith, S. M. (2007), 'Arabidopsis peroxisomal malate dehydrogenase functions in beta-oxidation but not in the glyoxylate cycle', *Plant J,* 50 (3), 381-390.

Preston, A. (2003), 'Choosing a cloning vector', *Methods Mol Biol,* 235, 19-26.

Rademacher, T., Hausler, R. E., Hirsch, H. J., Zhang, L., Lipka, V., Weier, D., Kreuzaler, F., and Peterhansel, C. (2002), 'An engineered phospho*enol*pyruvate carboxylase redirects carbon and nitrogen flow in transgenic potato plants', *Plant J,* 32 (1), 25-39.

Raines, C. A. (2003), 'The Calvin cycle revisited', *Photosynth Res,* 75 (1), 1-10.

Raines, C. A. (2011), 'Increasing photosynthetic carbon assimilation in C_3 plants to improve crop yield: current and future strategies', *Plant Physiol,* 155 (1), 36-42.

Ramazanov, Z. and Cardenas, J. (1992), 'Inorganic carbon transport across cell compartments of the halotolerant alga Dunaliella salina', *Physiol. Plant,* 85, 121–128.

Rao, S. K., Magnin, N. C., Reiskind, J. B., and Bowes, G. (2002), 'Photosynthetic and other phospho*enol*pyruvate carboxylase isoforms in the single-cell, facul-tative C_4 system of Hydrilla verticillata', *Plant Physiol,* 130 (2), 876-886.

Rao, V. S., Rao, S. K. , Reiskind, J. B., and Bowes, G. (2005), 'Carbonic anhydrase isoforms in the C_4 CCM of Hydrilla', *van der Est, A., Bruce, D., Photosynthesis: Fundamental Aspects to Global Perspectives Allen Press, Inc Kansas*, 954–955.

Rao, S., Reiskind, J., and Bowes, G. (2006), 'Light regulation of the photosynthetic phospho*enol*pyruvate carboxylase (PEPC) in Hydrilla verticillata', *Plant Cell Physiol,* 47 (9), 1206-1216.

Rao, S. K., Fukayama, H., Reiskind, J. B., Miyao, M., and Bowes, G. (2006), 'Identification of C_4 responsive genes in the facultative C_4 plant Hydrilla vertic-illata', *Photosynth Res,* 88 (2), 173-183.

Raven, J. A., Johnston, A. M. , Kübler, J. E. , Korb, R. , McInroy, S. G. , Handley, L. L. , Scrimgeour, C. M. , Walker, D. I. , Beardall, J. , Vanderklift, M. , Fredriksen, S. , and Dunton, K. H. (2002), 'Mechanistic interpretation of carbon isotope discrimination by marine macroalgae and seagrasses', *Funct. Plant Biol.,* 29, 355-378.

Read, B. A. and Tabita, F. R. (1994), 'High substrate specificity factor ribulose bisphosphate carboxylase/oxygenase from eukaryotic marine algae and properties of recombinant cyanobacterial Rubisco containing "algal" residue modifications', *Arch Biochem Biophys,* 312 (1), 210-218.

Reed, M. L. and Graham, D. (1981), 'Carbonic anhydrase in plants: distribution, properties and possible physiological roles', *Reinhold, L., Harbourne J. B., Swain, T., Eds. Progress in Phytochemistry. Oxford: Pergamon Press*, 47-94.

Reiskind, J. B., Madsen, T. V., VanGinkel, L. C., and Bowes, G. (1997), 'Evidence that inducible C_4 type photosynthesis is a chloroplastic CO_2-concentrating mechanism in Hydrilla, a submersed monocot', *Plant Cell and Environment,* 20, 211–220.

Robinson, S. P. and Portis, A. R. (1988), 'Involvement of stromal ATP in the light activation of ribulose-1,5-bisphosphate carboxylase/oxygenase in intact isolated chloroplasts', *Plant Physiol,* 86 (1), 293-298.

Sage, R. F., Pearcy, R. W., and Seemann, J. R. (1987), 'The Nitrogen Use Efficiency of C_3 and C_4 Plants : III. Leaf Nitrogen Effects on the Activity of Carbox-ylating Enzymes in Chenopodium album (L.) and Amaranthus retroflexus (L.)', *Plant Physiol,* 85 (2), 355-359.

Sage, R. F. (1999), 'Why C_4 photosynthesis. C_4 Plant Biology, edited by R.K. Mon-son and R.F. Sage.', *Academic Press San Diego,* 3, 3-16.

Sage, R. F. (2001), C_4 plants.Encyclopedia of Biodiversity *1: 575 – 598*

Sage, R. F. (2002), 'Variation in the k (cat) of Rubisco in C_3 and C_4 plants and some implications for photosynthetic performance at high and low tempera-ture', *J Exp Bot,* 53 (369), 609-620.

Sage, R. F. (2002), 'C_4 photosynthesis in terrestrial plants does not require Kranz anatomy', *Trends Plant Sci,* 7 (7), 283-285.

Sage, R. F. (2004), The evolution of C 4 photosynthesis. New phytologist 161, 341-370.

Sage, R. F. (2004), 'The evolution of C_4 photosynthesis', *New Phytologist,* 161, 341–370.

Sage, R. F., Christin, P.A., Edwards, E. J. (2011), 'The C(4) plant lineages of planet Earth', *J Exp Bot,* 62(9) 3155-69.

.

Salvucci, M. E. and Bowes, G. (1981), 'Induction of reduced photorespiratory activity in submersed and amphibious aquatic macrophytes', *Plant Physiol,* 67 (2), 335-340.

Salvucci, M. E. and Bowes, G. (1983), 'Two photosynthetic mechanisms mediating the low photorespiratory state in submersed aquatic angiosperms', *Plant Phys-iol,* 73 (2), 488-496.

Salvucci, M. E., Osteryoung, K. W., Crafts-Brandner, S. J., and Vierling, E. (2001), 'Exceptional sensitivity of Rubisco activase to thermal denaturation in vitro and in vivo', *Plant Physiol,* 127 (3), 1053-1064.

Sanger, F., Nicklen, S., and Coulson, A. R. (1977), 'DNA sequencing with chain terminating inhibitors', *Proc Natl Acad Sci U S A,* 74 (12), 5463-5467.

Sasaki, Y., Sone, T., Yoshida, S., Yahata, K., Hotta, J., Chesnut, J. D., Honda, T., and Imamoto, F. (2004), 'Evidence for high specificity and efficiency of multiple recombination signals in mixed DNA cloning by the Multisite Gateway system', *J Biotechnol,* 107 (3), 233-243.

Scheibe, R. (2004), 'Malate valves to balance cellular energy supply', *Physiol Plant,* 120 (1), 21-26.

Schmid, J. and Amrhein, N. (1995), 'Molecular organization of the shikimate pathway in higher plants', *Phytochemistry,* 4, 737-749.

Schofer, P., Brennicke, A. (2005), 'Pflanzen physiologie', Spektrum Akademischer Verlag; Auflage: 6.

Sentoku, N., Taniguchi, M., Sugiyama, T., Ishimaru, K., Ohsugi,R., Takaiwa, F., Toki, S. (2009), 'Analysis of the transgenic tobacco plants expressing Panicum miliaceum aspartate aminotransferase genes', *Plant Cell Reports,* 19 (6), 598-603.

Sharkey, T. D. (1985), 'O_2 insensitive photosynthesis in C_3 plants: its occurrence and a possible explanation', *Plant Physiol,* 78 (1), 71-75.

Sharkey, T. D., Seemann, J. R., and Berry, J. A. (1986), 'Regulation of Ribulose-1,5-Bisphosphate Carboxylase Activity in Response to Changing Partial Pressure of O_2 and Light in Phaseolus vulgaris', *Plant Physiol,* 81 (3), 788-791.

Sharkey, T. D. (1988), 'Estimating the rate of photorespiration in leaves', *Plant Phys-iol.,* 73, 147-152.

Sharkey, T. D., Badger, M. R., von Caemmerer, S., and Andrews, T. J. (2001), 'Increased heat sensitivity of photosynthesis in tobacco plants with reduced Rubisco activase', *Photosynth Res,* 67 (1-2), 147-156.

Sharkey, T. D. (2001), 'Photorespiration', *Encyclopedia of life sciences 1-5*.

Sharkey, T. D., Laporte, M., Lu, Y., Weise, S., and Weber, A. P. (2004), 'Engineering plants for elevated CO_2: a relationship between starch degradation and sugar sensing', *Plant Biol (Stuttg),* 6 (3), 280-288.

Sharkey, T. D. and Zhang, R. (2010), 'High temperature effects on electron and proton circuits of photosynthesis', *J Integr Plant Biol,* 52 (8), 712-722

Sheen, J. (1999), 'C_4 Gene Expression', *Annu Rev Plant Physiol Plant Mol Biol,* 50, 187-217.

Sheriff, A., Meyer, H., Riedel, E., Schmitt, J. M., and Lapke, C. (1998), 'The influence of plant pyruvate, orthophosphate dikinase on a C_3 plant with respect to the intracellular location of the enzyme', *Plant Sci.,* 136, 43–57.

Somerville, C. R. (2001), 'An Early Arabidopsis demonstration. Resolving a Few Issues Concerning Photorespiration', *Plant Physiol.,* 125 (1), 20-24.

Spencer, D., Anderson, L., Ksander, G., Klaine, S., and Bailey, F. (1994), 'Vegetative propagule production and allocation of carbon and nitrogen by monoecious Hydrilla verticillata (L.f.) Royle grown at two photoperiods', *Aquatic Botany,* 48, 121-132.

Stabenau, H., Winkler, U., and Saftel, W. (1984). Mitochondrial metabolism of glycolate in the alga Eremosphaera viridis. Zeitschrift fuer Pflanzenphysiologie 114, 413-420.

Stam, M., de Bruin, R., Kenter, S., van der Hoorn, R. A. L., van Blokland, R., Mol, J. N. M., and Kooter, J. M. (1997), 'Post-transcriptional silencing of chalcone synthase in Petunia by inverted transgene repeats', *Plant J.,* 12, 63–82.

Stemmer, W. P. (1994), 'DNA shuffling by random fragmentation and reassembly: in vitro recombination for molecular evolution', *Proc Natl Acad Sci U S A,* 91 (22), 10747-10751.

Sternberg, N. and Cohen, G. (1989), 'Genetic analysis of the lytic replicon of bacteriophage P1. II. Organization of replicon elements', *J Mol Biol,* 207 (1), 111-133.

Sternberg, N. (1990), 'Bacteriophage P1 cloning system for the isolation, amplification, and recovery of DNA fragments as large as 100 kilobase pairs', *Proc Natl Acad Sci U S A,* 87 (1), 103-107.

Stief, A., Winter, D. M., Stratling, W. H., and Sippel, A. E. (1989), 'A nuclear DNA attachment element mediates elevated and position-independent gene activity', *Nature,* 341 (6240), 343-345.

Stitt, M. and Sonnewald, U. (1995), 'Regulation of metabolism in transgenic plants', *Annu. Rev. Plant Physiol. Plant Mol. Biol.,* 46, 341–368.

Stitt, M. (1999), 'Nitrate regulation of metabolism and growth', *Curr Opin Plant Biol,* 2 (3), 178-186.

Streatfield, S. J., Weber, A., Kinsman, E. A., Hausler, R. E., Li, J., Post-Beittenmiller, D., Kaiser, W. M., Pyke, K. A., Flugge, U. I., and Chory, J. (1999), 'The phospho*enol*pyruvate/phosphate translocator is required for phe-nolic metabolism, palisade cell development, and plastid-dependent nuclear gene expression', *Plant Cell,* 11 (9), 1609-1622.

Sutherland, P. and McAlister-Henn, L. (1985), 'Isolation and expression of the Escherichia coli gene encoding malate dehydrogenase', *J Bacteriol,* 163 (3), 1074-1079.

Suzuki, S., Murai, N., Burnell, J. N., and Arai, M. (2000), 'Changes in photosynthetic carbon flow in transgenic rice plants that express C_4-type phospho*enol*pyruvate carboxykinase from Urochloa panicoides', *Plant Physiol,* 124 (1), 163-172.

Suzuki, S., Murai, N., Kasaoka, K., Hiyoshi, T., Imaseki, H., Burnell, JN., Arai, M. (2006), 'Carbon metabolism in transgenic rice plants that express phosphoenolpyruvate carboxylase and/or phosphoenolpyruvate carboxykinase', *Plant Science,*170 (5)1010-1019.

Svensson, P., Blasing, O. E., and Westhoff, P. (1997), 'Evolution of the enzymatic characteristics of C_4 phospho*enol*pyruvate carboxylase a comparison of the orthologous PPCA phospho*enol*pyruvate carboxylases of Flaveria trinervia (C_4) and Flaveria pringlei (C_3)', *Eur J Biochem,* 246 (2), 452-460.

Tachibana, K., Watanabe, T., Sekizawa, Y., and Takematsu, T. (1986). Accumulation of ammonia in plants treated with Bialaphos. Pesticide Sci 11, 33–37.

Takahashi, S., Bauwe, H., and Badger, M. (2007), 'Impairment of the photorespiratory pathway accelerates photoinhibition of photosystem II by suppression ofrepair but not acceleration of damage processes in Arabidopsis', *Plant Physiol,* 144 (1), 487-494.

Takeuchi, Y., Akagi, H., Kamasawa, N., Osumi, M., and Honda, H. (2000), 'Aberrant chloroplasts in transgenic rice plants expressing a high level of maize NADP-dependent malic enzyme', *Planta,* 211 (2), 265-274.

Tamoi, M., Nagaoka, M., Miyagawa, Y., Shigeoka, S. (2006). Contribution of Fructose-1,6-bisphosphatase and Sedoheptulose-1,7-bisphosphatase to the Photosynthetic Rate and Carbon Flow in the CalvinCycle in Transgenic Plants. *Plant and Cell Physiology*, 47 (3), 380-390.

Taniguchi, M., Taniguchi, Y., Kawasaki, M., Takeda, S., Kato, T., Sato, S., Tabata, S., Miyake, H., and Sugiyama, T. (2002), 'Identifying and characterizing plastidic 2-oxoglutarate/malate and dicarboxylate transporters in Arabidopsis thaliana', *Plant Cell Physiol,* 43 (7), 706-717.

Taniguchi, Y., Ohkawa, H., Masumoto, C., Fukuda, T., Tamai, T., Lee, K., Sudoh, S., Tsuchida, H., Sasaki, H., Fukayama, H., and Miyao, M. (2008), 'Over-production of C_4 photosynthetic enzymes in transgenic rice plants: an approach to introduce the C_4-like photosynthetic pathway into rice', *J Exp Bot,* 59 (7), 1799-1809.

Tolbert, N. E. (1997), 'The C2 Oxidative Photosynthetic Carbon Cycle', *Annu Rev Plant Physiol Plant Mol Biol,* 48, 1-25.

Tronconi, M. A., Fahnenstich, H., Gerrard Weehler, M. C., Andreo, C. S., Flugge, U. I., Drincovich, M. F., und Maurino, V. G. (2008), 'Arabidopsis NAD-malic enzyme functions as a homodimer and heterodimer and has a major impact on nocturnal metabolism', *Plant Physiol,* 146 (4), 1540-1552.

Tsang, E. W., Bowler, C., Herouart, D., Van Camp, W., Villarroel, R., Genetello, C., Van Montagu, M., and Inze, D. (1991), 'Differential regulation of superoxide dismutases in plants exposed to environmental stress', *Plant Cell,* 3 (8), 783-792.

Tsuchida, H., Tamai, T., Fukayama, H., Agarie, S., Nomura, M., Onodera, H., Ono, K., Nishizawa, Y., Lee, B. H., Hirose, S., Toki, S., Ku, M. S., Mat-suoka, M., and Miyao, M. (2001), 'High level expression of C_4-specific NADP-malic enzyme in leaves and impairment of photoautotrophic growth in a C_3 plant, rice', *Plant Cell Physiol,* 42 (2), 138-145.

Tsuzuki, M., Miyachi, S., and Berry, J. A. (1985), 'Intracellular accumulation of inorganic carbon and its active species taken up by Chlorella vulgaris 11h', *Inorganic Carbon Uptake by Aquatic Photosynthetic Organisms. Edited by Lucas, W. J. and Berry, J. A.*, 53-66.

Uemura, K., Anwaruzzaman, Miyachi, S., and Yokota, A. (1997), 'Ribulose-1,5-bisphosphate carboxylase/oxygenase from thermophilic red algae with a strong specificity for CO_2 fixation', *Biochem Biophys Res Commun,* 233 (2), 568-571.

Ueno, Y., Hata, S., and Izui, K. (1997), 'Regulatory phosphorylation of plant phospho*enol*pyruvate carboxylase: role of a conserved basic residue upstream of the phosphorylation site', *FEBS Lett,* 417 (1), 57-60.

Ueno, Y., Imanari, E., Emura, J., Yoshizawa-Kumagaye, K., Nakajima, K., Inami, K., Shiba, T., Sakakibara, H., Sugiyama, T., and Izui, K. (2000), 'Immunological analysis of the phosphorylation state of maize C_4 form phospho*enol*pyruvate carboxylase with specific antibodies raised against a synthetic phosphorylated peptide', *Plant J,* 21 (1), 17-26.

Utsunomiya, E. & Muto, S. (1993), 'Carbonic anhydrase in the plasmamembranes from leaves of C3and C4plants', *Physiologia Plantarum*, 88 (3), 413–419

Vain, P., Worland, B., Kohli, A., Snape, J. W., Christou, P., Allen, G. C., and Thompson, W. F. (1999), 'Matrix attachment regions increase transgenic rice plants and their progeny', *Plant J.,* 18 (3), 233-242.

Van Camp, W., Bowler, C., Villarroel, R., Tsang, E. W., Van Montagu, M., and Inze, D. (1990), 'Characterization of iron superoxide dismutase cDNAs from plants obtained by genetic complementation in Escherichia coli', *Proc Natl Acad Sci U S A,* 87 (24), 9903-9907.

Van der Straeten, D., Rodrigues-Pousada, R. A., Goodman, H. M., and Van Mon-tagu, M. (1991), 'Plant enolase: gene structure, expression, and evolution', *Plant Cell,* 3 (7), 719-735.

Vanderwinkel, E. D., Vlieghere, M. (1968), 'Physiology and genetics of isocitritase and the malate synthases of Escherichia coli', *Eur J Biochem,* 5 (1), 81-90.

van 't Hof, R. and de Kruijff, B. (1995), 'Characterization of the import process of a transit peptide into chloroplasts', *J Biol Chem,* 270 (38), 22368-22373.

Vaucheret, H. and Fagard, M. (2001), 'Transcriptional gene silencing in plants: targets, inducers and regulators', *Trends Genet,* 17 (1), 29-35.

von Caemmerer, S., Millgate, A., Farquhar, GD., Furbank, RT. (1997), 'Reduction of ribulose-1,5-bisphosphate carboxylase/oxygenase by antisense RNA in the C4 plant Flaveria bidentis leads to reduced assimilation rates and increased carbon isotope discrimination', *Plant Physiol* 113 (2), 469–477

von Caemmerer, S. and Furbank, R. T. (1999), 'Modelling of C_4 photosynthesis. In: Sage R, Monson RK, editors. C_4 plant biology', *Academic Press*, 173-211.

von Caemmerer, S. (2000), 'Biochemical Models of Leaf Photosynthesis', *CSIRO Publishing, Collingwood, Australia*.

von Caemmerer, S. and Furbank, R. T. (2003), 'The C(4) pathway: an efficient CO_2 pump', *Photosynth Res,* 77 (2-3), 191-207.

von Caemmerer, S. (2003), 'C_4 photosynthesis in a single C_3 cell is theoretically inefficient but may ameliorate internal CO_2 diffusion limitations of C_3 leaves', *Plant, Cell and Environment,* 26, 1191–1197.

von Caemmerer, S., Lawson, T., Oxborough, K., Baker, N. R., Andrews, T. J., and Raines, C. A. (2004), 'Stomatal conductance does not correlate with photosynthetic capacity in transgenic tobacco with reduced amounts of Rubisco', *J Exp Bot,* 55 (400), 1157-1166.

von Caemmerer, S. and Evans, J. R. (2010), 'Enhancing C_3 photosynthesis', *Plant Physiol,* 154 (2), 589-592.

Vooper T.G; Beever H. (1969), 'β Oxidation in Glyoxysomes from CastorBean Endosperm', *J Biol. Chem,* 244 (13), 3514-3520

Voznesenskaya, E. V., Franceschi, V. R., Kiirats, O., Freitag, H., and Edwards, G. E. (2001), 'Kranz anatomy is not essential for terrestrial C_4 plant photosynthesis', *Nature,* 414 (6863), 543-546.

Voznesenskaya, E. V., Franceschi, V. R., Kiirats, O., Artyusheva, E. G., Freitag, H., and Edwards, G. E. (2002), 'Proof of C_4 photosynthesis without Kranz anatomy in Bienertia cycloptera (Chenopodiaceae)', *Plant J,* 31 (5), 649-662.

Voznesenskaya, E. V., Koteyeva, N. K., Chuong, S. D., Akhani, H., Edwards, G. E., and Franceschi, V. R. (2005), 'Differentiation of cellular and biochemical features of the single-cell C_4 syndrome during leaf development in Bienertia cycloptera (Chenopodiaceae)', *Am J Bot,* 92 (11), 1784-1795.

Walker, R. P. and Leegood, R. C. (1996), 'Phosphorylation of phospho*enol*pyruvate carboxykinase in plants. Studies in plants with C_4 photosynthesis and Crassulacean acid metabolism and in germinating seeds', *Biochem J,* 317 (Pt 3), 653-658.

Walker, R. P., Acheson, R. M., Técsi, L. I., and Leegood, R. C. (1997), 'Phospho*enol*pyruvate carboxykinase in C_4 plants: its role and regulation', *Aust. J. Plant Physiol.,* 24, 459–468.

Wang, J., Tan, H., and Zhao, Z. K. (2007), 'Over-expression, purification, and characterization of recombinant NAD-malic enzyme from Escherichia coli K12', *Protein Expr Purif,* 53 (1), 97-103.

Werdan, K., Heldt, H. W., and Milovancev, M. (1975), 'The role of pH in the regulation of carbon fixation in the chloroplast stroma. Studies on CO_2 fixation in the light and dark', *Biochim Biophys Acta,* 396 (2), 276-292.

Westhoff, P. and Gowik, U. (2010), 'Evolution of C_4 photosynthesis looking for the master switch', *Plant Physiol,* 154 (2), 598-601.

Whitmarsh, J., Govindjee. (1995), 'Photosynthesis', *Encyclopedia for Applied Physics*. 13: 513-532

Whitney, S. M., Houtz, R. L., and Alonso, H. (2011), 'Advancing our understanding and capacity to engineer nature's CO_2-sequestering enzyme, Rubisco', *Plant Physiol,* 155 (1), 27-35.

Wild, A., Ziegler, C. (1989), 'The effect of bialaphos on ammonium assimilation and photosynthesis. I. Effect on the enzymes of ammonium-assimilation', *Naturforsch* 44, 97-102.

Wingler, A., Lea, P. J., and Leegood, R. C. (1997), 'Control of photosynthesis in barley plants with reduced activities of glycine decarboxylase', *Planta,* 202, 171-178.

Winter, K. and Holtum, J. A. (2007), 'Environment or development? Lifetime net CO_2 exchange and control of the expression of Crassulacean acid metabolism in Mesembryanthemum crystallinum', *Plant Physiol,* 143 (1), 98-107.

Wu, G., Truksa, M., Datla, N., Vrinten, P., Bauer, J.,Zank, T., Cirpus, P., Heinz, E., und Qiu, X. (2005),'Stepwise engineering to produce high yields of very long-chain polyunsaturated fatty acids in plants', Nat Biotechnol,23 (8), 1013-1017.

Yamaguchi, M., Tokushige, M., and Katsuki, H. (1973), 'Studies on regulatory functions of malic enzymes. II. Purification and molecular properties of nicotin amide adenine dinucleotide-linked malic enzyme from Eschericha coli', *J Bio-chem,* 73 (1), 169-180.

Zelitch, I., Schultes, N. P., Peterson, R. B., Brown, P., and Brutnell, T. P. (2009), 'High glycolate oxidase activity is required for survival of maize in normal air', *Plant Physiol,* 149 (1), 195-204.

Zhao, J. Z., Cao, J., Li, Y., Collins, H. L., Roush, R. T., Earle, E. D., and Shelton, A. M. (2003), 'Transgenic plants expressing two Bacillus thuringiensis toxins delay insect resistance evolution', *Nat Biotechnol,* 21 (12), 1493-1497.

Zhong, R., Richardson, E. A., und Ye, Z. H. (2007), 'Two NAC domain transcription factors, SND1 and NST1, function redundantly in regulation of secondary wall synthesis in fibers of Arabidopsis', *Planta,*225 (6), 1603-1611

Acknowledgements

My special thanks to Prof. Dr. Fritz Kreuzaler for his unlimited dedication and commitment towards this work. The critical reading, discussion and correction of this thesis by him made it possible for me to present this thesis in its present form.

Special thanks to Dr. Nikolaus Schlaich and Prof Dr.Christoph Peterhansel for their great help during my work.

I thank to Prof. Dr. Ursula Priefer for agreeing to be the examiner.

I wish to express my special thanks to Dr Bjorn Usadel and other members of Botany Institute for their kindness and cooperation

I would like to thank Raimund Knauf for his help in the green house and great care of my tobacco cultivers.

I thank the Institute for Biology I and RWTH Aachen University for financing my study from 2009 until its successful completion.

I thank my mother who always supports me in many situations. I remember my dad throughout my study and I get courage to complete my work. I also thank to Jayant and Bali for their many precious suggestions and advice.

I thank also Peter Subei for their skillful technical assistance. Special thanks to Vishal Saindane, Madhuri Saindane, Devendra Saindane, and Shankul Lohakare for their best wishes and help during this work.

I wish to acknowledge my endless thanks to Alexander Heil for his support and patience in many ways throughout this study.

Declaration / Erklärung

Herewith I declare that I have written this PhD thesis myself, using only the referenced literature.

Hiermit versichere ich, dass ich die vorliegende Doktorarbeit selbstständig verfasst and keine anderen, als die angebenen Hilfsmittel and Quellen verwendet habe.

Aachen, 2013